

RECLAMATION

Managing Water in the West

Design Standards No. 13

Embankment Dams

**Chapter 4: Static Stability Analysis
Phase 4 (Final)**



Mission Statements

The U.S. Department of the Interior protects America's natural resources and heritage, honors our cultures and tribal communities, and supplies the energy to power our future.

The mission of the Bureau of Reclamation is to manage, develop, and protect water and related resources in an environmentally and economically sound manner in the interest of the American public.

**Chapter Signature Sheet
Bureau of Reclamation
Technical Service Center**

Design Standards No. 13

Embankment Dams

Chapter 4: Static Stability Analysis

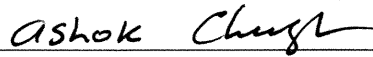
**DS-13(4)-6:¹ Phase 4 (Final)
October 2011**

Chapter 4 - Static Stability Analysis is an existing chapter within Design Standards No. 13 and was revised to include:

- Lowering of minimum factor of safety for reservoir operational conditions
- Current practices in slope stability analysis and computer programs
- Application to slope stability analysis for existing embankment dams
- Guidance papers for static slope stability analysis
- Minor corrections and editorial changes

¹ DS-13(4)-6 refers to Design Standards No. 13, chapter 4, revision 6.

Prepared by:




Ashok Chugh, P.E.
Civil Engineer, Geotechnical Engineering Group 1

7-6-2011

Date

Peer Review:

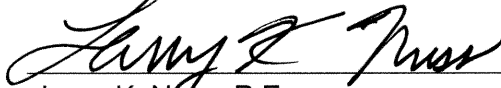


William Engemoen, P.E.
Geotechnical Engineer, Geotechnical Services Division

7/7/2011

Date

Security Review:

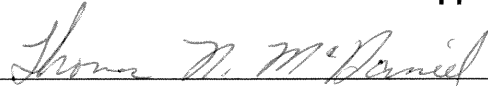


Larry K. Nuss, P.E.
Structural Engineer, Structural Analysis Group

7/19/2011

Date

Recommended for Technical Approval:




Thomas N. McDaniel, P.E.
Geotechnical Engineer, Geotechnical Engineering Group 2

7/6/2011

Date

Submitted:



Karen Knight, P.E.
Chief, Geotechnical Services Division

10/12/2012

Date

Approved:



Lowell Pimley, P.E.
Director, Technical Service Center

11/6/12

Date

Contents

	<i>Page</i>	
4.1	Introduction.....	4-1
4.1.1	Purpose.....	4-1
4.1.2	Scope.....	4-1
4.1.3	Deviations from Standard	4-1
4.1.4	Revisions of Standard	4-1
4.1.5	Applicability	4-1
4.2	Loading Conditions and Factor of Safety.....	4-2
4.2.1	General.....	4-2
4.2.2	Selection of Loading Conditions	4-2
4.2.3	Discussion of Loading Condition Parameters.....	4-3
4.2.4	Factor of Safety Criteria.....	4-5
4.3	Shear Strength of Materials.....	4-9
4.3.1	General Criteria.....	4-9
4.3.2	Shear Strength Data and Sources	4-9
4.3.3	Shear Strength Related to Loading Condition	4-11
4.3.4	Anisotropic Shear Strength.....	4-13
4.3.5	Residual Shear Strength.....	4-13
4.4	Determination of Pore Pressures	4-14
4.4.1	Phreatic Surface Method.....	4-14
4.4.2	Graphical Flow Net Method	4-14
4.4.3	Numerical Methods.....	4-14
4.4.4	Field Measurement (Instrumentation) Method	4-15
4.4.5	Hilf's Method.....	4-15
4.5	Slope Stability Analyses.....	4-16
4.5.1	Method of Analysis.....	4-16
4.5.2	Slip Surface Configuration	4-16
4.5.3	Slip Surface Location.....	4-17
4.5.4	Progressive Failure.....	4-17
4.5.5	Three-Dimensional Effect.....	4-18
4.5.6	Verification of Analysis	4-19
4.5.7	Existing Dams	4-20
4.5.8	Excavation Slopes.....	4-22
4.5.9	Back Analysis	4-22
4.5.10	Multi-Stage Stability Analysis for Rapid Drawdown.....	4-23
4.6	References	4-24

Appendices

- A Selection of Shear Strength Parameters
- B Spencer’s Method of Analysis
- C Computer Programs
- D Guidance Papers for Static Stability Analyses

Figures

	<i>Page</i>
4.5.7-1. B.F. Sisk Dam (near Los Banos, California). View showing upstream slope failure during reservoir drawdown	4-20
4.5.7-2. General cross section of B.F. Sisk Dam in the location of the slide during reservoir drawdown.....	4-21
4.5.7-3. Pine View Dam (near Ogden, Utah). View showing stability berm to improve performance of the dam during a seismic event.....	4-21
4.5.7-4. General cross section of Pine View Dam with stability berm.	4-22

Table

	<i>Page</i>
4.2.4-1 Minimum factors of safety	4-8

Chapter 4

Static Stability Analysis

4.1 Introduction

4.1.1 Purpose

This standard provides guidelines for accomplishing a thorough examination and satisfactory analytical verification of the static stability of an embankment dam. This will be accomplished through a discussion of applicable loading conditions, material properties, pore pressures to be considered, and appropriate minimum factors of safety that should be obtained for those loading conditions.

4.1.2 Scope

Criteria are presented for the determination of: (a) loading conditions and minimum factor of safety, (b) material strength properties, and (c) pore pressures. Methods for computing embankment stability under static loading are described in appendix B and are illustrated with numerical examples included therein.

4.1.3 Deviations from Standard

Stability analyses within the Bureau of Reclamation (Reclamation) should conform to this design standard. If deviations from the standard are required for any reason, the rationale for not using the standard should be presented in the technical documentation for the stability analyses. The technical documentation should follow the peer review requirements included in reference [1].

4.1.4 Revisions of Standard

This chapter will be revised as its use indicates. Comments or suggested revisions should be forwarded to the Chief, Geotechnical Services Division (86-68300), Bureau of Reclamation, Denver, Colorado 80225; they will be comprehensively reviewed and incorporated as needed.

4.1.5 Applicability

These stability analyses standards are applicable to the design and analysis of embankment dams founded on either soil or rock. While the methods discussed herein are also applicable to cut and natural slopes, analysis of cut and natural

slopes may involve factors not addressed herein. For design of small dams, refer to Reclamation publication cited in reference [2].

4.2 Loading Conditions and Factor of Safety

4.2.1 General

The loading conditions to be examined, for either a new or an existing dam, should be based on knowledge of the construction plan, reservoir operation plan, emergency and maintenance operation plans, and flood storage and release plans of the reservoir along with the behavior of the embankment and foundation materials with respect to the development of pore pressures in the dam and foundation.

Appropriate minimum factors of safety will be assigned for these loading conditions.

4.2.2 Selection of Loading Conditions

The loading conditions to be examined are:

- *Construction conditions.*—For a new dam, the end-of-construction condition must be analyzed. It may also be necessary to analyze stability for partial completion of fill conditions, depending on construction schedule and relationship of pore pressures with time.
- *Steady-state seepage conditions.*—For either a new or an existing dam, the stability of the downstream slope should be analyzed at the reservoir level that will control the development of the steady-state seepage surface in the embankment. This reservoir level is usually the top of active conservation storage, but may be lower or higher depending on anticipated reservoir operations.

Operational conditions.—For either a new or an existing dam, if the maximum reservoir surface is substantially higher than the top of active conservation surface, the stability of the downstream slope should be analyzed under maximum reservoir loading. The upstream slope should be analyzed for rapid drawdown conditions from the top of active conservation capacity water surface to the top of inactive capacity water surface and from the maximum water surface to the top of inactive storage water surface. The upstream slope should also be analyzed for rapid drawdown conditions from the top of active conservation water surface to an intermediate level if upstream berms are used.

- *Other conditions.*—Other loading conditions that need to be analyzed in some cases, if appropriate, include: (a) internal drainage plugged or partially plugged, (b) drawdown due to unusually high water use demands, (c) drawdown for the emergency release of the reservoir, (d) construction modifications, and (e) earthquake loading included in Chapter 13, Seismic Analysis and Design, of this Design Standards.

4.2.3 Discussion of Loading Condition Parameters

General guidelines for obtaining reservoir elevation, soil properties, and pore pressure parameters for analysis of different loading conditions are as follows:

- *Construction conditions.*—The end-of-construction condition can be examined either by effective stress concepts or by undrained shear strength concepts.
 - *Effective stress shear strength envelope method.*—The materials in the dam or foundation may develop excess pore pressures due to loading imposed by the overlying soil mass during construction. The effective stress method requires estimation of the change in pore pressure with respect to construction activities and time. Consideration should be given to monitor pore pressures during construction to ensure that the estimated pore pressures are not exceeded by a large margin [3]. The preferred methods for estimating pore pressures during and at the end of construction loading conditions are:
 - Conduct laboratory tests on representative samples of embankment and foundation materials to determine the initial pore air and pore water pressure.
 - Conduct laboratory tests to determine the pore pressure behavior with respect to time and applied load for each material.
 - Establish the expected construction schedule, determine pore pressure versus time function in the materials for that schedule, and check the stability of the upstream and downstream slopes.
 - If necessary, revise the schedule based on actual construction and recheck stability.
 - *Undrained shear strength envelope method.*—This method for determining soil shear strength does not involve measurement of pore air or pore water pressure in the soil sample; thus, it is relatively simpler than the effective stress shear strength envelope method described above. However, analysis in terms of undrained shear

Design Standards No. 13: Embankment Dams

strength implies that pore pressures occurring in laboratory tests on the material satisfactorily approximate field pore pressures and, therefore, the shear strength of those materials. Shear strength tests should be performed on specimens compacted to anticipated placement water contents and densities. Undrained shear strengths used in analyses should correspond to the range of effective normal consolidation stresses expected in the field [4].

- *Steady-state seepage conditions.*—The annual reservoir operation plan should be examined to determine the appropriate reservoir water elevation for use in estimating the location of the steady-state phreatic surface. Usually, it is the top of active storage or joint use pool elevation; although, it is possible that under certain operational plans, such an elevation (top of active storage or joint use pool) is reached for only a small fraction of time each year or it is reached in an oscillatory cycle. In either case, the effective reservoir elevation could be taken to be near the midpoint of the cycle. However, use of steady-state phreatic surface in stability analysis of a wide clay-core embankment dam is an accepted practice even though steady-state phreatic surface may not be expected to develop for a very long time.

For an existing dam, the appropriate elevation can usually be determined from operational records, specifically from reservoir operational plots of reservoir elevation versus time. Reservoir operational plots are available on most dams in the Reclamation inventory. Piezometric data, if available, can be used to estimate the phreatic surface in the embankment.

- *Operational conditions*
 - *Maximum reservoir level.*— If the phreatic surface under flood loading is significantly different (higher) from that of the steady-state condition for the active conservation pool, then the stability under this (higher phreatic surface) condition should be analyzed. A phreatic surface should be estimated for the maximum reservoir level. The maximum reservoir level may occur from a surcharge pool that drains relatively quickly or from a flood control pool that is not to be released for several months. The hydraulic properties (permeability) of materials in the upper part of the embankment affected by the reservoir fluctuations should be evaluated to determine whether a steady-state or transient analysis should be made when estimating the position of the phreatic surface. If the phreatic surface is significantly different (higher) from that of the steady-state condition for the active conservation pool, then the stability under this (higher phreatic surface) condition should be analyzed.
 - *Rapid drawdown conditions.*—During active conservation pool stages, embankments may become saturated by seepage. If, subsequently, the

reservoir pool is drawn down faster than pore water can drain from the soil voids, excess pore water pressure and unbalanced seepage forces result. Typically, rapid drawdown analyses are based on the conservative assumptions that: (1) pore pressure dissipation does not occur during drawdown in impervious material and (2) the phreatic surface on the upstream face coexists with the upstream face of the impervious zone and originates from the top of the inactive capacity water surface.

However, the critical elevation of drawdown with regard to stability of embankment may not coincide with the minimum pool elevation, and thus, intermediate drawdown levels should be considered.

- *Other conditions*
 - *Inoperable internal drainage.*—If uncertainties exist with regard to the success of internal drainage features or dewatering system designed to control the phreatic surface in an existing dam, then checks should be made using the phreatic surface developed assuming these features are not fully functioning.
 - *Unusual drawdown.*—All reservoir drawdown plans for maintenance or emergency release of the reservoir should be reviewed to determine the appropriate parameters for the stability analysis and the need for any modification of the usual phreatic surface assumption on the upstream face. Drought may cause reservoir drawdown and should be considered as such for the stability analysis. Intermediate drawdown levels would, in general, not be required to be examined.
 - *Construction modifications.*—All excavation plans in close vicinity to an existing embankment should be reviewed to determine the appropriate parameters for the stability analysis of the excavation and that of the embankment. Similarly, all dam raise plans should be reviewed to determine appropriate parameters for the stability analysis of the existing and the raised dam configurations including reservoir operations.

4.2.4 Factor of Safety Criteria

For each loading condition described previously, a recommended minimum factor of safety is provided. Deviations either higher or lower from these general criteria may be considered, but should be supported with an appropriate justification. The specific values selected need to consider: (a) the design condition being analyzed and the consequences of failure, (b) estimated reliability of shear strength parameters, pore pressure predictions, and other soil parameters, (c) presence of

Design Standards No. 13: Embankment Dams

structures within the embankment, (d) reliability of field and laboratory investigations, (e) stress-strain compatibility of embankment and foundation materials, (f) probable quality of construction control, (g) embankment height, and (h) judgment based on past experience with earth and rockfill dams.

For the purpose of slope stability analysis, the factor of safety is defined as the ratio of total available shear strength of the soil to shear stress required to maintain equilibrium along a potential surface of sliding. The factor of safety indicates a relative measure of stability for various conditions, but does not precisely indicate actual margin of safety. In addition, a relatively large factor of safety implies relatively low shear stress levels in the embankment or foundation and, hence, relatively small deformations. The minimum factors of safety for use in the design of slope stabilization should follow rationally from an assessment of a number of factors, which include the extent of planned monitoring of pore pressures and assumptions and uncertainties involved in the material strength.

The factor of safety criteria presented in this standard are based on the slope stability analysis being performed by limit equilibrium method using Spencer's procedure. A different procedure within the limit equilibrium method of analysis could give a different factor of safety for the same embankment cross section with the same material properties under the same loading conditions.

For the end-of-construction loading condition, excess pore pressures may be induced in impervious zones of the embankment or foundation because these soils cannot consolidate completely during the construction period. If effective stress shear strength parameters are used for the analysis, then excess pore pressures have an important influence on the factor of safety. A minimum factor of safety of 1.3 would be considered adequate if pore pressures are monitored during construction. However, if the effective stress shear strength envelope is used without any field monitoring of pore pressures, the minimum safety factor should be at least 1.4 to eliminate uncertainties involved in excess pore pressures.

A minimum factor of safety of 1.3 would also be adequate when the analysis is carried out in terms of undrained shear strength. However, if an undrained shear strength envelope is used, the laboratory testing performed to define the envelope must satisfactorily model the pore pressure behavior and state of stress anticipated under field loading conditions.

For the steady-state seepage condition under active conservation pool, a minimum factor of safety of 1.5 would be justified to take into account the uncertainties involved in material strengths, pore pressures in impervious material, and long-term loading. In addition, the failure of the downstream slope under a steady-state seepage condition is more likely to result in a catastrophic release of water, which definitely demands a higher safety margin than for the end-of-construction or rapid drawdown conditions.

For the operational conditions, a factor of safety of 1.2 for assumed steady-state seepage conditions under maximum reservoir water level during a probable maximum flood event would be justified if the duration of high flood pool is relatively short and the reservoir operations call for draining the flood storage quickly using spillway and outlet works facilities at the dam site, and restoring the reservoir to the active conservation pool. A higher factor of safety (approaching 1.5) might be required if the duration of flood storage above the active conservation pool is long and could potentially result in phreatic surface which is significantly higher than the steady-state phreatic surface under the active conservation pool.

For the rapid drawdown condition from active conservation pool (normal water surface) to inactive conservation pool, or other intermediate level, the loading due to unbalanced seepage forces may render the upstream slope unstable; however, the loading is of short duration, and the reservoir level is reduced during drawdown. Consequently, failure of the upstream slope would not likely release the reservoir. Hence, a minimum factor of safety of 1.3 is adequate, and in some cases, a lower factor of safety is acceptable with justification. Similarly, for the rapid drawdown condition from maximum reservoir surface (following a probable maximum flood) to active conservation pool, a factor of safety of 1.2 is adequate considering the short duration of the flood pool surcharge before returning to the normal pool. For the rapid drawdown below the active conservation pool, the minimum factor of safety of 1.3 applies.

For the other loading conditions, a minimum safety factor of 1.2 for drawdown at maximum outlet capacity, inoperable internal drainage, or failure of dewatering system is justified mainly because of infrequent occurrence and reliance on quick remedial action in the event of inoperable drainages and failure of dewatering system. However, if quick remedial action cannot be ensured in advance, higher factor of safety (approaching 1.3 or higher) should be required. For the construction modification, stability of the temporary excavation slopes and the resulting overall embankment stability during construction should have a minimum factor of safety of 1.3 for a conservative combination of ground water conditions and foundation soils during construction. However, all construction activities shall be well planned and executed under close supervision of qualified personnel.

Table 4.2.4-1 summarizes the minimum factors of safety required for various loading conditions.

Design Standards No. 13: Embankment Dams

Table 4.2.4-1. Minimum factors of safety based on two-dimensional limit equilibrium method using Spencer's procedure

Loading condition	Shear strength parameters*	Pore pressure characteristics	Minimum factor of safety
End of construction	Effective	Generation of excess pore pressures in embankment and foundation materials with laboratory determination of pore pressure and monitoring during construction	1.3
		Generation of excess pore pressures in embankment and foundation materials and no field monitoring during construction and no laboratory determination	1.4
		Generation of excess pore pressures in embankment only with or without field monitoring during construction and no laboratory determination	1.3
	Undrained strength		1.3
Steady-state seepage	Effective	Steady-state seepage under active conservation pool	1.5
Operational conditions	Effective or undrained	Steady-state seepage under maximum reservoir level (during a probable maximum flood)	1.2
	Effective or undrained	Rapid drawdown from normal water surface to inactive water surface	1.3
		Rapid drawdown from maximum water surface to active water surface (following a probable maximum flood)	1.2
Other	Effective or undrained	Drawdown at maximum outlet capacity (Inoperable internal drainage; unusual drawdown)	1.2
	Effective or undrained	Construction modifications (applies only to temporary excavation slopes and the resulting overall embankment stability during construction),	1.3

* For selection of shear strength parameters, refer to appendix A.

4.3 Shear Strength of Materials

Stability analyses of embankment dams and natural slopes require determination of shear strengths of materials involved along any potential failure surface. There are large volumes of information available related to the shear strength of soils; however, it is beyond the scope of this design standard to cover the topic in great detail. It is important to recognize that the selection of shear strengths for use in a numerical analysis of a slope (natural or manmade) should be a deliberate effort and involve the entire design team (i.e., designers, laboratory personnel, and geologists). A valuable reference for shear strength as it relates to slope stability is the textbook by Duncan and Wright [5]. The textbook by Lambe and Whitman [6] is a valuable general reference on the subject.

4.3.1 General Criteria

Stability analyses of embankment dams and natural slopes require the determination of shear strengths of the materials involved along any potential failure surface. Based on Mohr-Coulomb failure criterion with effective stress concepts, shear strength “S” (mobilized at failure) can be written as:

$$S = c' + (\sigma - u) \tan \phi'$$

where:

c' = Effective cohesion intercept

ϕ' = Effective angle of shearing resistance

u = Developed pore pressure on failure surface, at failure

σ = Total normal stress on failure surface due to applied load at failure

Based on undrained shear strength concepts, shear strength “ s_u ” can be written as:

$$s_u = f(\sigma_c')$$

which expresses the undrained shear strength as a function of σ_c' , the effective consolidation pressure prior to shear failure.

4.3.2 Shear Strength Data and Sources

Material shear strengths can be obtained from field testing, laboratory testing, or they can be estimated based on experience and judgment, depending on the design stage of the analysis. The analysis and decision regarding how to obtain shear strength parameters should also consider the sensitivity of the final slope stability on the strength parameters. For example, stability analysis may prove to be insensitive to small features such as gravel toe drains. Varying the strength value

Design Standards No. 13: Embankment Dams

of the drain material may not have a large impact on the computed stability, and it may therefore be prudent to use typical values in such a case.

For existing dams in Reclamation's inventory, project related earth material (EM) reports from Reclamation Materials Engineering and Research Laboratory provide site-specific soil strength data. However, caution should be exercised in using these past test data if the in situ stress conditions do not match with the stress conditions that were used in the laboratory tests. Guidance from experienced design staff should be solicited in deciding appropriateness of past test data.

In general, values for shear strength parameters to be used in appraisal or feasibility level design can be estimated based on judgment, previous experience and testing, local geologic data, or from tabulated data such as that included in appendix D from references [2] and [7]. For intermediate and final phases of design, shear strength parameters should be obtained from appropriate laboratory and field tests.

For fat clays, cyclic wetting and drying can reduce their shear strength to a fully softened state. Furthermore, if prior shear deformations have occurred in the foundation materials or material stress-strain behavior is strain softening, the shear strength of the clay may be at its residual strength value. Consolidated undrained (CU) tests with pore pressure measurements are used to measure fully softened strengths. Torsional ring shear and repeated direct shear tests are performed to determine residual shear strengths of clays in foundations, and natural and constructed slopes.

In situ shear strength testing can be performed in the field on foundation materials or embankment materials. Field testing methods include standard penetration test, vane shear test, cone penetration tests, and borehole shear device test. In situ tests are often used to estimate undrained shear strength parameters. References [8, 9] include details of in situ testing.

Laboratory shear strength testing is performed on disturbed or undisturbed samples of foundation and embankment materials to obtain shear strength parameters to be used in stability analyses. Appropriate laboratory shear strength tests include direct shear, repeated direct shear, triaxial shear, torsional ring shear, and simple shear tests. Shear strength tests should be supplemented with one-dimensional consolidation (oedometer) tests in order to ascertain the stress history of the material, particularly when determining undrained shear strength. Refer to appendix A for selection of proper laboratory tests that are compatible with field loading conditions. Reference [8] includes details of laboratory testing. Use of modern (state-of-the-art) sampling and testing equipment and procedures is advised.

Determination of the shear strength parameters is the most important phase of a stability analysis, yet the most difficult, especially for undrained strengths. It is difficult to obtain representative samples, avoid sample disturbance, simulate external loading and internal pore pressure conditions, and avoid inherent error in the testing methods. It is normally impossible to obtain samples that truly represent the range of materials existing in the field. Therefore, shear strength parameters are generally determined from samples representing extremes, and parameters are selected within the range. Loads and stresses on a sample in the laboratory are different from those on an element of soil located on a failure surface in the ground. Hence, judgment and experience play an extremely important role in the evaluation of test results to ensure that the parameters chosen are representative of the materials in place.

As a general rule, for significant projects, shear strength parameters should be obtained from appropriate laboratory and field tests. Regardless of the source of shear strength data (laboratory tests, field tests, published data), sensitivity analyses by varying the selected strength parameter values should always be performed to ensure safe design. Results of slope stability analyses, including sensitivity analyses, should be discussed with the experienced staff, and their concurrence with the design should be solicited.

4.3.3 Shear Strength Related to Loading Condition

The following loading conditions are usually evaluated for stability analysis of embankment dams: (1) end of construction, (2) steady-state seepage, and (3) rapid drawdown. The material shear strength parameters used in the analyses must correctly reflect the behavior of the material under each loading condition.

- End-of-construction loading can be analyzed by using either the undrained shear strength envelope or the effective stress strength envelope concept.
 - *Undrained shear strength.*—Applicable shear strength parameters of saturated fine-grained foundation soils can be determined from unconsolidated undrained (UU) triaxial shear tests without pore pressure measurements conducted on undisturbed samples. Undisturbed samples should be selected and tested from a range of depths in the foundation material. Field vane tests, if used, should also be conducted over a range of depths. Test specimens representing embankment materials should be compacted to anticipated placement densities and moisture contents and tested in UU triaxial compression. The confining pressures used in these tests shall correspond to the range of normal stresses expected in the field. Generally, the undrained shear strength envelopes are parallel to the normal stress axis for fully saturated fine-grained soils, but for partially saturated soils, envelopes have a curved portion in the low

Design Standards No. 13: Embankment Dams

normal stress range. This curved portion, or an approximation of it, should be used when the anticipated normal embankment stresses are in that range. UU triaxial shear test results approximate end-of-construction shear strengths of embankment zones consisting of impervious soils. These tests, performed on undisturbed samples, are also applicable to impervious foundation materials where the consolidation rate is slow compared to the fill placement rate.

- *Effective stress.*—Effective stress shear strength parameters are used in conjunction with the estimated embankment and foundation pore pressures generated by placement of the embankment materials. CU triaxial shear tests with pore pressure measurements are appropriate for clays and silts which, because of their low permeabilities, can be assumed to fail under undrained conditions. Consolidated drained (CD) triaxial shear tests or direct shear tests may be used for free-draining foundation and embankment materials. Shear strength of overconsolidated clay and clay-shale foundation materials could be obtained by using CU triaxial shear tests. If these clays have undergone prior shear deformation or the stress-strain behavior is strain softening, the residual strength may be appropriate and repeated direct shear or torsional ring shear tests should be used. When thixotropy is a possibility, shear strength parameters higher than residual may be considered.
- Steady-state seepage loading condition should be analyzed using effective stress shear strength parameters in conjunction with measured or estimated embankment and foundation pore pressures. The use of the CD triaxial shear test or the CU triaxial shear test with pore pressure measurements is appropriate. Sufficient back pressures should be used to effect nearly 100-percent saturation for both compacted samples of embankment materials and undisturbed foundation samples to ensure accurate pore pressure measurements. The use of the direct shear test is applicable for sands. It can also be used for silts and clays; however, the required rate of shearing would be very slow; therefore, it may not be practical. If prior shear deformation has occurred in the foundation materials or material stress-strain behavior is strain softening, residual strengths may be appropriate for these materials. If foundation materials consist of very soft clays, undrained shear strength of these materials should be determined as discussed above under the heading: *Undrained shear strength.*
- Rapid drawdown loading condition can be analyzed using effective stress shear strength parameters in conjunction with embankment and foundation pore pressures or using undrained shear strength developed as a result of consolidation stresses prior to drawdown. The CU triaxial shear test with pore pressure measurements is recommended for impervious and semipervious soils because such tests will provide both effective stress

shear strength parameters as well as undrained strength as a function of consolidation stress. Sufficient back pressures should be used to effect nearly 100-percent saturation to ensure accurate pore pressure measurements. CD triaxial shear test or direct shear test can be used if the material is highly permeable ($> 10^{-4}$ cm/s).

For testing of overconsolidated clay shales, considerations must be given to the geology of the damsite, the existence of bedding planes, and past shear deformations. CU triaxial shear tests with pore pressure measurements, CD triaxial shear tests, or direct shear tests may be used for these materials. Where potential failure surfaces follow existing shear planes, residual shear strengths from repeated direct shear tests or torsional ring shear tests are appropriate.

Shear strengths to be used for undrained strength analysis shall be based on the minimum of the combined CD and CU shear strength envelopes of embankment and foundation materials. Effective stresses used to determine the available undrained shear strength shall be the consolidation stresses developed prior to drawdown. The stability of upstream slopes needs to be analyzed for this loading condition.

4.3.4 Anisotropic Shear Strength

The undrained strength of clays varies with the orientation of the principal stress at failure and with the orientation of the failure plane. UU tests on vertical, inclined, and horizontal specimens provide the data to determine variation of undrained strength with direction of compression. Typically, the anisotropic shear strength is expressed by the variation in S_u with orientation of the failure plane [5].

4.3.5 Residual Shear Strength

Residual shear strength of clays may be determined by testing remolded soil samples via repeated direct shear test or ring shear test. However, because the testing procedures for repeated direct shear are still being standardized, professional guidance should be solicited when conducting these tests.

4.4 Determination of Pore Pressures

4.4.1 Phreatic Surface Method

Pore water pressures for steady-state seepage loading conditions can be estimated as hydrostatic pressures below the steady-state phreatic surface without introducing significant error. The steady-state phreatic surface can be estimated following established procedures developed by Casagrande [10], Pavlovsky [11], Cedergren [12], or others. In general, pore water pressures estimated from the phreatic surface method are conservative for zoned embankments; however, this method may underestimate the values for some special loading conditions such as infiltration of precipitation, artesian pressures in foundation, etc. Other methods of evaluating pore pressures should be used in such cases. It is acceptable to have multiple phreatic surfaces in a zoned embankment, one for each of the zones in the embankment and its foundation.

The phreatic surface method can also be used for determining pore pressures under rapid drawdown conditions. The phreatic surface from the steady seepage condition is modified in accordance with the following conservative assumptions: (1) pore pressure dissipation as a result of drainage does not occur during drawdown in impervious materials and (2) the water surface is lowered instantaneously from the top of active conservation water surface to the top of inactive conservation capacity water surface. The phreatic surface may be assumed to follow the upstream surface of the embankment. For embankments with semipervious shell materials, partial dissipation of pore pressures may be assumed in the shell material.

The phreatic surface method is not appropriate for determining pore pressures under end of construction or during construction loading conditions.

4.4.2 Graphical Flow Net Method

Under steady-state seepage conditions, flow net methods of analysis are used on transformed sections of the embankment and foundation to determine pore pressures. The values of horizontal to vertical permeability ratios depend on the method of compaction of embankment materials and/or geologic history of the foundation materials.

4.4.3 Numerical Methods

Numerical methods for determining pore pressures are excellent tools for rapid drawdown and steady-state seepage loading conditions for complex geometric

conditions and are the only way to compute pore pressures in three-dimensional space. However, the added degree of sophistication is not necessary in most cases. Finite element, finite difference, and boundary element are some of the well-known numerical methods that are used to determine pore pressures.

For estimating pore water pressure during rapid drawdown, numerical procedures that reflect the influence of dilatancy on the pore water pressure changes are based on stress changes during drawdown. These procedures are described in reference [5].

Permeabilities of all materials in the embankment and foundation must be known in order to get an accurate estimate of pressures and flow.

If necessary, numerical methods should be considered in the final phase of design.

All of the preceding methods are described in detail in Chapter 8, Seepage, of this design standard.

4.4.4 Field Measurement (Instrumentation) Method

The development of pore pressures during construction in either the foundation or in the embankment depends upon the soil properties and the amount of consolidation occurring during construction. Pore pressure observations made during construction should be compared with the predicted magnitudes of pore pressures for effective stress analysis to ensure that the actual pore pressures do not rise to a level that will cause instability. Pore pressure instrumentation (piezometers) to be used for observation during construction should be “no flow devices.”

If it is necessary to confirm stability of the dam during construction, the embankment and foundation should be adequately instrumented to monitor movement and pore pressures at critical sections corresponding to the stability analyses.

Pore pressures obtained from piezometers can be used directly for stability analyses of slopes of the embankment or natural slopes under steady-state or rapid drawdown conditions. Alternately, piezometer data can be converted into phreatic surface(s) in the embankment and foundation materials and used as such in stability calculations.

4.4.5 Hilf's Method

A detailed procedure for predicting a total stress versus pore water pressure curve from the results of a few laboratory consolidation tests and a large number of field

percolation-settlement tests is given by Hilf [3]. The procedure can be adapted to estimate pore water pressures during construction stages.

4.5 Slope Stability Analyses

4.5.1 Method of Analysis

Reclamation's preferred method of stability analysis of earth and rockfill embankments is limit equilibrium based on Spencer's procedure [13]. The procedure: (1) assumes the resultant side forces acting on each slice are parallel to each other, (2) satisfies complete statics, and (3) is adapted for calculating factor of safety and side-force inclination for circular and noncircular shear surface geometries. To facilitate stability analysis of embankments, Spencer's procedure is implemented in computer programs. Use of a particular computer program may be adopted with approval from appropriate line supervisors and managers. Additional comments on computer programs are included in appendix C.

For cohesionless materials ($c = 0$), the infinite slope method can be used to estimate the stability of the slope of an embankment [5].

Continuum mechanics based finite element or finite difference analysis, which satisfies static equilibrium and is capable of including stress changes due to varied elastic properties, heterogeneity of soil masses, and geometric shapes can be used to analyze stability of slopes at the discretion of the designer. Limit equilibrium based analysis, which uses Spencer's procedure, should also be conducted for comparison of results.

Sample calculations for stability analyses using Spencer's procedure are included in appendix B. References [5, 14] include useful information on slope stability calculations.

4.5.2 Slip Surface Configuration

There are two common slip surface configurations used for stability analysis. The circular arc slip surface is more applicable for analyzing essentially homogeneous or zoned embankments founded on thick deposits of fine-grained materials.

Noncircular slip surfaces, described by linear segments, are generally more applicable for zoned embankments on foundations containing one or several horizontal or nearly horizontal weak layers.

The slip surface resulting from an automatic search should only be regarded as a first approximation of the critical surface. For accurate results, several automatic

searches should be used, each with a different starting point. Selection of potential slip surface configuration requires experienced judgment in selecting the critical surface considering the stratigraphic conditions and structure of the slope.

4.5.3 Slip Surface Location

The location of critical slip surfaces should be related to the location of relatively weaker materials and zones of high pore pressure. The designer should evaluate the overall stability of the sliding mass and determine the location of slip surfaces with minimum factors of safety. In general, the following slip surfaces should be examined:

- Slip surfaces that may pass through either the fill material alone or through the fill and the foundation materials and which do not necessarily involve the crest of the dam.
- Slip surfaces that may pass through either the fill material alone or through the fill and the foundation materials and which include the crest of the dam.
- Slip surfaces which pass through major zones of the fill and the foundation.
- Slip surfaces that involve only the outer portion of the upstream or downstream slope. In this case, the infinite slope analysis may be appropriate for cohesionless materials.

The stability of downstream slopes should be analyzed for steady-state seepage loading condition. The stability of upstream slopes is generally not critical for steady-state seepage loading condition; however, stability of upstream slope for certain configurations of embankment zoning and foundation conditions (e.g., upstream sloping core, a downstream cutoff trench, and weak upstream foundation material that was not removed) should be analyzed.

4.5.4 Progressive Failure

Some common conditions that can lead to progressive failure are described in the following along with some possible solutions. There may be other modes of progressive failure [5, 15].

- Because of nonuniform stress distributions on potential failure surfaces, relatively large strains may develop in some areas and peak shear strengths may be reached progressively from area to area so that the total shear resistance will be less than if the peak shear strength was mobilized simultaneously along the entire failure surface. Where the stress-strain

Design Standards No. 13: Embankment Dams

curve for a soil exhibits a significant drop in shear stress after peak shear stresses are reached (strain softening stress-strain behavior), the possibility of progressive failure is increased, and the use of peak shear strengths in stability analyses would be unconservative. Possible solutions are to: (1) increase the required safety factor and use peak shear strengths or (2) use shear strengths that are less than peak shear strengths and use the typical required factors of safety. In certain soils or shale bedrock materials, it may even be necessary to use fully softened or residual shear strengths.

- Where embankments are constructed on foundations consisting of brittle, sensitive, highly plastic, or heavily overconsolidated clays or clay shales having stress-strain characteristics significantly different from those of the embankment materials, consideration should be given to: (1) increasing the required safety factor over the minimums required in table 4.2.4-1, (2) using shear strengths for the embankment materials at strains comparable to those in the foundation, or (3) using appropriate softened or residual shear strengths of the foundation soils.
- Progressive failure may also start along tension cracks resulting from longitudinal or transverse differential settlements occurring during or subsequent to construction or from shrinkage caused by drying. The maximum depth of cracking, assuming an infinite slope, can be estimated from the equation $(2c/\gamma) \tan (45 + \phi/2)$ with the limitation that the maximum depth assumed does not exceed 0.5 times the slope height. Shear resistance along the crack should be ignored, and the possibility that the crack will be filled with water should be considered in all stability analyses for embankments where this condition is possible.

4.5.5 Three-Dimensional Effect

Three-dimensional effect should be considered for the stability of upstream and downstream slopes of (i) embankments in narrow canyons, and (ii) the abutment-embankment contact area (groin). For a localized low strength material in the foundation, stress distribution in the longitudinal direction of the embankment and the resulting stability of the slope should be considered. Continuum mechanics based finite element or finite difference analysis of the embankment is recommended for evaluation of the three-dimensional effect. Limit equilibrium based analysis provides an alternative means to account for three-dimensional geometry (of shear surface) effects on factor of safety results.

Reference [16] should be consulted for creating a three-dimensional numerical model. Reference [17] includes useful information on the appropriate boundary conditions for three-dimensional numerical models.

4.5.6 Verification of Analysis

A designer must verify to his/her own satisfaction that his/her stability analysis is correct. The method of verification will depend on the designer's knowledge and experience. A designer that has a great deal of experience may be able to judge whether the factor of safety from a computer program appears reasonable, while a less experienced engineer may need a more detailed check, such as a hand solution for the critical surfaces.

As a minimum, any engineer doing a stability analysis should research the program that he is using so that he understands the assumptions, theory, methodology, and weaknesses inherent in that program. The engineer should have a good working knowledge of soil mechanics so that he/she can make intelligent selections of shear strength parameters and other properties used as input to the program. The engineer should double check all input data (material strengths, weights, pore pressures, and geometry) and in addition, ensure that input data are independently checked. The engineer should evaluate output from the computer program (computed stresses, forces, pore water pressures, and weights) to ensure that it is reasonable and not blindly accept the validity of factors of safety from the program.

There is a range of methods to check a stability program, such as calculating a solution by the same or different methods on the critical surface by hand or by using a different computer program; using computed stresses, forces, and weights from the output of the program to evaluate equilibrium condition of each slice; or using judgment based on comparing factors of safety and output to past experience. The ultimate goal being that the designer must verify the results of the analysis in a manner that ensures accuracy and with which he/she can submit the analysis to review with confidence.

Guidance on printed outputs from computer programs used for stability analyses is illustrated using sample problems included in appendix B. The printed output should have sufficient details to allow for an independent check and peer review of the stability analyses performed without re-doing the analyses. All input data should be checked for each slice. Pore-water pressure should be carefully assessed, especially when multiple phreatic surfaces are used to define pore-water pressures in different zones, or discrete pore water pressures data from field measurements are used. For a solution to be valid, the following characteristics should be met: (i) the interslice forces should be compressive; (ii) the interslice forces (thrust line) should be in the slide mass, preferably in the middle third; (iii) the interslice force inclination should be within reasonable bounds; and (iv) the normal forces on the base of slices should be compressive. Appropriate user's manual(s) of the computer program should be consulted for additional guidance to verify that the solution is reasonable.

4.5.7 Existing Dams

Slope stability analysis of an existing dam becomes necessary if the dam is to be raised to increase flood storage or to increase permanent storage of the reservoir. If an existing dam experiences slope failure (e.g., B.F. Sisk Dam in California, figures 4.5.7-1 and 4.5.7-2), slope stability analysis becomes an important part of investigations to understand the cause(s) of the failure and to design remedial measures. Other situations in which slope stability analysis of an existing dam may be necessary include: addition of stability berm to improve performance of the dam during a seismic event (e.g., Pineview Dam in Utah, figures 4.5.7-3 and 4.5.7-4) or if the observed performance of a dam, in some other manner, indicates signs of distress in the dam. In general, for a satisfactorily functioning dam with no performance-based deficiency needing remediation, slope stability analysis is not a required activity [18].

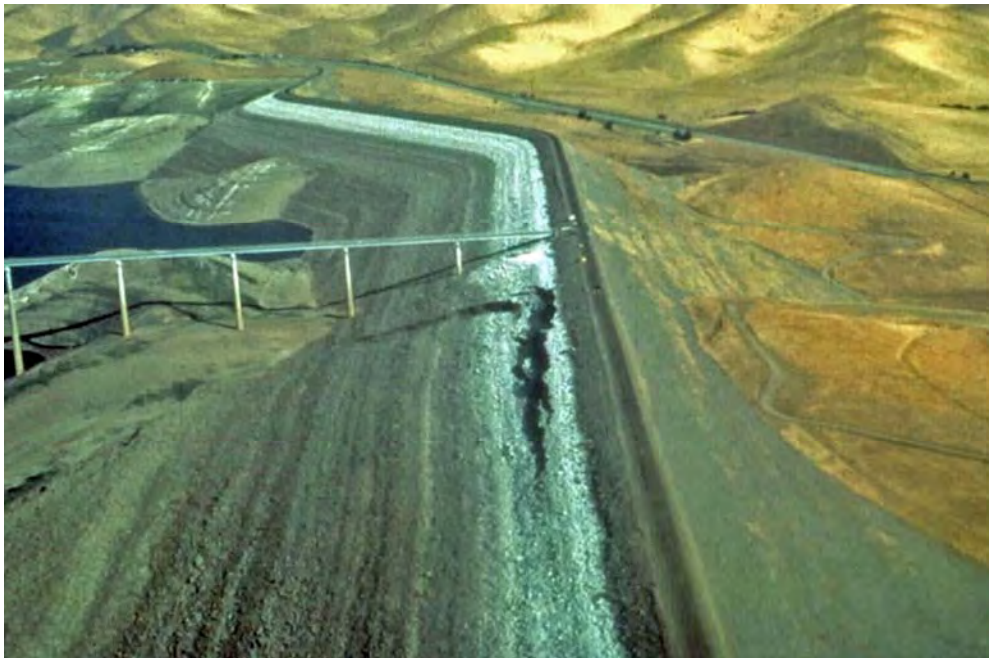


Figure 4.5.7-1. B.F. Sisk Dam (near Los Banos, California). View showing upstream slope failure during reservoir drawdown.

Design Standards No. 13: Embankment Dams

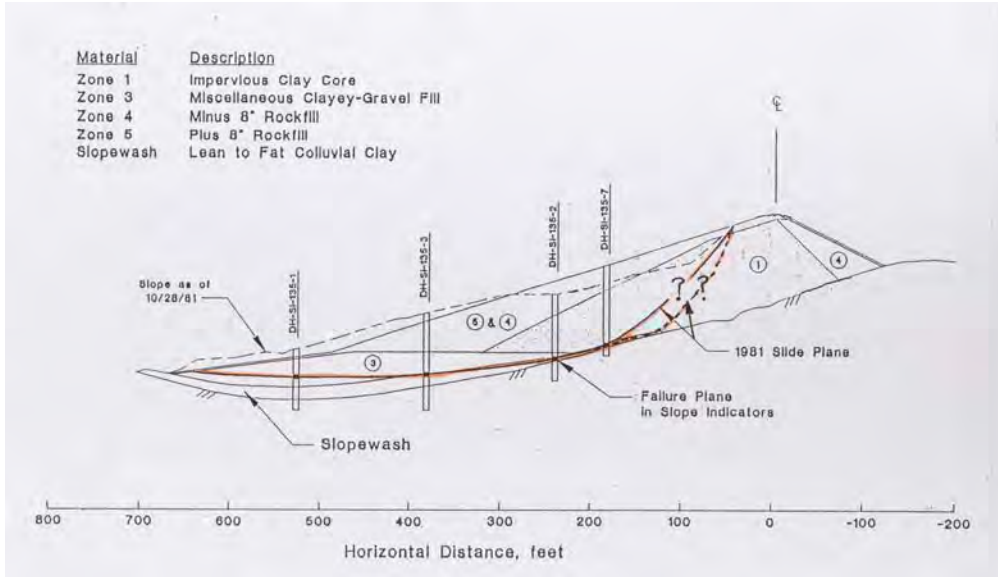


Figure 4.5.7-2. General cross section of B.F. Sisk Dam in the location of the slide during reservoir drawdown.



Figure 4.5.7-3. Pineview Dam (near Ogden, Utah). View showing stability berm to improve performance of the dam during a seismic event.

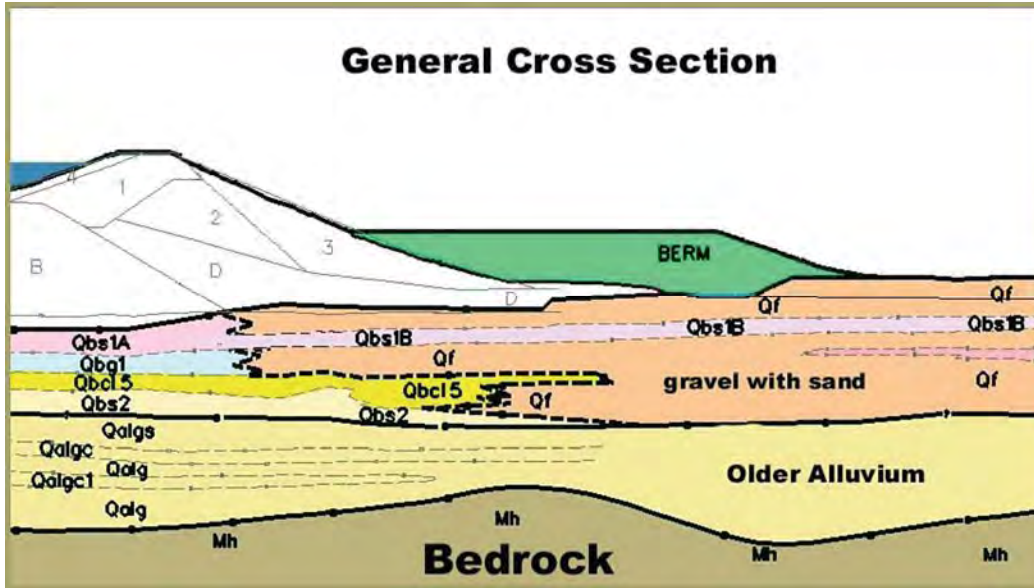


Figure 4.5.7-4. General cross section of Pineview Dam with stability berm.

4.5.8 Excavation Slopes

Excavation slope instability may result from: (i) failure to control seepage forces in and at the toe of the slope, (ii) too steep slopes for the shear strength of the materials being excavated, and (iii) insufficient shear strength of subgrade soils. Slope instability may occur suddenly, as the slope is being excavated, or after the slope has been standing for some time. Slope stability analyses are useful in sands, silts, and normally consolidated and overconsolidated clays. Care must be taken to select appropriate shear strength parameters. For excavation slopes in heavily overconsolidated clays, use of fully softened shear strength is considered appropriate. For cohesionless soils, failure surfaces are shallow and have circular configuration; for clays, the slip surfaces are wedge shaped and may be deep seated.

4.5.9 Back Analysis

When a slope fails by sliding, it can be used to gain insight into the conditions in the slope at the time of the failure by performing numerical model analyses of the site. The factor of safety at failure is taken to be 1.0. Following a significant slope failure, field and laboratory investigations are generally carried out. These investigations can provide some data for the numerical model (e.g., location and extent of the shear failure, unit weights of soils, ground water and pore water pressure). In numerical models, these data can be used to back-calculate shear strengths for the factor of safety to be 1.0. Depending on the extent of the field and laboratory investigations, and accuracy of the numerical models and methods of analysis, back-calculated shear strengths may provide useful information for

design of remedial measures. However, much experience and judgment are needed in numerical analyses and in assessing the results of numerical models. Reference [5] should be consulted as it has useful information on back analyses based on case studies of slope failures.

4.5.10 Multi-Stage Stability Analysis for Rapid Drawdown

During rapid drawdown, the stabilizing effect of the water on the upstream face of embankment is lost, but the pore-water pressures within the embankment may remain high. As a result, the stability of the upstream face of the dam can be much reduced. The dissipation of pore-water pressure in the embankment is largely influenced by the permeability and the storage characteristic of the embankment materials. Highly permeable materials drain quickly during rapid drawdown, but low permeability materials take a long time to drain.

For high permeability soils, an effective stress stability analysis using the initial and final steady-state phreatic surfaces and the associated reservoir loading is appropriate.

For low permeability soils, a multi-stage stability analysis which uses a combination of effective strength results and total strength (CU) results to estimate a worst-case scenario should be considered.

Two-stage stability computations consist of two complete sets of stability calculations for each trial shear surface: the first set is to calculate effective normal and the shear stresses along the shear surface for the pre-drawdown steady-state phreatic surface and full reservoir loading conditions; the second set is to calculate factor of safety for undrained loading due to sudden drawdown.

Three-stage stability computations consist of three complete sets of stability calculations for each trial shear surface the first two sets are the same as in two-stage stability computations. A third set of computations is performed if the undrained shear strength employed in the second stage computations for some of the slices is greater than the shear strength that would exist if the soil were drained.

Reference [5, 19] should be consulted for proper use of the multi-stage stability analysis for rapid drawdown.

4.6 References

- [1] Bureau of Reclamation, Technical Service Center Operating Guidelines, Denver, Colorado, 2005.
- [2] Bureau of Reclamation, *Design of Small Dams*, Denver, Colorado, 2004. (Table 5-1, Average engineering properties of compacted soils from the Western United States, is included in appendix D.)
- [3] Hilf, J.W., “Estimating Construction Pore Pressures in Rolled Earth Dams,” *Proceedings of the Second International Conference on Soil Mechanics and Foundation Engineering*, Rotterdam, pp. 234-240, 1948.
- [4] Lee, K.N., and Haley, S.C., “Strength of Compacted Clay at High Pressure,” *Journal of Soil Mechanics and Foundation Engineering*, pp. 1303-1332, 1968.
- [5] Duncan, J.M., and S.G. Wright, *Soil Strength and Slope Stability*, John Wiley and Sons, New Jersey, 2005.
- [6] Lambe, W.T., and R.V. Whitman, *Soil Mechanics*, John Wiley and Sons, New York, 1969.
- [7] Duncan, J.M., P. Byrne, K.S. Wong, and P. Mabry, “Strength, Stress-Strain and Bulk Modulus Parameters for Finite Element Analyses of Stresses and Movements in Soil Masses,” Report No. UCB/GT/80-01, University of California, Berkeley, California, 1980. (Tables 5 and 6 of this report are included in Appendix D.)
- [8] Bureau of Reclamation, *Earth Manual*, Denver, Colorado, 1998.
- [9] Clayton, C.R.I., M.C. Matthews, and N.E. Simons, *Site Investigation*, Blackwell Science, Cambridge, Massachusetts, 1995.
- [10] Casagrande, A., *Seepage Through Dams*, Contributions to Soil Mechanics, 1925-1940, Boston Society of Civil Engineers, Boston, Massachusetts, pp. 295-336, 1940.
- [11] Karpoff, K.P., *Pavlosky’s Theory of Phreatic Line and Slope Stability*, American Society of Civil Engineers, separate No. 386, New York, 1954.
- [12] Cedergren, H., *Seepage, Drainage, and Flow Nets*, John Wiley and Sons, Inc., New York, 1977.
- [13] Spencer, E., “Thrust Line Criterion in Embankment Stability Analysis,” *Geotechnique*, Vol. 23, No. 1, 1973.

- [14] Chugh, A.K., and J.D. Smart, "Suggestions for Slope Stability Calculations," *Computers and Structures*, Vol. 14, No. 1-2, pp. 43-50, 1981. (Copy of the paper is included in Appendix D.)
- [15] Chugh, A.K., "Variable Factor of Safety in Slope Stability Analysis," *Geotechnique*, Vol. 36, No. 1, 1986. (Copy of the paper is included in Appendix D.)
- [16] Chugh, A.K., and T.D. Stark, "An Automated Procedure for 3-Dimensional Mesh Generation," *Proceedings of the 3rd International Symposium on FALC and Numerical Modeling in Geomechanics*, Sudbury, Ontario, pp. 9-15, 2003. (Copy of the paper is included in Appendix D.)
- [17] Chugh, A.K., "On the Boundary Conditions in Slope Stability Analysis," *International Journal for Numerical and Analytical Methods in Geomechanics*, Vol. 27, pp. 905-926, 2003. (Copy of the paper is included in Appendix D.)
- [18] Peck, R.B., "The Place of Stability Calculations in Evaluating the Safety of Existing Embankment Dams," Civil Engineering Practice, *Journal of the Boston Society of Civil Engineers*, Boston, Massachusetts, Fall 1988, pp. 67-80. (Copy of the paper is included in Appendix D.)
- [19] Edris, E.V., Jr., and S.G. Wright, *User's Guide: UTEXAS3 Slope Stability Package, Vol. IV, User's Manual*, Instruction Report GL-87-1, Geotechnical Laboratory, Department of the Army, Waterways Experiment Station, U.S. Army Corps of Engineers, Vicksburg, Mississippi, 1992.
- [20] Germaine, J.T., and C.C. Ladd, "State-of-the-Art-Paper: Triaxial Testing of Saturated Soils," Advanced Triaxial Testing of Soil and Rock, ASTM STP 977, Donaghe, R.T., Chaney, R.C., and Silver, M.L., Eds., American Society for Testing and Materials, Philadelphia, Pennsylvania, 1988, pp. 421-459.
- [21] Abramson, L.W., T.S. Lee, S. Sharma, and G.M. Boyce, *Slope Stability and Stabilization Methods*, John Wiley and Sons, New Jersey, 2002.
- [22] Chugh, A.K., "User Information Manual, Slope Stability Analysis Program; SSTAB2 (A modified version of SSTAB1 by Wright, S.G.)," Bureau of Reclamation, Denver, Colorado, February 1992.
- [23] Johnson, S. J., "Analysis and Design Relating to Embankments; A State-of-the-Art Review," U.S. Army Engineer Waterways Experiment Station, Vicksburg, Mississippi, February 1975.

Design Standards No. 13: Embankment Dams

- [24] Wright, S.G., “SSTAB1 -A General Computer Program for Slope Stability Analyses,” Department of Civil Engineering, University of Texas at Austin, Texas, August 1974.
- [25] Edris, E.V., Jr., and S.G. Wright, *User’s Guide: UTEXAS2 Slope Stability Package, Vol. 1, User’s Manual*, Instruction Report GL-87-1, Geotechnical Laboratory, Department of the Army, Waterways Experiment Station, U.S. Army Corps of Engineers, Vicksburg, Mississippi, 1987.
- [26] Geo-Slope International, “Slope/W Slope Stability Analysis,” Geo-Slope International, 2007.
- [27] Itasca Consulting Group, Inc., *FLAC – Fast Lagrangian Analysis of Continua*, Minneapolis, Minnesota, 2006.
- [28] O. Hungr Geotechnical Research Inc., *CLARA-W – Slope Stability Analysis in Two or Three Dimensions for Microcomputers*, West Vancouver, British Columbia, 2010.
- [29] Itasca Consulting Group Inc., *FLAC3D – Fast Lagrangian Analysis of Continua in 3 Dimensions*, Minneapolis, Minnesota, 2002.

Appendix A

Selection of Shear Strength Parameters

Type of Test: Unconsolidated-Undrained (UU) Triaxial Compression test

Loading conditions and Mohr-Coulomb envelope are shown on figure A-1.

Use in Stability Analysis: Unconsolidated-undrained tests approximate the end-of-construction behavior of impervious embankment zones in which rate of consolidation is slow compared to rate of fill placement. Confining pressures used in the tests should encompass the range in total normal stresses which will act along potential failure surfaces through such impervious embankment zones. The UU strength is highly dependent on both compacted dry density and molding water content. Laboratory samples should be compacted to the dry density specified for the impervious embankment zones at water contents wet and dry of optimum within the range of compaction water content to be permitted in the specifications. Because the UU strength is dependent on dry density, it is desirable to obtain samples for testing by trimming cylindrical test samples from a specimen compacted in a Proctor mold. Figure A-2 shows the recommended procedure for a compaction test.

Remarks: Foundation materials which are stiff and fissured may fail under drained conditions (i.e., shear-induced pore pressure equal to zero) even though they are fine grained and subjected to short-term loading such as end-of-construction. Therefore, for these materials, an effective stress analysis assuming zero shear-induced pore pressures is more conservative and should be used instead of an analysis using UU results.

In general, and particularly for foundation materials, CU testing is preferred over UU testing because of the effects of sample disturbance and of high rate of strain in UU testing. These effects tend to offset each other, but not in a predictable way. Reference [20] should be consulted for a more detailed discussion on the relative merits of these two tests.

Design Standards No. 13: Embankment Dams

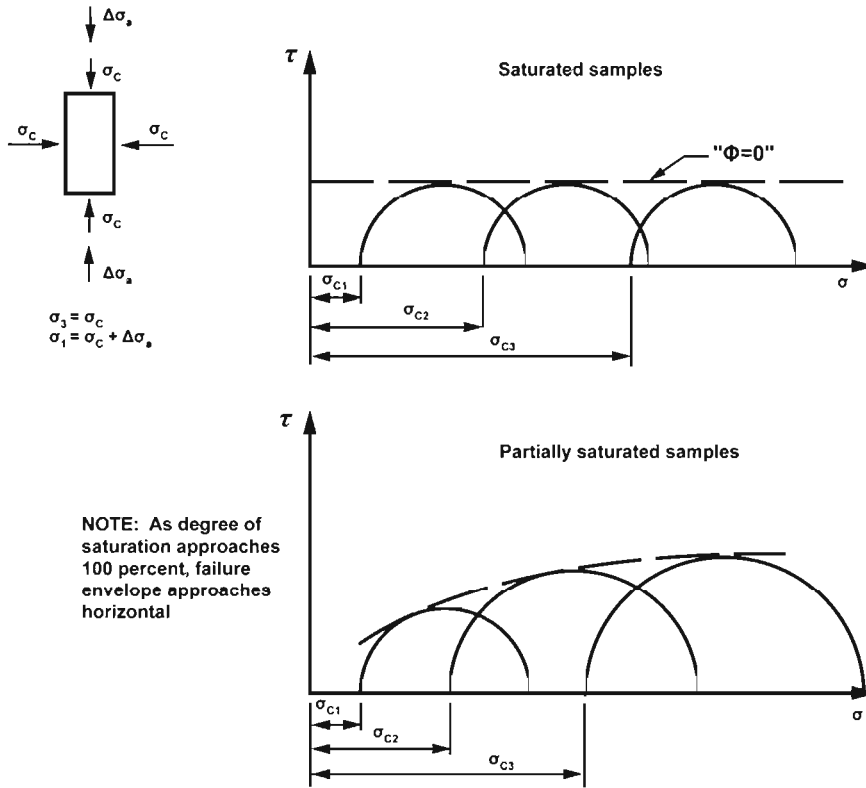


Figure A-1. Unconsolidated-Undrained (UU) triaxial compression test.

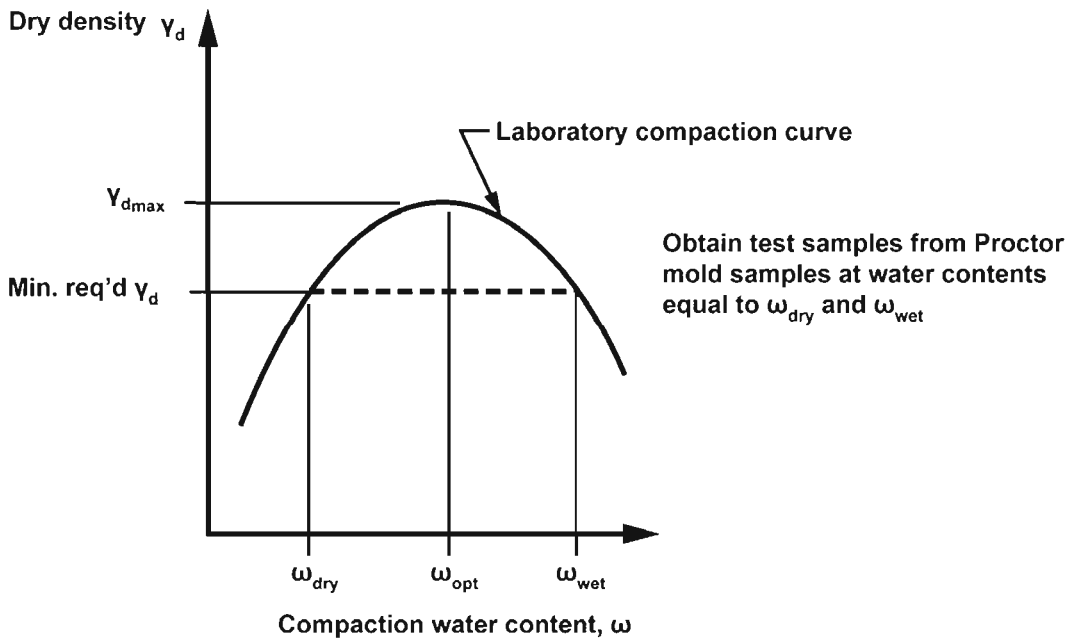


Figure A-2. Compaction test.

Type of Test: Consolidated-Undrained (CU) Triaxial Shear with pore pressure measurements test

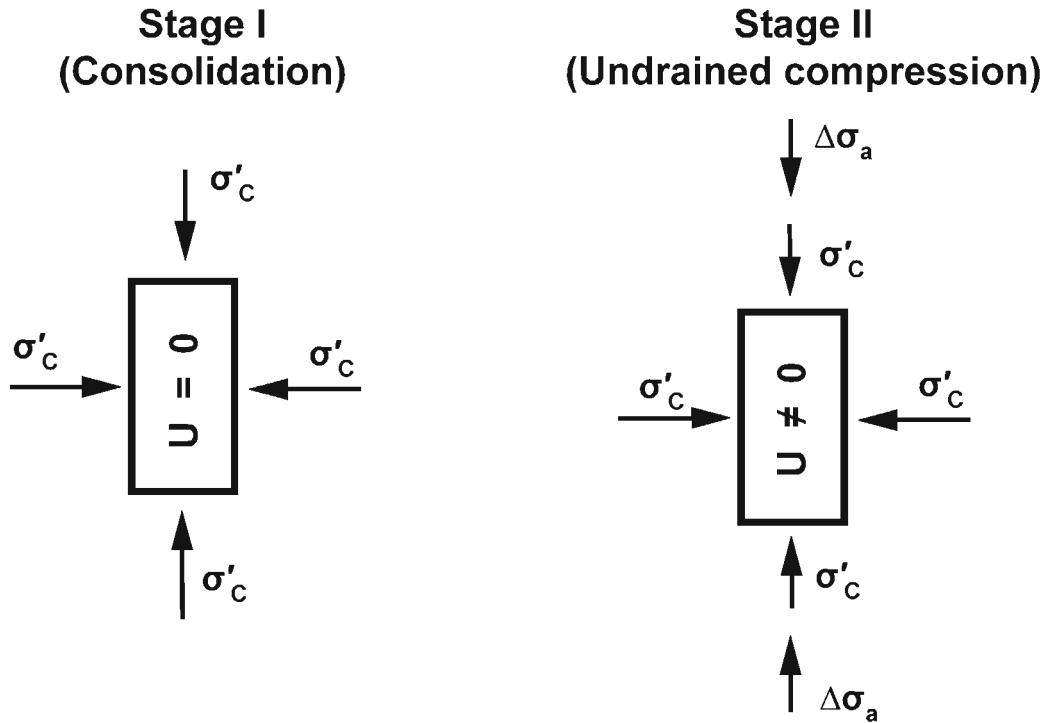
Loading condition and Mohr-Coulomb envelope are shown on figures A-3 and A-4.

Use in Stability Analysis: Consolidated undrained triaxial tests with pore pressure measurements have two primary uses in stability analyses: (1) they furnish effective stress shear strength parameters, ϕ' and c' , for use in analyses for steady-state seepage or other loading conditions where shear-induced pore pressures can be taken as zero (e.g., pervious zones in rapid drawdown or end-of-construction), and (2) they furnish undrained shear strengths as a function of effective consolidation pressure for saturated materials, for use in analyses for end-of-construction condition, or for analyses related to rapid drawdown conditions. As discussed in the main text, rapid drawdown analyses should use shear strengths obtained from a composite of the effective stress and undrained strength envelopes. The normal stress used to select the shear strength from the composite envelope should be the effective consolidation stress acting on the base of a **slice** prior to drawdown; refer to figure A-5 (i.e., the total normal stress minus the pore pressure taken from the steady-state flow net corresponding to pool level before drawdown).

Consolidation pressures used in the CU tests should encompass the range in effective normal stresses which will act along potential failure surfaces prior to drawdown. Because the undrained shear strength derived from the CU tests is highly dependent on both compacted dry density and molding water content, samples should be prepared as discussed for UU tests.

CU triaxial tests can be performed in compression or extension. The loading condition should be based on the expected state of stress at failure. Also, attention should be paid to choosing the consolidation conditions used. Modern computer automation and control allow for anisotropic or K_o consolidation to be employed in triaxial tests. Isotropic consolidation can lead to unconservative strength parameters if the in situ state of stress is anisotropic [20].

Remarks: Because derivation of the effective stress shear strength parameters from the CU tests depends on the accurate measurement of shear-induced pore pressures, samples must be pressure saturated to ensure 100-percent saturation. Complete saturation can be verified by applying an increment of all-around pressure with the drainage line to the sample closed, measuring the pore pressure induced in the sample, and computing the B coefficient (observed pore pressure divided by increment of all-around pressure). The B coefficient should be at least 0.95 before conducting the axial loading stage of the test.



At failure:

Total stresses

$$\sigma_3 = \sigma'_c$$

$$\sigma_1 = \sigma'_c + \Delta\sigma_a$$

Effective stresses

$$\sigma'_3 = \sigma_3 - U_f = \sigma'_c - U_f$$

$$\sigma'_1 = \sigma'_3 + \Delta\sigma_a = \sigma'_c + \Delta\sigma_a - U_f$$

where U_f = pore pressure at failure
induced by $\Delta\sigma_a$

Undrained shear strength $S_U = 0.5 \Delta\sigma_a \cos \Phi$

Figure A-3. Consolidated-Undrained (CU) triaxial compression test with isotropic consolidation.

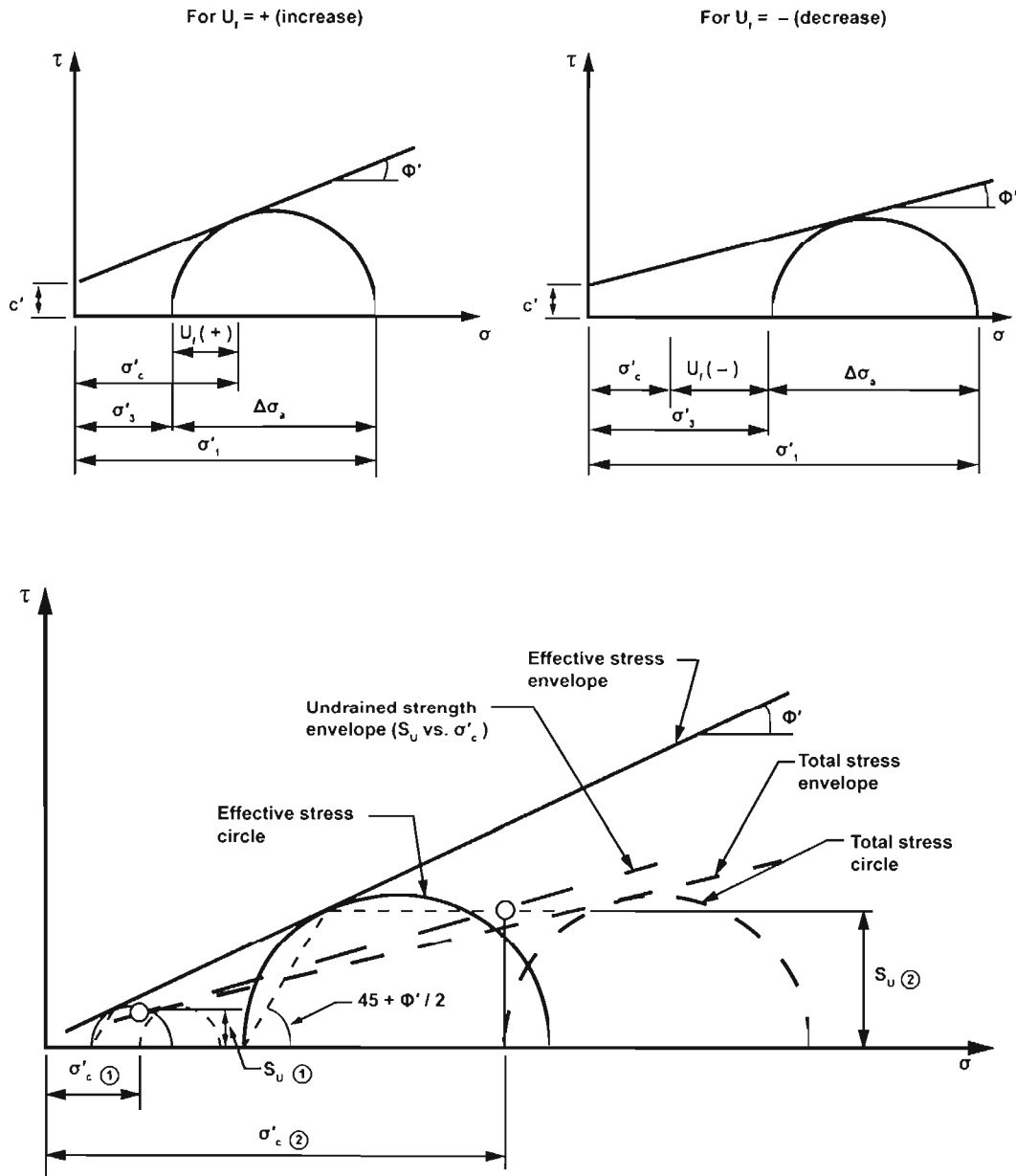


Figure A-4. Shear strength envelopes for Consolidated-Undrained (CU) triaxial compression test.

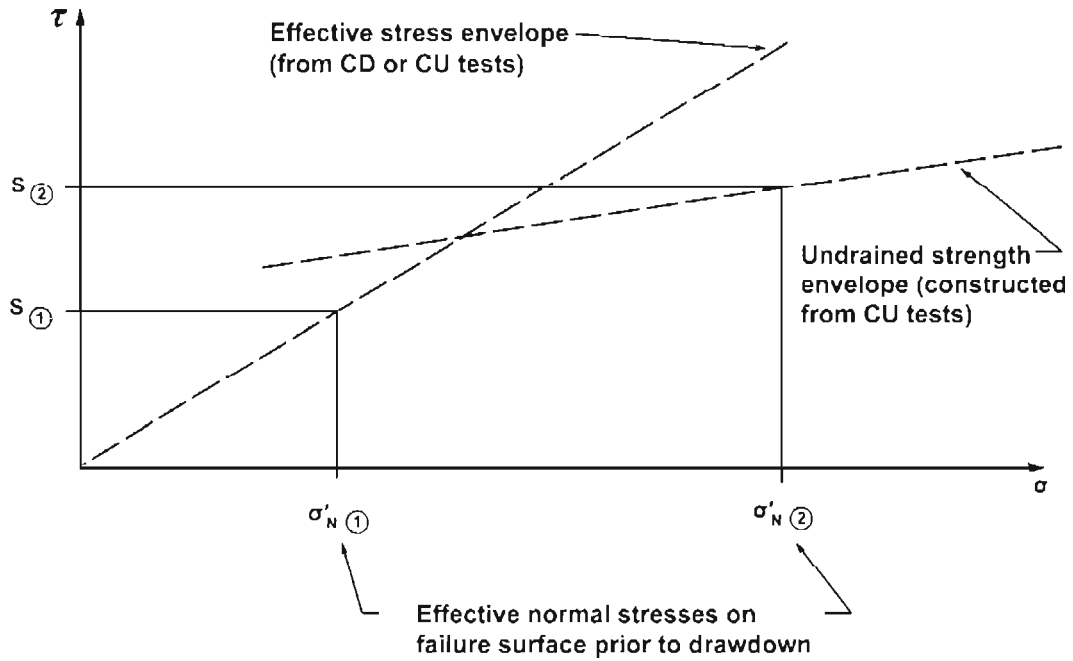


Figure A-5. Shear strength envelopes for Consolidated-Drained (CD) or Consolidated-Undrained (CU) triaxial compression test.

Type of Test: Consolidated-Drained (CD) Triaxial Shear test

Loading condition and Mohr-Coulomb envelope are shown on figure A-6.

Use in Stability Analysis: Consolidated drained triaxial tests are used to obtain the effective stress shear strength parameters, ϕ' and c' . These parameters are appropriate for use in effective stress analyses. Examples would be steady-state seepage for all embankment and foundation soils (except for natural soils such as overconsolidated clays or shales which may have been subjected to past shear deformations and for which the residual shear strength, determined from repeated direct shear or torsional ring shear tests, would be appropriate) or end-of-construction or rapid drawdown loading conditions for pervious soils only. The effective stress shear strength parameters from the CD test can be used in lieu of the parameters determined in the CU test to formulate the composite Mohr-Coulomb envelope for rapid drawdown analyses.

Because the effective stress shear strength parameters are a function largely of initial dry density for a given soil, samples should be prepared as discussed for UU tests.

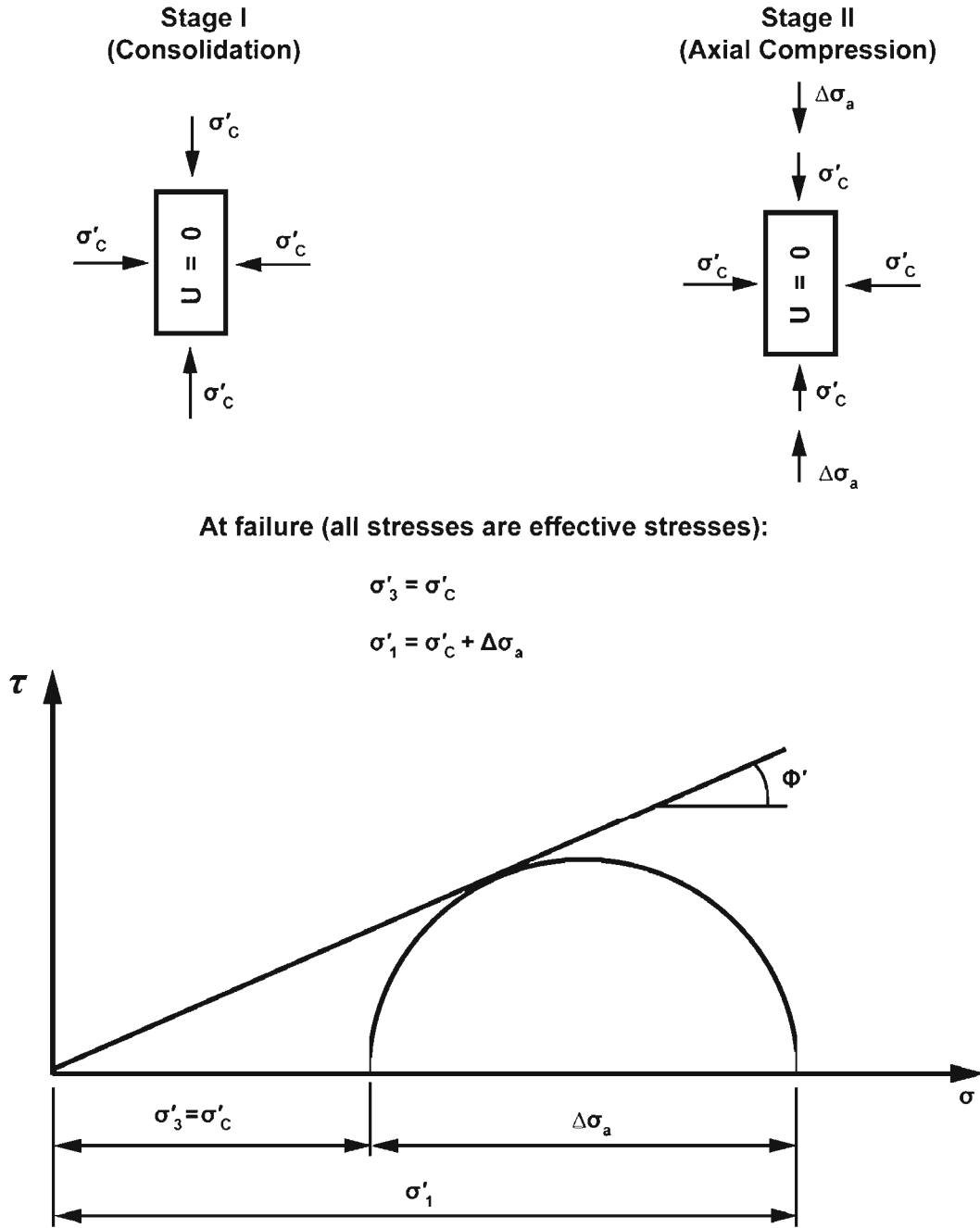


Figure A-6. Consolidated-Drained (CD) triaxial compression test with isotropic consolidation.

Type of Test: Direct Shear (DS) test

Loading condition and Mohr-Coulomb envelope are shown on figure A-7.

Use in Stability Analysis: The direct shear test can be used to determine drained shear strength parameters for many types of soil, provided the shear box is of adequate size according to the maximum grain size of the soil. Undisturbed or compacted samples can be tested. The test is also appropriate for determining fully softened strength (i.e., normally consolidated peak strength). Consolidation stresses should encompass the range of in situ stresses expected to occur on the anticipated failure surface.

In foundations consisting of highly overconsolidated clays or shales, prior deformations along bedding planes, shear zones, or faults may have occurred in the geologic past such that the maximum available shear strength along these discontinuities is the residual shear strength. Under such conditions, the direct shear test is appropriate for obtaining the residual strength. Samples should be oriented in the direct shear device such that shearing occurs parallel to the discontinuity so that the residual strength is measured. If the residual shear strength is used in analysis, somewhat lower factors of safety than shown in table 4.2.4-1 may be acceptable.

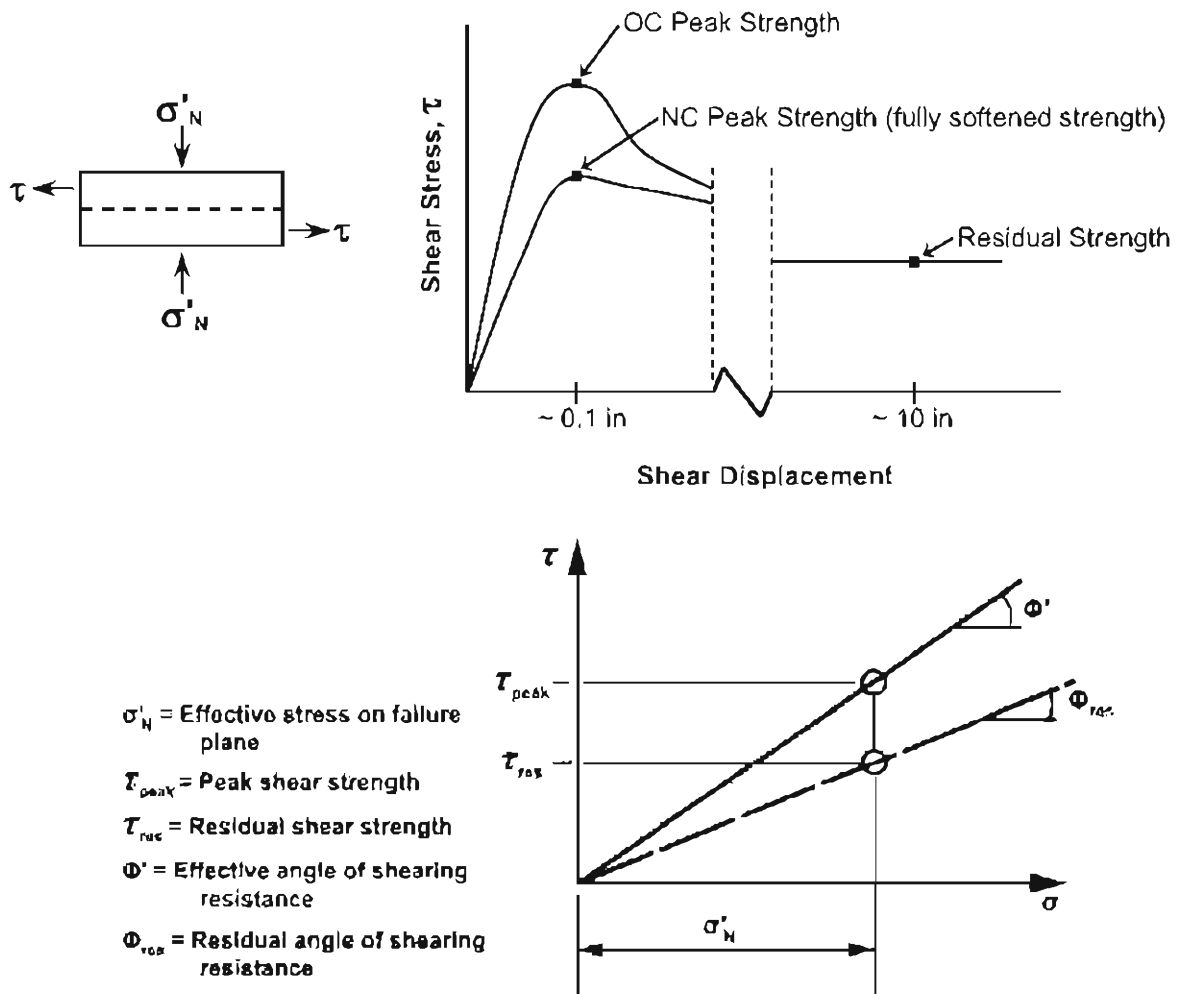


Figure A-7. Direct shear test.

Type of Test: Direct Simple Shear (DSS) test

Loading condition and Mohr-Coulomb envelope are shown in figure A-8 [21].

Use in Stability Analysis: The simple shear test imposes constant volume, undrained shearing. The strengths derived from this test can be used in a manner similar to the strengths derived from CU tests.

The simple shear state of stress corresponds to plane strain with constantly rotating principal stresses. The simple shear state of stress occurs in the field directly beneath embankment slopes. It should be noted that the state of stress within the specimen is not as uniform or well defined as for triaxial tests. Although the results are plotted in terms of the shear stress and normal effective stress on the horizontal plane and are useful for engineering purposes, the results cannot be directly compared to effective stress strengths derived from other tests.

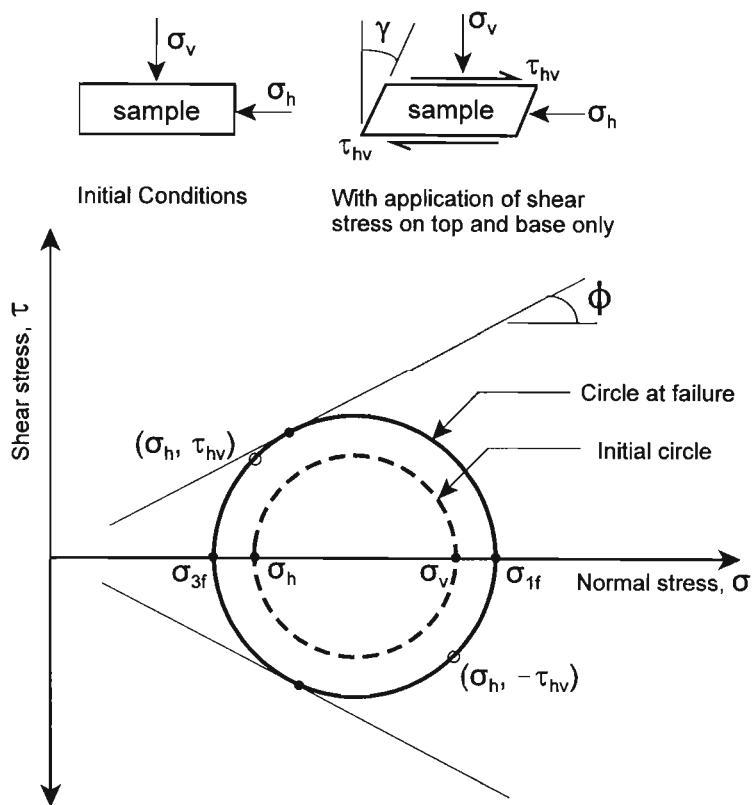


Figure A-8. Direct simple shear test.

Type of Test: Torsional Ring Shear test

Loading condition and Mohr-Coulomb envelope are shown in figure A-9.

Use in Stability Analysis: The torsional ring shear test can be used to determine fully softened and residual strengths of cohesive (silt and clay) materials. Testing is performed under drained conditions and is typically accomplished using reconstituted or slurry type specimens. The apparatus keeps the cross-sectional area of the shear surface constant during shear and shears the specimen continuously in one direction of rotation for any magnitude of displacement. This allows clay particles to become aligned parallel to the direction of shear and allows the residual condition to be reached. Fully softened strength is determined by testing slurry specimens. The fully softened strength is often taken to be the peak strength of the normally consolidated soil.

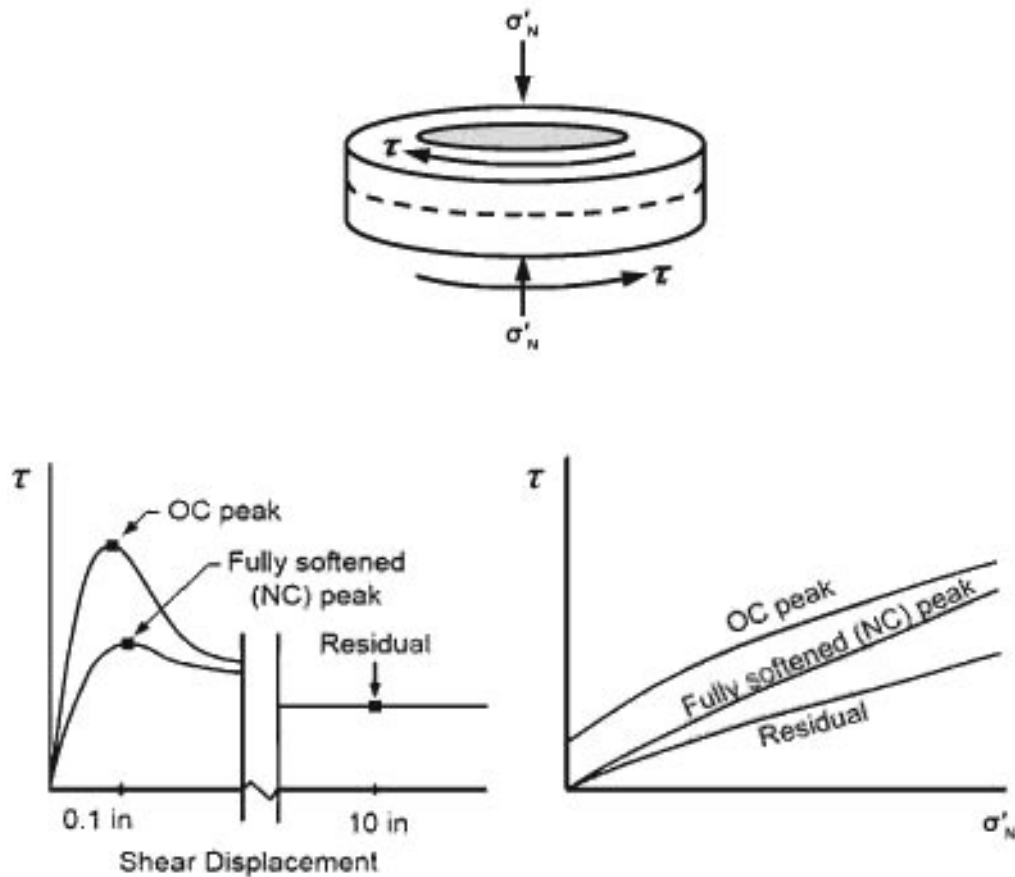


Figure A-9. Torsional ring shear test.

Appendix B

Spencer's Method of Analysis

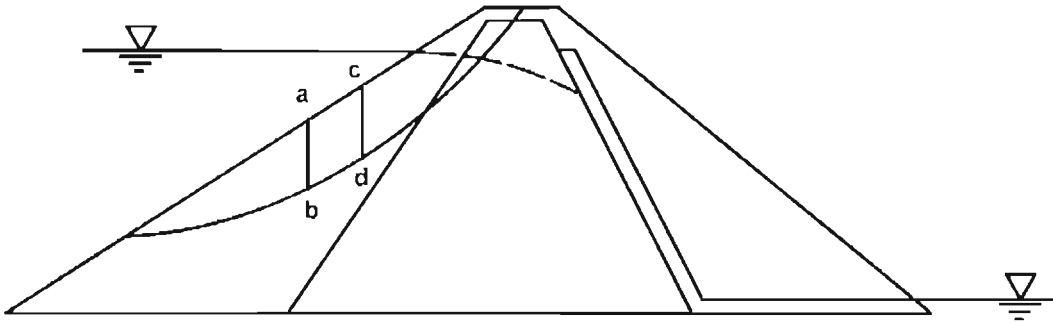
Figure B-1(a) is the general description of the slope stability problem. For any vertical slice, abdc, the forces acting on it are shown in figure B-1(b). H_L and H_R are the hydrostatic forces exerted by the subsurface water on the vertical boundaries of the slice (assumed to be known). Other forces acting on the free-body diagram of the slice figure B-1(b) are defined at the end of this appendix. The static equilibrium of forces acting on the slice shown in figure B-1(b) can be expressed as:

$$\begin{aligned}
 Z_R = Z_L + & \frac{\frac{1}{F} c' b \sec \alpha - W \sin \alpha + \frac{1}{F} (W \cos \alpha - U) \tan \phi'}{\cos(\delta - \alpha) \left[1 - \frac{1}{F} \tan(\delta - \alpha) \tan \phi' \right]} \\
 & + \frac{P \cos(\beta - \alpha) \left[\tan(\beta - \alpha) + \frac{1}{F} \tan \phi' \right]}{\cos(\delta - \alpha) \left[1 - \frac{1}{F} \tan(\delta - \alpha) \tan \phi' \right]} \\
 & + \frac{H_L \cos \alpha \left[1 + \frac{1}{F} \tan \alpha \tan \phi' \right]}{\cos(\delta - \alpha) \left[1 - \frac{1}{F} \tan(\delta - \alpha) \tan \phi' \right]} \\
 & - \frac{H_R \cos \alpha \left[1 + \frac{1}{F} \tan \alpha \tan \phi' \right]}{\cos(\delta - \alpha) \left[1 - \frac{1}{F} \tan(\delta - \alpha) \tan \phi' \right]}
 \end{aligned} \tag{1}$$

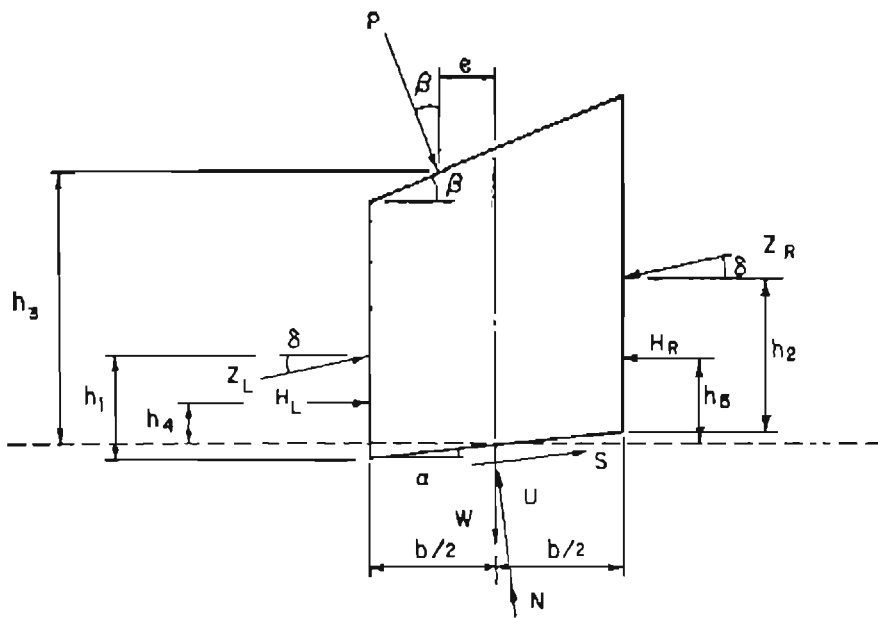
Design Standards No. 13: Embankment Dams

The moment equilibrium of the slice shown in figure B-1(b) can be expressed as:

$$\begin{aligned} h_2 &= \frac{Z_L}{Z_R} h_1 \\ &+ \frac{b}{2} [\tan\delta - \tan\alpha] \left[1 + \frac{Z_L}{Z_R} \right] \\ &+ \frac{P}{Z_R} \cos\beta \sec\delta [h_3 \tan\beta - e] \\ &+ \frac{1}{Z_R} \sec\delta [H_L h_4 - H_R h_5] \end{aligned} \tag{2}$$



(a) General slope stability problem description.



(b) Forces acting on a typical slice.

Figure B-1. Free body diagram of a typical slice.

Design Standards No. 13: Embankment Dams

The unknowns in equations (1) and (2) are Z_L , Z_R , h_1 , h_2 , δ , and F . The boundary conditions are defined in terms of $Z_{L,1}$, $h_{1,1}$ for the first slice and $Z_{R,1}$, $h_{2,1}$ for the last slice. By using an assumed value for the solution parameters (F , δ) and the known boundary conditions $Z_{L,1}$ and $h_{1,1}$ for slice 1, it becomes possible to use equations (1) and (2) in a recursive manner, slice by slice, and evaluate $Z_{R,i}$ and $h_{2,i}$ for the last slice. The solution of equations (1) and (2) proceeds along the following steps [14, 22]:

1. Assume some nonzero value for the factor of safety, F , and thrust line inclination, δ . (F , δ) are the solution parameters for the problem.
2. Knowing the boundary conditions on the left face of slice 1, i.e., $Z_{L,1}$ and $h_{1,1}$, calculate $Z_{R,1}$ and $h_{2,1}$ for the right face of slice 1. Because of material continuity between slices along vertical boundaries, $Z_{L,2} = Z_{R,1}$ and $h_{2,1} = h_{1,2}$. Thus, one can calculate $Z_{R,i}$ and $h_{2,i}$ for $i = 1$ to n , where n is the number of slices.
3. Compare the $Z_{R,i}$ and $h_{2,i}$ for the last slice against the known boundary conditions $Z_{R,1}$ and $h_{2,1}$ and the differences are due to error in values of (F , δ) assumed in step 1.
4. Adjust the values of (F , δ) and repeat steps 2 and 3 until the calculated values of $Z_{R,i}$ and $h_{2,i}$ for $i = n$ agree with the known boundary values $Z_{R,1}$ and $h_{2,1}$ to the desired accuracy.
5. The refined value of (F , δ) for which the boundary conditions are satisfied is taken as a solution to the slope stability problem.

There are special nonlinear numerical procedures such as Newton-Raphson algorithm and/or quasi-Newton algorithm for solving transcendental equations which are used in the computer program SSTAB2 [22] for making adjustments to (F , δ) values at the beginning of each new iteration past the first calculation cycle.

The input data for the example problems included herein are formatted for use in the computer program SSTAB2 [22]. A different format for data preparation will be required for use of other computer programs.

Meaning of Symbols

b	Width of slice
c'	Cohesion with respect to effective stress
e	Eccentricity of external force
F	Factor of safety
H_L	Hydrostatic force on the left side of a slice
H_R	Hydrostatic force on the right side of a slice
h_1	Location of left interslice force above slip surface
h_2	Location of right interslice force above slip surface
h_3	Location of external force above slip surface
h_4	Location of left hydrostatic force above slip surface
h_5	Location of right hydrostatic force above slip surface
$h_{1,i}$	Location of boundary force at toe of slide mass
$h_{2,1}$	Location of boundary force at head of slide mass
$h_{1,i}$	Location of interslice force on the left face of slice i
$h_{2,i}$	Location of interslice force on the right face of slice i
n	Number of slices
P	External force acting on slice
U	Force exerted by the pore water on the base of a slice
W	Weight of slice
Z	Interslice force
$Z_{L,1}$	Force boundary condition at toe of slide mass
$Z_{R,1}$	Force boundary condition at head of slide mass
Z_L	Calculated interslice force on the left face of a slice
Z_R	Calculated interslice force on the right face of a slice
α	Angle of inclination of base of slice
β	Angle of inclination of top of slice
δ	Angle of inclination of interslice force
φ'	Angle of internal friction

Example Problem A

Example Problem A illustrates an analysis of the upstream slope of a zoned earthfill embankment under end-of-construction loading condition. In this example, the embankment and the foundation are described by six types of materials as shown on the figure B-2. The input data for this problem are described and a listing of the input and output data is included at the end of the description.

Profile lines were specified as described in the user's information manual of the computer program SSTAB2 [22]. Shear strengths of six material types are described on the figure B-3. Because of undrained strength analysis concept, pore pressures were not considered. Submerged weights of foundation, materials were used which are below the ground-water table. The factor of safety for a single circular shear surface, shown on figure B-3 is computed. The center of the circle is located at the coordinates $x = 222.0$, $y = 378.0$, and passes through the upstream toe of the embankment. The circle is subdivided into slices by using maximum arc length of 30 feet. The initial values assumed for the factor of safety and side force inclination are 2.0 and 25° , respectively. A maximum of 40 iterations is permitted in order to satisfy force and moment equilibrium of the last slice within 100 lb and 100 lb-ft, respectively. The input for the computer program is listed in table B-A.1. The output from the program is illustrated in tables B-A.2 and B-A.3. A free-body diagram of a typical slice is shown on figure B-3. Horizontal E-forces for a typical slice as obtained from table B-A.3 are divided by cosine of the side force inclination (δ) to obtain side forces Z_L and Z_R . Typical force polygons for two slices are shown on figure B-3 where ϕ_D is the mobilized angle of friction of the base material of the slice and c_m is the mobilized cohesion intercept. Error of closure of each force polygon must be zero, based on the formulation of Spencer's method in the computer program. It should also be noted that horizontal side forces are always positive for all slices. The factor of safety of the failure mass as shown on figure B-3 is 1.318. By comparing with the required factor of safety of 1.3 (table 4.2.4-1), the upstream slope meets the minimum factor of safety criteria for the end-of-construction loading condition.

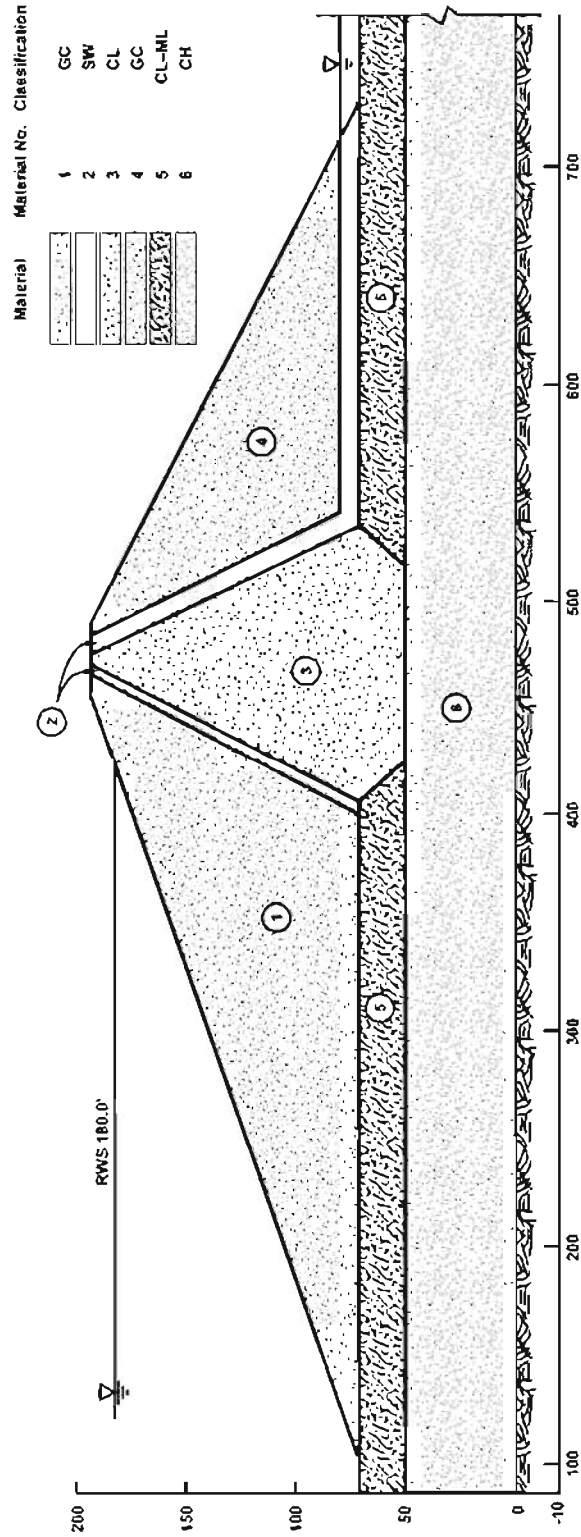


Figure B-2. Cross section of an embankment dam used for example problems.

Table B-A.1 Input data for end-of-construction loading

1						
Example Problem A						
9	6					62.4
3	1					
100.0	70.0					
460.0	190.0					
465.0	190.0					
3	2					
400.0	70.0					
465.0	190.0					
470.0	190.0					
4	3					
405.0	70.0					
470.0	190.0					
475.0	190.0					
535.0	70.0					
3	2					
475.0	190.0					
485.0	190.0					
540.0	80.0					
3	4					
485.0	190.0					
490.0	190.0					
710.0	80.0					
2	2					
540.0	80.0					
710.0	80.0					
5	5					
0.0	70.0					
100.0	70.0					
400.0	70.0					
405.0	70.0					
425.0	50.0					
4	5					
515.0	50.0					
535.0	70.0					
730.0	70.0					
1000.0	70.0					
2	6					
0.0	50.0					
1000.0	50.0					
0.0		35.0	135.0	0	0	
0.0		30.0	130.0	0	0	
1200.0		5.0	135.0	0	0	
0.0		30.0	125.0	0	0	
200.0		2.0	128.0	0	0	
2000.0		10.0	63.0	0	0	
0						
0						
0						
1						
End of construction loading u/s						
7						
0.0	70.0					
100.0	70.0					
460.0	190.0					
480.0	190.0					
710.0	80.0					
730.0	70.0					
1000.0	70.0					
1						
1						
222.0	378.0	99999	0.0	30.0	100.0	70.0
0.0						
2.0	25.0	100.0	100.0	40	1	0.1
1						
2						

Table B-A.2 Output for end-of-construction loading—slice information

NO.	S L I C E		WEIGHT (LBS/FT)	N F O R M A T I O N			COHESION (PSF)	FRICTION ANGLE (DEGS)	P O R E P R E S S U R E (PSF)	B O U N D A R Y F O R C E S A T S U R F A C E		C H A R A C T E R I S T I C O F S I D E - F O R C E I N C L I N A T I O N	S H A P E S O F F A C T O R O F S A F E T Y
	LEFT C E N T E R R I G H T	LEFT C E N T E R R I G H T		COHESION (PSF)	FRICTION ANGLE (DEGS)	B I F U R C A T I O N S T R E S S (PSF)				F O R C E - L O C A T I O N (L B S)	X		
1	100.00	70.00	0.	0.00	35.00	0.00	0.00	35.00	0.00	0.	0.00*	1.000	1.000
2	100.00	70.00	0.	0.00	35.00	0.00	0.00	35.00	0.00	0.	0.00*	1.000	1.000
3	114.18	65.11	35822.	200.00	2.00	0.00	200.00	2.00	0.00	0.	0.00*	1.000	1.000
4	128.36	60.23											
5	142.92	56.65	106016.	200.00	2.00	0.00	200.00	2.00	0.00	0.	0.00*	1.000	1.000
6	157.48	53.06											
7	166.48	51.53	96162.	200.00	2.00	0.00	200.00	2.00	0.00	0.	0.00*	1.000	1.000
8	175.49	50.00											
9	190.41	48.57	200576.	2000.00	10.00	0.00	2000.00	10.00	0.00	0.	0.00*	1.000	1.000
10	205.34	47.14											
11	213.67	46.93	131084.	2000.00	10.00	0.00	2000.00	10.00	0.00	0.	0.00*	1.000	1.000
12	222.00	46.72											
13	236.98	47.40	266277.	2000.00	10.00	0.00	2000.00	10.00	0.00	0.	0.00*	1.000	1.000
14	251.96	48.08											
15	260.24	49.04	162734.	2000.00	10.00	0.00	2000.00	10.00	0.00	0.	0.00*	1.000	1.000
16	268.51	50.00											
17	283.25	52.78	308006.	200.00	2.00	0.00	200.00	2.00	0.00	0.	0.00*	1.000	1.000
18	297.98	55.55											
19	312.41	59.65	313981.	200.00	2.00	0.00	200.00	2.00	0.00	0.	0.00*	1.000	1.000
20	326.83	63.74											
21	335.41	66.87	188712.	200.00	2.00	0.00	200.00	2.00	0.00	0.	0.00*	1.000	1.000
22	344.00	70.00											
23	357.67	76.15	294475.	0.00	35.00	0.00	0.00	35.00	0.00	0.	0.00*	1.000	1.000
24	371.35	82.29											
25	384.42	89.65	265099.	0.00	35.00	0.00	0.00	35.00	0.00	0.	0.00*	1.000	1.000
26	397.48	97.01											
27	398.74	97.81	24410.	0.00	35.00	0.00	0.00	35.00	0.00	0.	0.00*	1.000	1.000
28	400.00	98.60											
29	402.50	100.23	47460.	0.00	35.00	0.00	0.00	35.00	0.00	0.	0.00*	1.000	1.000
30	405.00	101.85											
31	415.00	109.03	178129.	0.00	35.00	0.00	0.00	35.00	0.00	0.	0.00*	1.000	1.000
32	425.00	116.20											
33	425.02	116.22	375.	0.00	35.00	0.00	0.00	35.00	0.00	0.	0.00*	1.000	1.000
34	425.04	116.24											
35	429.47	119.79	71543.	0.00	30.00	0.00	0.00	30.00	0.00	0.	0.00*	1.000	1.000
36	433.90	123.35											
37	444.98	133.45	153169.	1200.00	5.00	0.00	1200.00	5.00	0.00	0.	0.00*	1.000	1.000
38	456.06	143.56											
39	458.03	145.56	23116.	1200.00	5.00	0.00	1200.00	5.00	0.00	0.	0.00*	1.000	1.000
40	460.00	147.56											
41	462.50	150.20	26636.	1200.00	5.00	0.00	1200.00	5.00	0.00	0.	0.00*	1.000	1.000
42	465.00	152.84											
43	467.50	155.60	23107.	1200.00	5.00	0.00	1200.00	5.00	0.00	0.	0.00*	1.000	1.000
44	470.00	158.36											
45	472.50	161.25	19409.	1200.00	5.00	0.00	1200.00	5.00	0.00	0.	0.00*	1.000	1.000
46	475.00	164.13											

Table B-A.2 Output for end-of-construction loading—slice information

NO.	S L I C E I N F O R M A T I O N								PORE PRESSURE (PSF)	BOUNDARY FORCES AT SURFACE		CHARACTERISTIC OF SIDE-FORCE INCLINATION	SHAPE FACTOR OF SAFETY
	WEIGHT (LBS/FT)		COHESION (PSF)	FRICTION ANGLE (DEGS)	DIPUR. STRESS (PSF)	COHESION (PSF)	FRICTION ANGLE (DEGS)	FORCE-LOCATION (LBS)					
	LEFT CENTER RIGHT	LEFT CENTER RIGHT						X					
	473.00	164.13										1.000	
24	477.50	167.16	15289.	1700.00	5.00	0.00	1200.00	5.00	0.00	0.	0.00	1.000	1.000
	480.00	170.19										1.000	
25	481.50	172.09	6796.	1200.00	5.00	0.00	1200.00	5.00	0.00	0.	0.00	1.000	1.000
	483.01	173.98										1.000	
26	484.00	175.27	3319.	0.00	30.00	0.00	0.00	30.00	0.00	0.	0.00	1.000	1.000
	485.00	176.56										1.000	
27	485.79	177.59	1969.	0.00	30.00	0.00	0.00	30.00	0.00	0.	0.00	1.000	1.000
	486.57	178.63										1.000	
28	487.90	180.28	1892.	0.00	30.00	0.00	0.00	30.00	0.00	0.	0.00	1.000	1.000
	489.03	181.94										1.000	
29	489.52	182.60	345.	0.00	30.00	0.00	0.00	30.00	0.00	0.	0.00	1.000	1.000
	490.00	183.26										1.000	
30	490.93	183.93	128.	0.00	30.00	0.00	0.00	30.00	0.00	0.	0.00	1.000	1.000
	491.05	184.71										1.000	

Table B-A.3 Output for end-of-construction loading—solution information

S O L U T I O N I N F O R M A T I O N
 FACTOR OF SAFETY = 1.318 (0 ITERATIONS)
 SIDE FORCE INCLINATION = -14.83 DEGREES

SLICE NO.	XAVG	TOTAL NORMAL STRESS (PSF)	NOMINAL SHEAR STRESS (PSF)	L I N E O F T H R U S T			HORIZONTAL E-FORCE (LBS)	LENGTH (FEET)	SHEAR FORCE (LBS)	EFFECTIVE PHI REQD (DEGREES)	N/NCOSA	SHEAR ST/NORMAL ST
				X	YT (TOT)	FRACTION						
0				100.0	70.0	0.0000	0.			0.000		
1	100.0	0.	0.	100.0	70.0	0.4530	0.	0.00	0.00	14.834	2.128	0.531
2	114.2	1519.	192.	128.4	68.9	0.4495	20288.	29.99	5759.84	9.566	1.345	0.126
3	142.9	4036.	259.	157.5	66.3	0.3654	56746.	29.99	7760.28	11.594	1.176	0.064
4	166.5	5747.	304.	175.5	66.1	0.3560	79825.	18.27	5556.06	12.120	1.104	0.053
5	190.4	7844.	2568.	205.3	62.1	0.2580	178933.	29.99	77007.02	11.887	1.178	0.327
6	213.7	8705.	2683.	222.0	62.8	0.2517	227276.	16.66	44709.03	12.318	1.107	0.308
7	237.0	9384.	2774.	252.0	66.2	0.2492	297641.	29.99	83188.35	13.413	1.058	0.296
8	260.2	9948.	2849.	268.5	68.9	0.2479	325665.	16.66	47482.64	14.175	1.026	0.286
9	283.2	9985.	416.	298.0	79.7	0.3008	282521.	29.99	12488.89	14.285	0.989	0.042
10	312.4	10115.	420.	326.8	95.4	0.3865	211766.	29.99	12592.25	14.517	1.004	0.042
11	335.4	9988.	417.	344.0	110.8	0.5019	156419.	18.27	7609.92	14.834	1.029	0.042
12	357.7	8845.	4701.	371.4	113.8	0.4025	176252.	29.99	140967.52	14.834	0.988	0.531
13	384.4	7758.	4123.	397.5	121.7	0.3425	169802.	29.99	123644.14	14.834	1.007	0.531
14	398.7	7116.	3782.	400.0	122.6	0.3368	168022.	2.98	11264.94	14.834	1.027	0.531
15	402.5	6924.	3680.	405.0	124.5	0.3251	163924.	5.96	21941.48	14.834	1.033	0.531
16	415.0	6226.	3309.	425.0	132.8	0.2677	140753.	24.62	81443.86	14.834	1.059	0.531
17	425.0	5682.	3020.	425.0	132.9	0.2676	140692.	0.06	170.64	14.834	1.084	0.531
18	429.5	5578.	2444.	433.9	137.3	0.2406	122653.	11.36	27757.83	14.834	1.136	0.438
19	445.0	4922.	1238.	456.1	152.8	0.2049	50619.	29.99	37116.60	0.000	1.304	0.251
20	458.0	3929.	1172.	460.0	156.0	0.1997	39513.	5.62	6581.50	0.000	1.361	0.298
21	462.5	3458.	1140.	465.0	160.4	0.2031	26960.	7.27	8291.80	0.000	1.373	0.330
22	467.5	2861.	1101.	470.0	165.1	0.2122	16671.	7.45	8197.87	0.000	1.374	0.385
23	472.5	2249.	1060.	475.0	170.2	0.2361	8976.	7.64	8100.82	0.000	1.353	0.471
24	477.5	1586.	1016.	480.0	175.4	0.2617	4444.	7.86	7982.52	0.000	1.281	0.641
25	481.5	966.	975.	483.0	176.9	0.1999	3714.	4.84	4717.69	14.834	1.107	1.009
26	484.0	929.	407.	485.0	178.8	0.2053	2132.	3.26	1325.64	14.834	1.490	0.438
27	485.8	693.	303.	486.6	180.4	0.2173	1177.	2.60	788.37	14.834	1.510	0.438
28	487.8	420.	184.	489.0	182.9	0.2491	239.	4.12	759.51	14.834	1.535	0.438
29	489.5	193.	85.	490.0	184.2	0.4714	65.	1.64	138.76	14.834	1.557	0.438
30	490.5	66.	29.	491.1	184.7	0.0000	0.	1.79	51.77	-14.834	1.570	0.438

AVERAGE FACTOR-OF-SAFETY = 1.318

SUM= 0.795E+06

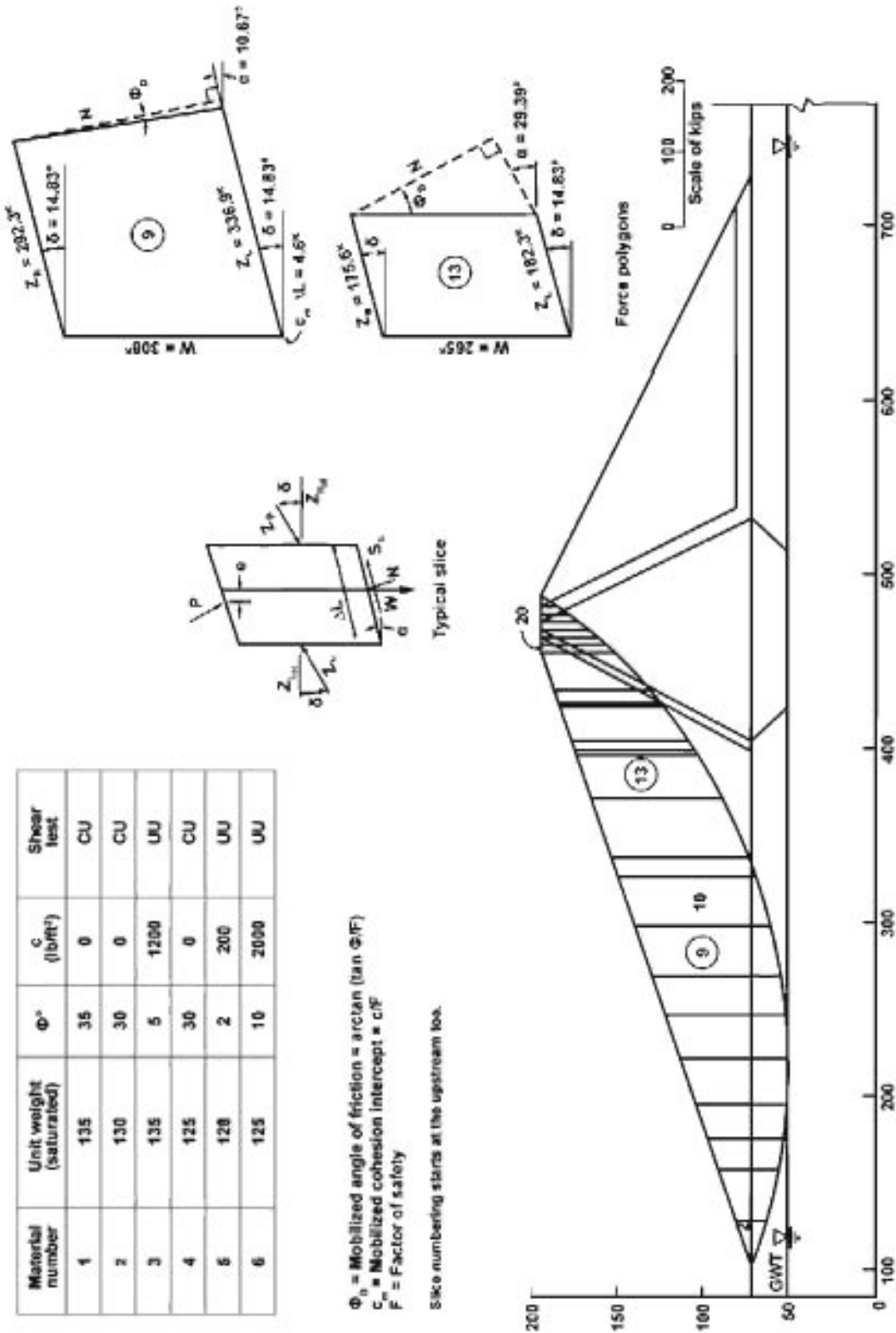


Figure B-3. Stability analysis of the upstream slope for end-of-construction loading.

Example Problem B

Example problem B presents a stability analysis of the upstream slope of the zoned earthfill dam as shown on figure B-2 under rapid drawdown loading condition using effective stress envelope concept. The input data were prepared in accordance with the user's manual of the computer program SSTAB2 [22]. Shear strength of six material types is described on figure B-4. With coarse granular soils, dissipation generally occurs so rapidly that no measurable additional pore pressure actually develops. Thus, the pore pressures are hydrostatic in granular soils like shell material in the example problem. In low permeability medium, excess pore pressures are caused during undrained loading. Effective stress analysis by using pore pressures measured by piezometers assume that the stress path to failure has an A_f value of 0.5 ($1 - \sin \phi'$) where A_f is the Skempton's A-parameter at failure and ϕ' is the effective friction angle [23]. This may not coincide with actual A_f values developed in undrained shear. If the actual A_f value is less than 0.25 to 0.33, pore pressures measured by piezometers are conservative. However, if substantial shear-induced pore pressures are developed ($A_f > 0.25$ to 0.33) the pore pressures by piezometric method renders too high shear strengths. In this case, excess pore pressures are computed by using the following relationship:

$$\Delta u = B [\Delta \sigma_3 + A_f (\Delta \sigma_1 - \Delta \sigma_3)]$$

where:

A_f and B are the Skempton's parameters,
 Δu = excess hydrostatic pressure,
 $\Delta \sigma_3$ = change in confining stress, and
 $\Delta \sigma_1$ = change in applied load.

Estimation of shear induced pore pressures can be eliminated by using undrained strength of cohesive materials. In the example problem, CL-ML and CH materials in foundation are assumed to have A_f values less than 0.33 and, thus, the piezometric method is applicable to obtain pore pressures. The phreatic surface intersects the upstream slope at the inactive conservation pool water surface at elevation 100.00 feet (after drawdown reservoir level), then follows the upstream slope (which satisfies Skempton's pore pressure coefficient, $B = 1$) until it reaches the active conservation pool (before drawdown reservoir level) and then follows the steady-state phreatic surface. If upstream shell material is very pervious, pore pressures should not be considered in that material. The factor of safety for a single circular shear surface is computed. The center of the circle is located at the coordinates $x = 220.0$, $y = 375.0$, and the surface passes through the upstream toe of the embankment. The circular arc is subdivided into slices by using maximum arc lengths of 15 feet. The initial values assumed for the factor of safety and side force inclination are 2.0 and 25° , respectively. A maximum of

Design Standards No. 13: Embankment Dams

40 iterations is permitted in order to satisfy force and moment equilibrium equations of the last slice within 100 lb and 100 ft-lb, respectively. The input listing is shown in table B-B.1 and the output from the program is illustrated in tables B-B.2 and B-B.3. A free-body diagram of a typical slice is shown on figure B-4 to describe internal and external forces. Typical force polygons for two slices are shown on the same figure, where ϕ_D is the mobilized angle of friction and c_m is the mobilized cohesion intercept. Based on the formulation of Spencer's method, the forces must be in equilibrium for every slice and, thus, the error of closure of each polygon must be zero. The horizontal E-forces must be positive for all slices unless tensile crack develops in which case, crack should be assumed in accordance with the procedures in the user's manual. The factor of safety of the failure mass as shown in table B-B.3 is 1.278 and by comparing with the required factor of safety of 1.3, the upstream slope did not meet the minimum factor of safety criteria under rapid drawdown condition.

Table B-B.1 Input data for rapid drawdown (effective stress)

1	2	3	4	5	6	7	8	9	10	11	12	
Example	12	9							10	0	11	62.4
Problem	3	1										
B	430.0	180.0										
	460.0	190.0										
	465.0	190.0										
	3	2										
	100.0	70.0										
	430.0	180.0										
	459.5834	180.0										
	3	3										
	459.5834	180.0										
	465.0	190.0										
	470.0	190.0										
	3	4										
	400.0	70.0										
	459.5834	180.0										
	464.5834	180.0										
	4	5										
	464.5834	180.0										
	470.0	190.0										
	475.0	190.0										
	515.0	110.0										
	4	6										
	405.0	70.0										
	464.5834	180.0										
	515.0	110.0										
	535.0	70.0										
	3	3										
	475.0	190.0										
	485.0	190.0										
	540.0	80.0										
	3	7										
	485.0	190.0										
	490.0	190.0										
	710.0	80.0										
	2	4										
	540.0	80.0										
	710.0	80.0										
	5	8										
	0.0	70.0										
	100.0	70.0										
	400.0	70.0										
	405.0	70.0										
	425.0	50.0										
	4	8										
	515.0	50.0										
	535.0	70.0										
	730.0	70.0										
	1000.0	70.0										
	2	9										
	0.0	50.0										
	1000.0	50.0										
	0.0				40.0	125.0	0	0				
	0.0				40.0	135.0	0	5				
	0.0				35.0	122.0	0	0				
	0.0				35.0	130.0	0	5				
	500.0				28.0	126.0	0	0				
	300.0				28.0	135.0	0	5				
	0.0				35.0	125.0	0	5				
	0.0				25.0	128.0	0	5				
	400.0				29.0	125.0	0	5				
	0											
	0											
	0											
	12											

Design Standards No. 13: Embankment Dams

Table B-B.1 Input data for rapid drawdown (effective stress)

0.0	70.0	1872.0	10			
100.0	70.0	1872.0	10			
190.0	100.0	0.0	10			
0.0	100.0		11			
190.0	100.0		11			
430.0	180.0		11			
459.5834	180.0		11			
464.5834	180.0		11			
515.0	110.0		11			
540.0	80.0		11			
710.0	80.0		11			
1000.0	80.0		11			
1						
Rapid drawdown loading u/s (effective stress)						
7						
0.0	70.0					
100.0	70.0					
460.0	190.0					
490.0	190.0					
710.0	80.0					
730.0	70.0					
1000.0	70.0					
1						
1						
220.0	375.0	99999	0.0	15.0	100.0	70.0
0.0						
2.0	25.0	100.0	100.0	40	1	0.1
1						
2						

Table B-B.2 Output for rapid drawdown (effective stress) – slice information

NO.	S L I C E		WEIGHT (LBS/FT)	COHESION (PSF)	FRICTION ANGLE (DEGS)	RIFUR. STRESS (PSF)	COHESION (PSF)	FRICTION ANGLE (DEGS)	PORE PRESSURE (PSF)	BOUNDARY FORCES AT SURFACE		CHARACTERISTIC OF SIDE-FORCE INCLINATION	SHAPE OF FACTOR OF SAFETY
	LEFT CENTER RIGHT	LEFT CENTER RIGHT								FORCE-LOCATION (LBS)	M		
1	100.00	70.00	0.	0.00	10.00	0.00	0.00	40.00	1871.98	2.	100.00	1.000	1.000
2	107.04	63.41	9121.	0.00	25.00	0.00	0.00	25.00	2033.32	25608.	106.84	1.000	1.000
3	121.23	62.57	27267.	0.00	25.00	0.00	0.00	25.00	2335.69	21562.	120.98	1.000	1.000
4	135.63	56.38	44798.	0.00	25.00	0.00	0.00	25.00	2597.24	17277.	135.31	1.000	1.000
5	150.20	54.85	61526.	0.00	25.00	0.00	0.00	25.00	2817.41	12787.	149.75	1.000	1.000
6	164.92	51.99	77278.	0.00	25.00	0.00	0.00	25.00	2995.75	6179.	164.20	1.000	1.000
7	174.95	50.37	90982.	0.00	25.00	0.00	0.00	25.00	3097.20	1738.	174.80	1.000	1.000
8	183.79	49.31	79689.	400.00	29.00	0.00	400.00	29.00	3163.08	1691.	181.72	1.000	1.000
9	197.48	48.10	107491.	400.00	29.00	0.00	400.00	29.00	3393.93	0.	0.00	1.000	1.000
10	212.46	47.42	119114.	400.00	29.00	0.00	400.00	29.00	3748.42	0.	0.00	1.000	1.000
11	219.98	47.24	349.	400.00	29.00	0.00	400.00	29.00	3925.57	0.	0.00	1.000	1.000
12	227.50	47.42	129262.	400.00	29.00	0.00	400.00	29.00	4061.25	0.	0.00	1.000	1.000
13	242.48	48.10	137795.	400.00	29.00	0.00	400.00	29.00	4330.00	0.	0.00	1.000	1.000
14	256.19	49.31	120556.	400.00	29.00	0.00	400.00	29.00	4539.92	0.	0.00	1.000	1.000
15	269.83	51.14	149679.	0.00	25.00	0.00	0.00	25.00	4709.32	0.	0.00	1.000	1.000
16	284.60	53.76	152714.	0.00	25.00	0.00	0.00	25.00	4853.00	0.	0.00	1.000	1.000
17	299.22	57.05	154598.	0.00	25.00	0.00	0.00	25.00	4951.89	0.	0.00	1.000	1.000
18	313.64	61.01	154747.	0.00	25.00	0.00	0.00	25.00	5005.78	0.	0.00	1.000	1.000
19	327.85	65.62	153199.	0.00	25.00	0.00	0.00	25.00	5014.56	0.	0.00	1.000	1.000
20	337.52	69.05	53644.	0.00	25.00	0.00	0.00	25.00	4999.80	0.	0.00	1.000	1.000
21	346.91	72.89	148221.	0.00	10.00	0.00	0.00	10.00	4954.51	0.	0.00	1.000	1.000
22	360.60	79.03	142364.	0.00	10.00	0.00	0.00	10.00	4857.17	0.	0.00	1.000	1.000
23	373.99	85.77	133050.	0.00	10.00	0.00	0.00	10.00	4715.04	0.	0.00	1.000	1.000

Table B-B.2 Output for rapid drawdown (effective stress) – slice information

NO.	S L I C E		WEIGHT (LBS/FT)	C O H E S I O N (P S F)	F R I C T I O N A N G L E (D E G S)	B I F U R C A T I O N S T R E S S (P S F)	C O H E S I O N (P S F)	F R I C T I O N A N G L E (D E G S)	P O R E P R E S S U R E (P S F)	B O U N D A R Y F O R C E S A T S U R F A C E		C H A R A C T E R I S T I C S I D E - F O R C E I N C L I N A T I O N	S H A P E S O F F A C T O R O F S A F E T Y
	LEFT C E N T E R R I G H T	LEFT C E N T E R R I G H T								Y	X		
	380.61	89.29										1.000	
24	387.06	93.12	126409.	0.00	10.00	0.00	0.00	40.00	4520.40	0.	0.00	1.000	1.000
	393.51	96.94										1.000	
25	396.76	99.02	61197.	0.00	10.00	0.00	0.00	40.00	4361.86	0.	0.00	1.000	1.000
	400.00	101.09										1.000	
26	402.50	102.77	45943.	0.00	10.00	0.00	0.00	40.00	4247.14	0.	0.00	1.000	1.000
	405.00	104.15										1.000	
27	411.09	108.82	106714.	0.00	10.00	0.00	0.00	40.00	4048.36	0.	0.00	1.000	1.000
	417.18	113.19										1.000	
28	421.09	116.23	64154.	0.00	10.00	0.00	0.00	40.00	3793.96	0.	0.00	1.000	1.000
	425.00	119.27										1.000	
29	426.50	120.49	23699.	0.00	10.00	0.00	0.00	40.00	3640.86	0.	0.00	1.000	1.000
	428.01	121.71										1.000	
30	429.00	122.53	15350.	0.00	15.00	0.00	0.00	35.00	3565.26	0.	0.00	1.000	1.000
	430.00	123.36										1.000	
31	433.65	126.50	53650.	0.00	15.00	0.00	0.00	35.00	3338.67	0.	0.00	1.000	1.000
	437.30	129.63										1.000	
32	442.80	134.73	72565.	300.00	28.00	0.00	300.00	28.00	2824.60	0.	0.00	1.000	1.000
	448.30	139.83										1.000	
33	453.56	145.18	59294.	300.00	28.00	0.00	300.00	28.00	2172.95	0.	0.00	1.000	1.000
	458.82	150.52										1.000	
34	459.20	150.93	3890.	300.00	28.00	0.00	300.00	28.00	1813.86	0.	0.00	1.000	1.000
	459.58	151.34										1.000	
35	459.79	151.56	7098.	300.00	28.00	0.00	300.00	28.00	1774.48	0.	0.00	1.000	1.000
	460.00	151.79										1.000	
36	462.29	154.30	21464.	300.00	28.00	0.00	300.00	28.00	1603.54	0.	0.00	1.000	1.000
	464.58	156.82										1.000	
37	464.79	157.85	1799.	300.00	28.00	0.00	300.00	28.00	1413.90	0.	0.00	1.000	1.000
	465.00	157.29										1.000	
38	467.50	160.17	19413.	300.00	28.00	0.00	300.00	28.00	984.94	0.	0.00	1.000	1.000
	470.00	163.85										1.000	
39	471.82	165.23	11525.	300.00	28.00	0.00	300.00	28.00	294.31	0.	0.00	1.000	1.000
	473.64	167.42										1.000	
40	474.32	168.25	3716.	500.00	28.00	0.00	500.00	28.00	0.00	0.	0.00	1.000	1.000
	475.00	169.09										1.000	
41	478.19	173.17	13362.	500.00	28.00	0.00	500.00	28.00	0.00	0.	0.00	1.000	1.000
	481.39	177.25										1.000	
42	483.19	179.69	4558.	0.00	35.00	0.00	0.00	35.00	0.00	0.	0.00	1.000	1.000
	485.00	182.13										1.000	
43	486.16	183.74	1788.	0.00	35.00	0.00	0.00	35.00	0.00	0.	0.00	1.000	1.000
	487.32	185.36										1.000	
44	488.66	187.28	912.	0.00	35.00	0.00	0.00	35.00	0.00	0.	0.00	1.000	1.000
	490.00	189.19										1.000	
45	490.21	189.48	21.	0.00	35.00	0.00	0.00	35.00	0.00	0.	0.00	1.000	1.000
	490.41	189.79										1.000	

Table B-B.3 Output for rapid drawdown (effective stress) – solution information

S O L U T I O N I N F O R M A T I O N												
FACTOR OF SAFETY = 1.278 (0 ITERATIONS)												
SIDE FORCE INCLINATION = -13.59 DEGREES												
SLICE NO.	XAVG	TOTAL NORMAL STRESS (PSF)	NOMINAL SHEAR STRESS (PSF)	L I N E O F T H R U S T			HORIZONTAL E-FORCE (LBS)	LENGTH (FEET)	SHEAR FORCE (LBS)	EFFECTIVE PHI REQD (DEGREES)	N/COSA	SHEAR ST/NORMAL ST
				X	Y(TOT)	FRACT(OM)						
0				100.0	70.0	0.0000	0.			0.000		
1	100.0	2548.	444.	100.0	70.0	0.5750	3.	0.00	0.60	13.592	1.622.047	0.657
2	107.0	2991.	349.	114.1	70.3	0.5577	28484.	15.00	5241.28	13.592	5.239	0.365
3	121.2	4135.	657.	128.4	70.0	0.5078	63384.	15.00	9847.50	13.592	2.385	0.365
4	135.6	5108.	916.	142.9	69.7	0.4751	101854.	15.00	13743.68	13.592	1.770	0.365
5	150.2	5927.	1135.	157.5	69.4	0.4506	141468.	15.00	17023.97	13.592	1.479	0.365
6	164.9	6606.	1318.	172.3	69.4	0.4307	180174.	15.00	19762.79	13.592	1.301	0.365
7	174.9	7001.	1425.	177.6	69.5	0.4246	193342.	5.32	7574.95	13.592	1.212	0.365
8	183.8	7340.	1521.	190.0	69.0	0.3963	231757.	12.50	27639.28	13.462	1.190	0.505
9	197.5	8041.	2329.	205.0	69.0	0.3737	274900.	15.00	34937.70	13.401	1.125	0.501
10	212.5	8636.	2434.	220.0	69.7	0.3582	314374.	15.00	36502.48	13.402	1.088	0.498
11	220.0	8903.	2477.	220.0	69.7	0.3582	314478.	6.04	104.15	13.402	1.072	0.497
12	227.5	9119.	2507.	235.0	71.0	0.3468	346946.	15.00	37607.82	13.442	1.058	0.496
13	242.5	9493.	2593.	250.0	72.7	0.3378	377381.	15.00	38291.59	13.512	1.036	0.495
14	256.2	9749.	2573.	262.4	74.6	0.3314	395947.	12.54	32261.53	13.592	1.020	0.494
15	269.8	9855.	1878.	277.2	77.8	0.3325	401310.	15.00	28168.40	13.592	1.003	0.365
16	284.6	9977.	1876.	291.9	81.5	0.3335	399309.	15.00	28048.45	13.592	0.999	0.365
17	299.2	10006.	1845.	306.5	85.7	0.3350	389871.	15.00	27668.42	13.592	1.000	0.365
18	313.7	9947.	1804.	320.9	90.3	0.3375	373135.	15.00	27050.82	13.592	1.006	0.365
19	328.0	9804.	1748.	335.0	95.5	0.3418	349433.	15.00	26217.49	13.592	1.017	0.365
20	337.5	9670.	1704.	340.0	97.5	0.3440	339471.	5.32	9060.46	13.592	1.026	0.365
21	346.9	9272.	2835.	353.8	102.0	0.3330	324817.	15.00	42526.23	13.592	1.018	0.657
22	360.6	8974.	2638.	367.4	107.1	0.3228	303447.	15.00	39566.52	13.592	1.035	0.657
23	374.0	8412.	2428.	380.6	112.5	0.3127	276298.	15.00	36419.76	13.592	1.058	0.657
24	387.1	7991.	2209.	393.5	118.4	0.3021	244451.	15.00	33126.78	13.592	1.088	0.657
25	396.8	7467.	2040.	400.0	121.5	0.2962	226662.	7.70	15706.78	13.592	1.116	0.657
26	402.5	7193.	1935.	405.0	124.0	0.2914	212225.	6.02	11647.58	13.592	1.135	0.657
27	411.1	6743.	1771.	417.2	130.5	0.2775	174806.	15.00	26560.54	13.592	1.167	0.657
28	421.1	6198.	1579.	425.0	135.0	0.2667	149501.	9.90	14630.31	13.592	1.211	0.657
29	426.5	5884.	1473.	428.0	136.8	0.2620	139570.	3.87	5707.08	13.592	1.239	0.657
30	429.0	5819.	1235.	430.0	138.1	0.2598	132437.	2.59	3193.80	13.592	1.272	0.548
31	433.7	5482.	1173.	437.3	142.9	0.2505	106599.	9.63	11310.85	13.592	1.298	0.548
32	442.8	4798.	1056.	448.3	150.6	0.2329	69280.	15.00	15841.93	11.200	1.953	0.535
33	453.6	3925.	964.	458.8	158.8	0.2130	37458.	15.00	14460.50	5.195	1.416	0.550
34	459.2	3443.	915.	459.6	159.5	0.2121	35345.	1.12	1022.28	4.395	1.448	0.560
35	459.8	3397.	910.	460.0	159.9	0.2118	34206.	0.61	556.12	3.921	1.452	0.561
36	462.3	3116.	864.	464.6	164.2	0.2219	22487.	6.81	5882.71	0.000	1.467	0.571
37	464.8	2826.	822.	465.0	164.6	0.2238	21509.	0.63	515.24	0.000	1.480	0.582
38	467.5	2439.	840.	470.0	170.1	0.2610	11659.	7.63	6406.34	0.000	1.462	0.578
39	471.8	1809.	865.	473.6	174.6	0.3184	6899.	5.69	4924.78	0.000	1.396	0.571
40	474.1	1377.	964.	475.0	176.0	0.3319	5910.	2.15	2073.86	0.000	1.263	0.700
41	478.2	970.	795.	481.4	160.9	0.2899	3065.	10.35	8233.31	13.592	1.221	0.820
42	483.2	651.	357.	485.0	164.5	0.3052	1179.	6.08	2170.09	13.592	1.458	0.548
43	486.2	392.	215.	487.3	187.1	0.2710	412.	3.98	853.68	13.592	1.493	0.548
44	488.7	170.	93.	490.0	193.7	1.0000	9.	4.68	437.00	13.592	1.526	0.548
45	490.2	25.	14.	490.2	189.8	0.0000	-1.	0.73	9.99	-13.592	1.547	0.548
AVERAGE FACTOR-OF-SAFETY				1.278								
SUM-								0.732E+06				

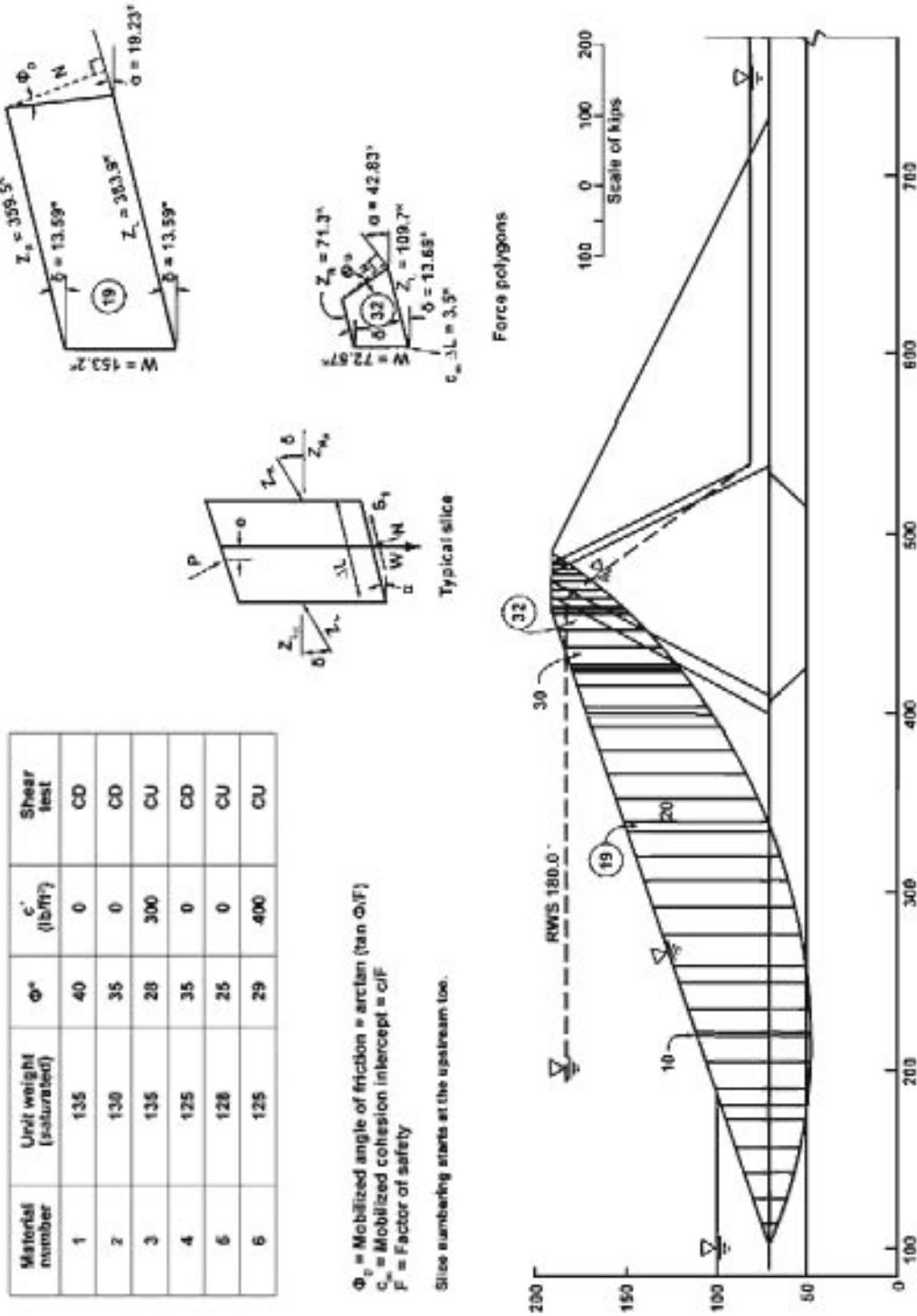


Figure B-4. Stability analysis of the upstream slope under rapid drawdown loading (effective stress concept).

Example Problem C

Example problem C presents a stability analysis of the upstream slope of the zoned earthfill dam as shown on figure B-2 under rapid drawdown loading condition using undrained strength envelope concept. The analysis is done in two steps: the first step includes analysis of the upstream slope at predrawdown level under steady-state seepage condition. The second step involves the analysis of the slope at the after-drawdown level and by incorporating undrained shear strengths of the sliding mass at normal stresses corresponding to steady-state condition from step 1.

The input data were prepared in accordance with the user's manual of the computer program SSTAB2 [22] for predrawdown level. Effective shear strength of six materials is described on figure B-5. Phreatic surface method is used to determine pore pressures at the base of slices. The factor of safety for a single circular shear surface is computed. The center of the circle is located at the coordinates $x = 220.0$, $y = 375.0$, and the failure surface passes through the upstream toe of the embankment. The circular arc is subdivided into slices by using maximum arc lengths of 15 feet. The initial values assumed for the factor of safety and side force inclination are 2.0 and 25° , respectively. A maximum of 40 iterations is permitted in order to satisfy force and moment equilibrium equations of the last slice within 100 lb and 100 ft-lb, respectively.

The input listing is shown in table B-C.1 and the output is listed in tables B-C.2 and B-C.3. Typical slice and force polygons are shown on figure B-5. Force polygons illustrated are for predrawdown condition.

The computer program SSTAB2 is not equipped with the formulation of two-step analysis. Hence, using the normal forces (effective) from the first step, and by obtaining corresponding undrained shear strength as shown by the bilinear shear strength envelope on figure B-5, the factor of safety of the failure mass after-drawdown condition is computed. The computation is illustrated in table B-C.4.

The computed factor of safety is 1.38 and, thus, it meets the minimum factor of safety criteria of the upstream slope under rapid drawdown condition.

Design Standards No. 13: Embankment Dams

Table B-C.1 Input data for rapid drawdown (undrained strength)

1					
Example	Problem C				
12	9	0	0	0	62.4
3	1				
430.0	180.0				
460.0	190.0				
465.0	190.0				
3	2				
100.0	70.0				
430.0	180.0				
459.5834	180.0				
3	3				
459.5834	180.0				
465.0	190.0				
470.0	190.0				
3	4				
400.0	70.0				
459.5834	180.0				
464.5834	180.0				
4	5				
464.5834	180.0				
470.0	190.0				
475.0	190.0				
515.0	110.0				
4	6				
405.0	70.0				
464.5834	180.0				
515.0	110.0				
535.0	70.0				
3	3				
475.0	190.0				
485.0	190.0				
540.0	80.0				
3	7				
485.0	190.0				
490.0	190.0				
710.0	80.0				
2	4				
540.0	80.0				
710.0	80.0				
5	8				
0.0	70.0				
100.0	70.0				
400.0	70.0				
405.0	70.0				
425.0	50.0				
4	8				
515.0	50.0				
535.0	70.0				
730.0	70.0				
1000.0	70.0				
2	9				
0.0	50.0				
1000.0	50.0				
0.0		40.0	125.0	0	0
0.0		40.0	72.6	0	0
0.0		35.0	122.0	0	0
0.0		35.0	67.6	0	0
500.0		28.0	126.0	0	0
300.0		28.0	72.6	0	0
0.0		35.0	125.0	0	0
0.0		25.0	65.6	0	0
400.0		29.0	62.6	0	0
0					
0					
0					
1					

Table B-C.1 Input data for rapid drawdown (undrained strength)

Rapid drawdown loading u/s (total stress)

7						
0.0	70.0					
100.0	70.0					
460.0	190.0					
490.0	190.0					
710.0	80.0					
730.0	70.0					
1000.0	70.0					
1						
1						
220.0	375.0	99999	0.0	15.0	100.0	70.0
0.0						
2.0	25.0	100.0	100.0	40	1	0.1
1						
2						

Table B-C.2 Output for rapid drawdown (undrained strength) – slice information

NO.	S L I C E		WEIGHT (LBS/FT)	COHESION (PSF)	FRICTION ANGLE (DEGS)	BIFUR. STRESS (PSF)	COHESION (PSF)	FRICTION ANGLE (DEGS)	PORE PRESSURE (PSF)	BOUNDARY FORCES AT SURFACE		CHARACTERISTIC SHAPES OF SIDE-FORCE INCLINATION	FACTOR OF SAFETY
	LEFT CENTER RIGHT	LEFT CENTER RIGHT								FORCE-LOCATION (LBS)	X		
1	100.00	70.00	0.	0.00	10.00	0.00	0.00	40.00	0.00	0.	0.00	1.000	1.000
2	107.04	67.41	4787.	0.00	25.00	0.00	0.00	25.00	0.00	0.	0.00	1.000	1.000
3	114.08	64.83	14320.	0.00	25.00	0.00	0.00	25.00	0.00	0.	0.00	1.000	1.000
4	128.38	60.31	23546.	0.00	25.00	0.00	0.00	25.00	0.00	0.	0.00	1.000	1.000
5	142.68	56.45	32369.	0.00	25.00	0.00	0.00	25.00	0.00	0.	0.00	1.000	1.000
6	157.53	51.25	40697.	0.00	25.00	0.00	0.00	25.00	0.00	0.	0.00	1.000	1.000
7	172.32	50.73	16332.	0.00	25.00	0.00	0.00	25.00	0.00	0.	0.00	1.000	1.000
8	177.58	50.00	51003.	400.00	29.00	0.00	400.00	29.00	0.00	0.	0.00	1.000	1.000
9	192.49	48.40	57792.	400.00	29.00	0.00	400.00	29.00	0.00	0.	0.00	1.000	1.000
10	207.47	47.48	53015.	400.00	29.00	0.00	400.00	29.00	0.00	0.	0.00	1.000	1.000
11	222.00	47.24	68365.	400.00	29.00	0.00	400.00	29.00	0.00	6.	0.00	1.000	1.000
12	234.99	47.59	73003.	400.00	29.00	0.00	400.00	29.00	0.00	0.	0.00	1.000	1.000
13	242.48	49.10	249.96	400.00	29.00	0.00	400.00	29.00	0.00	0.	0.00	1.000	1.000
14	256.19	49.31	262.42	400.00	29.00	0.00	400.00	29.00	0.00	0.	0.00	1.000	1.000
15	269.83	51.14	277.24	0.00	25.00	0.00	0.00	25.00	0.00	0.	0.00	1.000	1.000
16	284.60	53.76	291.95	0.00	25.00	0.00	0.00	25.00	0.00	0.	0.00	1.000	1.000
17	299.22	55.24	306.30	0.00	25.00	0.00	0.00	25.00	0.00	0.	0.00	1.000	1.000
18	313.68	58.86	320.87	0.00	25.00	0.00	0.00	25.00	0.00	0.	0.00	1.000	1.000
19	327.95	63.15	335.03	0.00	25.00	0.00	0.00	25.00	0.00	0.	0.00	1.000	1.000
20	337.52	65.62	340.00	0.00	25.00	0.00	0.00	25.00	0.00	0.	0.00	1.000	1.000
21	346.91	68.09	352.83	0.00	20.00	0.00	0.00	40.00	0.00	0.	0.00	1.000	1.000
22	357.83	69.05	360.60	0.00	20.00	0.00	0.00	40.00	0.00	0.	0.00	1.000	1.000
23	367.17	70.00	373.99	0.00	20.00	0.00	0.00	40.00	0.00	0.	0.00	1.000	1.000
24	380.61	72.90	387.06	0.00	20.00	0.00	0.00	40.00	0.00	0.	0.00	1.000	1.000
25	393.51	75.81	393.51	0.00	20.00	0.00	0.00	40.00	0.00	0.	0.00	1.000	1.000

Table B-C.2 Output for rapid drawdown (undrained strength) – slice information

NO.	S L I C E		WEIGHT (LBS/FT)	P A R A M E T E R S				PORE PRESSURE (PSF)	BOUNDARY FORCES AT SURFACE		CHARACTERISTIC SHAPES OF SIDE-FORCE INCLINATION	FACTOR OF SAFETY
	LEFT CENTER RIGHT	LEFT CENTER RIGHT		COHESION (PSF)	FRICTION ANGLE (DEGS)	BIFUR. STRESS (PSF)	COHESION (PSF)		FRICTION ANGLE (DEGS)	FORCE-LOCATION (LBS)		
	393.51	96.94									1.000	
24	396.76	99.02	32911.	0.00	10.00	0.00	0.00	40.00	0.00	0.	0.00	1.000
	400.00	101.09									1.000	
25	402.50	102.77	24707.	0.00	10.00	0.00	0.00	40.00	0.00	0.	0.00	1.000
	405.00	104.45									1.000	
26	411.09	108.82	57388.	0.00	10.00	0.00	0.00	40.00	0.00	0.	0.00	1.000
	417.18	113.19									1.000	
27	421.09	116.23	34501.	0.00	10.00	0.00	0.00	40.00	0.00	0.	0.00	1.000
	425.00	119.27									1.000	
28	426.50	120.49	12745.	0.00	10.00	0.00	0.00	40.00	0.00	0.	0.00	1.000
	428.01	121.71									1.000	
29	429.00	122.53	8250.	0.00	15.00	0.00	0.00	35.00	0.00	0.	0.00	1.000
	430.00	123.36									1.000	
30	433.65	126.50	29270.	0.00	15.00	0.00	0.00	35.00	0.00	0.	0.00	1.000
	437.30	129.63									1.000	
31	442.80	134.73	41501.	300.00	18.00	0.00	300.00	28.00	0.00	0.	0.00	1.000
	448.30	139.83									1.000	
32	453.56	145.18	36436.	300.00	18.00	0.00	300.00	28.00	0.00	0.	0.00	1.000
	458.82	150.52									1.000	
33	459.20	150.93	2505.	300.00	18.00	0.00	300.00	28.00	0.00	0.	0.00	1.000
	459.58	151.34									1.000	
34	459.79	151.56	1358.	300.00	18.00	0.00	300.00	28.00	0.00	0.	0.00	1.000
	460.00	151.79									1.000	
35	462.29	154.30	14115.	300.00	18.00	0.00	300.00	28.00	0.00	0.	0.00	1.000
	464.58	156.82									1.000	
36	464.79	157.05	1210.	300.00	18.00	0.00	300.00	28.00	0.00	0.	0.00	1.000
	465.00	157.29									1.000	
37	467.50	160.17	14489.	300.00	18.00	0.00	300.00	28.00	0.00	0.	0.00	1.000
	470.00	163.05									1.000	
38	471.82	165.23	10453.	300.00	18.00	0.00	300.00	28.00	0.00	0.	0.00	1.000
	473.64	167.42									1.000	
39	474.32	168.25	5716.	500.00	18.00	0.00	500.00	28.00	0.00	0.	0.00	1.000
	475.00	169.09									1.000	
40	478.19	173.17	13362.	500.00	18.00	0.00	500.00	28.00	0.00	0.	0.00	1.000
	481.38	177.25									1.000	
41	483.19	179.89	4558.	0.00	15.00	0.00	0.00	35.00	0.00	0.	0.00	1.000
	485.00	182.33									1.000	
42	486.16	183.74	1788.	0.00	15.00	0.00	0.00	35.00	0.00	0.	0.00	1.000
	487.32	185.36									1.000	
43	488.66	189.28	932.	0.00	15.00	0.00	0.00	35.00	0.00	0.	0.00	1.000
	490.00	189.79									1.000	
44	490.21	189.49	21.	0.00	15.00	0.00	0.00	35.00	0.00	0.	0.00	1.000
	490.41	189.79									1.000	

Table B-C.3 Output for rapid drawdown (undrained strength) – solution information

S O L U T I O N I N F O R M A T I O N
 FACTOR OF SAFETY = 2.262 (0 ITERATIONS)
 SIDE FORCE INCLINATION = -16.53 DEGREES

SLICE NO.	XAVG	TOTAL NORMAL STRESS (PSF)	NOMINAL SHEAR STRESS (PSF)	LINE OF THRUST			HORIZONTAL E-FORCE (LBS)	LENGTH (FEET)	SHEAR FORCE (LBS)	EFFECTIVE PHI REQD (DEGREES)	N/XCOS α	SHEAR ST/NORMAL ST
				X	YT(TOT)	FRACTION						
0				100.0	70.0	0.0000	0.			0.000		
1	100.0	0.	0.	100.0	70.0	0.4667	0.	0.00	0.00	16.533	1.843	0.371
2	107.0	451.	91.	114.1	69.5	0.4739	3640.	15.00	1394.08	16.533	1.505	0.206
3	121.2	1264.	265.	128.4	67.2	0.3590	13230.	15.00	3970.00	16.533	1.411	0.206
4	135.6	2019.	416.	142.0	65.9	0.3390	27058.	15.00	6241.65	16.533	1.331	0.206
5	150.2	2664.	539.	157.5	65.2	0.3332	43619.	15.00	8236.38	16.533	1.263	0.206
6	164.9	3227.	665.	172.3	65.1	0.3313	61585.	15.00	9976.31	16.533	1.206	0.206
7	174.9	3569.	736.	177.6	65.2	0.3313	68069.	5.32	3911.30	16.533	1.173	0.206
8	185.0	4017.	1161.	192.3	64.9	0.3149	91814.	15.00	17416.86	16.165	1.188	0.289
9	200.0	4388.	1252.	207.5	65.5	0.3095	114582.	15.00	18781.04	16.069	1.141	0.285
10	213.7	4674.	1322.	220.0	66.6	0.3082	132274.	12.54	16974.97	16.093	1.105	0.283
11	227.5	4904.	1378.	235.0	68.3	0.3080	151269.	15.00	20674.16	16.196	1.076	0.281
12	242.5	5100.	1427.	250.0	70.6	0.3084	167259.	15.00	21896.46	16.359	1.050	0.280
13	256.2	5234.	1459.	262.4	72.9	0.3090	178296.	12.54	18294.92	16.533	1.032	0.279
14	269.8	5282.	1085.	277.2	76.8	0.3189	182371.	15.00	16268.62	16.533	1.007	0.206
15	284.6	5320.	1097.	291.9	81.1	0.3282	182769.	15.00	18448.60	16.533	1.000	0.206
16	299.2	5329.	1098.	306.3	85.9	0.3279	179432.	15.00	16475.95	16.533	0.998	0.206
17	313.7	5291.	1091.	320.9	91.3	0.3492	172418.	15.00	16358.16	16.533	1.000	0.206
18	328.0	5208.	1074.	335.0	97.3	0.3635	161886.	15.00	16102.77	16.533	1.007	0.206
19	337.5	5133.	1058.	340.0	99.6	0.3696	157351.	5.32	5624.56	16.533	1.014	0.206
20	346.9	4925.	1827.	353.8	104.3	0.3615	154004.	15.00	27400.72	16.533	1.005	0.371
21	360.6	4682.	1737.	367.4	109.5	0.3551	147402.	15.00	26045.99	16.533	1.015	0.371
22	374.0	4405.	1634.	380.6	115.2	0.3493	137985.	15.00	24505.90	16.533	1.031	0.371
23	387.1	4098.	1520.	393.3	121.3	0.3434	126260.	15.00	22799.37	16.533	1.051	0.371
24	396.8	2852.	1429.	400.0	124.5	0.3400	119528.	7.70	11002.65	16.533	1.070	0.371
25	402.5	2694.	1370.	408.0	127.1	0.3370	113997.	6.02	8249.00	16.533	1.084	0.371
26	411.1	2440.	1276.	417.2	133.7	0.3272	99455.	15.00	19137.66	16.533	1.107	0.371
27	421.1	2133.	1162.	425.0	138.0	0.3178	89508.	9.90	11804.19	16.533	1.138	0.371
28	426.5	2958.	1097.	428.0	139.8	0.3131	85584.	3.87	4252.19	16.533	1.158	0.371
29	429.0	2938.	909.	430.0	141.0	0.3113	82555.	2.59	2361.04	16.533	1.195	0.310
30	433.7	2804.	869.	437.3	145.6	0.3027	71289.	9.63	8258.66	16.533	1.217	0.310
31	442.8	2592.	742.	448.3	153.2	0.2889	53012.	15.00	11127.89	13.477	1.278	0.286
32	453.6	2290.	671.	458.8	161.0	0.2684	35387.	15.00	10662.55	7.860	1.344	0.293
33	459.2	2122.	631.	459.6	161.6	0.2666	34339.	1.12	705.20	7.243	1.384	0.298
34	459.8	2104.	627.	460.0	161.9	0.2654	33660.	0.61	383.19	6.888	1.388	0.298
35	462.3	1964.	594.	464.6	165.5	0.2629	26502.	6.81	4044.19	1.972	1.406	0.303
36	464.8	1829.	563.	465.0	165.9	0.2628	25881.	0.63	352.47	0.815	1.425	0.308
37	467.5	1804.	557.	470.0	170.0	0.2596	18270.	7.63	4246.77	0.000	1.449	0.309
38	471.8	1752.	544.	473.6	173.5	0.2709	12590.	5.69	3099.74	0.000	1.491	0.311
39	474.3	1599.	597.	475.0	174.9	0.2774	10731.	2.15	1283.43	0.000	1.467	0.373
40	478.2	1166.	495.	481.4	180.7	0.2676	4376.	10.35	5126.66	16.533	1.467	0.429
41	483.2	729.	226.	489.0	184.3	0.2717	1634.	6.08	1372.40	16.533	1.632	0.310
42	486.2	440.	136.	487.3	186.8	0.3036	529.	3.98	541.23	16.533	1.676	0.310
43	488.7	192.	59.	490.9	188.9	0.0000	-47.	4.68	277.65	-16.533	1.716	0.310
44	490.2	28.	9.	490.4	189.8	0.0000	-60.	0.73	6.36	-16.533	1.743	0.310

AVERAGE FACTOR-OF-SAFETY = 2.262

SUM= 0.442E+06

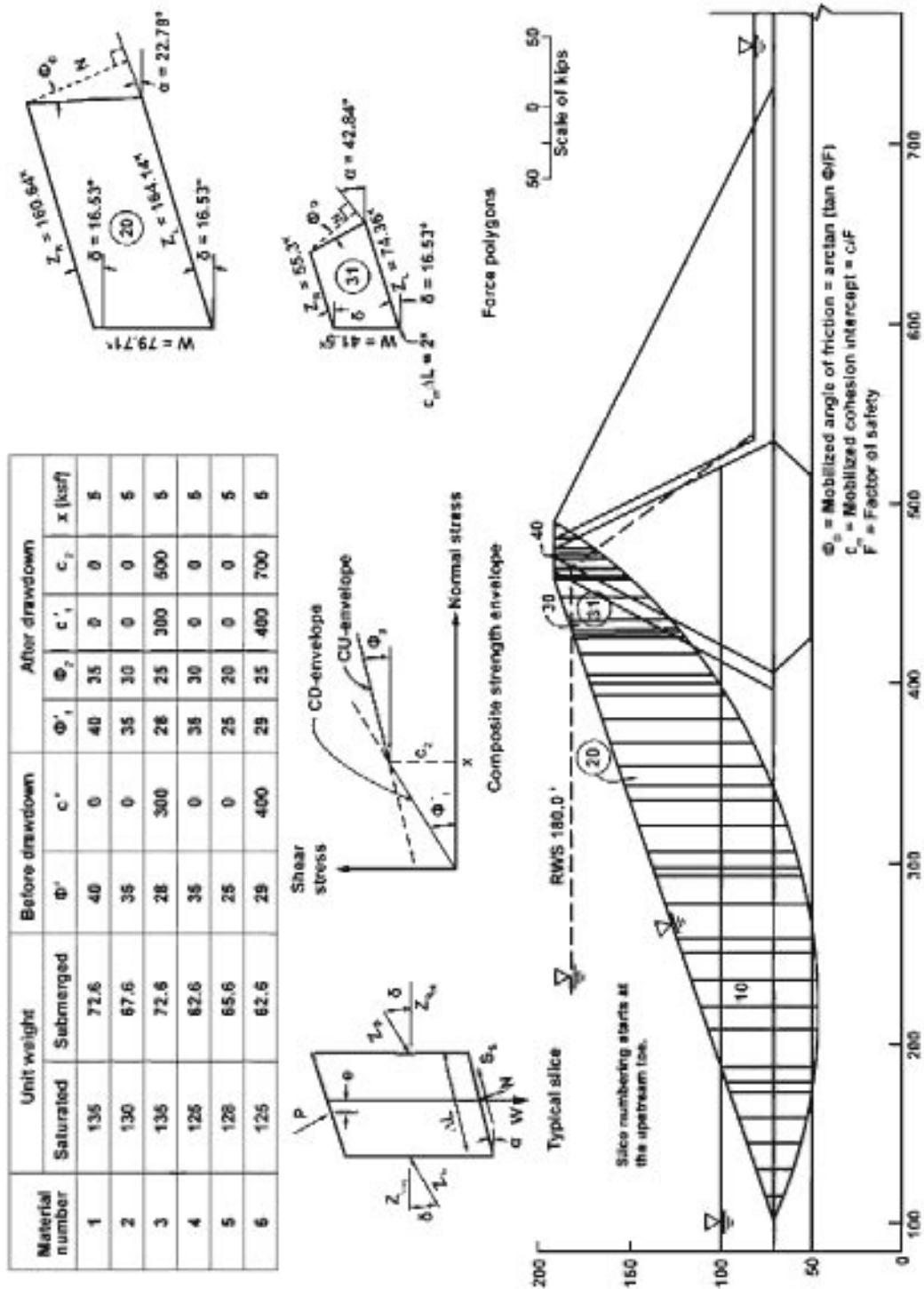


Figure B-5. Stability analysis of the upstream slope under rapid drawdown loading (undrained strength envelope concept).

Design Standards No. 13: Embankment Dams

Table B-C.4 Computation of factor of safety for after-drawdown condition

Slice	N _D	tan φ	N _D tan φ	cΔL	W	W sin α*
1	0.02	0.839	0.017		0.0	0.0
2	12.75	0.4663			4.78	-1.65
3	23.13	0.4663			14.32	-4.32
4	32.55	0.4663			23.55	-6.06
5	41.0	0.4663			32.37	-6.89
6	48.5	0.4663			40.7	-6.84
7	18.87	0.4663	82.44		16.33	-2.25
8	58.26	0.5543		6.0	42.01	-4.64
9	63.49	0.5543		6.0	58.66	-4.03
10	56.52	0.5543		5.02	68.79	-1.58
11	71.0	0.5543		6.0	0.2	0.0
12	74.0	0.5543	179.24	6.0	78.19	1.79
13	63.7	0.4663	29.7	8.78	86.72	5.95
14	77.94	0.364			78.39	8.66
15	79.05	0.364			99.94	15.2
16	79.47	0.364			105.65	20.83
17	79.2	0.364			110.3	26.67
18	78.3	0.364			113.85	32.55
19	27.45	0.364	143.40		116.31	38.32
20	72.23	0.839			41.62	14.92
21	69.0	0.839			117.61	45.55
22	65.22	0.839			116.93	50.17
23	60.99	0.839			115.17	54.13
24	29.54	0.839			112.39	57.3
25	22.2	0.839			41.79	22.43
26	51.71	0.839			14.49	7.92
27	31.23	0.839			42.53	23.69
28	11.56	0.839	347.1		91.51	53.23
29	7.78	0.700			38.66	23.44
30	27.72	0.700	24.85		28.09	17.41
31	40.56	0.5317			21.94	13.83
32	36.38	0.5317			64.01	41.54
33	2.54	0.5317			67.85	46.13
34	1.37	0.5317		15.75	55.98	39.9
35	14.37	0.5317			5.69	4.16
36	1.24	0.5317			22.13	16.38
37	15.12	0.5317			18.7	14.12
38	11.27	0.5317			15.08	11.62
39	3.91	0.5317		6.25	13.36	10.53
40	13.72	0.5317	74.69		4.56	3.66
41	5.11	0.7			1.79	1.45
42	2.02	0.7			0.91	0.75
43	1.04	0.7	5.72		0.02	0.02
			Σ887.2	Σ59.8		Σ685.99

* Additional resisting moments due to the boundary hydrostatic forces on the lower slices are neglected.

$$F = \frac{\sum N_D \tan \phi + \sum C\Delta L}{\sum W \sin \alpha} = \frac{887.2 + 59.8}{685.99} = 1.38$$

Example Problem D

Example problem D illustrates an analysis of the downstream slope of an embankment dam as shown on figure B-2 under steady-state seepage condition. Selected shear strength parameters and type of triaxial tests to obtain the parameters are shown on figure B-6. The input for the computer program is listed in table B-D.1 and the output is shown in tables B-D.2 and B-D.3. A free-body diagram of a typical slice and force polygons of two slices are illustrated on figure B-6. The maximum arc length of slices is limited to 15 feet. The factor of safety of the failure mass as shown in table B-D.3 is 1.443. By comparing with the required factor of safety of 1.5 (table 4.2.4-1), the downstream slope did not meet the minimum factor of safety criteria.

Design Standards No. 13: Embankment Dams

Table B-D.1 Input data for steady seepage condition

Example	Problem D	10	0	11	62.4
1					
12	9				
3	1				
430.0	180.0				
460.0	190.0				
465.0	190.0				
3	2				
100.0	70.0				
430.0	180.0				
459.5834	180.0				
3	3				
459.5834	180.0				
465.0	190.0				
470.0	190.0				
3	4				
400.0	70.0				
459.5834	180.0				
464.5834	180.0				
4	5				
464.5834	180.0				
470.0	190.0				
475.0	190.0				
515.0	110.0				
4	6				
405.0	70.0				
464.5834	180.0				
515.0	110.0				
535.0	70.0				
3	3				
475.0	190.0				
485.0	190.0				
540.0	80.0				
3	7				
485.0	190.0				
490.0	190.0				
710.0	80.0				
3	4				
540.0	80.0				
710.0	80.0				
1000.0	80.0				
5	8				
0.0	70.0				
100.0	70.0				
400.0	70.0				
405.0	70.0				
425.0	50.0				
4	8				
515.0	50.0				
535.0	70.0				
730.0	70.0				
1000.0	70.0				
2	9				
0.0	50.0				
1000.0	50.0				
0.0		40.0	125.0	0	0
0.0		40.0	135.0	0	5
0.0		35.0	122.0	0	0
0.0		35.0	130.0	0	5
500.0		28.0	126.0	0	0
300.0		28.0	135.0	0	5
0.0		35.0	125.0	0	5
0.0		25.0	128.0	0	5
400.0		29.0	125.0	0	5
0					
0					
0					

Table B-D.1 Input data for steady seepage condition

11							
0.0	70.0	6864.0	10				
100.0	70.0	6864.0	10				
430.0	180.0	0.0	10				
0.0	180.0		11				
430.0	180.0		11				
459.5834	180.0		11				
464.5834	180.0		11				
515.0	110.0		11				
540.0	80.0		11				
710.0	80.0		11				
1000.0	80.0		11				
1							
Steady seepage analysis							
6							
0.0	70.0						
100.0	70.0						
460.0	190.0						
490.0	190.0						
710.0	80.0						
1000.0	80.0						
1							
1							
650.0	375.0	99999	0.0	15.0	730.0	70.0	
0.0							
2.0	25.0	100.0	100.0	40	1	0.1	
1							
2							

Table B-D.2 Output for steady seepage condition – slice information

No.	S L I C E		I N F O R M A T I O N	WEIGHT (LBS/FT)	COHESION (PSF)	FRICTION ANGLE (DEGS)	BIFUR. STRESS (PSF)	COHESION (PSF)	FRICTION ANGLE (DEGS)	PORE PRESSURE (PSF)	BOUNDARY FORCES AT SURFACE		CHARACTERISTIC SHAPES OF	
	LEFT CENTER RIGHT	LEFT CENTER RIGHT									FORCE-LOCATION (LBS)	X	SIDE-FORCE INCLINATION	FACTOR OF SAFETY
1	408.13	172.71		9730.	0.00	10.00	0.00	0.00	40.00	306.65	3672.	412.59*	1.000	1.000
2	418.02	161.44		10285.	0.00	10.00	0.00	0.00	40.00	1387.4E	1299.	441.03*	1.000	1.000
3	425.00	154.69		10605.	0.00	10.00	0.00	0.00	40.00	1771.90	274.	426.67*	1.000	1.000
4	427.50	151.60		10645.	0.00	10.00	0.00	0.00	40.00	2176.79	0.	0.00*	1.000	1.000
5	430.00	149.11		10741.	0.00	15.00	0.00	0.00	35.00	2520.07	0.	0.00*	1.000	1.000
6	434.26	145.13		10431.	300.00	28.00	0.00	300.00	28.00	2911.34	0.	0.00*	1.000	1.000
7	438.52	141.12		10601.	300.00	28.00	0.00	300.00	28.00	3364.76	0.	0.00*	1.000	1.000
8	440.21	139.61		10431.	300.00	28.00	0.00	300.00	28.00	3524.71	0.	0.00*	1.000	1.000
9	441.99	138.11		10463.	300.00	28.00	0.00	300.00	28.00	3640.50	0.	0.00*	1.000	1.000
10	447.64	133.30		10331.	300.00	28.00	0.00	300.00	28.00	3737.84	0.	0.00*	1.000	1.000
11	453.19	128.48		10454.	300.00	28.00	0.00	300.00	28.00	3833.38	0.	0.00*	1.000	1.000
12	456.49	126.08		10081.	300.00	28.00	0.00	300.00	28.00	3977.16	0.	0.00*	1.000	1.000
13	459.58	123.67		10346.	300.00	28.00	0.00	300.00	28.00	4063.40	0.	0.00*	1.000	1.000
14	459.79	123.51		10205.	300.00	28.00	0.00	300.00	28.00	4207.31	0.	0.00*	1.000	1.000
15	460.00	123.36		10688.	300.00	28.00	0.00	300.00	28.00	4244.68	0.	0.00*	1.000	1.000
16	462.29	121.66		10406.	300.00	28.00	0.00	300.00	28.00	4375.06	0.	0.00*	1.000	1.000
17	464.58	119.96		10304.	300.00	28.00	0.00	300.00	28.00	4432.26	0.	0.00*	1.000	1.000
18	464.79	119.81		76975.	0.00	35.00	0.00	0.00	35.00	0.00	0.	0.00*	1.000	1.000
19	465.00	119.66		53556.	0.00	35.00	0.00	0.00	35.00	0.00	0.	0.00*	1.000	1.000
20	467.50	117.83		149795.	0.00	35.00	0.00	0.00	35.00	184.41	0.	0.00*	1.000	1.000
21	470.00	116.11		147761.	0.00	35.00	0.00	0.00	35.00	466.75	0.	0.00*	1.000	1.000
22	472.50	114.41		14435.	0.00	35.00	0.00	0.00	35.00	612.16	0.	0.00*	1.000	1.000
23	475.00	112.70		143244.	0.00	35.00	0.00	0.00	25.00	731.92	0.	0.00*	1.000	1.000
	480.00	109.50		68.54										
	485.00	106.30												
	487.50	104.80												
	490.00	103.29												
	496.55	99.64												
	503.10	95.99												
	509.05	93.02												
	515.00	90.04												
	521.42	87.18												
	527.85	84.31												
	531.42	82.85												
	535.00	81.40												
	537.50	80.93												
	540.00	79.48												
	547.09	77.04												
	554.18	74.60												
	561.37	72.49												
	568.57	70.38												
	569.29	70.19												
	570.00	70.00												
	577.30	68.27												
	584.60	66.54												

Table B-D.2 Output for steady seepage condition – slice information

NO.	S L I C E		I N F O R M A T I O N							PORE PRESSURE (PSF)	BOUNDARY FORCES AT SURFACE		CHARACTERISTIC SHAPES OF	
	X	Y	WEIGHT (LBS/FT)	COHESION (PSF)	FRICTION ANGLE (DEGS)	BIFUR. STRESS (PSF)	COHESION (PSF)	FRICTION ANGLE (DEGS)	FORCE-LOCATION (LBS)		X	SIDE-FORCE INCLINATION	FACTOR OF SAFETY	
	LEFT CENTER RIGHT	LEFT CENTER RIGHT												
	584.60	66.54											1.000	
24	591.97	65.16	137050.	0.00	25.00	0.00	0.00	25.00	925.99	0.	0.00		1.000	
	599.34	63.78											1.000	
25	606.77	62.79	128954.	0.00	25.00	0.00	0.00	25.00	1076.31	0.	0.00		1.000	
	614.20	61.72											1.000	
26	621.67	61.09	119604.	0.00	25.00	0.00	0.00	25.00	1192.55	0.	0.00		1.000	
	629.14	60.37											1.000	
27	636.63	60.06	107271.	0.00	25.00	0.00	0.00	25.00	1244.47	0.	0.00		1.000	
	644.12	59.74											1.000	
28	647.06	59.71	38516.	0.00	25.00	0.00	0.00	25.00	1266.03	0.	0.00		1.000	
	650.00	59.68											1.000	
29	657.50	59.86	88153.	0.00	25.00	0.00	0.00	25.00	1256.61	0.	0.00		1.000	
	660.99	60.04											1.000	
30	672.47	60.58	72584.	0.00	25.00	0.00	0.00	25.00	1212.12	0.	0.00		1.000	
	679.95	61.11											1.000	
31	687.40	62.00	53616.	0.00	25.00	0.00	0.00	25.00	1123.25	0.	0.00		1.000	
	694.85	62.89											1.000	
32	702.24	64.13	37504.	0.00	25.00	0.00	0.00	25.00	990.15	0.	0.00		1.000	
	709.64	65.38											1.000	
33	709.82	65.41	486.	0.00	25.00	0.00	0.00	25.00	910.42	0.	0.00		1.000	
	710.00	65.44											1.000	
34	717.33	67.09	24568.	0.00	25.00	0.00	0.00	25.00	808.39	0.	0.00		1.000	
	724.65	68.65											1.000	
35	727.32	69.32	7409.	0.00	25.00	0.00	0.00	25.00	666.17	0.	0.00		1.000	
	730.00	70.00											1.000	
36	730.00	70.00	5.	0.00	35.00	0.00	0.00	35.00	623.97	0.	0.00		1.000	
	730.00	70.00											1.000	
37	737.21	72.08	14848.	0.00	35.00	0.00	0.00	35.00	494.48	0.	0.00		1.000	
	744.41	74.15											1.000	
38	751.51	76.57	6340.	0.00	35.00	0.00	0.00	35.00	214.37	0.	0.00		1.000	
	758.61	78.98											1.000	
39	759.98	79.49	182.	0.00	35.00	0.00	0.00	35.00	31.81	0.	0.00		1.000	
	761.35	80.00											1.000	

Table B-D.3 Output for steady seepage condition – solution information

S O L U T I O N I N F O R M A T I O N
 FACTOR OF SAFETY = 1.443 (ITERATIONS)
 SIDE FORCE INCLINATION = 17.94 DEGREES

SLICE NO.	XAVG	TOTAL NORMAL STRESS (PSF)	NOMINAL SHEAR STRESS (PSF)	L I N E O F T H R U S T			HORIZONTAL E-FORCE (LBS)	LENGTH (FEET)	SHEAR FORCE (LBS)	EFFECTIVE PHI REDD (DEGREES)	N/WCOS α	SHEAR ST/NORMAL ST
				X	YT(TOT)	FRACTION						
0				408.1	172.7	0.0000	0.			0.000		
1	413.1	912.	61.	418.0	166.1	0.3187	10834.	15.00	915.16	17.936	2.130	0.582
2	421.5	1508.	302.	425.8	160.3	0.2567	23138.	10.13	3063.86	17.936	1.534	0.582
3	427.5	2692.	481.	430.0	156.3	0.2318	33771.	7.06	3411.20	17.936	1.394	0.582
4	434.3	3410.	717.	438.5	149.7	0.2669	54931.	11.69	6381.91	17.936	1.232	0.582
5	440.2	4187.	803.	441.9	147.2	0.1982	64781.	4.52	3654.17	17.936	1.283	0.485
6	447.6	5094.	1011.	453.4	139.1	0.1784	102203.	15.00	15166.49	13.122	1.239	0.464
7	456.5	6206.	1253.	459.6	134.9	0.1701	124293.	7.84	9838.20	11.861	1.194	0.442
8	459.8	6618.	1348.	460.0	134.7	0.1696	125823.	0.52	704.02	11.795	1.179	0.436
9	462.3	6862.	1394.	464.6	131.7	0.1680	142732.	5.70	7958.08	11.172	1.169	0.431
10	464.8	7097.	1444.	465.0	131.5	0.1678	144276.	0.51	744.25	11.021	1.159	0.430
11	467.5	7307.	1563.	470.0	128.4	0.1666	162382.	6.13	9598.82	9.403	1.146	0.425
12	472.5	7894.	1784.	475.0	125.5	0.1660	179632.	6.05	10792.88	9.501	1.123	0.417
13	480.0	8185.	2095.	485.0	120.1	0.1655	211088.	11.87	24878.55	12.176	1.094	0.409
14	487.5	8682.	2416.	490.0	117.6	0.1651	225147.	5.83	14058.69	13.200	1.071	0.401
15	496.8	8955.	2681.	502.1	111.5	0.1774	255407.	15.00	40204.99	15.301	1.048	0.389
16	509.1	9125.	2990.	515.0	106.5	0.1884	274101.	13.30	39772.73	16.796	1.025	0.396
17	521.4	9199.	3250.	527.6	101.7	0.2004	285135.	14.07	45731.16	17.936	1.010	0.394
18	531.4	9188.	3459.	535.0	99.7	0.2126	279921.	7.72	34418.23	17.936	0.994	0.485
19	537.5	9299.	3511.	540.0	98.4	0.2213	275116.	5.35	24152.99	17.936	0.995	0.485
20	547.1	9416.	3481.	554.2	95.1	0.2463	257711.	15.00	67193.57	17.936	0.997	0.485
21	561.4	9499.	3382.	568.6	92.4	0.2747	234690.	15.00	65730.21	17.936	1.005	0.485
22	569.3	9509.	3317.	570.0	92.2	0.2778	232111.	1.48	6402.30	17.936	1.011	0.485
23	577.3	9340.	2783.	584.6	88.3	0.2857	223819.	15.00	41723.08	17.936	1.005	0.321
24	592.0	9105.	2643.	599.3	84.9	0.2951	209991.	15.00	39644.52	17.936	1.014	0.323
25	606.8	8747.	2479.	614.2	82.0	0.3069	191154.	15.00	37180.84	17.936	1.027	0.323
26	621.7	8259.	2287.	629.1	79.7	0.3224	169126.	15.00	34301.62	17.936	1.045	0.323
27	636.6	7634.	2065.	644.1	78.1	0.3444	142038.	15.00	30972.78	17.936	1.068	0.323
28	647.1	7124.	1803.	650.0	77.6	0.3557	131239.	5.88	11132.35	17.936	1.088	0.323
29	657.5	6520.	1701.	665.0	76.8	0.3956	103464.	15.00	25514.37	17.936	1.110	0.323
30	672.5	5531.	1396.	680.0	76.8	0.4637	76667.	15.00	20935.74	17.936	1.146	0.323
31	687.4	4371.	1049.	694.9	77.5	0.5908	53259.	15.00	15740.80	17.936	1.186	0.323
32	702.2	3024.	687.	709.6	77.9	0.8477	36024.	15.00	9856.02	17.936	1.226	0.321
33	709.8	2267.	439.	710.0	77.9	0.8570	35707.	0.37	161.43	17.936	1.239	0.321
34	717.3	2038.	307.	724.7	77.7	0.7948	23358.	15.00	5958.18	17.936	1.272	0.323
35	727.3	1725.	342.	730.0	77.6	0.7562	19197.	5.51	1886.28	17.936	1.324	0.323
36	730.0	1779.	561.	730.0	77.6	0.7562	19193.	0.00	2.26	17.936	1.462	0.485
37	737.2	1448.	461.	744.4	79.0	0.8352	8514.	15.00	6941.18	17.936	1.522	0.485
38	751.5	665.	219.	758.6	79.9	0.9366	193.	15.00	3278.09	17.936	1.661	0.485
39	760.0	102.	34.	761.4	75.2	0.0000	0.	2.92	100.27	-17.936	1.761	0.485

AVERAGE FACTOR-OF-SAFETY = 1.443

SUM= 0.722E+06

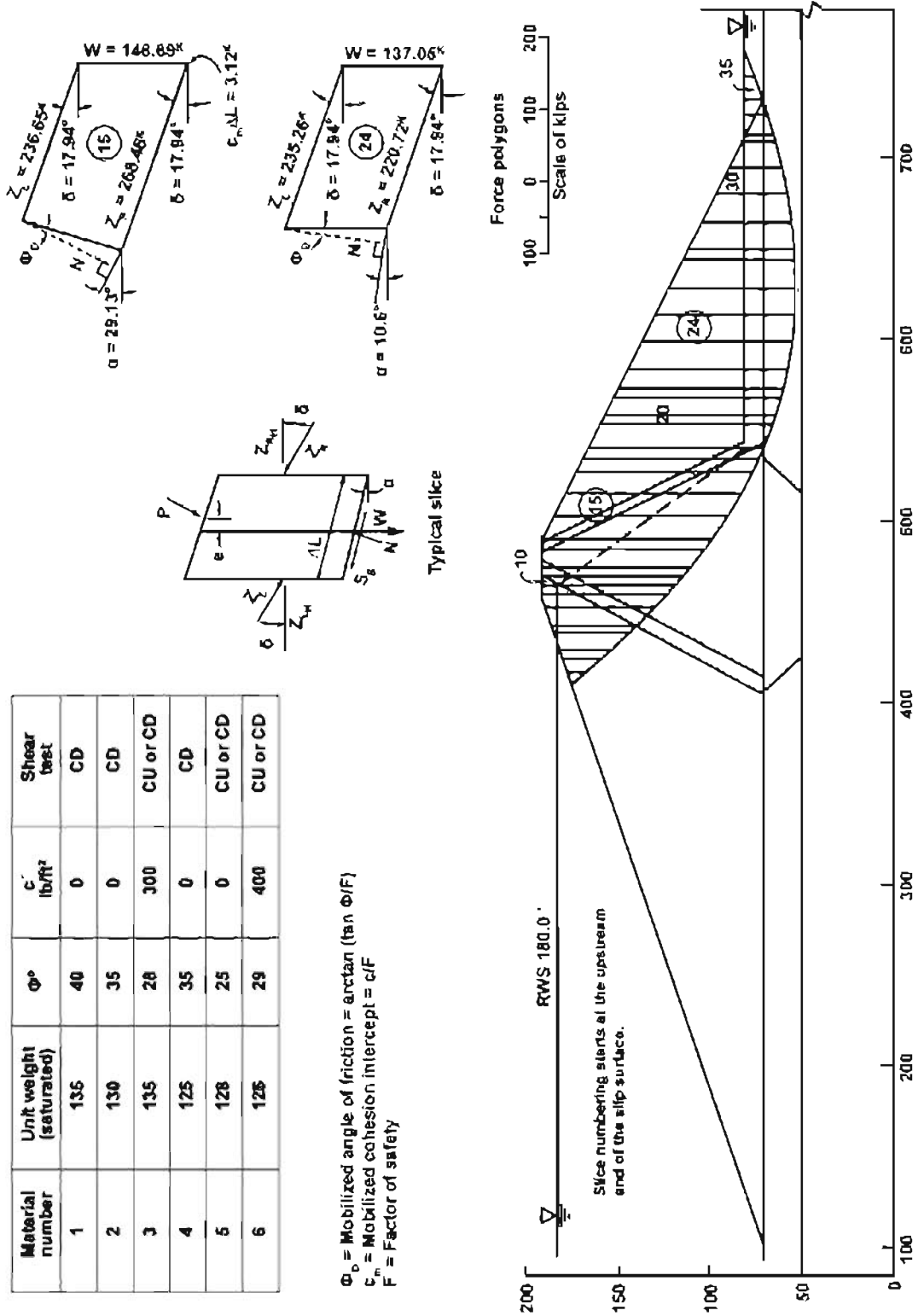


Figure B-6. Stability analysis of the downstream slope for steady-state seepage condition.

Appendix C

Computer Programs

Two-dimensional analysis using limit equilibrium method

In limit equilibrium method, only static equilibrium of slide mass is considered. In a given soil deposit, the slide mass geometry is defined by a shear surface. The material properties required for analysis are density or unit weight of soils and their shear strengths. Boundary conditions are generally included implicitly in the formulation of the equilibrium equations which are solved using numerical methods [17].

There are several procedures devised to solve a slope stability problem using the limit equilibrium method and some of these procedures have been implemented in computer programs to facilitate computations. The difference between various procedures relate to the assumptions that are made in order to achieve statical determinacy – some of these procedures satisfy only force equilibrium equations or only moment equilibrium equation, and others satisfy both force and moment equilibrium equations. Additional limitations of the various procedures apply to the geometry of the slip surface, i.e. circular, non-circular, log-spiral, etc.

The Bureau of Reclamation prefers use of slope stability analysis procedures which satisfy complete statics and accommodate general slip surface geometry - Spencer's procedure is one of them. It is similar to but simpler than Morgenstern and Price procedure which also satisfies complete statics but requires additional information (variations in interslice force inclination) not commonly available as a priori – Spencer's procedure assumes the inclination of interslice forces to be the same (i.e., parallel). The Bureau of Reclamation prefers use of Spencer's procedure for slope stability analysis.

There are several computer programs which implement Spencer's procedure – SSTAB2 [22] is one of them, developed at the Bureau of Reclamation by modifying SSTAB1 [24]; others include UTEXAS2 [25], UTEXAS3 [19], SLOPE/W [26], amongst others. All of these computer programs have been used in the Bureau of Reclamation with approval from line supervisors and managers.

Two-dimensional analysis using continuum mechanics method

In continuum mechanics method, force equilibrium and strain compatibility equations of engineering mechanics are considered and the differential equations relating forces and displacements in a solid are solved using numerical procedures. Unlike limit equilibrium based solution procedures for slope stability analysis, continuum mechanics based solution procedures require their adaptation for solving slope stability problems. Also, continuum mechanics based solution procedures require data for deformation properties (for elastic and plastic deformations) in addition to the data for shear strength parameters and material density or unit weight. Boundary conditions are explicitly stated as a part of the input data. In a continuum model, shear surface is not defined as a

Design Standards No. 13: Embankment Dams

priori – instead, it is determined as a part of the solution. The problem is solved successively using reduced values of shear strength parameters, c' and ϕ' , (by a scalar factor) until the model becomes unstable (i.e. the solution fails to converge). The scalar factor for reduction in shear strength parameters for which the numerical model becomes unstable is taken as the factor of safety and the interface between the elements undergoing displacements and elements with virtually no-displacements is taken as the shear surface.

There are several procedures devised to solve the force-displacement equations of engineering mechanics. In Reclamation, finite element and finite difference based solution procedures are commonly used.

For slope stability analysis, when needed, we use finite difference based computer program FLAC [27] for continuum mechanics based slope stability analysis. The same problem is also analyzed using the limit-equilibrium based Spencer's solution procedure and computed factor of safety and associated shear surface results are compared.

Engineering judgments are used in deciding relevance of the results to the project and issues of interest/concern.

Three-dimensional analysis using limit equilibrium and continuum mechanics methods

Stability of natural or manmade slopes is affected by its lateral extent in the third dimension. Three-dimensional solution procedures are extensions of their two-dimensional counterparts, and use the same solution strategies. However, the addition of the third dimension increases the complexity of the problem solving methodologies.

For the limit-equilibrium based solution, we use computer program CLARA-W [28] for 3-dimensional slope stability analysis. CLARA-W has 3D extension of Spencer's procedure. The same problem is also analyzed in 2-dimensions using the limit-equilibrium based Spencer's solution procedure and results compared.

For the continuum mechanics based solution, we use finite difference based computer program FLAC3D [29] for 3-dimensional slope stability analysis. FLAC3D is a 3D extension of FLAC program.

Engineering judgments are used in deciding relevance of the results to the project and issues of interest/concern.

Note: There are other commercially available computer programs based on limit equilibrium and continuum mechanics methods which can be used for static stability analyses. The programs named herein have been used in Reclamation

and their inclusion is for convenience; however, no endorsement or recommendation of their use is implied.

Appendix D

Guidance Papers for Static Stability Analyses

- Part 1* The Place of Stability Calculations in Evaluating the Safety of Existing Embankment Dams
- Part 2* Suggestions for Slope Stability Calculations
- Part 3* Variable Factor of Safety in Slope Stability Analysis
- Part 4* On the Boundary Conditions in Slope Stability Analysis
- Part 5* An Automated Procedure for 3-Dimensional Mesh Generation
- Part 6* Average Engineering Properties of Compacted Soils from the Western United States
- Part 7* Strength, Stress-Strain and Bulk Modulus Parameters for Finite Element Analyses of Stresses and Movements in Soil Masses

Each of these documents is self-explanatory, and no additional comments are considered necessary.

Appendix D

Part 1 The Place of Stability Calculations in Evaluating the Safety of
Existing Embankment Dams
by Ralph B. Peck

This article was published in the *Civil Engineering Practice, Journal of the Boston Society of Civil Engineers Section/ASCE*, Volume 3, Number 2, pp. 67-80, 1988. It is reproduced here with permission of the publisher.

CIVIL ENGINEERING PRACTICE •

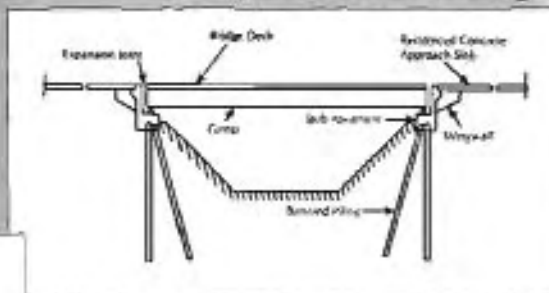
JOURNAL OF THE BOSTON SOCIETY OF CIVIL ENGINEERS SECTION/ASCE

FALL 1988

VOLUME 3, NUMBER 2

ISSN: 0886-9685

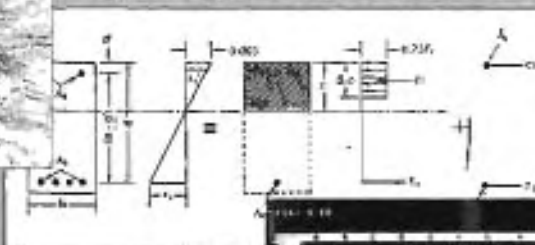
Integral Abutment Bridges



Early Iron Bridges



Lightweight Concrete Roof Slabs



Engineering Design Using Spreadsheets



Also in This Issue:

Electron Inactivation of Pathogens
Concrete Formwork
BSCES Honorary Members



Existing Embankment Dam Safety

The Place of Stability Calculations in Evaluating the Safety of Existing Embankment Dams

Thorough investigations of site conditions and construction records should have precedence over stability analyses for determining the safety of embankment dams.

RALPH B. PECK

THE PURPOSE of evaluating the safety of an existing embankment dam is to ensure that the catastrophic loss of the reservoir will not occur. Many reports in which the safety of existing dams is evaluated relate the safety to the results of stability analyses. Yet, seismic considerations aside, stability analyses are often irrelevant and may even be misleading.

To be sure, one of the great achievements of soil mechanics has been the development of

limit-equilibrium methods of stability analyses. Every soils student learns about them. Sophisticated computer programs exist for carrying them out. They have an important place in embankment dam engineering, primarily in design, but they can be misleading in evaluating dam safety if too much dependence is placed on the numerical values of factors of safety derived from them.

Purposes of Stability Analysis in Design

Before the implications of stability analyses with respect to the safety of existing dams can be considered, the ways in which such analyses are useful in design should be reviewed. The discussion herein is limited to limit-equilibrium analyses. Other techniques are required for investigating seismic behavior and liquefaction.

In practice, the slopes for embankment dams are not chosen on the basis of stability calculations; they are chosen by precedent. The initial

selection is based on the designer's judgment that takes into account foundation conditions, economics, the availability of materials, logistics and a whole series of technical and non-technical considerations. Having tentatively selected both exterior and interior slopes, the designer carries out stability analyses to ensure that conventional factors of safety are achieved. This application of stability analyses is a legitimate step in design.

Furthermore, inasmuch as every embankment dam differs in some respect from any other, it is useful to have a basis for comparing the proposed dam with others whose performance is known. Factors of safety provided by stability analyses for the proposed design and for existing dams constitute such a basis.

Moreover, stability analyses are valuable in comparing the efficiencies of various arrangements of the zoning of the dam. The analyses can provide insights regarding the relative merits and economies of placing superior or inferior materials of different costs in different parts of the embankment.

Stability analyses assist greatly in avoiding shear failures during construction. Many dams have experienced upstream or downstream sliding failures during construction because of weak seams in the foundation. Such failures can often be predicted and avoided by careful investigation and appraisal of the foundation conditions and appropriate equilibrium analyses.

In addition, failures during construction have been known to occur as a consequence of pore pressures induced in relatively impervious zones by the addition of fill. These failures can be predicted by suitable equilibrium analyses combined with investigations of pore-pressure coefficients in the relevant materials and studies of the rates of dissipation. These failures also can be avoided by implementing a monitoring program that ensures that sufficient dissipation of excessive pressures occurs by instituting appropriate waiting periods during filling.

Finally, stability analyses are used to provide assurance that a dam will not fail under operating conditions. A large enough factor of safety is specified to guard against downstream sliding under a full reservoir and, in addition, an

appropriate factor of safety is specified against an upstream failure resulting from rapid draw-down.

All these uses of stability analyses are legitimate parts of design. They require knowledge of foundation conditions and of the pertinent properties of the various materials involved. The necessary information from the field and the analyses are usually developed in successive steps of increasing refinement.

Stability Analyses of Existing Dams

The application of stability analyses in the design phase makes use of idealized or generalized soil properties, assumed known geometries and idealized surfaces of sliding. In contrast, if the factor of safety of an existing embankment dam is to be determined correctly, facts rather than idealizations are needed. Obtaining these facts is no simple task.

First, both the external and internal geometry of the dam must be ascertained, which may be difficult if reliable as-built drawings of the dam are not available. Second, the properties of the materials need to be determined, either from good records as they were actually placed or by investigation. The geometry of the surface of sliding can be determined by measurements if possible, or it can be established realistically from knowledge of the subsurface conditions. The shear strengths have to be ascertained in terms of effective-stress parameters along the surface of sliding including that portion of the surface within the foundation. The pore pressures on the actual surface of sliding (or on the potential surface of sliding if the actual one is not known) must be determined as well.

All these data are at best expensive to evaluate realistically, and in many instances may be impractical to determine. Obtaining them may necessitate exploratory work within and beneath the dam, itself often an undertaking detrimental to the safety of the dam.

Indeed, it is fair to say that if good construction records are unavailable, it may be impractical or virtually impossible to get adequate data for calculating the factor of safety reliably. However, this limitation is only one of several considerations leading to the conclusion that stability analyses may be irrelevant or mislead-

ing with respect to predicting the safety of an existing dam.

Failure of Embankment Dams

Embankment dams can fail either catastrophically or non-catastrophically. A catastrophic failure of whatever nature is defined as one that results in the uncontrolled loss of the reservoir with consequent loss of life and damage to property. It is the avoidance of catastrophic failures that justifies the authority given to regulatory bodies to require assessments of dam safety and to mandate remedial measures where safety appears to be questionable or inadequate. It is the legitimate goal of government, through regulatory bodies, to avoid future St. Francis (California), Teton (Idaho), Johnstown (Pennsylvania) or Baldwin Hills (California) catastrophes. Non-catastrophic failures, which may be expensive, annoying or embarrassing, should also be avoided. Owners of dams may be well advised to evaluate the probability of such failures and to take steps to prevent them. Yet, since their consequences fall far short of the calamities associated with the flood following a catastrophic failure, they fall outside the domains of public safety and the regulatory powers of government, and they do not fall within the scope of this study.

Catastrophic failures have one of four causes: overtopping, piping by backward erosion, liquefaction, or downstream sliding at high reservoir (possibly associated with toe failure due to piping by heave). The first three of these types of failures — overtopping, backward erosion and liquefaction — cannot be predicted by stability analyses. Hence, the legitimate application of stability analyses to catastrophic failure is restricted to downstream sliding, with or without loss of toe support, when there is enough water in a reservoir to do catastrophic damage if released.

Non-catastrophic failures can occur by downstream or upstream sliding, including sliding originating in the foundation, when there is no pool or when the pool is so small that its release is inconsequential. In addition, failures can occur by rapid drawdown, but such failures are not in themselves catastrophic even if the reservoir contains a high pool.

Rapid drawdown has led to significant

damage in a number of instances, but there appears to be no record of catastrophic loss of a reservoir resulting from this mode of failure. Therefore, it is not included as a cause of catastrophic failure. However, the potential for catastrophic failure exists if a rapid drawdown slide could block outlet works and if spillway capacity would be inadequate to prevent overtopping in the event of such blockage. Under these circumstances the potential for a rapid drawdown requires assessment.

Critical Periods for Sliding

If an embankment dam were to fail under conditions that could be appropriately defined by a limit-equilibrium analysis, it would do so at one of three critical periods. The first of these is during construction. As the embankment rises, the factor of safety against a slope failure, and particularly against foundation failure, decreases. Such a slide would not be catastrophic unless the pool had been allowed to rise against the embankment as it was being placed. Under these circumstances, whatever pool had been accumulated might escape and cause flooding.

The second critical period is the first filling of the reservoir. If the dam survives the initial filling and if there is no blowup at the toe, the dam can be considered safe (in effect, proof-tested) against failure by piping due to heave.

The third critical period is achievement of maximum pore pressure under a full reservoir. If the dam has not failed when this condition has been reached, its safety against downstream slope failure has been demonstrated. Under many circumstances, including the presence of relatively thin cores or ample well-drained downstream shells, pore-pressure maxima follow so rapidly after the first filling that the survival of the first filling can be considered to be a demonstration of the ultimate safety of the dam under full-reservoir conditions. However, if the impervious section of the dam is thick and impermeable enough to create a time lag between the rise of the reservoir and the rise of piezometric levels in the core or supporting downstream zones, pore-pressure equilibrium may not occur for several years after the reservoir is first filled and the critical period may be delayed. So-called

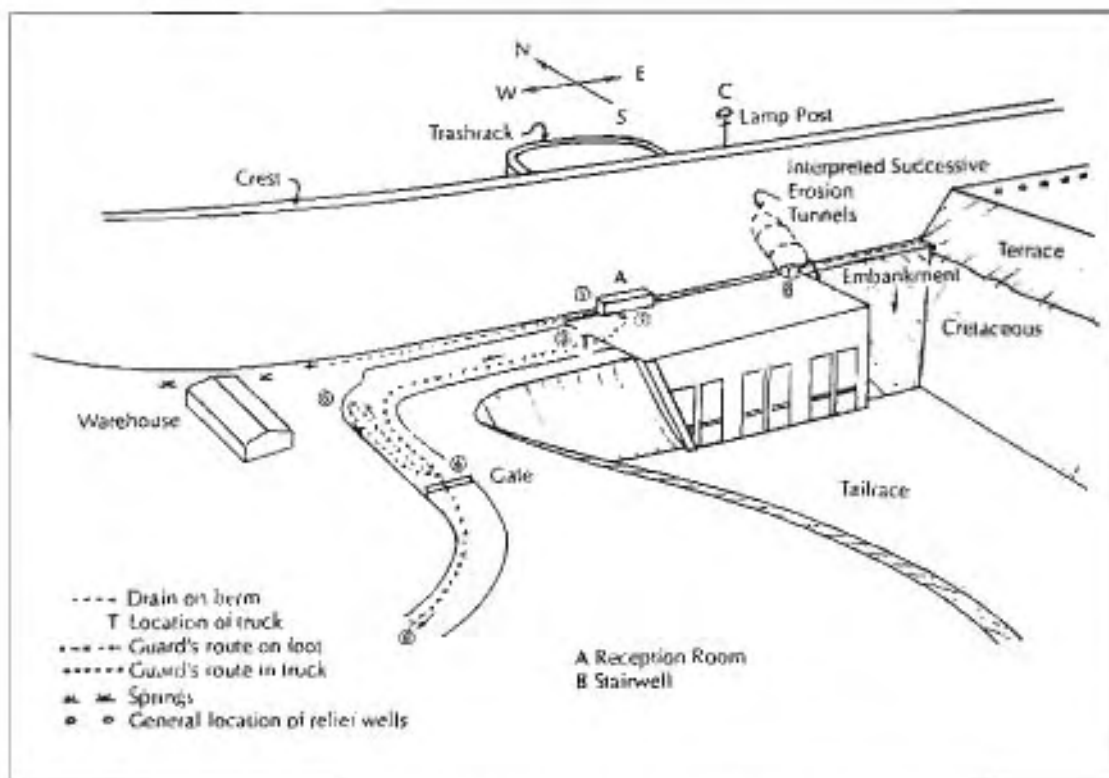


FIGURE 1. Principal features of the Walter Bouldin Dam as related to its failure.

homogeneous dams, especially in regions of high intensity of rainfall, are potentially vulnerable, and at least one failure, a small dam near Ponce, Puerto Rico, has occurred under these conditions.

In principle, it remains generally correct to postulate that if a dam survives the first filling and the corresponding pore-pressure increases under the filled condition, its safety against failure of the downstream slope has been demonstrated. There is one possible exception to this statement.

If the factor of safety is so close to unity that cyclic loading by the pool causes strain softening and critical loss of strength, the factor of safety may decrease. Aside from this special case, surviving the first filling and corresponding pore-pressure increase ensures that the dam is safe against catastrophic failure by any mode to which an equilibrium analysis is applicable.

Failure of Walter Bouldin Dam

Notable for its absence from the listed causes of catastrophic failure is upstream sliding leading

to overtopping. Yet, the official cause of failure of Walter Bouldin Dam in Alabama, as set forth in reports of the Federal Power Commission, is an upstream slide that occurred without preceding drawdown and that breached the crest of the dam.^{1,2,3} The failure resulted in loss of the reservoir within a few hours.

It is important to the profession and to the public that the failure of Walter Bouldin Dam be correctly explained, as it would otherwise be necessary to include upstream sliding as a cause of catastrophic failure. In this case, the failure was clearly the result of subsurface erosion. The official reports and other sources can be consulted for details about the dam and of the investigations after the failure.⁴ The investigations disclosed shortcomings in both design and construction. However, these shortcomings were not responsible for the failure. The investigators did not ignore the possibility of piping, but they concentrated their attention with respect to piping on zones where seepage had been noted and extensive observational and control measures had been

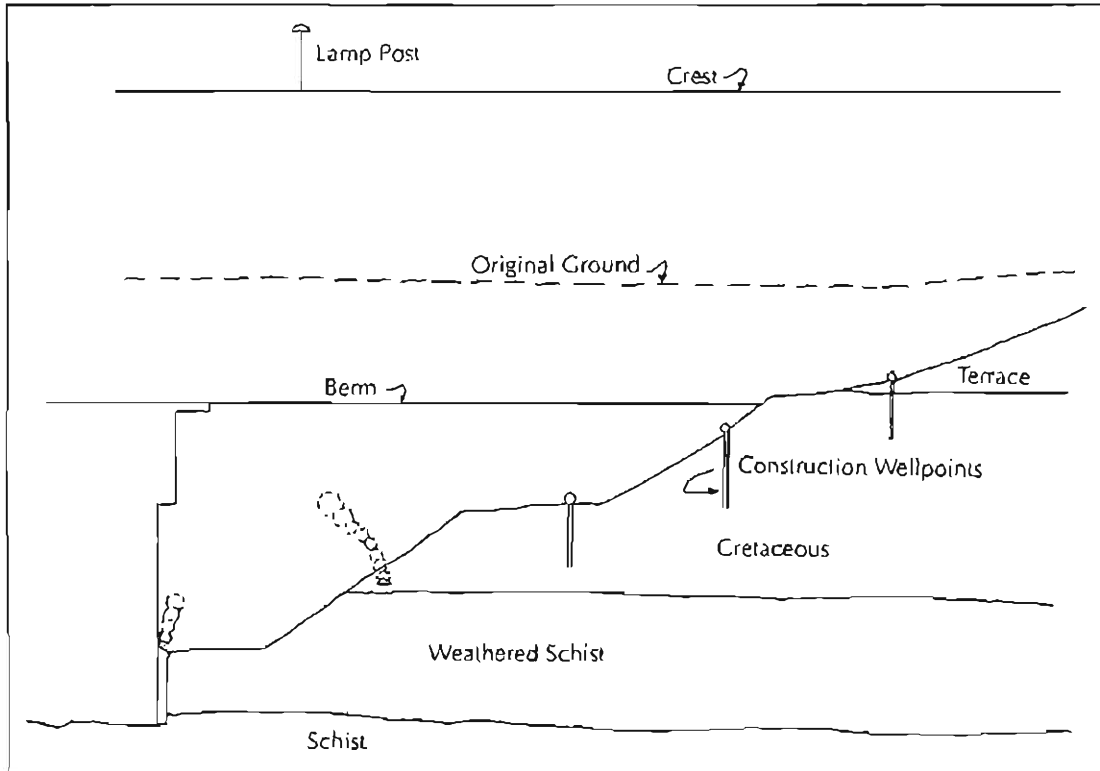


FIGURE 2. Longitudinal section through the east end of the Walter Bouldin power house and the junction with east wing dam.

established. They discounted the likelihood of piping at a lower elevation where it probably occurred.

The essential features of the project included an earth dam about 165 feet high across the deepest part of a valley, flanked on the west and east by wing dams founded on Pleistocene terrace deposits at a higher level. A power house was embedded in the downstream slope of the highest part of the dam; the roof of the power house was at the same elevation as a berm on the downstream slope. The power house's foundation extended into Precambrian schist bedrock overlain by Cretaceous sediments consisting largely of slightly cohesive sands and silts with layers of stiff clay. Beneath the wing dams these sediments were overlain in turn by the terrace deposits. The relationships are shown diagrammatically in Figure 1. Figure 2 depicts a longitudinal section of the area through the east end of the power house and its junction with the east wing dam; it shows the excavation made through the Cretaceous soils

into the schist to reach suitable foundation support for the power house raft.

There was one eyewitness to the events leading up to the failure: Mr. Sanford, the night guard. He was interrogated many times in the course of the ensuing investigation and recounted a remarkably consistent series of recollections. As a non-technical person, he had no hypotheses about the causes of failure and apparently had no reason to report other than what he experienced.

The chronology of Sanford's activities on the cloudy, moonless night of the failure can be traced with reference to Figure 1, a simplified sketch of the power house and dam as seen from downstream. He went on duty about 9:45 p.m., made his first routine inspection starting at his office in the reception room (A) at the northwest corner of the roof of the power house, and returned about midnight without having observed anything unusual. After reading the Sunday paper for some time in the reception room, he glanced out a west window



FIGURE 3. Development of erosion tunnel through Teton Dam. (USBR photo.)

(1) and noticed that the paved gutter along the north edge of the roof was running nearly full of muddy water. He was unable to see the drain or embankment directly north of the reception area, because there were no windows on that side of the building. Recognizing that something was wrong, he called his supervisor. The time was 1:10 a.m. Before he completed his brief call, water was coming beneath the door into the room. At first, it was one or two inches deep, but it quickly became deeper.

By this time he had decided to leave. As he did so, he looked around from (2) and saw that muddy water was now flowing over the powerhouse roof, apparently gushing from the northeast corner near the back stairwell (B). He waded through water, now 4 to 6 inches deep, to his truck (T) and drove from (3) to the gate (4). At (4) he got out of the truck, opened the gate, and looked back for a few minutes. He observed that the light (C), which was located 26 feet east of the power house on the crest of the dam, was illuminated, but he could not observe many other details of the dam because of the intervening switchyard and other objects. He thought he saw a cavity behind the stairwell and mist rising behind it, possibly from beyond the crest of the dam.

He then noticed that the water on the road and on the powerhouse roof was getting shallower, so he decided to walk back for a closer look. He stopped (5) in front of the warehouse and while standing there heard rocks begin to fall on the roof and on some of the equipment it supported. There was then an electric flash and the lights went out, including the one at (C). The clock in the control room was later found to have stopped at 1:33 a.m., about 23 minutes after Sanford's phone call to his supervisor. Shortly thereafter, other plant personnel arrived; by that time they could see, with the aid of their automobile lights, that a gap existed in the crest of the dam and that water was pouring through.

Sanford's account is fully compatible with the progressive collapsing of the roof of an erosion tunnel that had penetrated through the dam at the east end of the power house, as suggested schematically in Figure 1. When the elevation of the tunnel reached that of the berm, water was able to flow over the power house roof. As erosion progressed, one of the successive collapses partially blocked the tunnel and the flow decreased, prompting Sanford to return as far as the warehouse. The final collapse, accompanied by falling riprap, breached

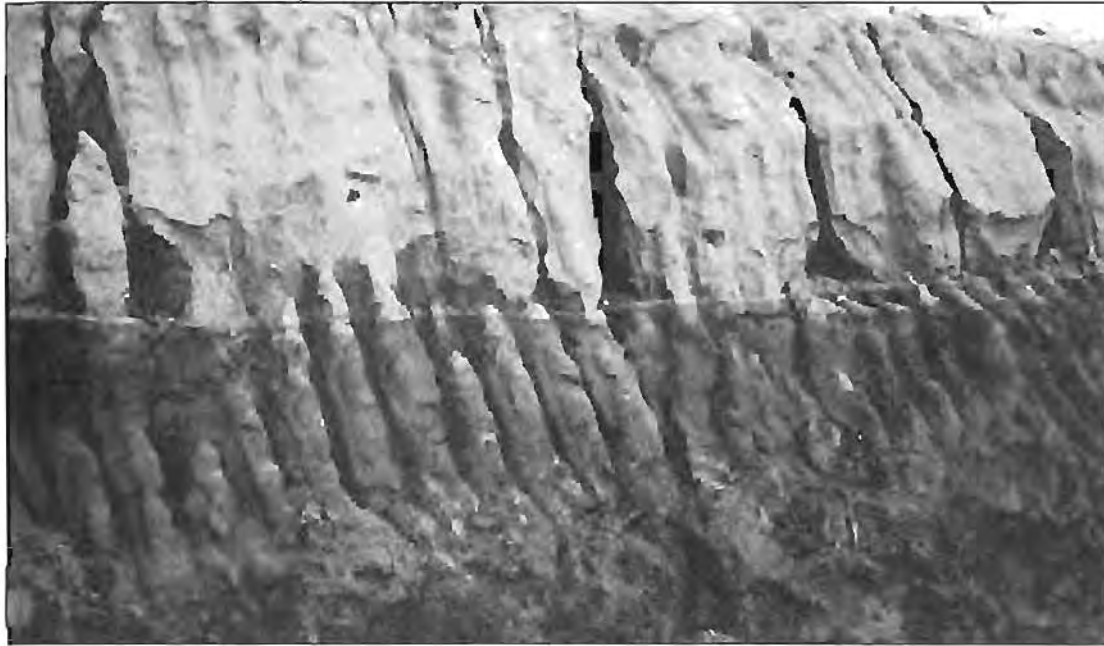


FIGURE 4. Erosion of cut slope in Cretaceous soils during Bouldin Dam reconstruction.

the crest. The similarity of the events to the development of the erosion tunnel through Teton Dam is evident (see Figure 3).

The official reports concluded that the failure started as an upstream slide extensive enough to breach the crest to a level below the reservoir surface, whereupon the water flowed through the gap and initiated the erosion. This scenario is incompatible with Sanford's account. Foremost among the facts that cannot be explained by the upstream slide hypothesis is that the light at the crest of the dam, located where the gut ultimately developed, remained illuminated for more than 20 minutes after muddy water began to flow over the roof of the power house. Had overtopping occurred through a slide-produced gap, the lamp post or its power supply cables would have been among the first casualties, and the events described by Sanford would have taken place in the dark. Furthermore, the temporary decrease in the flow that he observed when he reached the gate is characteristic of blockage caused by collapse of material overlying a tunnel, whereas the flow through an open channel would only have increased with time. It is also noteworthy that the horizontal thickness of the dam at the water line was some 64 feet. To allow

the reservoir to escape, a slide would have had to extend upstream at least this distance. The extent of such a slide parallel to the axis of the dam would have had to be of comparable magnitude, several times greater than the 26 feet from the end of the power house to the lamp post at (C). Thus, the crest light would have disappeared with the first earth movement. Yet, it continued to function for at least twenty minutes after the dam was releasing water.

From the time that Sanford first detected trouble, his description fits the classic mechanism of the upward development of an erosion tunnel. The scenario would not be complete, however, unless a set of physical conditions existed that would permit the initial undetected development of such a tunnel. The official reports correctly noted that seepage was expected by the designers and had occurred extensively at the downstream toes of the east and west wing dams where they rested on permeable terrace deposits. Relief wells had been installed, along with other remedial and observation works, to control the seepage. Indeed, the record is replete with references to the attention given to the prevention of piping at and above the Tertiary-Cretaceous interface. The investigators, however, discounted the



FIGURE 5. Erosion tunnel at the contact of two layers of Cretaceous soils in excavation at the Bouldin damsite. Note the vertical joint in the cohesive gravelly material.

possibility of piping in the underlying Cretaceous materials, although these materials contained many slightly cohesive, highly erodible sands and silts (see Figures 4 and 5).

The foundation raft of the power house was cast inside formwork in an excavation extending a few feet into somewhat weathered schist underlying the Cretaceous beds. An approximate section through the edge of the raft and adjacent materials is shown in Figure 2. The geometry of the backfilled zone would have favored seepage along its boundaries. Seepage could also have developed readily through the joints and more pervious zones in the Cretaceous deposits. Indeed, the excavation for the power house and intake structure required dewatering by well points; three tiers were installed, the lower two of which were entirely in the Cretaceous beds. Thus, avenues for

seepage were undoubtedly present. Backward erosion could have gone unobserved below tailwater level for a long time until finally an erosion tunnel reached the reservoir and permitted concentrated destructive flows to cause rapid enlargement and failure.

The course of events before the tunnel reached the level of the power house roof is speculative, but the existence of conditions favorable to the development of a tunnel by backward erosion is not. Neither are the events observed after the tunnel reached the level of the power house roof. The conclusion seems inescapable that failure actually occurred by piping, and that any supposed shortcomings in the construction of the embankment, even if they existed, were irrelevant.

The official reports postulate an upstream slide without the destabilizing influence of a drawdown. This explanation in itself is logically questionable. An earlier shallow drawdown slide in the steep upstream slope had occurred, however, and had been repaired by dumping crushed stone and rockfill in the affected area. The investigators reasoned that the strength of the clayey materials under the dumped fill had gradually deteriorated as their moisture content increased, and that at the time of failure the strength had reduced to the extent that the slide was reactivated. This hypothesis, like that of any upstream slide, is incompatible with the events recounted by Sanford and with the extent of a slide that would have been required to lower the top of the dam below reservoir level.

In short, the failure of Walter Bouldin Dam occurred because of piping by backward erosion. As no other example of catastrophic failure and loss of reservoir has been attributed to an upstream slide, it may be concluded that a dam that has successfully survived construction will not experience a catastrophic upstream slope failure. Any analysis that indicates otherwise must be erroneous. Further, a stability analysis to investigate the safety of the upstream slope under full reservoir is irrelevant. If an upstream slope does not fail during construction, its factor of safety must exceed unity under the more favorable condition of reservoir loading. Rapid drawdown may induce a failure, but such a failure is shallow and has never been known to cut back into

the embankment far enough to permit overtopping and cause the catastrophic loss of a reservoir.

There is a remote possibility that a dam consisting of fine-grained soils possessing shear strength due to capillarity, or containing stiff cohesive materials susceptible to swelling, may lose strength when submerged if the thickness of stable upstream shell material is inadequate. The upstream slopes of dams containing such materials are usually fairly flat and failure surfaces would tend to be shallow, with consequences similar to those of drawdown failures. Again, no catastrophic failure of this type is known.

If Walter Bouldin Dam is eliminated from the category of failure by upstream sliding, then it may be concluded that once a reservoir has been filled and the associated pore-pressure increases have been achieved, the factor of safety is at least equal to unity with respect to limit-equilibrium conditions, and that any calculation showing a factor of safety less than unity must be in error.

Downstream Slope Failures

The factor of safety of a dam that survives its first filling and the associated increases in pore pressure will increase with time, unless this factor of safety is so close to unity that cyclic loading produced by fluctuations in the level of the pool causes strain softening and a critical loss of strength. If, however, the factor of safety is indeed so close to unity, downstream slope failure will be preceded by progressive and increasing increments of movement at successive full pool levels. Any calculation showing a factor of safety appreciably different from unity under these conditions must be erroneous. Stability calculations are thus irrelevant in assessing the safety of such a structure; observations of movement must take their place. If successive periods of full reservoir are accompanied by decreasing increments of movements, the stability of the structure is increasing. If the contrary occurs, the stability may be decreasing. Stability calculations may be useful in judging the influence of various remedial measures, but the computed magnitudes of the factor of safety are meaningless. An outstanding example of the irrelevance of

stability calculations under conditions of decreasing increments of movement is Gardiner Dam on the South Saskatchewan River in Canada. The case of this dam illustrates the limitations of equilibrium stability analyses.

Behavior of Gardiner Dam

Conception, design and construction of Gardiner Dam took place during the quarter century in which understanding of shear strength was undergoing its most radical revisions, and at each step in the evolution of the design the geotechnical studies reflected the new frontiers of knowledge. The following history is greatly abbreviated, perhaps beyond tolerable limits, but since the project has been exceptionally well documented, the interested reader can readily learn the details.^{5,6,7}

At the site the South Saskatchewan River flows in a valley cut into the Cretaceous Bearpaw formation, of which the main shale member at the site, the Snakebite, is of high plasticity and contains bentonite or bentonitic zones with liquid limits ranging up to about 300. The depth of the shale bedrock valley at the site is about 75 m, but the bottom 30 m are filled with alluvium. The valley is bordered by wide zones of slump or landslide topography giving testimony to the propensity for stability problems during excavation and fill placement (see Figure 6).

In 1943, the Prairie Farm Rehabilitation Administration of Canada (PFRA) began studies for an irrigation project involving a dam across the river. Total stress stability analyses were the rule at the time, and the initial design was based on two sets of undrained peak-strength parameters: $c = 15$ to 20 psi, $\phi = 10^\circ$; and $c = 20$ psi, $\phi = 0^\circ$. Circular surfaces of sliding were assumed, and a factor of safety, $FS = 2.7$, was adopted for the end-of-construction condition.

The early geotechnical studies were carried out by Robert Peterson with equipment representing the latest Harvard designs. Subsequently, Arthur Casagrande, engaged as a consultant, turned the emphasis to a study of the slumped slopes in the vicinity supplemented by laboratory tests on a few select samples, by a test drift in which surfaces of sliding in the shale could be observed, by instrumentation to detect movements and by installation of



FIGURE 6. Landslide topography downstream of Gardiner Dam.

piezometers. Backfiguring the undrained strengths of the shales from the observed natural slumped slopes, on the assumption of circular surfaces of sliding, led to the conclusion that the most appropriate values for design were $c = 3$ psi and $\phi = 3^\circ$. A factor of safety of 1.1 was considered adequate for the end of construction because the interpretation was believed to be conservative. Even so, the design slopes required flattening.

During the early stages of construction from 1959 to 1961, however, minor excavations reactivated slips at calculated factors of safety greater than unity, according to analyses based on the design parameters, and a re-evaluation was undertaken. By now, effective stress analyses had become the norm. When the reactivated slips were backfigured, with composite surfaces of sliding and with piezometric levels assumed to be near the upper surface of the shale, shear parameters $c' = 0$, $\phi' = 8.5^\circ$ to 11.5° were found. A reanalysis of the slumped slopes as they existed before construction activities, carried out under the same premises, indicated $c' = 0$, $\phi' = 5^\circ$ to 7° . The design was then revised on the basis of $c' = 0$, $\phi' = 9^\circ$ in the foundation, and the slopes were flattened accordingly.

A minimum value $FS = 1.4$ was postulated

for short surfaces of sliding; $FS = 1.2$ was considered sufficient for long surfaces emerging near the toe at locations where stabilizing fill could be added, and $FS = 1.3$ was required where such stabilization would not be practical because of physical constraints. Construction proceeded on this basis through 1964. Although up to 0.3 m of foundation displacement toward the river channel was noted during stage construction on the west side of the river, the deformations were considered acceptable because there was no visible indication of upstream cracks in the embankment or of overthrusting at the toe. As piezometric data accumulated, the calculations were refined by incorporation of observed values of the pore-pressure ratio, r_u .

However, when the river-section embankment was raised from a height of 26 m to 47 m in 1965, horizontal displacements of as much as 0.8 m took place in the downstream direction. In 1966, when the dam was raised only 11 m from this height to nearly its full height at the center line, further movements of about 0.3 m occurred. The slopes, which had already been flattened after each redesign, were flattened once more. The final slopes were extended to a distance of about 1,200 m downstream to

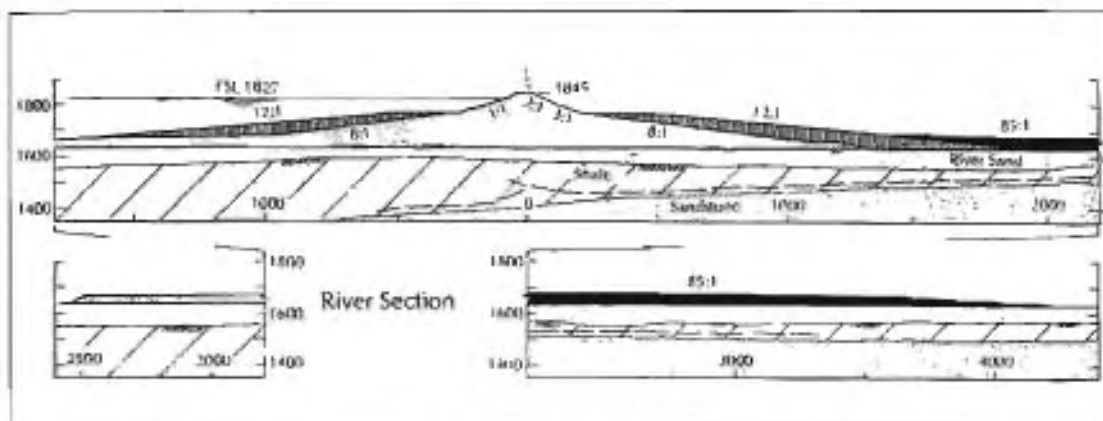


FIGURE 7. Successive stages in flattening of slopes of Gardiner Dam (after PFRA 1980).

prevent an overthrust from developing from the ancient shear zone located some 50 m below the valley floor. Three of the successive stages in the flattening of the slopes are shown in Figure 7. Although the increment of fill near the crest had produced a disproportionately large increment of movement, the rate slowed rapidly, and the embankment was completed to its designed crest elevation. In all, a maximum displacement of over 2 m occurred in the region about 150 m downstream of the center line. The displacement was associated with an upstream-downstream compression of the downstream shell, as the displacement at the toe of the embankment 1,200 m downstream of the center line was less than 1 cm during the same time interval.

The reservoir was raised for the first time, although not to full pool, in 1967. The raising was marked by a substantial increment of downstream displacement. Each annual rise of the reservoir has been accompanied by an additional increment, although a trend for the magnitude of the increments to decrease is evident if the different peak annual reservoir levels are taken into account. However, in view of the large movements already experienced during construction, the reservoir-induced movements prompted further evaluation of the structure's safety. Many factors were taken into account, including the numerous features of the design that were introduced to cope with the large movements that had been anticipated:

- a cross-section capable of accommodat-

ing substantial deformations without rupture of the core;

- the remoteness of the possibility of cracking and leakage through the core;
- the great depth of the preexisting shear surface below the river bed; and,
- the extensive installations of slope indicators, piezometers and other means of field observations provided to permit close surveillance.

Indeed, this and subsequent evaluations by the PFRA and its ongoing Boards of Consultants, which have enhanced confidence in the inherent safety of the dam, have placed principal dependence on the results of the observational program and the favorable trends that it has disclosed.

In his 1964 Rankine Lecture, Skempton introduced the concept of residual strength on surfaces along which large displacements had occurred.⁸ It had by then become apparent that the surface of sliding constituting the seat of principal movement was an ancient shear zone in the hard shale near the base of the Snakebite member. The zone extended from an area beneath the upstream shell of the dam to at least 1,200 m downstream of the crest. According to Skempton's concepts, it should certainly have been at residual strength.

Reversing direct-shear tests on samples from the shear zone indicated $c_r' = 0$, $\phi_r' = 2.7^\circ$ to 3.3° ; rotational-shear tests indicated $c_r' = 0$, $\phi_r' = 3.5^\circ$ to 4.5° . Back analyses using measured piezometric levels and composite surfaces of

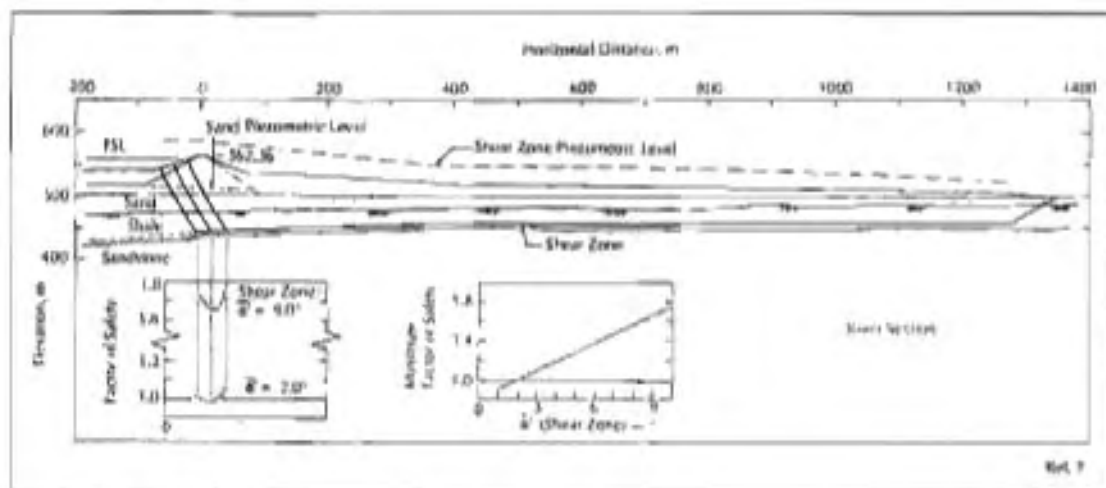


FIGURE 8. Results of stability calculation for the river section of the Gardiner Dam on the basis of the best information available in 1979.

sliding corresponded to $c_r' = 0$, ϕ_r' ranging from 2° to 7° . (In reality, three different embankments make up Gardiner Dam — all experiencing a similar history. Part of the range in the shear parameters may be ascribed to differences in the geometry and geology of the sections.) Although the shear-strength parameters from the tests and back calculations are in general agreement and leave little doubt that the residual strength is the pertinent parameter, the range in back-calculated values of ϕ demonstrates that the margin of uncertainty in such stability calculations is still appreciable.

One of the most recently published examples of such a calculation for the river section is illustrated in Figure 8.⁷ It represents a parametric study in which the factor of safety was calculated for various residual friction angles from 2° to 9° . The composite surface of sliding included the observed shear zone in the foundation, an active segment (taken at 3 different positions) along which peak strength was assumed, and a passive segment at the downstream end at a location corresponding to observation. Measured piezometric levels along the shear zone and in the embankment were used. The results show that for $FS = 1.0$ a residual friction angle of only 2° is needed, but even at this small value a maximum shearing displacement of over 2 m occurred during construction. The calculations illustrated are for full pool, but similar calculations for low pool,

corresponding to conditions at the end of winter, show a negligible influence of pool elevation on the factor of safety. Inasmuch as each application of the reservoir load has actually produced a distinct increment of displacement amounting to several millimeters, it is apparent that even these calculations are not yet at a stage where they are definitive predictors of behavior.

Considering the talent that was brought to bear on this project over a period of more than forty years; the degree of care and sophistication in soil testing; the data obtained from some 83 slope indicators, over 500 piezometers and an even greater number of surface reference points; and the care and continuity with which the observations have been carried out, there arises an inescapable conclusion. Forty years of research have reached the point where a limit-equilibrium stability analysis can indeed demonstrate that the calculated factor of safety of the structure is equal to the known value of approximately unity. Even so, the analysis is still deficient inasmuch as it does not yet realistically account for the influence of the water level in the reservoir. The analysis is still deficient in spite of the outstanding resources of the PFRA and the unusual effort that has been expended as compared to the investigations possible in connection with the usual dam-safety assessments.

The unusual geometry and physical proper-

ties of the mass undergoing movement in Gardiner Dam impose inherent limitations on limit-equilibrium analyses. The limitations have been recognized, and finite-element studies have been carried out with sophisticated refinements.⁹ By assigning what appeared to be reasonable values to the physical properties of the various materials involved, and by adjusting these values as required to achieve agreement between predicted and observed behavior, a model was developed that could reproduce deformations similar to those in the field, including the pattern of response to cyclic reservoir operation. Prediction over many load cycles, however, was not satisfactory. Although the study provided valuable insight into the behavior of the dam, it is clear, nevertheless, that no such finite-element study, without the calibration afforded by extensive observational data, can yet be depended on to indicate the degree of safety of this or probably any other existing dam.

Conclusions

The foregoing discussion leads to the conclusion that stability analyses are unreliable bases for assessing the stability of an existing dam with respect to catastrophic failure. The conclusion strictly applies only to static conditions; insight regarding the behavior in an earthquake may be gained by analysis, although not generally by limit-equilibrium analyses.

If the pool has been filled and pore-pressure equilibrium has been reached, the results of stability analyses may be assessed as follows:

1. If the calculated factor of safety is less than unity, it must be erroneous.
2. If the calculated factor of safety is greater than unity, the results merely indicate the obvious. The calculation is unnecessary to show that the dam is standing. Furthermore, no definitive conclusion about the degree of safety can be drawn from the numerical value of a computed factor of safety: hence, satisfying some prescribed criterion for this value is not in itself a suitable indicator of safety.
3. If progressive movements are occurring, a calculation is irrelevant because the

factor of safety is obviously close to unity. The actual safety can be assessed only on the basis of monitoring the movements and associated events. The procedure is exemplified by the studies at Gardiner Dam, where the crucial observations were those indicating decreasing increments of movement under successive comparable reservoir fillings. Nevertheless, if the calculated factor of safety is approximately unity, limit-equilibrium calculations may be useful in judging the effectiveness of various alternatives for increasing the safety. This use of equilibrium analysis is justifiable, and its effectiveness has been demonstrated not only with respect to dams, but with respect to many natural slopes. It should be clear, however, that the absolute value of the factor of safety resulting from any of the calculations is of no significance.

Stability analyses are tools for the guidance of the investigator. They have their limitations with respect to evaluating the stability of existing dams. It is not meant that they should never be performed. However, the numerical values for the factor of safety should carry little if any weight in judging the actual safety of the structure with respect to catastrophic failure.

The great danger in placing too much emphasis on stability calculations is that they may be regarded as a substitute for the much more difficult and expensive field investigations and historical research needed to establish the real character of the structure in question. Some dam owners may prefer the relatively small expenditure for a perfunctory stability study in contrast to costly and time-consuming field studies. Of greater importance, because of the greater potential danger, some regulatory bodies may take more comfort in orderly stability calculations based on unsupported or unverifiable assumptions than in qualitative judgments based on experience and careful investigation. Yet, the former may have little or no relation to the real safety of the dam, whereas the latter are essential in assessing the likelihood or possibility of a catastrophic failure.

This discussion quite possibly conveys a negative impression about our ability to deter-

mine whether or not an existing embankment dam is demonstrably safe against a catastrophic failure. This impression is not the intention of this study, nor would it be a correct summarization. On the contrary, a sound engineering appraisal can almost always be reached, but such an appraisal will often require painstaking field investigations; searches for construction records and, if they are found, their assessment and interpretation; inspection of all visible features; location and interpretation of maintenance records; and in many instances installation and monitoring of instruments and devices capable of disclosing not only present behavior but also future trends. The latter requirements may sometimes preclude an immediate evaluation of the safety of the dam, and they may sometimes prove to be expensive. On the contrary, they may also sometimes establish the safety quickly and beyond reasonable doubt. However, factors of safety derived from stability analyses, even when based on what appear to be the most reasonable of assumptions, are dangerous substitutes for the thorough investigations that are needed to reach sound, even if qualitative, judgments.

ACKNOWLEDGEMENTS — *A scenario concerning the failure of Walter Bouldin Dam, quite similar to that described herein, was developed independently and roughly concurrently by Thomas M. Leps. It is contained in Advanced Dam Engineering for Design, Construction, and Rehabilitation, R. B. Jansen, ed., Van Nostrand Reinhold, 1988. The Prairie Farm Rehabilitation Administration (PFRA), Agriculture Canada, provided data concerning Gardiner Dam and granted permission to publish the account contained in this article. This permission, as well as review and comments by the PFRA engineering staff and by J. G. Watson, are gratefully acknowledged. Thanks are also extended to John Dumnichiff, who critically reviewed the entire manuscript. This article was originally prepared as the Third Casagrande Lecture presented to the Boston Society of Civil Engineers Section/ASCE on October 14, 1987.*



RALPH B. PECK received the degrees of C.E. and D.C.E. from Rensselaer Polytechnic Institute in 1934 and 1937, respectively, and studied soil mechanics at Harvard from 1938 to 1939. He was a professor of civil engineering at the University of Illinois from 1943 to 1974. He now resides in Albuquerque, New Mexico, and is a consultant on dams, tunnels and landslides. An honorary member of ASCE, he has received numerous awards from that Society. He is a member of the National Academy of Engineering and, in 1974, received the National Medal of Science from President Gerald Ford.

REFERENCES

1. "Report on Investigation by Atlanta Regional Office Staff of Walter Bouldin Dam (Project No. 2146). Failure of February 10, 1975," September 1975.
2. "Investigation of Failure, Walter Bouldin Dam and Safety of Other Dams of the Alabama Power Company." Federal Power Commission, Bureau of Power, February 1976.
3. "Report to the Federal Energy Regulatory Commission, Walter Bouldin Dam Failure and Reconstruction," Office of Electric Power Regulation, FERC, Washington, DC, September 1978.
4. Sowers, G.F., "Reflections on the Design of Earth Structures," Contribution to the Fifth Nabor Carrillo Lecture by Raul J. Marsal, Mexico, 1980, pp. 133-141.
5. Peterson, R., Jaspas, J.L., Rivard, P.J., and Iverson, N.L., "Limitations of Laboratory Shear Strength in Evaluating Stability of Highly Plastic Clays," *Proc. Research Conf. on Shear Strength of Cohesive Soils*, ASCE, Boulder, CO, 1960, pp. 765-791.
6. "The Design and Construction of Gardiner Dam and Associated Works," PFRA, Canadian Gov't Publ. Ctr., Hull, 1980, 382 pp.
7. Jaspas, J.L., and Peters, N., "Foundation Performance of Gardiner Dam," *Can. Geol. Journal*, Vol. 16, No. 4, 1979, pp. 758-788.
8. Skempton, A.W., "Long-Term Stability of Clay Slopes," *Geotechnique*, Vol. 14, No. 2, 1964, pp. 77-101.
9. Morgenstern, N.R., and Simmons, J.V., "Analysis of the Movements of Gardiner Dam," *Proc. 4th Int. Conf. on Numerical Methods in Geomechanics*, Edmonton, Vol. 3, 1982, pp. 1003-1027.

Appendix D

Part 2 Suggestions for Slope Stability Calculations
by Ashok K. Chugh and John D. Smart

This article was published in *Computers and Structures*, Volume 14, Number 1-2,
pp. 43-50, 1981.

SUGGESTIONS FOR SLOPE STABILITY CALCULATIONS

ASHOK K. CHUGH† and JOHN D. SMART‡

Water and Power Resources Service, Engineering and Research Center, D222, P.O. Box 25007, Denver, CO 80225, U.S.A.

(Received 21 January 1980; received for publication 3 July 1980)

Abstract—Considerations for the selection of potential slide surface geometry in slope stability calculations by the limit equilibrium method are presented. Relations between the solution variables and the Mohr-Coulomb strength parameters for no failure on the interslice boundaries are derived. Also included are the relations between the solution variables for effective and total stress considerations. The materials are assumed to be "no-tension" type. Significance of evaluating the calculated response for the individual slices making up the potential slide mass is indicated.

NOMENCLATURE

b	width of slice
c'	cohesion with respect to effective stress
e	eccentricity of the external force P
E	horizontal component of interslice force
F	factor of safety
H	force exerted by the pore water on the interslice boundary
h	height of force above slip surface
i	ground slope
K_A	coefficient of active earth pressure
N	force normal to base of slice
P	external force acting on the slice
S	total shear force
T	interslice force for the back wedge
W	weight of slice or back wedge
Z	interslice force
U	force exerted by the pore water on the base of the slice
α	slope of base of slice
β	slope of the top of slice
δ	slope of interslice force
θ	backrest angle with horizontal

INTRODUCTION

The problem of slope stability is an important part of geotechnical engineering. As a result much has been said and written in the technical literature about various methods of analyses—their merits, complexities and simplifying assumptions, justifications for their use in actual practice, and about comparison of results obtained from their use [1, 4, 6–8, 12–14]. § Most of the slope stability analysis procedures have been converted into computer programs for their fast and accurate implementation [3, 15]. Frequent occurrence of slope design problems combined with availability of the computers, makes it reasonable to assert that at present almost every geotechnical engineer has an access to one or more of the slope stability analysis computer codes and that these codes are frequently used in engineering practice.

Amongst the different methods of analyses, limit equilibrium methods satisfying the three equations of statics are now being used extensively for estimating the stability of both natural slopes and man-made embankments [5–8, 12]. The method of slices, considering the interslice forces, as presented by Spencer [10, 11, 13], is representative of the modern versions of limit equilibrium methods. It seeks the solution of the slope stability equations, starting with an assumed value of factor of safety F and thrust inclination δ , satisfying the boundary conditions at the toe and head of the slide mass. The other parameters, such as interslice forces, their magnitude, location and direction, do not play an active role in the solution scheme but are calculated as a part of the iteration procedure. In this presentation, the boundary conditions are considered as being distinct from the interslice forces.

The objectives of the present paper are to present suggestions for:

1. Geometrical configuration of a critical segmented failure surface.
2. Interrelationship of the mathematical solution for total and effective stress considerations; and
3. Limits imposed by the material strength on the validity of the mathematical solution.

The materials are assumed to be homogeneous and isotropic and obey the Mohr-Coulomb strength hypothesis. An example of stability analysis of a natural slope is included. The following terms used in this paper are defined as follows:

Backrest: Geometric configuration of the heel of a segmented failure surface.

Thrust: Resultant force on interslice boundary. The words "no-tension" and "cohesionless" are implied to have identical meaning.

Figure 1 is a general description of the problem. For any vertical slice, $abcd$, the forces acting are shown in Fig. 1(b). H_L and H_R are the hydrostatic forces exerted by the subsurface water on the vertical boundaries of the slice (assumed to be known). Other forces acting on the free body diagram of a slice are defined in the Nomen-

†Civil Engineer, U.S. Bureau of Reclamation.

‡Supervisory Civil Engineer, U.S. Bureau of Reclamation.

§References included in this paper are representative, but not a complete list, of the works on the subject.

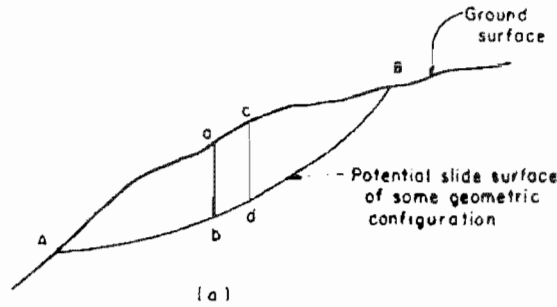
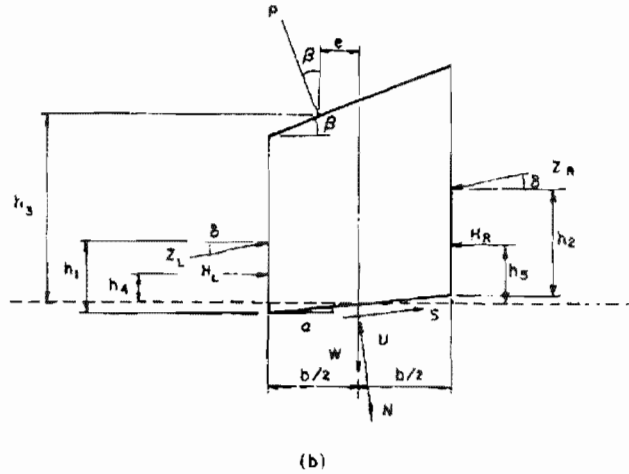


Fig. 1(a). General slope stability problem description.



$$\text{Available shear strength} = \frac{1}{F} \left(c' + \frac{N}{b \sec \alpha} \tan \phi' \right) b \sec \alpha$$

Fig. 1(b). Forces acting on a typical slice.

clature. Considering static equilibrium of the forces:

$$Z_R = Z_L + \frac{\frac{1}{F} c' b \sec \alpha - W \sin \alpha + \frac{1}{F} (W \cos \alpha - U) \tan \phi'}{\cos(\delta - \alpha) \left[1 - \frac{1}{F} \tan(\delta - \alpha) \tan \phi' \right]}$$

$$+ \frac{P \cos(\beta - \alpha) \left[\tan(\beta - \alpha) + \frac{1}{F} \tan \phi' \right]}{\cos(\delta - \alpha) \left[1 - \frac{1}{F} \tan(\delta - \alpha) \tan \phi' \right]}$$

$$+ \frac{H_L \cos \alpha \left[1 + \frac{1}{F} \tan \alpha \tan \phi' \right]}{\cos(\delta - \alpha) \left[1 - \frac{1}{F} \tan(\delta - \alpha) \tan \phi' \right]}$$

$$- \frac{H_R \cos \alpha \left[1 + \frac{1}{F} \tan \alpha \tan \phi' \right]}{\cos(\delta - \alpha) \left[1 - \frac{1}{F} \tan(\delta - \alpha) \tan \phi' \right]}$$

$$h_2 = \frac{Z_L}{Z_R} h_1 + \frac{b}{2} [\tan \delta - \tan \alpha] \left[1 + \frac{Z_L}{Z_R} \right]$$

$$+ \frac{P}{Z_R} \cos \beta \sec \delta [h_3 \tan \beta - e]$$

$$+ \frac{1}{Z_R} \sec \delta [H_L h_4 - H_R h_5]$$

In the derivation of eqns (1) and (2), and elsewhere in this paper, the factor of safety (F) is defined as the ratio of the total shear strength available on the slip surface to the total shear force required to reach a condition of limiting equilibrium.

GEOMETRIC CONFIGURATION

For circular configuration of potential slide surfaces, most computer programs have a routine that optimizes on a circle that gives a minimum factor of safety [3, 15]. This optimization is generally in the neighborhood of the initial estimate for the center of rotation of critical circle provided by a designer.

For a segmented geometry of potential slide surfaces, generally a discrete calculation is performed for the stability determination along the specified configuration. The critical elements of a slope that should be considered in the selection of a segmented failure surface geometry are:

1. The profile of the weak material responsible for the occurrence of slope stability problem.
2. The profiles of the underlying and overlying relatively stronger material.
3. The pore water pressure distribution.
4. The length of the potential slide surface.
5. The indication of localized weak material zones.

The order in which the above elements are mentioned

is not important. While these elements influence the choice of large segments of potential slide surfaces for analysis, they do not, per se, assist in estimating the toe and heel of the slide surface[2].

CRITICAL BACKREST INCLINATION

The critical backrest of a segmented slide surface should be such as to give the least contribution to the overall factor of safety against sliding. For a planar backrest of the failure surface, the forces acting on the wedge of material are shown in Fig. 2. Pore water pressure is not considered in the following derivation. Summing forces along the backrest plane:

$$S = W \sin \theta - T \cos (\theta - \delta) \quad (3)$$

Summing forces normal to the backrest plane:

$$N = W \cos \theta + T \sin (\theta - \delta) \quad (4)$$

For the Mohr-Coulomb material, shear strength along the backrest plane is:

$$\begin{aligned} \text{shear strength} &= c \cdot AC + N \tan \phi \\ &= c \frac{h_0 \cos i}{\sin (\theta - i)} \\ &\quad + \frac{1}{2} \gamma h_0^2 \frac{\cos \theta \cos i}{\sin (\theta - i)} \cos \theta \tan \phi \\ &\quad + T \sin (\theta - \delta) \tan \phi \end{aligned} \quad (5)$$

The expression for the factor of safety from equations (3) and (5) is:

$$F = \frac{c h_0 \cos i + \frac{1}{2} \gamma h_0^2 \frac{\cos \theta \cos i}{\sin (\theta - i)} \cos \theta \tan \phi + T \sin (\theta - \delta) \tan \phi}{W \sin \theta - T \cos (\theta - \delta)} \quad (6)$$

Thus for the backrest to yield the least F , its orientation should be such as to give the minimum value for the thrust, T .

For a given material and ground slope, the thrust T depends upon W and δ , Fig. 2. For the planar backrest of the failure surface, T is a function of (θ, δ) .

At the instant of shear failure, from eqn (6)

$$\begin{aligned} w \sin \theta - T \cos (\theta - \delta) \\ &= c \frac{h_0 \cos i}{\sin (\theta - i)} + \frac{1}{2} \gamma h_0^2 \frac{\cos \theta \cos i}{\sin (\theta - i)} \cos \theta \tan \phi \\ &\quad + T \sin (\theta - \delta) \tan \phi \\ T &= \frac{\frac{1}{2} \gamma h_0^2 \cos \theta \cos i \sin (\theta - \phi) - c h_0 \cos i \cos \phi}{\cos (\theta - \delta - \phi) \sin (\theta - i)} \end{aligned} \quad (7)$$

For a cohesionless material, eqn (7) becomes

$$T = \frac{1}{2} \gamma h_0^2 K_A \quad (8)$$

where

$$K_A = \frac{\cos \theta \cos i \sin (\theta - \phi)}{\cos (\theta - \delta - \phi) \sin (\theta - i)} \quad (9)$$

Differentiating $K(\theta, \delta)$ with respect to δ and equating it to zero, one gets

$$\delta = \theta - \phi \quad (10)$$

Similarly differentiating $K(\theta, \delta)$ with respect to θ , equating it to zero, and substituting eqn (10), leads to the transcendental equation:

$$\sin (\theta - \phi) \sin (\theta - i) \tan \theta - \sin (\phi - i) = 0 \quad (11)$$

The solutions of the eqn (11) are graphed in Fig. 3 for several values of i . The corresponding values of K_A , the coefficient of active earth pressure, are evaluated from

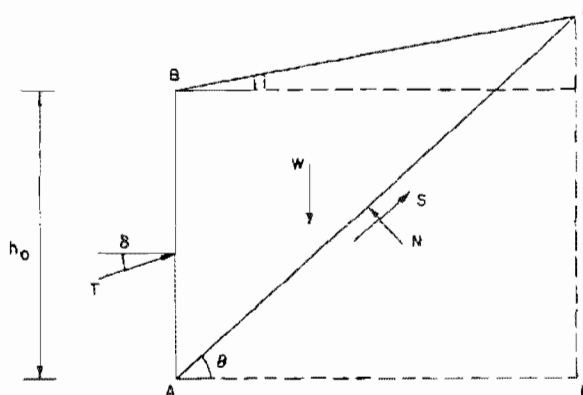


Fig. 2. Forces acting on the backrest portion of a slide mass.

$$\begin{aligned} W &= \frac{1}{2} AB \cdot AD \cdot \gamma \\ \tan \theta &= \frac{CE + DE}{AD} \\ \tan i &= \frac{CE}{AD} \\ DE &= h_0 \\ AD &= \frac{h_0 \cos \theta \cos i}{\sin (\theta - i)} \\ W &= \frac{1}{2} \gamma h_0^2 \frac{\cos \theta \cos i}{\sin (\theta - i)} \end{aligned}$$

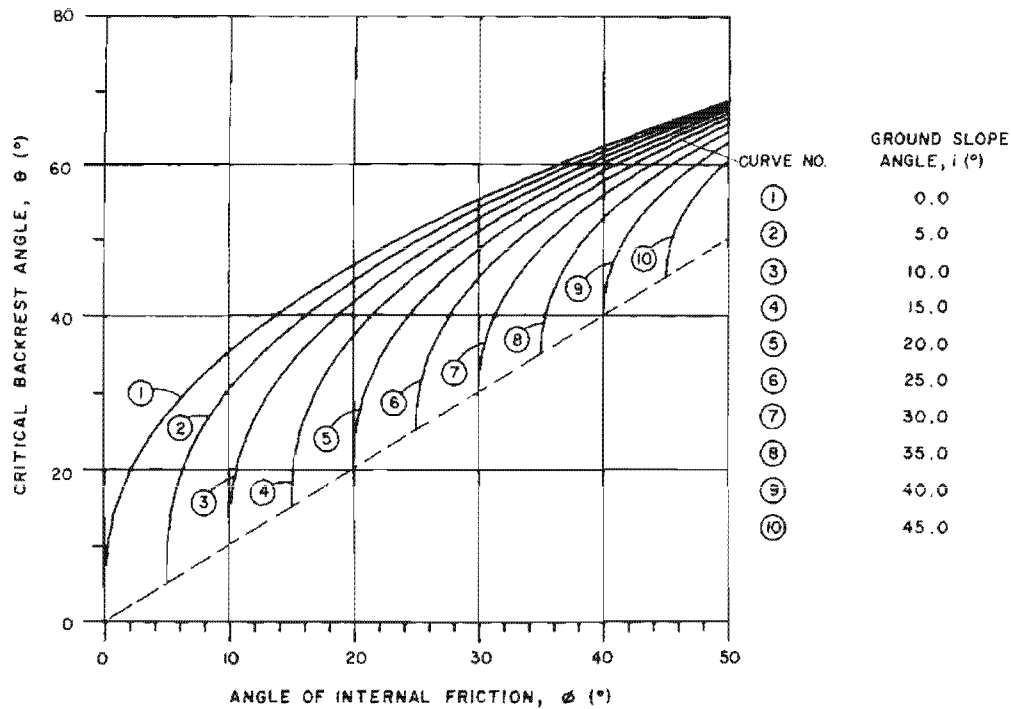


Fig. 3. Solution of eqn (11) to first approximation.

Table 1. Values of K_A

i		ϕ IN DEGREES								
DEG.	SLOPE	5	10	15	20	25	30	35	40	45
0	0	.735	.604	.504	.423	.355	.296	.244	.199	.160
5	1:1.5	.992	.698	.563	.463	.383	.316	.258	.209	.166
10	1:5.7		.970	.654	.517	.418	.340	.275	.220	.174
15	1:3.7			.933	.602	.467	.371	.295	.234	.183
20	1:2.7				.883	.545	.414	.322	.250	.193
25	1:2.1					.821	.485	.359	.273	.207
30	1:1.7						.750	.422	.305	.225
35	1:1.4							.671	.359	.251
40	1:1.2								.587	.297
45	1:1.0									.500

RELATION OF THRUST AND ITS INCLINATION FOR EFFECTIVE AND TOTAL STRESS

For the interslice forces to be statically equivalent for the effective and total stress, Fig. 4(a, b):

$$T \cos \delta = T' \cos \delta' + H \tag{12}$$

$$T \sin \delta = T' \sin \delta' \tag{13}$$

$$T(h_0 - h) \cos \delta = T'(h_0 - h') \cos \delta' + H \left(h_0 - \frac{1}{3} h_1 \right) \tag{14}$$

Equations (12)–(14) ensure the horizontal, vertical, and moment equivalence respectively of the interslice forces for the total and the effective stress. From eqn (13)

$$T' = T \frac{\sin \delta}{\sin \delta'} \tag{15}$$

From eqns (12) and (15)

$$\tan \delta' = \frac{T \sin \delta}{T \cos \delta - H} \tag{16}$$

From eqns (14)–(16), one gets

$$h' = \frac{\left[T \cos \delta - \frac{1}{3} H \frac{h_1}{h} \right] h}{T \cos \delta - H} \tag{17}$$

Equations (15)–(17) relate the interslice force, its location, and orientation for total and effective stress. However eqns (12)–(17) do not account for the effect of the hydrostatic forces on the interslice boundaries on the calculated factor of safety, F . It is essential, therefore, to include these hydrostatic forces in the derivation of slope stability equations as shown in eqns (1) and (2).

LIMITS ON THRUST LINE INCLINATION AND ITS MAGNITUDE

Considering the vertical equilibrium of shear force acting on the interslice boundary and the mobilized shear

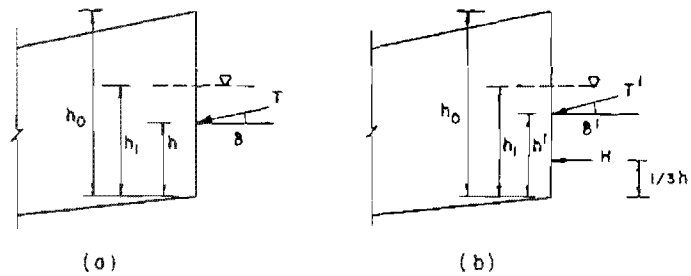


Fig. 4. Total and effective interslice forces.

strength, Fig. 4(b):

$$T' \sin \delta' = \frac{1}{F} [c' h_0 + T \cos \delta' \tan \phi']$$

$$\tan \phi' = F \tan \delta' - \frac{c' h_0}{T'} \sec \delta'. \quad (18)$$

Therefore, in a cohesionless material, ($c' = 0$), the necessary condition for no shear failure on the interslice boundaries is:

$$\delta' \leq \phi'. \quad (19)$$

The corresponding inclination of the thrust for total stress is obtained from eqns (16) and (18):

$$\tan \phi' = F \frac{1}{1 - \frac{H}{T} \sec \delta} \tan \delta. \quad (20)$$

Since $\left(\frac{1}{1 - (H/T) \sec \delta}\right)$ must be ≥ 1 , it follows from eqn (20) that

$$\delta \leq \phi'. \quad (21)$$

Similarly from eqn (16), it follows that:

$$\delta \leq \delta' \quad (22)$$

and from eqns (15) and (22) that:

$$T' \leq T. \quad (23)$$

It is perhaps clear that equality in eqns (21)–(23) holds for $H = 0$.

LOCATION OF THRUST LINE

The slope stability eqns (1) and (2) deal primarily with the equilibrium of forces acting on the free body diagram of a typical intermediate slice. Therefore, the location of the thrust line on the interslice boundaries in terms of h_1 and h_2 is of direct significance. If the calculated location of the thrust line for a particular slice is outside the sliding mass, a tension of some magnitude and extent is implied. For no tension on the interslice boundaries, it is imperative that the thrust line be located within the sliding mass for every interslice boundary. A further assumption for normal stress distribution (such as linear) on the interslice boundary shall further define the bounds (such as middle third) within which the thrust line must be located for no tension. Since the limit equilibrium solution procedure does not consider the tensile charac-

ter of the material, it is important that a designer consider the results of this calculation along with the calculated value of the factor of safety.

COMMENTS

In the derivation for critical backrest inclination presented, it is presumed that the total factor of safety of a segmented failure surface is composed of the factor of safety of its various constituents, i.e.

$$F = \sum_{i=1}^n f_i$$

where f_i is the contribution of the i th segment and n is the total number of segments making up the geometry of the potential slide surface. Therefore, for a slide surface to have the least factor of safety the contribution of each unit should be minimized.

In a wedge type of slope stability analysis, where the back and toe wedges of material are replaced by horizontal forces exerted by them on the middle wedge and the factor of safety of the slope is calculated by considering the equilibrium of the forces acting on the middle wedge, the backrest angle for maximum horizontal force is greater than the backrest angle that gives the least interslice force, T , used in eqn (6). Since this type of wedge analysis implies occurrence of shear failure condition on the vertical interfaces between the wedges, it gives a lower value for the computed factor of safety of the slope. For stability of natural slopes and embankments, this assumption of shear failure on the vertical interfaces of slices is unrealistic and gives unduly lower estimates of the factor of safety, and hence results in more extensive remedial treatment(s) than may be necessary to meet a design criterion of factor of safety. Alternatively, it could lead a designer into remedying a smaller zone, the middle wedge, of a potentially large slide mass and thus underestimate the extent of essential treatment. In any case, a wedge type of analysis for slope stability problems is unrealistic and is not recommended for general use.

Since slope stability problems generally occur in geologic formations and embankments composed of different materials and complicated by complex pore water pressure distribution, it is essential that a designer make a parametric study on the backrest and exit slopes for a segmented failure geometry. Figure 3 may be used in making an initial estimate for the backrest angle.

Since there is no way in general to predict what a solution to a nonlinear system, while satisfying the prescribed boundary conditions, may calculate for the various slices making up a slope, it is important to keep in mind the physics of the actual problem in interpreting the calculated response. Assuming com-

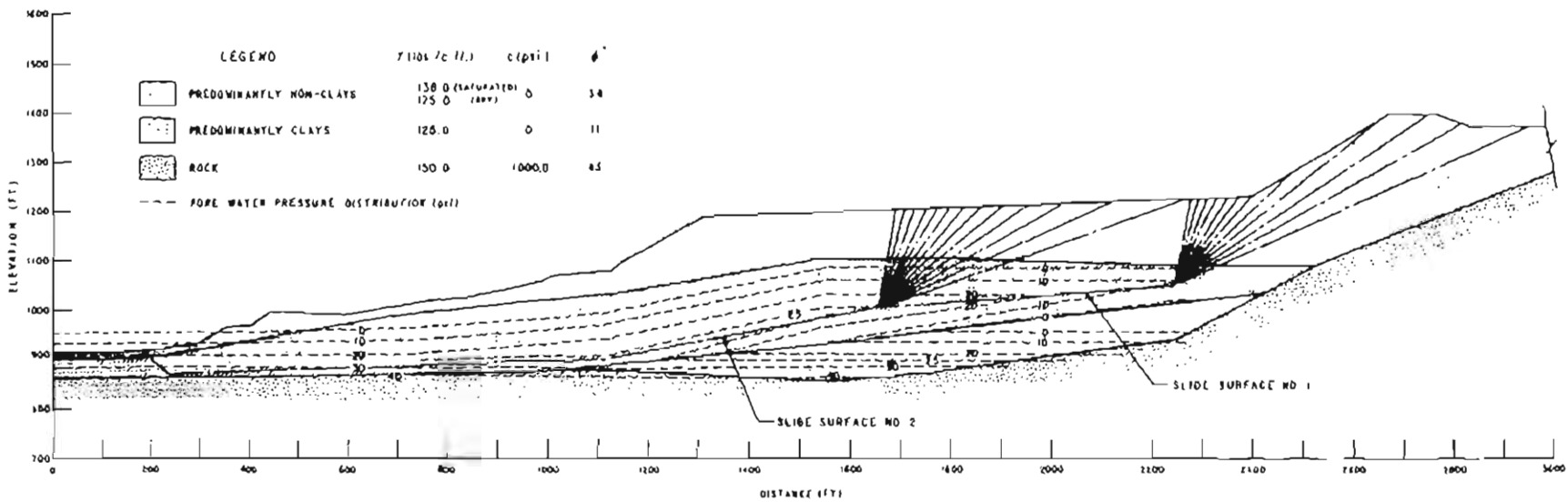
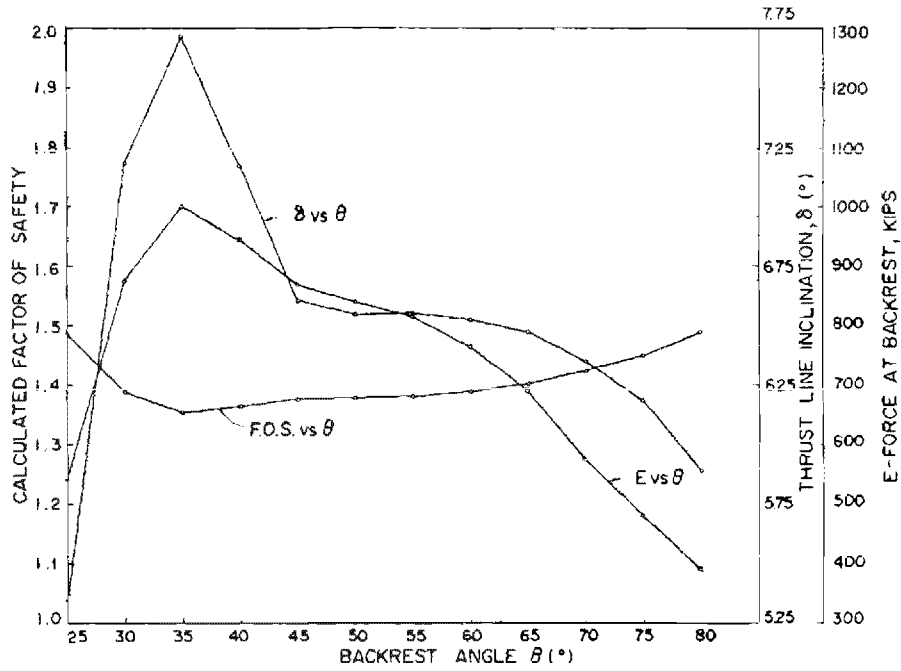
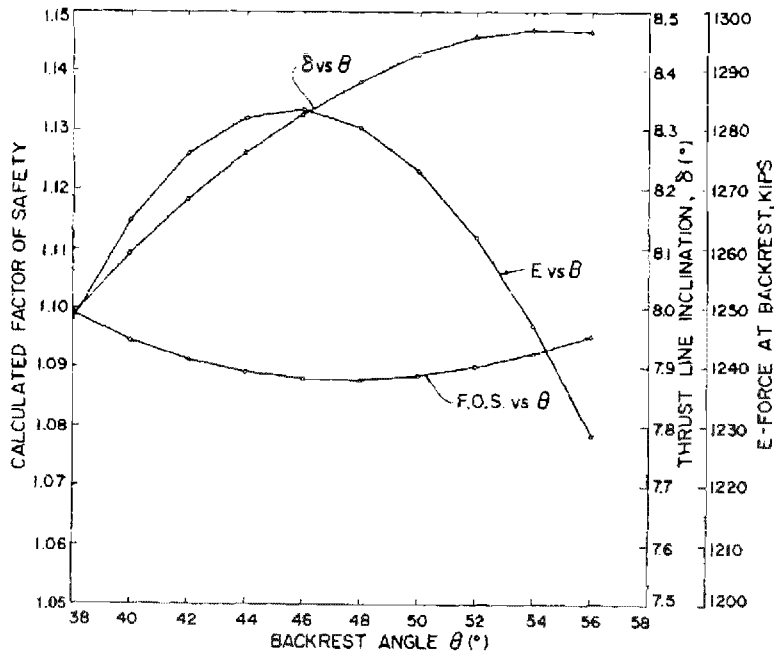


Fig. 5. Example problem.



COULEE DAM N-E AREA; LONG SLIDE SURFACE #1

Fig. 6. Parametric study results, slide surface No. 1.



COULEE DAM N-E AREA; LONG SLIDE SURFACE #2

Fig. 7. Parametric study results, slide surface No. 2.

pression to be positive, the calculated negative interslice forces imply the presence of tensile normal stresses in the soil mass. Unless the solution scheme is formulated to account for the tensile character of the material, the calculated results for the (F, δ) pair can be quite meaningless. Similar comments apply for the solutions that give thrust line inclination δ in violation of the limits imposed by eqns (19) or (22) for the ideal material

assumed. Even in actual geologic formations, the limits imposed by these equations cannot be grossly violated by a nonlinear solution and still be acceptable.

A poor mathematical solution does not necessarily imply a poor nonlinear solution procedure; it can also indicate a poor physical model. An evaluation of the intermediate response of a poor mathematical solution to a nonlinear system generally reveals the bad character of

the physical model. A designer should take into consideration both of the above possibilities in interpreting the computed response of a slope stability problem.

It is assumed, in these comments, that there is only one real value of F and of δ that will satisfy both the force and moment conditions of equilibrium.

SAMPLE PROBLEM

Figure 5 illustrates a section located in the Coulee Dam northeast area downstream of the Grand Coulee Dam in the State of Washington. The identification of potential slide surfaces in the hillside is of interest. For slope stability analysis, the geologic makeup of the site is assumed to be composed of four materials. Their broad identification and estimated properties are given in Fig. 5. The pore water pressure distribution in the hillside is shown in Fig. 5. The geometry of the segmented slide surfaces analyzed are also marked in this figure. The analyses were performed using the computer code STABLY [15] available at the U.S. Bureau of Reclamation, Engineering and Research Center. This computer program implements the method of slices satisfying the three equations of static equilibrium and calculates a constant value for the factor of safety and a constant inclination for the interslice forces. The effect of backrest angle on the calculated factor of safety, inclination of the interslice force, and the horizontal component of the interslice force are shown in Figs. 6 and 7. It should perhaps be mentioned that each potential slide surface was analyzed individually. For the slide surface No. 2, the calculated least factor of safety corresponds to backrest angle of 48° , Fig. 7. The critical backrest angles for the surface topography and the two material strength values, from Fig. 3, are: $\theta = 35^\circ$ for $\phi = 11^\circ$ and $\theta = 58^\circ$ for $\phi = 34^\circ$. The average of these two critical backrest angles is 46.5° . The corresponding values for the critical backrest angle assuming validity of $45 + \phi/2$ would be 50.5° and 62° with the mean value of 56.25° . Thus, the backrest angle corresponding to the least factor of safety tends to agree with the values indicated by Fig. 3 rather than $45 + \phi/2$ [2].

It should be mentioned that these analyses were performed using the existing conditions of surface topography, interpreted material horizons, tested material properties for predominantly clay materials (residual strength) and estimated material properties for predominantly non-clay materials, and interpreted pore water pressure distribution for the steady-state river operation (tailbay elevation 955.0 ft). The residual strength value for clay materials used in these calculations tends to align with the lower end of the range of strength values obtained to date by both the back

calculations of known past slides in the area and laboratory tests. The results of calculated factor of safety as far as they apply to the specific site are preliminary and do not reflect the remedial treatment alternatives under study to improve stability.

SUMMARY

The selection of potential slide surface geometry in slope stability analysis by the limit equilibrium method deserves a careful consideration. A close scrutiny of the calculated results of slope stability analysis in terms of interslice forces—their magnitude, direction, and location is of significant importance and should be considered along with the factor of safety.

REFERENCES

1. W. F. Chen, *Limit Analysis and Soil Plasticity*. Elsevier, Amsterdam (1975).
2. J. M. Duncan and A. L. Buchignani, *An Engineering Manual for Slope Stability Studies*. Department of Civil Engineering, University of California (Mar. 1975).
3. D. G. Fredlund, Slope stability analysis. *User's Manual*. Department of Civil Engineering, University of Saskatchewan (1974).
4. D. G. Fredlund and J. Krahn, Comparison of slope stability methods of analysis. *Canadian Geotechnical J.* 14, 429-439 (1977).
5. T. C. Hopkins, D. L. Allen and R. C. Deen, *Effects of Water on Slope Stability*. Kentucky Bureau of Highways (1975).
6. T. W. Lambe and R. V. Whitman, *Soil Mechanics*. pp. 352-373. Wiley, New York (1969).
7. K. T. Law and P. Lumb, A limit equilibrium analysis of progressive failure in the stability of slopes. *Canadian Geotechnical J.* 15, 113-122 (1978).
8. N. R. Morgenstern and V. E. Price, The analysis of the stability of general slip surfaces. *Geotechnique* 15, 70-93 (1965).
9. M. G. Salvadori and M. L. Baron, *Numerical Methods in Engineering*, pp. 18-20. Prentice-Hall, New Jersey (1961).
10. E. Spencer, A method of analysis of the stability of embankments assuming parallel interslice forces. *Geotechnique*, 11-26 (1967).
11. E. Spencer, Thrust line criterion in embankment stability analyses. *Geotechnique*, 85-100 (1973).
12. K. Terzaghi and R. B. Peck, *Soil Mechanics in Engineering Practice*, pp. 361-459. Wiley, New York (1967).
13. S. G. Wright, A study of slope stability and the undrained shear strength of clay shales. Ph.D. dissertation, University of California, Berkeley (1969).
14. H. J. Hovland, A three-dimensional slope stability analysis method. *J. Geotechnical Engng Div. Am. Soc. Civil Engrs*, 103(GT9), 971-986 (1977).
15. S. G. Wright, SSTAB1—A general computer program for slope stability analyses. Department of Civil Engineering, University of Texas at Austin (1974).

Appendix D

Part 3 Variable Factor of Safety in Slope Stability Analysis
by Ashok K. Chugh

This article was published in *Géotechnique*, Volume 36, No. 1, pp. 57-64, 1986.

Variable factor of safety in slope stability analysis

A. K. CHUGH*

The use of a variable factor of safety in slope stability analysis procedures based on the limit equilibrium method is presented. The proposed procedure consists of defining a characteristic that describes the variation in the factor of safety along a slip surface and the analysis procedure seeks to determine a scalar factor that in combination with the characteristic and the interslice force inclination satisfies the boundary conditions in a slope stability problem. A possible form of the characteristic for frictional materials is discussed. A case study is included to illustrate the application of the ideas presented. No new assumptions or unknowns are introduced and all equations of static equilibrium are satisfied.

L'article décrit l'utilisation d'un facteur de sécurité variable dans l'analyse de la stabilité des pentes basées sur la méthode d'équilibre limite. La méthode proposée consiste à définir une caractéristique qui décrit la variation du facteur de sécurité le long d'une surface de glissement, tandis que la méthode analytique cherche à déterminer un facteur scalaire qui en combinaison avec la caractéristique et l'inclinaison de la force entre les tranches remplit les conditions limites dans un problème de stabilité de pente. On discute une forme possible de la caractéristique pour les matériaux pulvérulents et on présente un cas concret pour illustrer l'application des idées exprimées. La méthode proposée n'introduit aucune nouvelle hypothèse ni inconnues et toutes les équations de l'équilibre statique sont satisfaites.

KEYWORDS: analysis; case history; dams; failure; slopes; stability.

INTRODUCTION

Slope stability analysis of embankment dams and natural slopes in geotechnical engineering practice is usually performed by the limit equilibrium method. In this method of analysis, sufficient assumptions are made to enable the problem to be solved using only equations for static equilibrium and a failure equation. There is no unique set of assumptions that have usually been made. Thus, there are different solution procedures available each subscribing to a different set of assumptions. The more modern of the solution

procedures commonly used for the slope stability studies are by Morgenstern & Price (1965), Spencer (1967), Sarma (1973) and Janbu (1973). Their use in practice is a matter of individual or organizational preference, availability of a particular computer procedure and past experience.

One of the assumptions common to all slope stability analysis procedures based on the limit equilibrium method is a single value factor of safety F for the entire shear surface, i.e. the factor of safety is the same for all locations along the shear surface. The factor of safety is generally defined as the ratio of the total shear resistance available on a shear surface to the total shear force required to reach a condition of limit equilibrium. The factor of safety is thus considered to account for uncertainties in the shear strength values for the materials.

A shear surface in a typical slope stability problem passes through a variety of distinctly different materials—each with different shear strength characteristics. While peak shear strengths for some materials along a shear surface may be usable, it is possible to have only residual shear strengths available for others for a slope stability problem involving an embankment fill and its foundations. The level of uncertainty in the shear strengths of materials along a shear surface may not necessarily be the same. Thus, the assumption of identical factors of safety everywhere along a shear surface is not realistic (see, for example, Bishop, 1967, 1971; Chowdhury, 1978).

The objectives of this Paper are

- (a) to present a procedure for calculating a variable factor of safety along a shear surface within the framework of the limit equilibrium method
- (b) to present a possible form of characteristic for a variable factor of safety for frictional materials
- (c) to present a geometric interpretation of the constant and variable factor of safety assumption in slope stability analysis by the limit equilibrium method.

A case study is included to illustrate the application of ideas presented.

Discussion on this Paper closes on 1 July 1986. For further details see inside back cover.

* US Department of the Interior, Denver.

CALCULATIONS FOR FACTOR OF SAFETY

The factor of safety in a slope stability analysis is defined by

$$F = \frac{\text{Available shear strength along a shear surface}}{\text{Driving shear stress along the shear surface}} \quad (1)$$

The available shear strength at a point in a soil deposit depends on the shear strength parameters (c' , ϕ') of the soil and the induced effective normal stress at that location. In the conventional slope stability analysis procedures in which the slide mass is divided into slices, equation (1) is applied for each slice. Typically, the derivation of the slope stability equations leads to the following (Chugh, 1984). (The equations included here are for the finite formulation of Morgenstern & Price (1965) adapted to Spencer's (1967) procedure. However, the ideas presented for a variable factor of safety can be adapted to any other procedure based on the limit equilibrium method.)

For static equilibrium of forces acting on the slice shown in Fig. 1(b)

$$\begin{aligned} Z_R = Z_L & \\ & \times \frac{\cos(\delta_L - \alpha)[1 - (1/F)\tan(\delta_L - \alpha)\tan\phi']}{\cos(\delta_R - \alpha)[1 - (1/F)\tan(\delta_R - \alpha)\tan\phi']} \\ & + [(1/F)c'b \sec\alpha - W \sin\alpha \\ & \quad + (1/F)(W \cos\alpha - U)\tan\phi'] \\ & \times \{\cos(\delta_R - \alpha)[1 - (1/F)\tan(\delta_R - \alpha)\tan\phi']\}^{-1} \\ & + \frac{P \cos(\beta - \alpha)[\tan(\beta - \alpha) + (1/F)\tan\phi']}{\cos(\delta_R - \alpha)[1 - (1/F)\tan(\delta_R - \alpha)\tan\phi']} \\ & + \frac{H_L \cos\alpha[1 + (1/F)\tan\alpha\tan\phi']}{\cos(\delta_R - \alpha)[1 - (1/F)\tan(\delta_R - \alpha)\tan\phi']} \\ & - \frac{H_R \cos\alpha[1 + (1/F)\tan\alpha\tan\phi']}{\cos(\delta_R - \alpha)[1 - (1/F)\tan(\delta_R - \alpha)\tan\phi']} \end{aligned} \quad (2)$$

For moment equilibrium of the forces acting on the slice shown in Fig. 1(b)

$$\begin{aligned} h_2 = \frac{Z_L \cos\delta_L}{Z_R \cos\delta_R} h_1 & \\ & + \frac{b}{2} \frac{1}{\cos\alpha \cos\delta_R} \left[\sin(\delta_R - \alpha) \right. \\ & \left. + \frac{Z_L}{Z_R} \sin(\delta_L - \alpha) \right] \\ & + \frac{P}{Z_R} \cos\beta \sec\delta_R (h_3 \tan\beta - e) \\ & + \frac{1}{Z_R} \sec\delta_R (H_L h_4 - H_R h_5) \end{aligned} \quad (3)$$

(see Fig. 1 for the meanings of the various symbols).

The variation in side force inclination in equations (2) and (3) is defined as (Spencer, 1973)

$$\tan\delta = \lambda f(x) \quad (4)$$

where $f(x)$ is a predefined characteristic shape function and λ is a scalar factor to be determined. This formulation for variable interslice force inclination does not increase the number of unknowns (Spencer, 1967).

Equations (2) and (3) are recurring relations and allow the boundary value problem to be solved as an initial value problem for an assumed value of the factor of safety F , the side force inclinations δ and the known boundary conditions at the left-hand side of the shear surface (Chugh, 1982): see Fig. 1.

The idea of incorporating a variable factor of safety in a slope stability analysis follows very closely the idea used for the variable interslice force inclination in that a characteristic shape for its variation along a shear surface is predefined and the solution procedure is required to calculate a scalar factor which scales the characteristic. Thus, for equation (1)

$$T g(x) = \frac{\text{Available shear strength along a slice base}}{\text{Driving shear stress along the slice base}} \quad (5)$$

where T is the unknown scalar factor and $g(x)$ is the characteristic shape for the variation in factor of safety along the slip surface. For $g(x) = 1$, equations (1) and (5) lead to $T = F$. The definition of the variable factor of safety according to equation (5) introduces only one unknown—the same as for the constant factor of safety assumption. The solution procedure for calculating T from equation (5) is similar to the procedure used for calculating F from equation (1). The effect of using equation (5) in the slope stability analysis is to change the distribution of induced shear stress and normal stress along a shear surface.

CHARACTERISTIC SHAPE FOR VARIABLE FACTOR OF SAFETY

The shear stress distribution in materials along a shear surface, for the constant factor of safety assumption, depends on the normal stress distribution and the values of the shear strength parameters, i.e. induced shear stresses are higher in materials with higher c' , ϕ' values—all else being equal. Thus, if σ'_n at two points in two different materials were the same, the present analysis would indicate two different values of

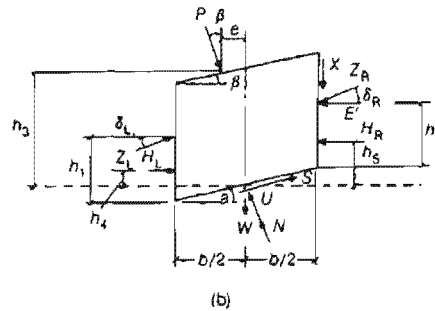
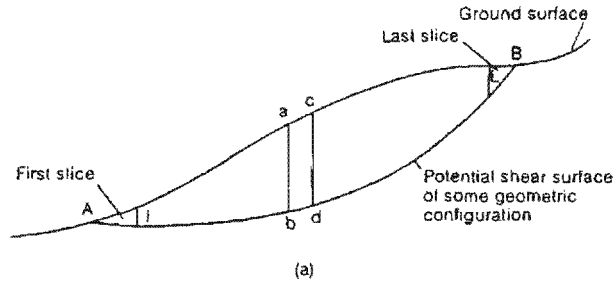


Fig. 1. General description of the limit equilibrium analysis of a soil deposit: (a) slope stability problem; (b) forces acting on a typical slice

shear stress and their magnitude would depend on the values of c' , ϕ' for these materials. Intuitively though, it would be expected that the shear stresses at these points would depend on the coefficient of lateral stress and inclination of the shear surface at these locations. If these were nearly the same, the induced shear stresses would be expected to be about the same as well.

It has been observed in the analysis results of several problems that the normal stress distribution along a shear surface is generally smooth; the difference in normal stress distribution along a shear surface is relatively small for different interslice force inclination assumptions, shear strength parameter values for the soils in a deposit and methods of analysis. However, the induced shear stresses differ appreciably along the shear surface. The results of deformation analysis by the finite element method indicate that the ratio of induced shear stress to induced effective normal stress along a shear surface is reasonably constant. This observation needs to be further confirmed with additional studies.

If $(\tau/\sigma_n)_{induced}$ were to be held constant for frictional materials along a shear surface, then it could be used to define the characteristic shape function $g(x)$ in equation (5). The procedure then consists of making a slope stability analysis for $g(x) = 1.0$ in equation (5), i.e. a constant factor

of safety assumption and a preselected interslice force inclination assumption, and finding $(\sigma_n', \tau)_{induced}$ at the base of each slice. Now $g(x)$ is redefined as $(\tau/\sigma_n')_{induced}$ and the calculations are repeated—all else being the same. The procedure is repeated until $(\tau/\sigma_n')_{induced}$ is constant along the shear surface. If the calculated value of the induced shear stress is greater than the available shear strength then only a shear stress equal to the available shear strength need be used in calculating $g(x)$. The numerical procedure is generally able to achieve convergence in two or three iterations. The value of $T g(x)$ then defines the factor of safety along the slip surface.

GEOMETRIC INTERPRETATION OF FACTOR OF SAFETY

Constant factor of safety

Equation (1) is the commonly accepted definition of the factor of safety in slope stability analysis by the limit equilibrium method. By this definition, the normal and shear stresses induced along a shear surface are such that their plot maintains a constant proportion (equal to the factor of safety value) to the corresponding normal and shear stress strength plots at every point along the shear surface. Thus, for the computed $F > 1$ the $(\sigma_n', \tau)_{induced}$ plots below the

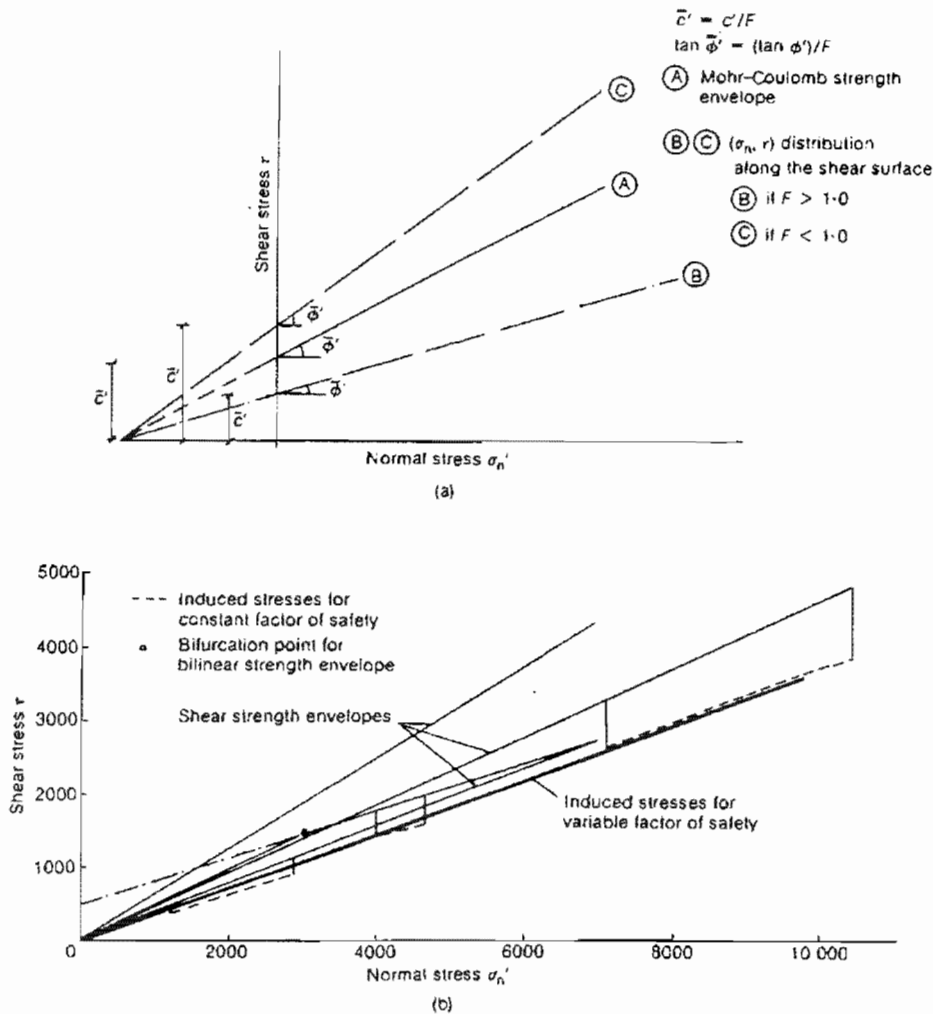


Fig. 2. Geometric interpretation of the factor of safety: (a) constant factor of safety; (b) variable factor of safety

$(\sigma_n', \tau)_{\text{strength}}$ data; for computed $F < 1$ the $(\sigma_n', \tau)_{\text{induced}}$ plots above the $(\sigma_n', \tau)_{\text{strength}}$ data; for computed $F = 1$ the $(\sigma_n', \tau)_{\text{induced}}$ plots on the $(\sigma_n', \tau)_{\text{strength}}$ data (Fig. 2(a)).

Although $F < 1$ is routinely calculated in slope stability analysis of earth slopes for assigned values of material strengths and pore pressure conditions, the calculated $(\sigma_n', \tau)_{\text{induced}}$ values are not acceptable as these stresses plot in a non-admissible stress space according to the theory of plasticity. The most shear stress that can be sustained by a frictional material is equal to its shear strength for the corresponding induced normal stress. Thus, an analysis procedure should not calculate F to be less than unity, with $F = 1$ being interpreted as a failure condition.

Variable factor of safety

Equation (5) is proposed to define a variable factor of safety along a slip surface. According to this definition a distribution of induced normal and shear stresses is sought along a slip surface that plots as a single continuous curve in the (σ_n', τ) plane (see Fig. 2(b)). The F value at any point along the slip surface is still defined as the ratio of available shear strength to the driving shear stress at that point. Since $(\sigma_n', \tau)_{\text{induced}}$ values fall on one curve and there may be several strength curves, one for each material along the shear surface, the ratio of mobilized shear strength to shear stress induced is different, and hence the factor of safety along the shear surface is varying.

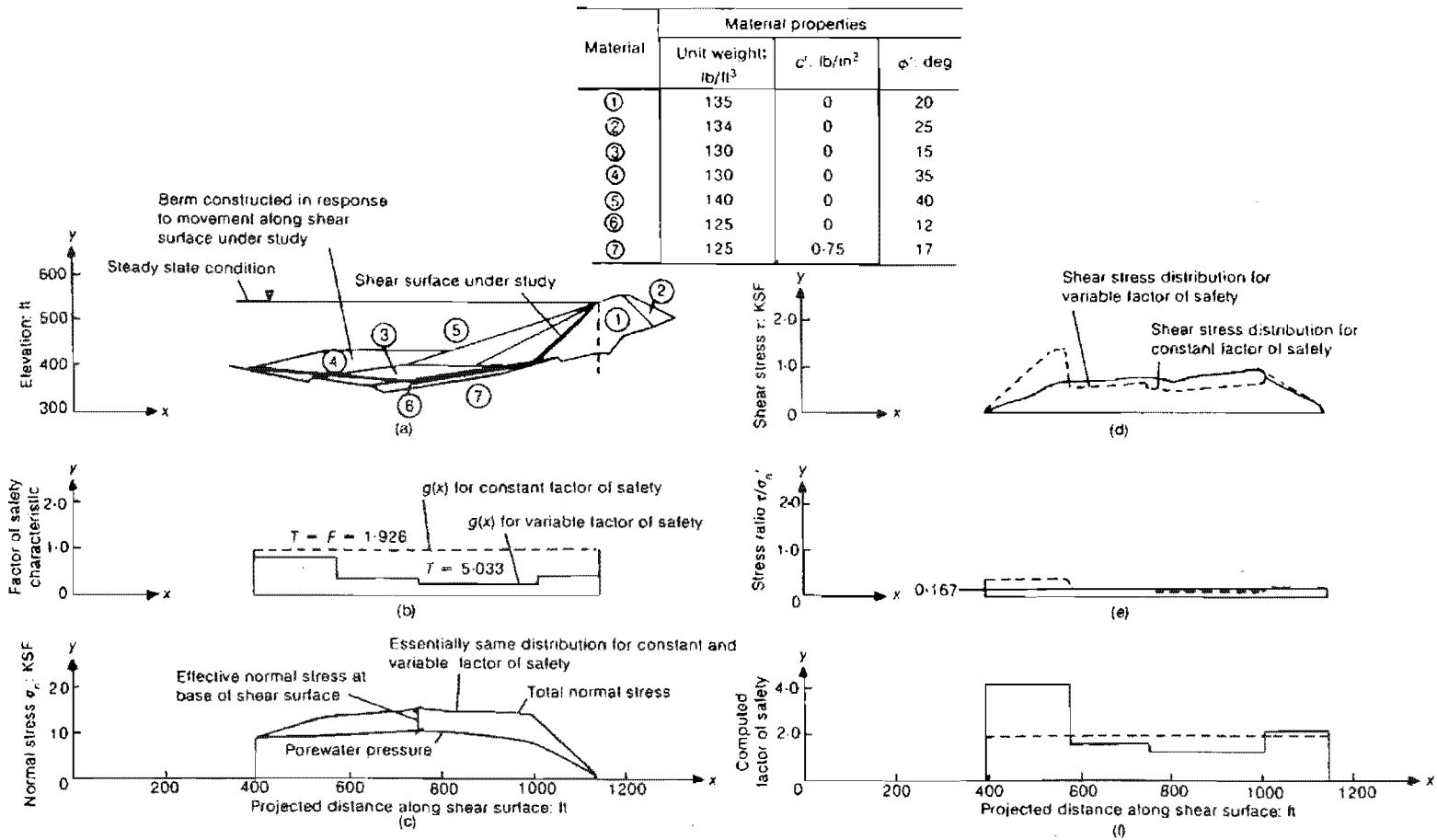


Fig. 3. Sample problem (reservoir water elevation, 540 ft)

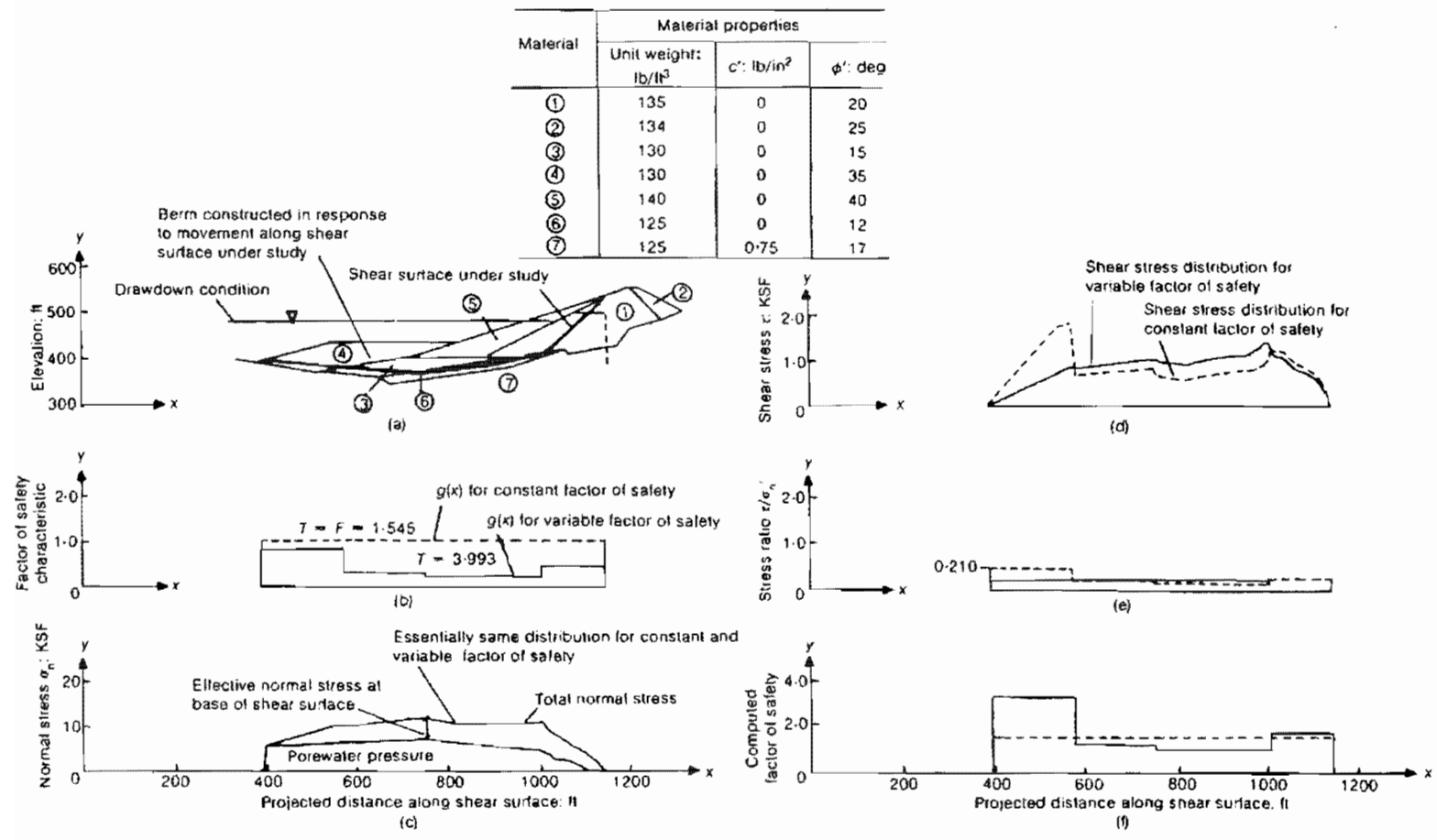


Fig. 4. Sample problem (reservoir water elevation, 480 ft)

CASE STUDY

Figure 3(a) shows a part of an embankment dam cross-section and its foundation zones. The shear strength properties of different materials in the embankment and its foundations are shown in the table included in the figure. There was a slip failure at this site. As a result, the upstream berm was constructed and the facility put back to use.

Recently, during the reservoir drawdown, internal sliding at the old slip surface has been detected by the instrumentation; some cracking at the crest of the dam has occurred, but there has not been a gross movement of the embankment materials or a noticeable change in the embankment geometry. Thus, the problem needs to be analysed to seek answers to questions like

- (a) is there a failure?
- (b) where is the failure localized?
- (c) how safe is the upstream portion of the dam?
- (d) can the reservoir be filled without any major rehabilitation work?

The shear surface geometry and the pore pressure data for use in this study are shown in Fig. 3.

The slope stability analyses were performed using the computer program SSTAB2 (Chugh, 1981). This computer program is based on the limit equilibrium method; it satisfies all the statics equations; it provides for use of a constant or a variable interslice force inclination and a constant or a variable factor of safety along the slip surface according to the ideas presented in this Paper.

The conventional slope stability analysis of the sample problem, using constant interslice force inclination and constant factor of safety assumptions, yields $F = 1.93$ for high level steady state reservoir operation and $F = 1.55$ for the reservoir drawdown. The normal stress, the shear stress and the ratio of shear stress to effective normal stress along the shear surface, as obtained through these calculations, are shown in Figs 3(c)–3(e) and 4(c)–4(e) for the high level steady state reservoir operation and reservoir drawdown conditions respectively. It is not possible to draw any inference of actual or impending distress along the shear surface from these results of conventional slope stability calculations.

A similar slope stability analysis of the sample problem using the variable factor of safety ideas presented in this Paper, all else being the same, give the stress distributions shown superimposed on their counterpart results for the constant F assumption. There is no appreciable difference in the normal stress distribution, but the shear stress distribution is much improved and more as would be expected considering the shear surface geometry, i.e. peak shear stress occurs where the

shear surface geometry has the sharpest change in direction. The computed factors of safety along the shear surface are shown in Figs 3(f) and 4(f) for the conditions analysed. The computed factor of safety in the 12° material for the drawdown condition is 1.01. It is higher in other materials. The shear surface under the berm has a factor of safety of 3.33. For this sample problem, the results indicate that the local shear failure should occur in the 12° material. Once this happens, movement should occur in the 12° material which will cause tensile stresses in the materials above the back rest portion of the shear surface. Thus, the tension cracks at the crest of the dam are a consequence of internal failure in the 12° material and define the extent of the active wedge. Since the factor of safety along the shear surface under the berm area is substantially higher than 1.0, gross movement along the shear surface could not have occurred. Filling of the reservoir, without any repair work, should only improve the stability of the embankment because of the buttressing effect of the water.

CONCLUSIONS

The use of a variable factor of safety in slope stability analysis of problems of practical importance is generally of considerable interest in seeking answers to questions that influence design decisions. The proposed procedure provides a means to calculate variations in the factor of safety along a shear surface within the framework of the limit equilibrium method. The choice of the characteristic function $g(x)$ defining the relative safety factor along a shear surface is a difficult issue and needs further study. The proposed procedure of making $g(x)$ equal to the ratio of shear stress to effective normal stress for purely frictional materials is reasonable. The resulting shear stress distribution along the shear surface is generally smooth and more likely to occur in nature than that implied by the constant factor of safety assumption.

REFERENCES

- Bishop, A. W. (1967). Progressive failure—with special reference to the mechanism causing it. *Proc. Geotechnical Conf. Oslo* 2, 142–154.
- Bishop, A. W. (1971). The influence of progressive failure on the choice of the method of stability analysis. *Géotechnique* 21, No. 2, 168–172.
- Chowdhury, R. N. (1978). *Slope analysis*. New York: Elsevier.
- Chugh, A. K. (1981). *User information manual for slope stability analysis program SSTAB2*. Denver: Engineering and Research Center, US Bureau of Reclamation.
- Chugh, A. K. (1982). Slope stability analysis for earthquakes. *Int. J. Numer. Analyt. Meth. Geomech.* 6, No. 3, 307–322.

- Chugh, A. K. (1984). *Variable interslice force inclination in slope stability analysis*. Internal Report, Engineering and Research Center, Bureau of Reclamation, Denver.
- Janbu, N. (1973). Soil stability computations. In *Embankment dam engineering*, Casagrande volume, pp. 47-87 (eds R. C. Hirschfeld and S. J. Poulos). New York: Wiley.
- Morgenstern, N. R. & Price, V. E. (1965). The analysis of the stability of general slip surfaces. *Géotechnique* 15, No. 1, 79-93.
- Sarma, S. K. (1973). Stability analysis of embankments and slopes. *Géotechnique* 23, No. 3, 423-433.
- Spencer, E. (1967). A method of analysis of the stability of embankments assuming parallel interslice forces. *Géotechnique* 17, No. 1, 11-26.
- Spencer, E. (1973). Thrust line criterion in embankment stability analysis. *Géotechnique* 23, No. 1, 85-100.

Appendix D

Part 4 On the Boundary Conditions in Slope Stability Analysis
by Ashok K. Chugh

This article was published in *International Journal for Numerical and Analytical Methods in Geomechanics*, Volume 27, pp. 905-926, 2003.

On the boundary conditions in slope stability analysis

Ashok K. Chugh^{*,†}

U.S. Bureau of Reclamation, Denver, Colorado 80225, U.S.A.

SUMMARY

Boundary conditions can affect computed factor of safety results in two- and three-dimensional stability analyses of slopes. Commonly used boundary conditions in two- and three-dimensional slope stability analyses via limit-equilibrium and continuum-mechanics based solution procedures are described. A sample problem is included to illustrate the importance of boundary conditions in slope stability analyses. The sample problem is solved using two- and three-dimensional numerical models commonly used in engineering practice. Copyright © 2003 John Wiley & Sons, Ltd.

KEY WORDS: boundary conditions; slope stability; two- and three-dimensional analysis

1. INTRODUCTION

Slope stability problems in geomechanics are boundary value problems and boundary conditions play an important role in the development of internal stresses in the medium and hence influence the calculated factor of safety (FoS). Some slope problems can be analysed adequately via two-dimensional (2-D) numerical models, while others require a three-dimensional (3-D) model for a correct assessment of the slope performance. Use of appropriate boundary conditions is important in both 2-D and 3-D analyses.

In geotechnical engineering practice, slope stability analysis is generally performed using 2-D and 3-D computer programs based on limit equilibrium method. 2-D analyses are more common than 3-D analyses, and the 2-D FoS results are generally considered to be conservative. Geotechnical literature is rich in limit-equilibrium-based 2-D analysis papers; however, 3-D analysis papers are relatively few [1–3]. References included in this paper are representative and not a complete list of works on the subject. Duncan [4] gives a current state-of-the-art in slope stability analysis and includes an extensive list of references on the subject.

Arellano and Stark [3] used a commercially available limit-equilibrium-based computer program *CLARA* [5] to show that for a translational shear surface of sliding in 3-D introduction of shear resistance along the two sides of the slide mass that parallel the direction of movement can cause significant difference in the computed FoS values. Arellano and Stark [3] introduced approximations to include the shear resistance along the two sides of the slide mass to overcome some of the limitations with *CLARA*, and suggested use of a continuum-mechanics-based analysis procedure which provide an effective alternative means to solve slope stability problems in 2-D and 3-D [6–8].

*Correspondence to: A. K. Chugh, U.S. Bureau of Reclamation, Denver, Colorado 80225, U.S.A.

†E-mail: achugh@do.usbr.gov

The objectives of this paper are to describe: (1) boundary conditions implicit in the limit-equilibrium-based 2-D and 3-D solution procedures and (2) boundary conditions commonly used in continuum-mechanics-based 2-D and 3-D solution procedures. The significance of boundary conditions on the computed FoS is illustrated using one of the parametric slope model cases from Arellano and Stark [3] and solving it using commercially available continuum-mechanics-based explicit finite difference computer programs *FLAC* [9] and *FLAC3D* [10] in 2-D and 3-D, respectively. The work reported was carried out as a sequel to Arellano and Stark [3].

It should be noted that the two methods of slope stability analysis referred to in this paper are: (1) the limit equilibrium method and (2) the continuum mechanics method. Within the limit equilibrium method, there are several procedures, e.g. Bishop, Janbu, Morgenstern-Price, Spencer among others (each makes different assumptions to render the problem statically determinate). Within the continuum mechanics method, finite difference, finite element, and boundary element are different procedures (each uses a different solution strategy).

For ease of presentation, the nomenclature shown in Figure 1 is used in this paper. A slope is considered to lie in the xz plane and the width of the slope is in the y -direction. Displacements are expressed using the symbols u , v , w for the x , y and z faces, respectively. Stresses are expressed using the stress symbols shown in Figure 1. According to this convention, tension is positive, compression is negative, and the shear stresses shown in Figure 1 are positive.

2. CONCEPTUAL MODELS AND BOUNDARY CONDITIONS

The conceptual model of a slope stability problem is different in the limit-equilibrium and continuum-mechanics methods. Boundary conditions need to be consistent with the conceptual model. Also, emphasis on prescribing boundary conditions is different in the two methods. Therefore, the conceptual model, model size, and boundary conditions for each method are described separately.

2.1. *Limit-equilibrium-based conceptual slope model*

Figure 2 shows a schematic of a slope model in both 2-D and 3-D. In 2-D, the model of failure usually envisaged consists of a train of vertical blocks resting on a curved slip surface. These blocks are attached to each other and to the slip surface with a rigid-plastic glue which conforms to the Terzaghi–Coulomb shear strength criterion. The blocks themselves are considered to be rigid and their properties are not related to those of soil. It is in the nature of this model that no deflection occurs prior to failure and that when failure does take place all the blocks begin to slide slowly downwards together—without accelerating. Strictly, the model is applicable only if the radius of curvature of the slip surface is constant; variation in the radius would produce distortion in the blocks which are assumed to be rigid [11,12]. However, this limitation is commonly disregarded. In 3-D, the 2-D conceptual model extends in the y -direction to the natural boundaries such as end-walls of the slide mass or abutments, and the 2-D vertical blocks become 3-D columns.

2.1.1. Model size and boundary conditions. In limit-equilibrium-based 2-D and 3-D solution procedures, the size of the model needs to cover the slide mass including the shear surface but

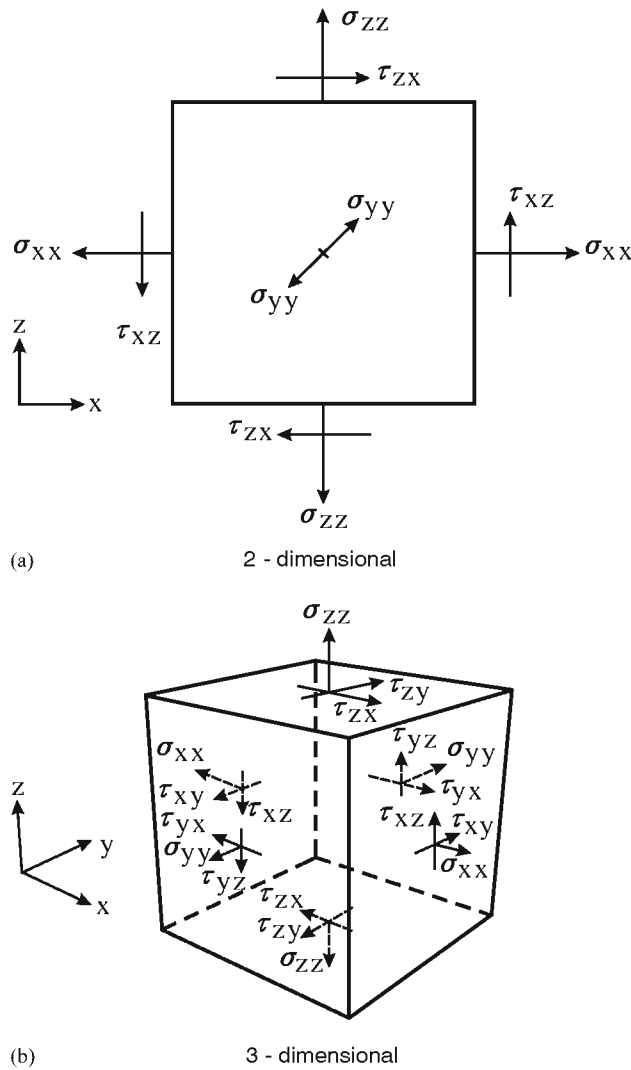


Figure 1. Description of state of stress on an element of soil (stresses shown are positive).

any extension of the model past this requirement is only for the user's reference and convenience. Also, boundary conditions are built into the solution procedure, and the user is not required to specify them explicitly in a data file. The boundary conditions implicit in 2-D and 3-D solution procedures are as described below.

2.1.2. *2-D model boundary conditions.* Figure 2(a) shows a sketch of a 2-D slope of a unit width in the y -direction and the slide mass divided into vertical slices. The boundary conditions apply at the head and at the toe of the slip surface, and at the two faces of the slope in the y -direction.

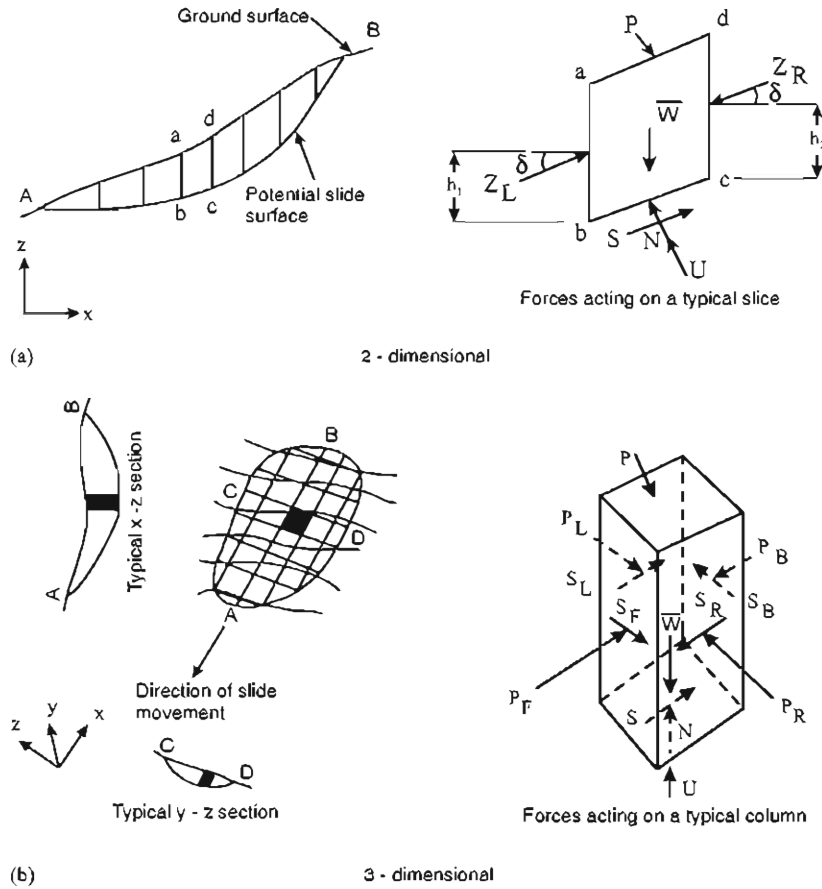


Figure 2. Limit-equilibrium based slope models and boundary conditions.

The applicable boundary conditions are:

- (a) Applied force Z_L and its location h_1 at the toe of the slip surface.
- (b) Applied force Z_R and its location h_2 at the head of the slip surface. In the case of a tension crack with water, Z_R is the force exerted by the water in the tension crack, and h_2 is the location of the water force. If there is no water in the tension crack, Z_R and h_2 are zero, and the bottom of the tension crack becomes the end of the shear surface. The water force acts horizontally.
- (c) Plane strain in the y -direction. This implies the out-of-plane displacement, v , and shear stresses, τ_{yx} and τ_{yz} , on the y -faces are zero. However, the normal stress, σ_{yy} , on the y -faces is not zero. Since equilibrium of forces and moments in the xz plane is of interest, this out-of-plane force is not considered in the equilibrium equations—however, it is present.

2.1.3. 3-D model boundary conditions. Figure 2(b) shows a sketch of a 3-D slope and the slide mass divided into vertical columns. The boundary conditions (a) and (b) of the 2-D case are

extended in the y -direction and the boundary condition (c) of the 2-D case is applied to the end boundaries in the y -direction. However, in order to include the shear resistance along the parallel sides of the slide mass, Arellano and Stark [3] added an external horizontal and vertical side force equivalent to the shear resistance due to the at-rest earth pressure acting on the vertical sides at the centroid of the two parallel sides in calculating 3-D FoS results using the computer program *CLARA* [5].

One of the objectives of this paper is to study the effects of different boundary conditions at the slope-abutment contact on the computed FoS using a continuum-mechanics-based 3-D analysis procedure.

2.2. *Continuum-mechanics-based conceptual slope model*

Figure 3 shows schematics of a slope model in 2-D and 3-D. The conceptual model of failure in 2-D and 3-D is a deformable, bounded material body with Terzaghi–Coulomb yield strength. Under the action of gravity and externally applied loads, the material body deforms causing

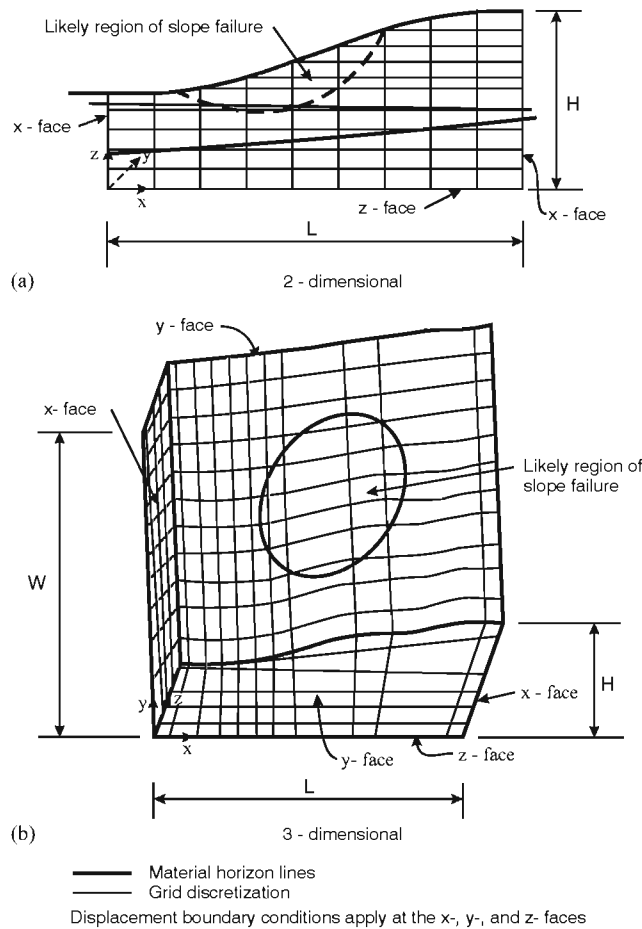


Figure 3. Continuum based slope models and boundary conditions.

relative deformations that produce strains and stresses in the material body. If stresses at a location in the material body exceed the Terzaghi–Coulomb yield strength, the excess of stresses is shared by the neighbouring under-stressed locations. When stresses at a sufficient number of locations reach their yield strength, a mechanism is formed along which continuous movement or sliding occurs. Thus, in a continuum model, a shear surface develops as a part of the solution, and is always the one with the lowest FoS. The deformational behaviour of the bounded mass is controlled by the geometry of the medium, deformational properties of the materials, gravity and external loads, and boundary conditions. The FoS is determined using a strength reduction technique [13] in which the slope problem is solved repeatedly using reduced soil shear strength values until the numerical model becomes unstable (indicating slope failure), and the resulting FoS is the ratio of the soil's initial shear strength to the reduced shear strength at failure.

2.2.1. Model size and boundary conditions. For a continuum-mechanics-based solution to be meaningful, the slope model needs to extend past the location where slope failure is likely to occur. Also, all of the exterior of the slope model constitutes its boundary and boundary conditions need to be expressed in terms of applied forces or displacements in the input data. It should be mentioned that at any one location on the body, either a displacement or a stress condition can be prescribed, but not both. In continuum-mechanics-based solution procedures, it is common to set every point free to displace and free of all stresses, and the user defines the non-zero stress and/or restrained displacement boundary conditions via input data. A displacement restraint is either nil (completely free) or full (completely fixed)—partial restraints are generally not allowed.

2.2.2. 2-D model boundary conditions. Figure 3(a) shows a sketch of a continuum model of a slope with a unit width in the y -direction and the material body divided into a grid. Every node in the grid including the boundaries has two degrees of freedom, i.e. displacements u and w in the x - and z -directions, respectively. The commonly used boundary conditions are:

- (a) No displacement in the x -direction at the ends of the slope model ($u = 0$ at $x = 0$ and at $x = L$). These boundaries are placed far enough from the region where slope failure is likely to occur.
- (b) No displacement at the base of the slope model ($u = w = 0$ at $z = 0$). This boundary is placed far enough from the region where slope failure is likely to occur.
- (c) Plane strain in the y -direction. This implies the out-of-plane displacement, v , and shear stresses, τ_{yx} and τ_{yz} , on the y -faces are zero. However, the normal stress, σ_{yy} , on the y -faces is not zero.

2.2.3. 3-D model boundary conditions. Figure 3(b) shows a sketch of a continuum model of a slope in 3-D and the material body divided into a grid. Every node in the grid including the boundaries has three degrees of freedom, i.e. displacement u , v , and w in the x -, y -, and z -directions, respectively; and a user can constrain any or all components of displacement at any location in the model including the boundaries. The commonly used boundary conditions are:

- (a) No out-of-plane displacement in the x -direction at the model ends ($u = 0$ on the end yz planes in the x -direction). These boundaries are placed far enough from the region where slope failure is likely to occur.

- (b) No displacement at the base of the slope model ($u = v = w = 0$ for the xy plane at $z = 0$). This boundary is placed far enough from the region where slope failure is likely to occur.
- (c) Displacement constraints in the y -direction at the model ends ($v = 0$ or $u = v = w = 0$ for the xz planes at $y = 0$ and $y = W$ are the commonly prescribed conditions). The displacement $v = 0$ boundary condition is used to represent a contact with a rigid, smooth abutment that can provide a reacting thrust but no in-plane shear restraint. The displacement boundary condition $u = v = w = 0$ is used to represent a rigid contact with no possibility of movement.

2.3. Appropriate 3-D model and boundary conditions

The option of explicitly specifying boundary conditions is available in continuum-mechanics-based solution procedures. Selection of appropriate boundary conditions for a slope problem should be derived from the field conditions being analysed. For example, the boundary conditions at the y -faces for a laboratory model of a slope built in a wooden container with glass walls are different than the boundary conditions at the y -faces for a slope with rock or soil abutments commonly encountered in the field.

The boundary conditions described for the x - and z -directions of a 3-D model are appropriate so long as the boundaries are placed far enough away from the region where slope failure is likely to occur. The following recommendations are suggested for establishing the boundary conditions in the y -direction of a 3-D model:

- (1) Extend the 3-D continuum model past the ends of the slope to include the presence of abutments.
- (2) Place the model boundary conditions at the ends of the extended continuum model.
- (3) Introduce interfaces between the slope and the abutments to allow for relative movements at the slope-abutment contact.
- (4) Use the displacement condition of $u = 0$, $v = 0$, and $w = 0$ at the extended model boundaries.

3. SAMPLE PROBLEM

Figure 4 shows the parametric slope model of Arellano and Stark [3]. Arellano and Stark [3] used three slope inclinations ($1H: 1V$; $3H: 1V$; and $5H: 1V$); for each slope inclination, seven width (W) to height (H) ratios ($W/H = 1, 1.5, 2, 4, 6, 8,$ and 10); and for each pair of the slope inclination and W/H ratio, four combinations of $\varphi_{\text{upper}}/\varphi_{\text{lower}}$ values ($\varphi_{\text{upper}}/\varphi_{\text{lower}} = 1, 1.5, 3,$ and 3.75). The $5H: 1V$ slope was selected to illustrate the effects of boundary conditions on computed factor of safety results for the four combinations of $\varphi_{\text{upper}}/\varphi_{\text{lower}}$ values. The friction angle of the upper material was 30° , and the friction angle for the lower material was assigned values of $8^\circ, 10^\circ, 20^\circ$ and 30° . Values of $W/H = 1, 2, 5,$ and 10 were considered.

For W/H less than 5 or 10, a 2-D plane strain analysis is not considered appropriate because of the close proximity of the end abutments, and thus cannot provide a reasonable estimate of the FoS for the slope. For these conditions, a 3-D analysis should be used. However, for illustration purposes, 2-D and 3-D analyses were performed using the continuum-mechanics-based explicit finite difference computer programs *FLAC* [9] and *FLAC3D* [10], respectively. For

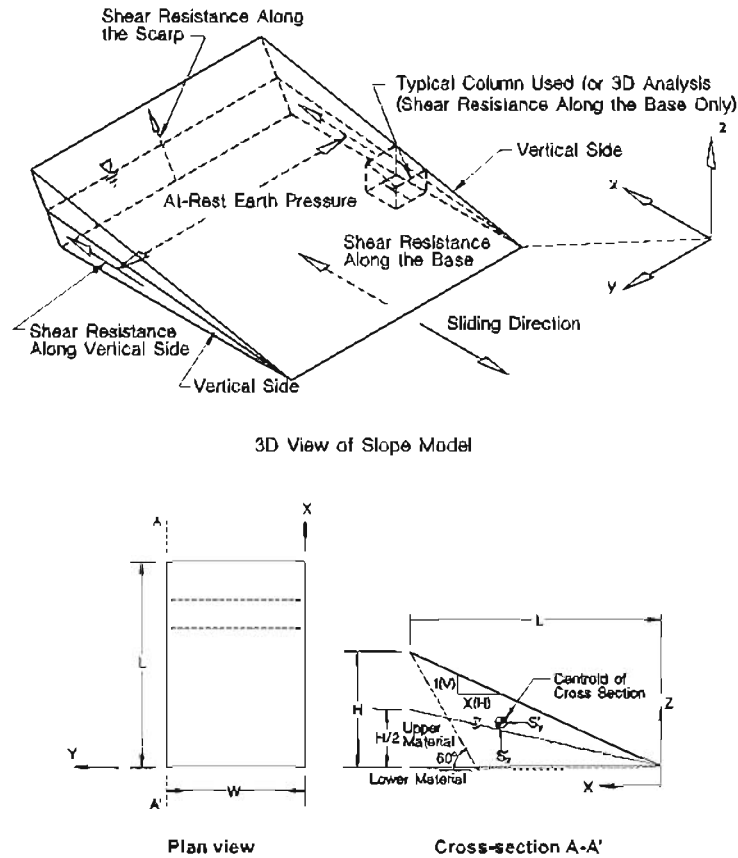


Figure 4. Sample problem showing details of the parametric slope model used by Arellano and Stark [3] (reproduced by permission of the publisher, ASCE).

comparison purposes, the problem was also solved using a limit-equilibrium-based 2-D analysis procedure *SSTAB2* [14] which implements Spencer's procedure [15]. The material properties that were used to perform the *FLAC*, *FLAC3D*, and *SSTAB2* analyses are shown in Table I. In all of these analyses, the following slope geometry parameters were used: height (H) = 10 m, length (L) = 58.8 m and width (W) = 10 m. In the continuum models of the sample problem, the geometric space covered is 176.4 m (3 times the slope length L) in the x -direction, 20 m (2 times the slope height H) in the z -direction, and 10 m (1 time the slope width W) or 22 m (slope width W plus two 6-m wide end blocks for abutments) in the y -direction. For $W/H = 2, 5,$ and 10 , the continuum model included two 6-m wide end blocks for abutments and the model width in the y -direction was 32, 62, and 112 m, respectively.

3.1. Arellano and Stark results

The 2-D and 3-D values of FoS calculated using *CLARA* without applying the Arellano and Stark [3] modification are shown in Table II. Also included in Table II are the 3-D values of FoS calculated using *CLARA* with the Arellano and Stark [3] modification for $W/H = 1, 2, 5,$

Table I. Material properties for stability analyses of the sample Problem.

Material	Density	Material strength		Elastic constants	
	ρ (kg/m ³)	c (Pa)	φ (°)	Bulk modulus (Pa)	Shear modulus (Pa)
Upper material	1733	0	30	3e7	1e7
Lower material	1835	0	8; 10; 20; 30	3e6	1e6
Bottom block	1836	0	40	3e8	1e8
End blocks	2500	50	45	3e9	1e9
Interface	N/A	0	30	Normal stiffness (Pa/m) 1e7	Shear stiffness (Pa/m) 1e6

Unit weight γ (N/m³) = Density \times 9.81; N/A—not applicable.

Table II. FoS results* for the sample problem from Arellano and Stark [3].

$\varphi_{\text{lower material}}$	CLARA		Arellano and Stark [3] modification of CLARA			
	2-D	3-D	3-D			
			$W/H = 1$	$W/H = 2$	$W/H = 5$	$W/H = 10$
8°	0.90	0.90	2.85	1.45	1.05	1.00
10°	1.00	1.00	3.18	1.63	1.23	1.13
20°	1.70	1.70	4.80	2.58	2.00	1.82
30°	2.50	2.50	6.58	3.58	2.85	2.57

*The FoS values given are scaled from the graphical presentation of results in Arellano and Stark [3].

and 10. The FoS values were scaled from the graphical presentation of results in Arellano and Stark [3].

3.2. SSTAB2 results

The FoS and interslice force inclination, δ , results from *SSTAB2* for the four values of φ_{lower} are given in Table III. The shear surfaces used in the *SSTAB2* analyses were the same as those used by Arellano and Stark [3].

3.3. FLAC results

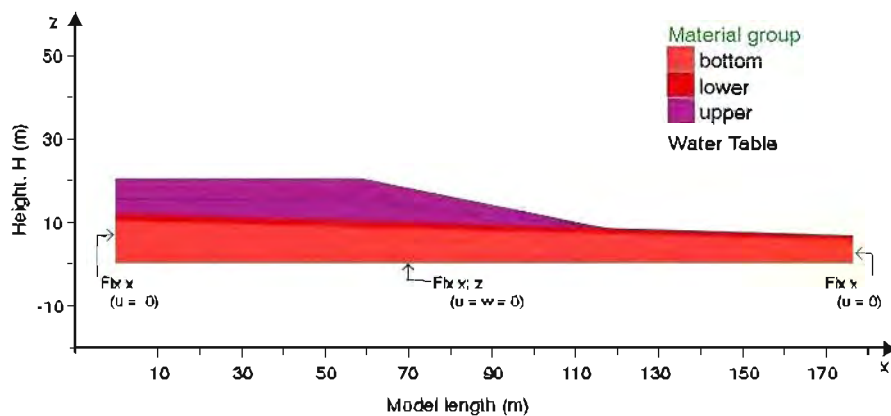
Figure 5 shows the *FLAC* 2-D model of the slope with end extensions in the x - and z -directions, the water table, and the boundary conditions used. The FoS results for the four cases analysed, i.e. four values of φ_{lower} , are shown in Table III. The *FLAC* values of FoS are in general agreement with those from *SSTAB2* and *CLARA* 2-D (Table II). Figure 6 shows contour plots of maximum shear strain rate and the velocity vectors at the instant of numerical instability for each of the values of φ_{lower} analysed. The maximum shear strain rate and velocity vector plots are helpful in identifying the location and shape of failure surface. However, in Figure 6, the shear strain rate plots are hidden from view because of the superimposed velocity vector plots; the location and geometry of the associated shear surface for each case is taken to be along the

Table III. *FLAC* (Figure 5) and *SSTAB2* FoS results for the sample problem.

$\varphi_{\text{lower material}}$	<i>FLAC</i> 2-D	<i>SSTAB2</i> 2-D	
		FoS	δ°
8°	0.85	0.78	12.55
10°	1.01	0.93	12.69
20°	1.64	1.62	13.02
30°	2.22	2.37	13.13

Table IV. *FLAC3D* model No. 1 (Figure 7) FoS results for the following boundary conditions ($W/H = 1$).

$\varphi_{\text{lower material}}$	Boundary constraint(s) used at the y -faces of the numerical model		
	Fix y	Fix x, y	Fix x, y, z
8°	0.89	1.42	1.41
10°	1.04	1.57	1.57
20°	1.71	2.26	2.26
30°	2.32	2.82	2.82

Figure 5. *FLAC* model for the sample problem.

path where the velocity vectors essentially vanish as it marks the boundary between stable and unstable portions of the deposit.

3.4. *FLAC3D* model No. 1 results

In this model, the width W is 10 m in the y -direction. Figure 7 shows the *FLAC3D* model of the slope with end extensions in the xz plane, the water surface, the viewing information, and the boundary conditions used. For each of the values of φ_{lower} , three sets of analyses were conducted for $W/H = 1$ using the boundary conditions of $v = 0$ (fix y); $u = v = 0$ (fix x, y); and $u = v = w = 0$ (fix x, y, z) at the ends of the slope in the y -direction. Application of each of these y -direction boundary conditions represents a particular condition: (a) the $v = 0$ (fix y) boundary

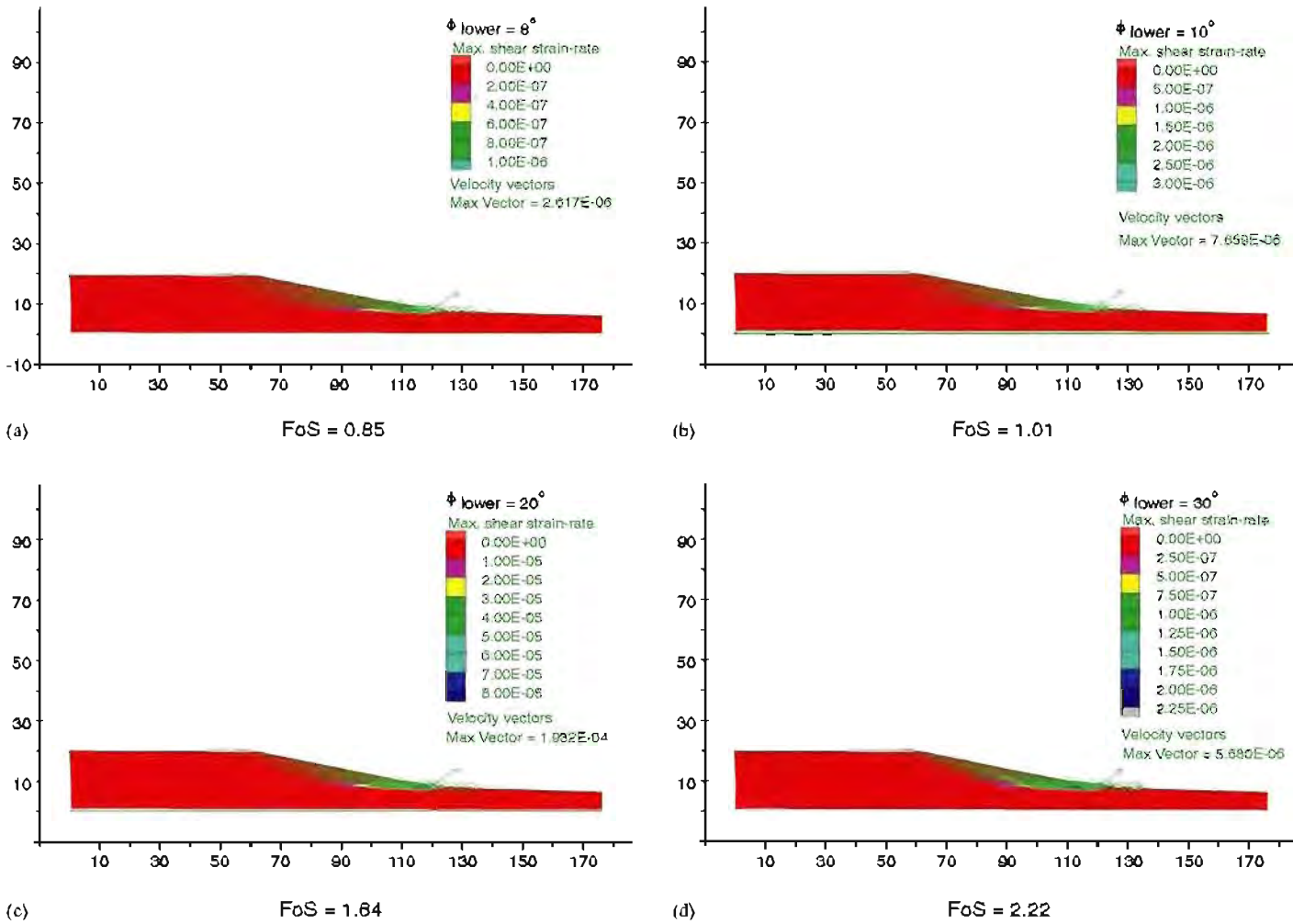


Figure 6. *FLAC* model results for the four values of ϕ_{lower} .

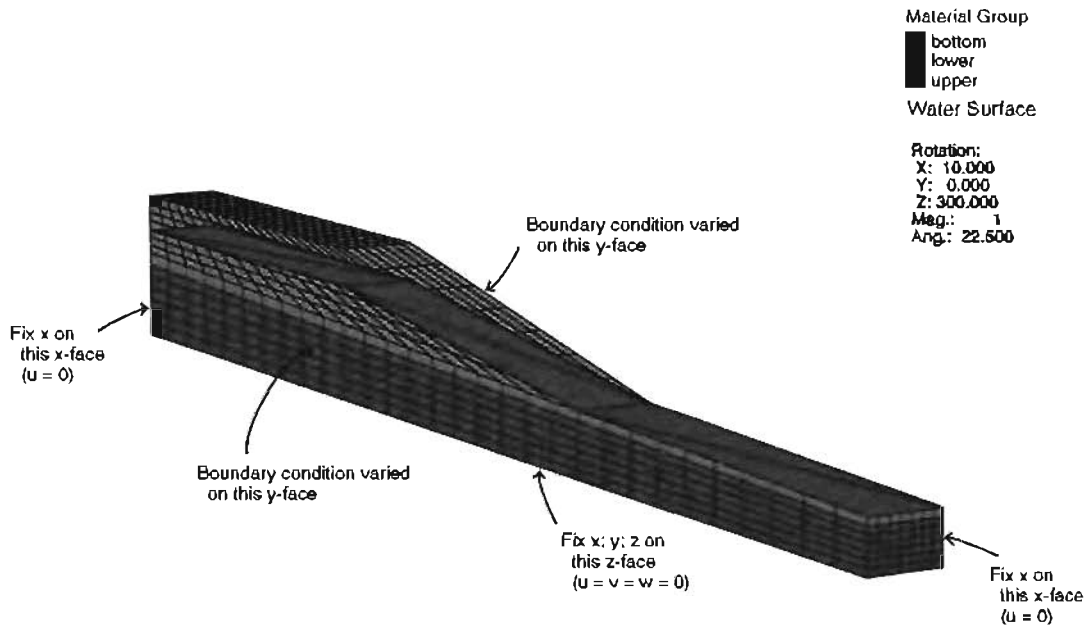


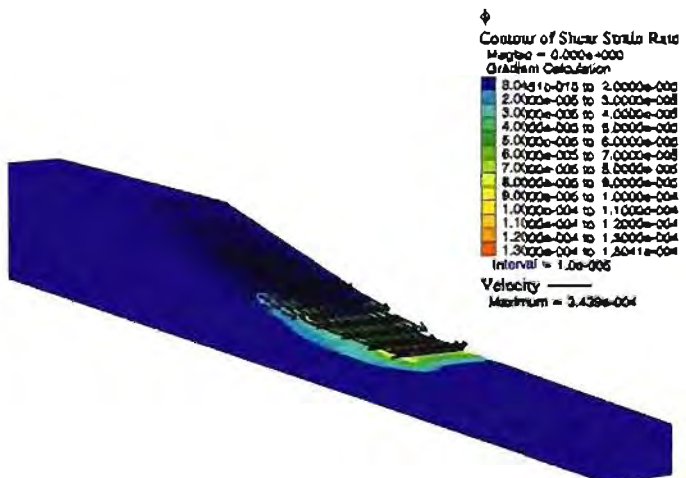
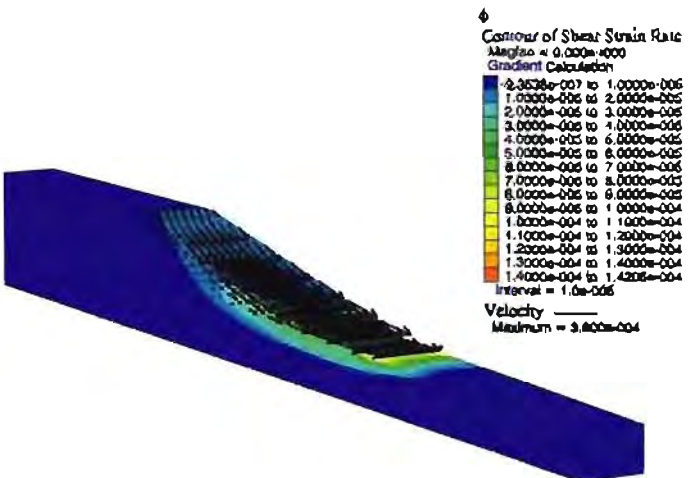
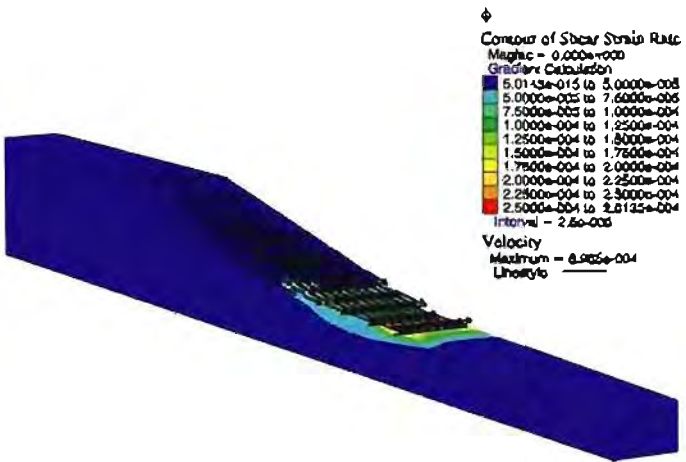
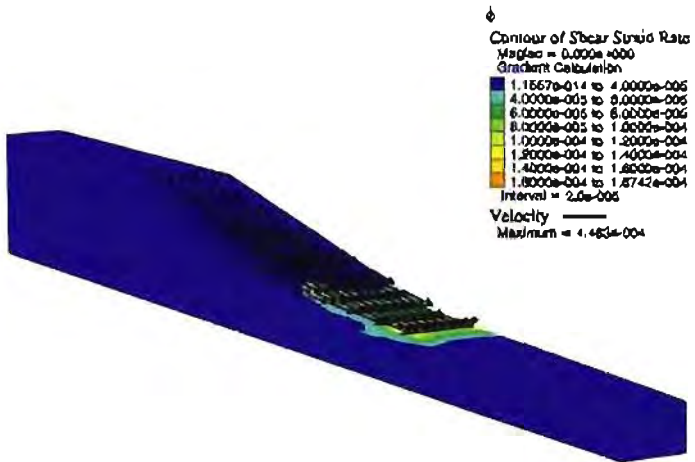
Figure 7. *FLAC3D* model No. 1 for the sample problem ($W/H = 1$).

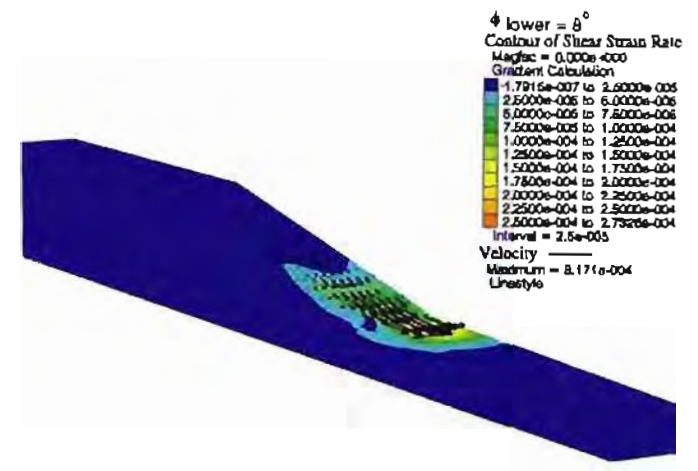
condition is similar to the implicit boundary condition in *CLARA 3D*; (b) the $u = v = 0$ (fix x, y) boundary condition should model the conditions imposed by the modification proposed by Arellano and Stark [3] to include side shear resistance; and (c) the $u = v = w = 0$ (fix x, y, z) boundary condition is used commonly in practice. The FoS values for each of the assigned boundary conditions in the y -direction for the four values of ϕ_{lower} are shown in Table IV. *FLAC3D* model No. 1 results are compared with Arellano and Stark [3] values of FoS (Table II).

For the fixed y boundary conditions, *FLAC3D* FoS values (Table IV) are similar to those from *CLARA 3D* shown in Table II. For the fixed x, y boundary conditions, *FLAC3D* FoS values differ from those of Arellano and Stark [3] 3-D shown in Table II for $W/H = 1$. For the fixed x, y, z boundary conditions, *FLAC3D* FoS values are similar to the *FLAC3D* values for the fixed x, y boundary conditions shown in Table IV. However, this does not mean that the two sets of boundary conditions (fixed x, y and fixed x, y, z) are the same or that they will always lead to the same results.

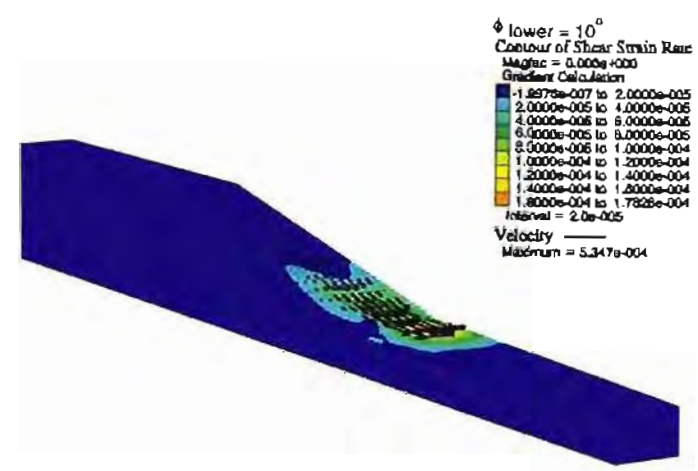
Figure 8 shows contour plots of maximum shear strain rate and the velocity vectors at the instant of numerical instability for each of the values of ϕ_{lower} and the three boundary

Figure 8. *FLAC3D* model No. 1 results for the sample problem with $W/H = 1$ and the boundary condition of $v = 0$ (fix y) in the y -direction: (a) FoS = 0.89, (b) FoS = 1.04, (c) FoS = 1.71 and (d) FoS = 2.32. *FLAC3D* model No. 1 results for the sample problem with $W/H = 1$ and the boundary condition of $u = v = 0$ (fix x, y) in the y -direction: (e) FoS = 1.42, (f) FoS = 1.57, (g) FoS = 2.26 and (h) FoS = 2.82. *FLAC3D* model No. 1 results for the sample problem with $W/H = 1$ and the boundary condition of $u = v = w = 0$ (fix x, y, z) in the y -direction: (i) FoS = 1.41, (j) FoS = 1.57, (k) FoS = 2.26 and (l) FoS = 2.82.

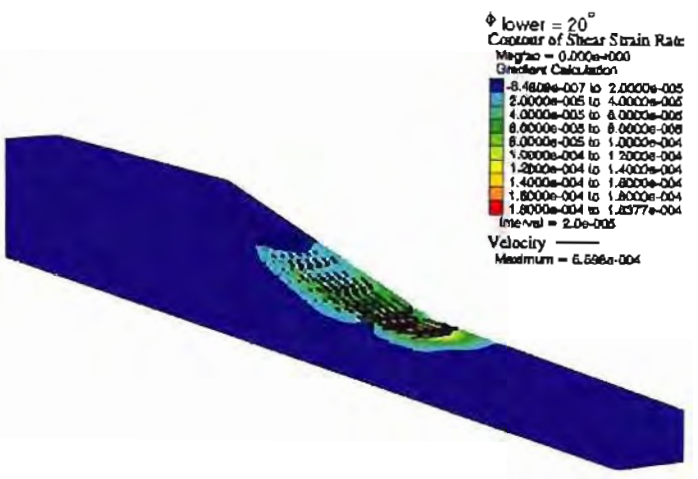




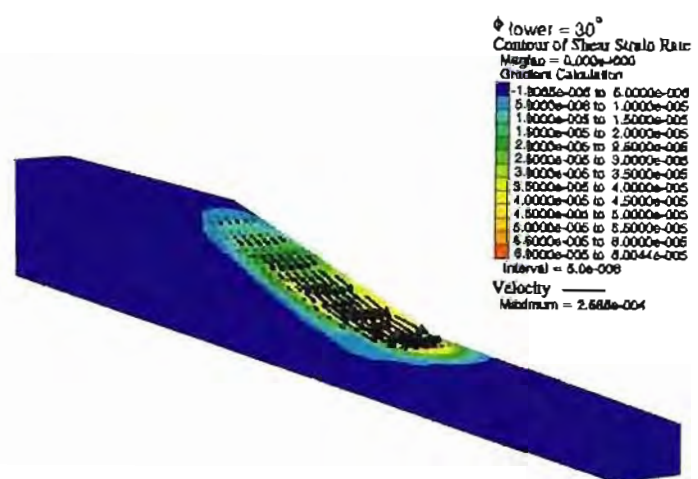
(e) FoS = 1.42



(f) FoS = 1.57



(g) FoS = 2.26



(h) FoS = 2.82

Figure 8. (Continued)

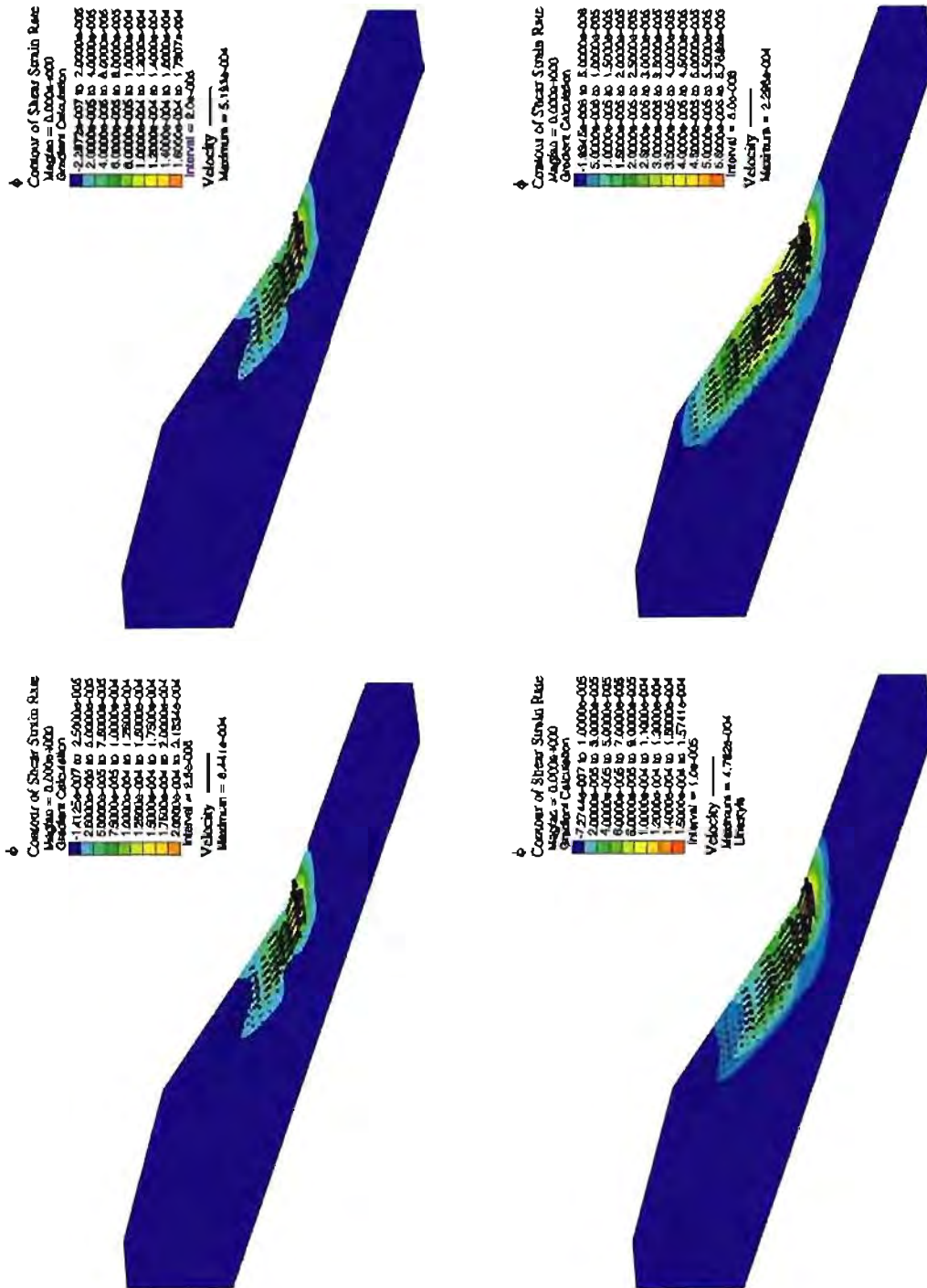


Figure 8. (Continued)

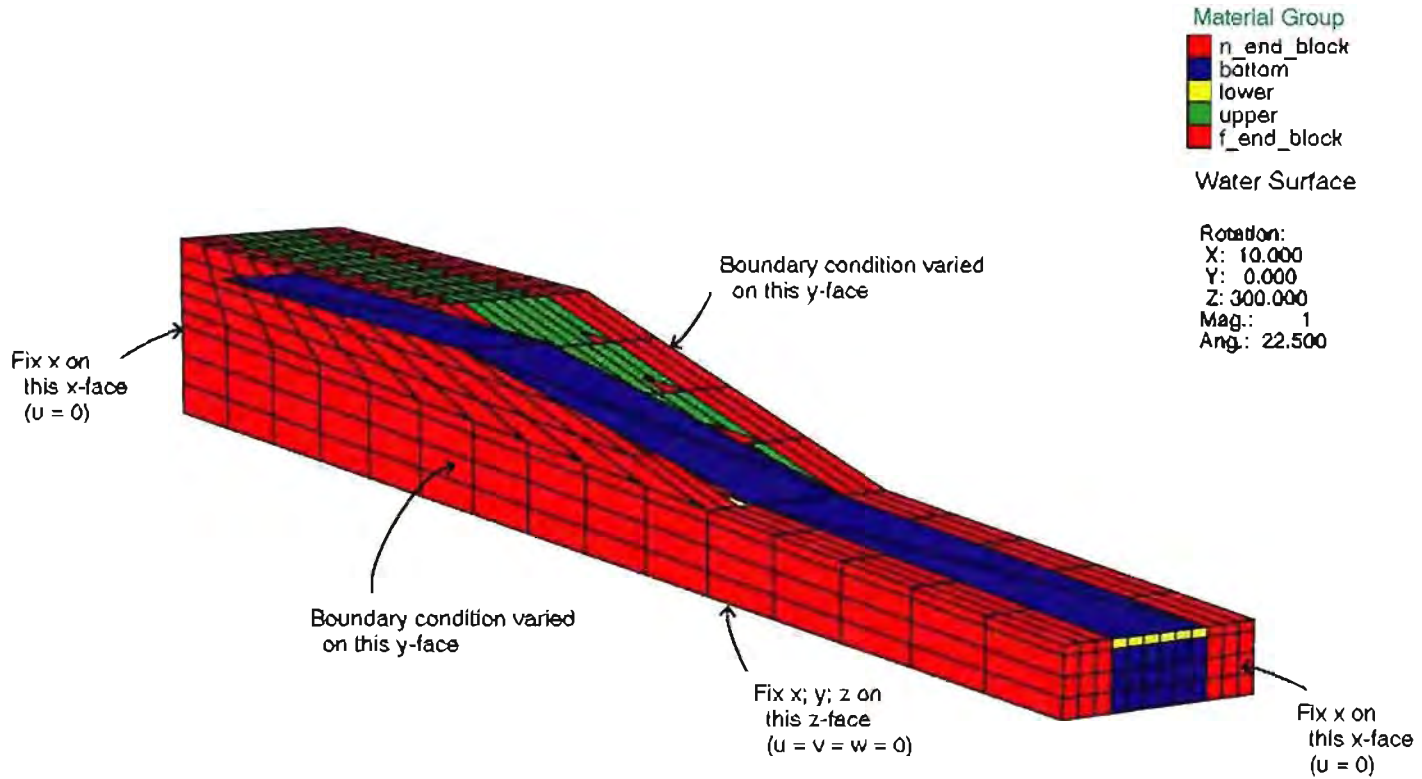


Figure 9. *FLAC3D* model No. 2 for the sample problem ($W/H = 1$).

conditions analysed; the viewing information for the 3-D model is the same as used in Figure 7. As mentioned for the *FLAC* results, the location and geometry of the associated shear surface for each case is interpreted to be along the path where the velocity vectors essentially vanish.

3.5. *FLAC3D* model No. 2 results

Figure 9 shows the suggested 3-D model for the slope. It has the same end extensions in the xz plane as in the *FLAC3D* model No. 1 (Figure 7); in addition, in the y -direction, it has two end blocks to represent abutments, and the contacts between the slope and abutments are represented by interfaces. The viewing information for the 3-D model, the water surface, and the boundary conditions used are shown in Figure 9. Three sets of analyses were conducted for $W/H = 1$ using the boundary conditions of $v = 0$ (fix y); $u = v = 0$ (fix x, y); and $u = v = w = 0$ (fix x, y, z) at the far ends of the abutments in the y -direction. The conditions represented by each of the y -direction boundary condition are the same as described for the *FLAC3D* model No. 1. The property values for the end blocks and interfaces used to perform the *FLAC3D* analyses are included in Table I. *FLAC3D* FoS values for this model are given in Table V.

Figure 10 shows the contour plots of maximum shear strain rate and the velocity vectors at the instant of numerical instability for each of the four values of ϕ_{lower} and the three boundary conditions analysed; the viewing information for the 3-D model is the same as used in Figure 9. As mentioned before, the location and geometry of the associated shear surface for each case is interpreted to be along the path where the velocity vectors essentially vanish.

3.6. Additional *FLAC3D* model No. 2 results

The *FLAC3D* model No. 2 was also used to analyse the sample problem for $W/H = 2, 5$, and 10 for the boundary condition of $u = v = w = 0$ (fix x, y, z) at the far ends of the abutments in the y -direction. The *FLAC3D* FoS results for all four values of W/H are shown in Table VI.

Table V. *FLAC3D* model No. 2 (Figure 9) FoS results for the following boundary conditions ($W/H = 1$).

$\phi_{\text{lower material}}$	Boundary constraint(s) used at the y -faces of the numerical model		
	Fix y	Fix x, y	Fix x, y, z
8°	1.74	1.75	1.74
10°	1.90	1.89	1.89
20°	2.52	2.52	2.52
30°	3.02	3.02	3.01

Table VI. *FLAC3D* model No. 2 (Figure 9) FoS results for the $u = v = w = 0$ (fix x, y, z) boundary condition at the y -faces of the numerical model for the following W/H values.

$\phi_{\text{lower material}}$	$W/H = 1$	$W/H = 2$	$W/H = 5$	$W/H = 10$
8°	1.74	1.38	1.11	1.01
10°	1.89	1.53	1.26	1.17
20°	2.52	2.16	1.92	1.85
30°	3.01	2.67	2.48	2.42

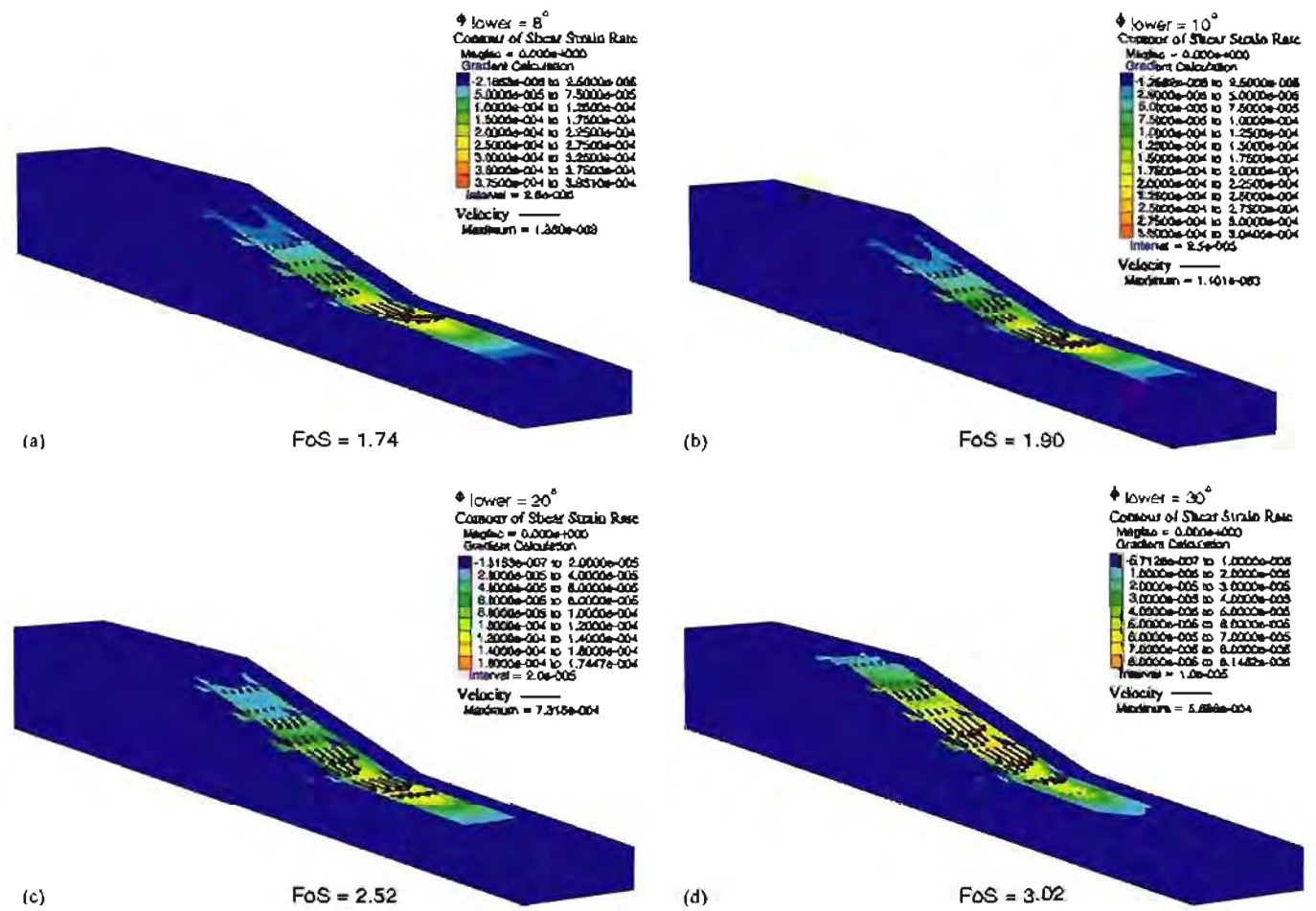


Figure 10. *FLAC3D* model No. 2 results for the sample problem with $W/H = 1$ and the boundary condition of $v = 0$ (fix y) in the y -direction: (a) FoS = 1.74, (b) FoS = 1.90, (c) FoS = 2.52 and (d) FoS = 3.02. *FLAC3D* model No. 2 results for the sample problem with $W/H = 1$ and the boundary condition of $u = v = 0$ (fix x, y) in the y -direction: (e) FoS = 1.75, (f) FoS = 1.89, (g) FoS = 2.52 and (h) FoS = 3.02. *FLAC3D* model No. 2 results for the sample problem with $W/H = 1$ and the boundary condition of $u = v = w = 0$ (fix x, y, z) in the y -direction: (i) FoS = 1.74, (j) FoS = 1.89, (k) FoS = 2.52 and (l) FoS = 3.02.

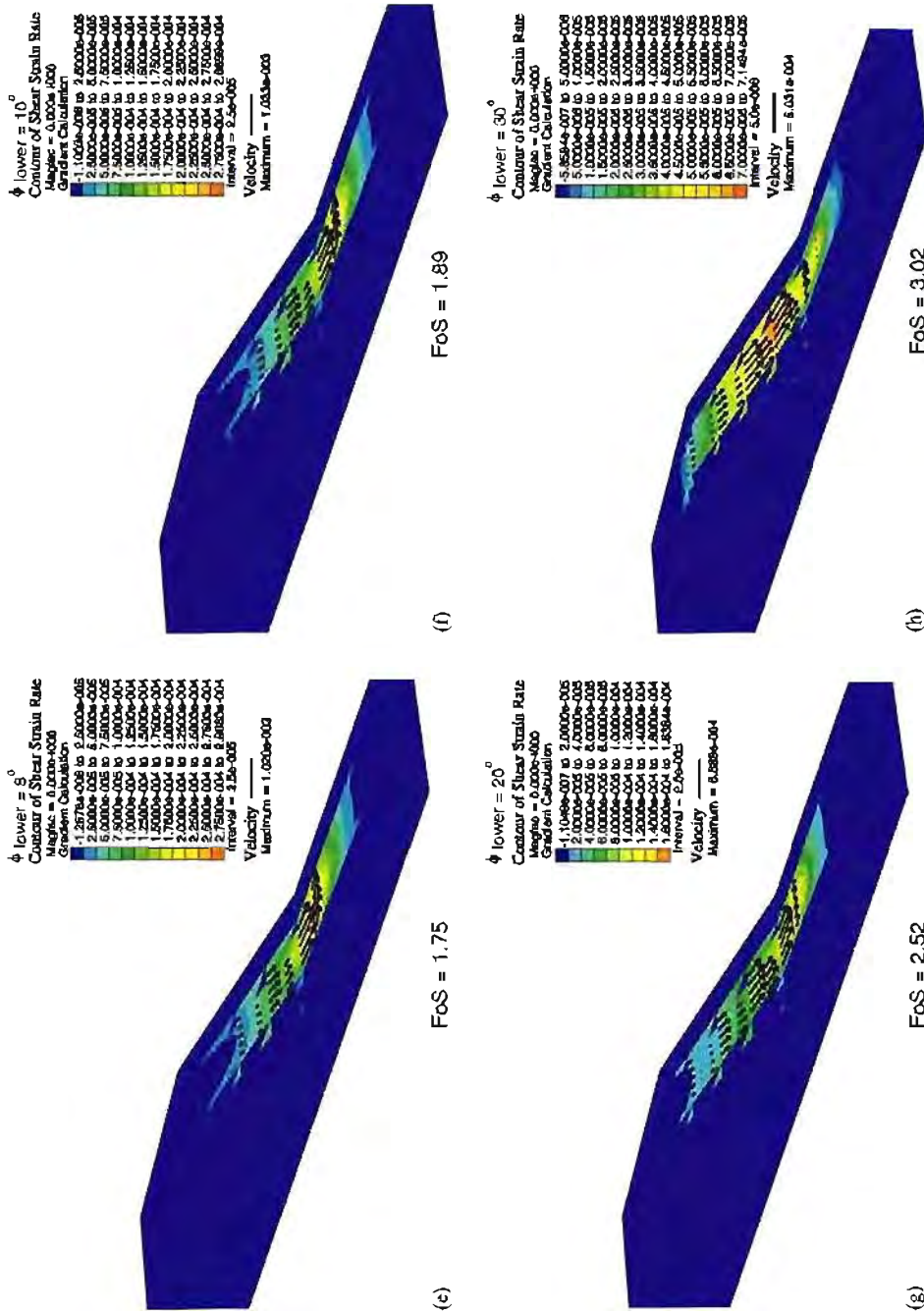


Figure 10. (Continued)

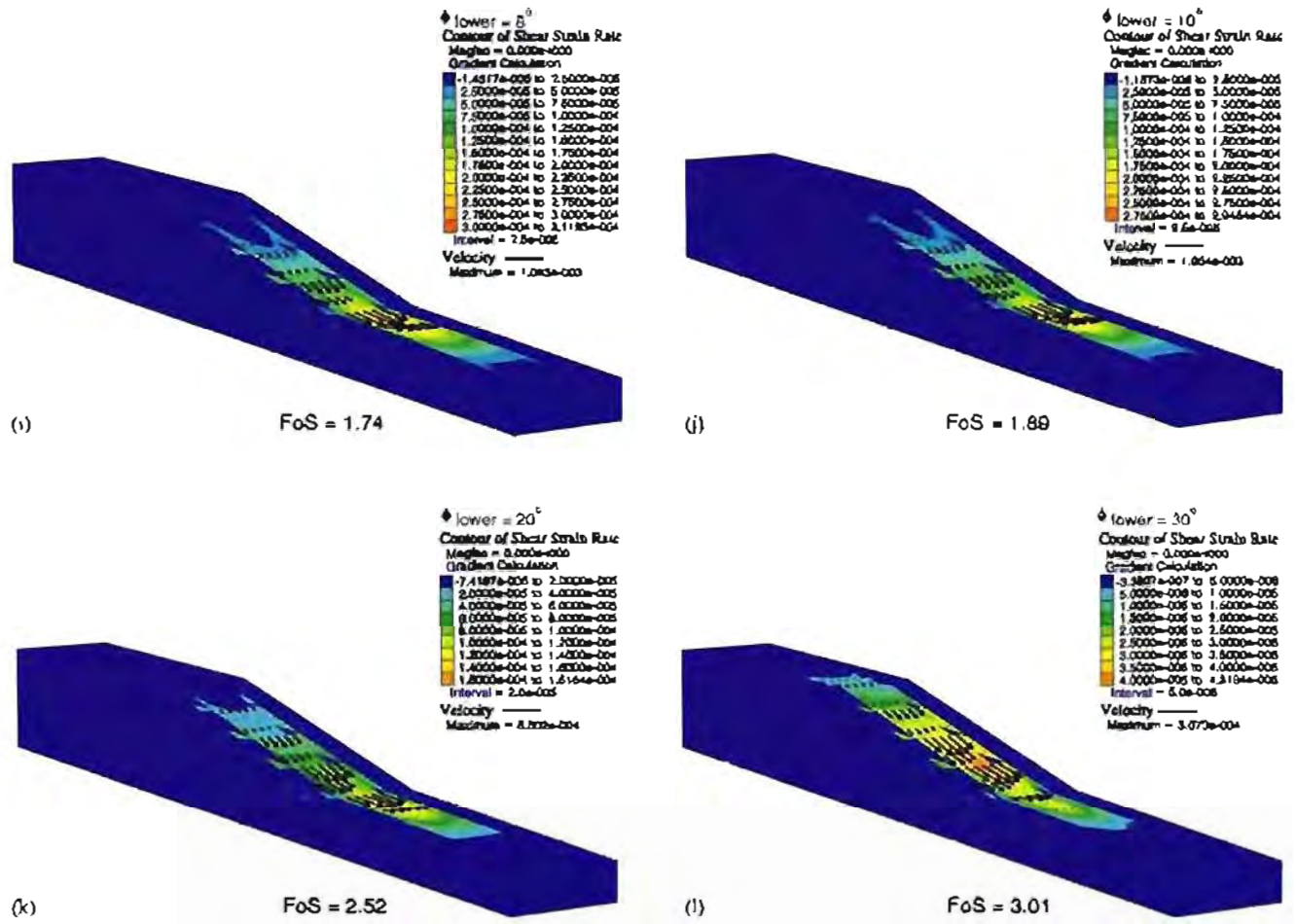


Figure 10. (Continued)

4. COMMENTS ON ANALYSIS RESULTS

For W/H ratio greater than 5, the differences between 2-D FoS and 3-D FoS values tend to lose significance (Tables II, III and VI), i.e. the 2-D FoS results approximate the 3-D FoS results reasonably well. For W/H ratio less than 5, the differences between 2-D and 3-D FoS values are significant. For the 3-D FoS results, the choice of an acceptable answer depends on the physical conditions being analysed via the numerical model. For a laboratory model with smooth but rigid walls, the fixed y boundary condition seems appropriate, and the FoS values from *CLARA* 3D (Table II) and *FLAC3D* (Table IV) are about the same. However, for field conditions where the end walls are rigid and rough abutments, $u = v = w = 0$ (fix x, y, z) boundary conditions are more appropriate, and *FLAC3D* results (Tables IV and V) will be more reflective of the slope behaviour. Between *FLAC3D* model No. 1 and *FLAC3D* model No. 2, *FLAC3D* model No. 2 is more representative of field conditions; therefore, use of *FLAC3D* model No. 2 results in Table VI should be appropriate.

5. SUMMARY AND CONCLUSIONS

- (1) Limit-equilibrium-based slope stability analysis procedures use different assumptions to render slope stability problems statically determinate. Some solution procedures only satisfy moment equilibrium or force equilibrium equations of statics, while others satisfy both force and moment equilibrium requirements of statics. For 2-D FoS calculations, solution procedures that satisfy complete statics, e.g. Spencer [15], are usually used in dam engineering practice. A similar trend is observed in the development of 3-D FoS solution procedures [16], and their use in engineering practice shall follow the advisory for 2-D procedures. In either case, it is essential that the user of these procedures and corresponding software understand the theories, assumptions, and calculations implemented.
- (2) If spatial variations of geometry, pore-water pressure, and/or material properties indicate that 3-D effects may be significant, it is suggested that the problem be analysed using a 3-D analysis software.
- (3) In a 3-D slope stability analysis, contribution of shear resistance along the two sides of a slide mass that parallel the direction of movement to the FoS is an item of interest.
- (4) It is easier to visualize model displacement boundary conditions than stress boundary conditions from the physical boundaries of a slope problem. However, for stress boundary conditions, one needs to think through the state of stress at a point, especially the shear stresses which are complimentary and exist in pairs. Inconsistencies in stress boundary conditions can lead to unpleasant consequences in computed FoS results. In continuum-mechanics-based solution procedures, use of displacement boundary conditions is recommended.
- (5) Initial stresses in a continuum model can be introduced via applied loads, boundary displacements, or by specifying their values. Any consistent state of stress can be present in the continuum body. However, the model must be in equilibrium under the applied loads, initial stresses, and boundary conditions.
- (6) In 3-D analyses, the failure surface geometry and location shall likely be different at different sections in the y -direction.

ACKNOWLEDGEMENTS

The author would like to express his sincere thanks to Professors D. Vaughan Griffiths, O. Hungr, and Timothy D. Stark for their interest and several conversations on the subject matter of the paper.

REFERENCES

1. Hovland HJ. Three-dimensional slope stability analysis method. *Journal of the Geotechnical Engineering Division*, ASCE, 1977; **103**(GT9):971–986.
2. Stark TD, Eid HT. Performance of three-dimensional slope stability methods in practice. *Journal of Geotechnical and Geoenvironmental Engineering* 1998; **124**(11):1049–1060.
3. Arellano D, Stark TD. Importance of three-dimensional slope stability analysis in practice. In *ASCE Geotechnical Special Publication No. 101: Slope Stability 2000*, Griffiths DV, Fenton GA, Martin TR (eds). ASCE: New York, 2000; 18–32.
4. Duncan JM. State of the art: limit equilibrium and finite-element analysis of slopes. *Journal of Geotechnical Engineering*, ASCE, 1996; **122**(7):577–596.
5. Hungr O. *CLARA: Slope stability analysis in two or three dimensions for IBM or compatible microcomputers*. O. Hungr Geotechnical Research Inc.: West Vancouver, British Columbia, 1988.
6. Griffiths DV, Lane PA. Slope stability analysis by finite elements. *Geotechnique* 1999; **49**(3):387–403.
7. Zetter AH, Poisel R, Roth W, Preh A. Slope stability analysis based on the shear reduction technique in 3D. In *Flac and Numerical Modeling in Geomechanics*, Detournay C, Hart R. (eds). Balkema: Rotterdam, 1999; 11–21.
8. Dawson EM, Roth WH, Drescher A. Slope stability analysis by strength reduction. *Geotechnique* 1999; **49**(6): 835–840.
9. Itasca Consulting Group. *FLAC—Fast Lagrangian Analysis of continua*. Itasca Consulting Group: Minneapolis, Minnesota, 2000.
10. Itasca Consulting Group. *FLAC3D—Fast Lagrangian Analysis of continua in 3 dimensions*. Itasca Consulting Group: Minneapolis, Minnesota, 2002.
11. Spencer E. Personal communications, 1984.
12. Peck RB. Personal communications, 1989.
13. Zienkiewicz OC, Humpheson C, Lewis RW. Associated and non-associated visco-plasticity and plasticity in soil mechanics. *Geotechnique* 1975; **25**(4):671–689.
14. Chugh AK. *User information manual for slope stability analysis program SSTAB2*. U.S. Bureau of Reclamation: Denver, Colorado, 1992.
15. Spencer E. A method of analysis of the stability of embankments assuming parallel interslice forces. *Geotechnique* 1967; **17**(1):11–26.
16. Huang C-C, Tsai C-C, Chen Y-H. Generalized method for three-dimensional slope stability analysis. *Journal of Geotechnical and Geoenvironmental Engineering* 2002; **128**(10):836–848.

Appendix D

Part 5 An Automated Procedure for 3-Dimensional Mesh Generation
by A.K. Chugh and T.D. Stark

This article was published in *Proceedings of the 3rd International Symposium on FLAC and Numerical Modeling in Geomechanics*, Sudbury, Ontario, pp. 9-15, 2003.

An automated procedure for 3-dimensional mesh generation

Ashok K. Chugh

Bureau of Reclamation, Denver, CO 80225-0007, USA

Timothy D. Stark

University of Illinois, Urbana, IL 61801-2352, USA

ABSTRACT: An automated procedure is presented to generate a 3-dimensional mesh for numerical analysis of engineering problems. The procedure is simple, effective and efficient, and can be applied to represent complex geometries and material distributions. A listing of the program that was used for the sample problem of a landfill slide is included.

1 INTRODUCTION

One of the essential tasks in a 3-dimensional (3-D) numerical analysis is to represent the geometry and distribution of materials in the numerical model. *FLAC3D* provides means to facilitate mesh generation and the built-in programming language *FISH* can be used to develop and implement additional program instructions during execution of a data file.

In geotechnical engineering, surface geometry, distribution of materials, and water table conditions usually vary from one location to the next and pose a difficult set of conditions to represent in a numerical model. In order to facilitate the analysis of landslides, a simple procedure was devised to represent complex surface geometry, subsurface material horizons, and water table conditions. The objectives of this paper are to present: (1) a simple method to describe field geometry and conditions for a 3-D numerical model of a slope problem; (2) a simple procedure for automatic generation of a 3-D mesh; and (3) an illustration of the use of the procedure for analysis of a large slide in a landfill. A listing of the program for the landfill slide is included in the paper. This program listing is in the *FISH* language and uses some of the functions available in the *FISH* library.

2 CONCEPTUAL MODEL

The conceptual model for the generation of a 3-D mesh follows the conventional procedure of portraying spatial variations of materials in 3-D via a series of 2-dimensional (2-D) cross-sections. This technique is commonly used by engineers and

geologists in constructing visual models of complex geologic sites where a number of 2-D cross-sections are used to represent the field conditions. In these representations, linear variations between material horizons in consecutive 2-D cross-sections are used to depict the 3-D spatial variability of a site. The accuracy of the representation is improved by using closely spaced 2-D cross-sections.

The 3-D mesh generation procedure presented herein follows the conventional practices used by engineers in constructing 2-D numerical meshes by hand for geotechnical problems to be solved using methods other than *FLAC3D*. For example, in the creation of a 2-D numerical model of a slope to be analyzed using a limit-equilibrium based procedure, it is a common practice to define profile lines via a set of data points followed by specifications of their connectivities. Also, in the creation of a 2-D model of a continuum to be solved by a finite-element based procedure, it is a common practice to discretize the continuum into a network of zones; assign identification numbers to the grid points; define the coordinates of the grid points; and then specify the connectivity of grid points.

Thus, in the conceptual model for the generation of a 3-D mesh in *FLAC3D*, use is made of defining a series of 2-D cross-sections at representative locations of a site; defining each of the 2-D sections as an assemblage of data points with line-segment connections; and organizing the data for an efficient and effective discretization of the volume.

3 WATER TABLE

The water table surface is specified using the water table data of individual 2-D cross-sections and

through the use of 3-point planar polygons between consecutive 2-D cross-sections. This scheme allows incorporation of non-coplanar variations in the water table surface in the entire 3-D model.

4 DESCRIPTION OF THE PROCEDURE

In geotechnical engineering, the ground-surface geometry is obtained using contour maps that are prepared from land or aerial survey of the area. The subsurface material horizons are estimated from geologic data and information obtained from exploratory boring logs. The subsurface water conditions are estimated from field observations, piezometers installed at various depths, and/or from water levels in borings. Subsurface data are used to develop contour maps of the subsurface geology and water conditions.

From these contour maps, the region-of-interest, and the locations of significant cross-sections are identified; information for 2-D cross-sections are read and tabulated; and 2-D cross-sections are drawn for an understanding of the site details and preparation of input data for a 2-D analysis. In general, the cross-sectional data for a site varies from one location to the next — these variations may be caused by changes in the ground surface and (or) in subsurface material horizons, discontinuity of some materials, or a combination of these or some other variations.

In the proposed procedure, the following steps are followed: (For ease of presentation, 2-D cross-sections are assumed to lie in x-z plane and the x,y,z coordinate system follow the right hand rule.)

1. The following steps are used for creating an orderly assemblage of field data for 3-D discretization of the continuum of the region-of-interest:

- (a) On the site map, select values of x, y, and z coordinates that completely circumscribe the 3-D region-of-interest;
- (b) Mark locations of all significant 2-D cross-sections oriented in the same and preferably parallel direction;
- (c) For each 2-D cross-section, tabulate (x,y,z) coordinates of end-points of all line segments for each profile line and the water table (for parallel 2-D cross-sections, y-coordinate shall have same constant value between two consecutive cross-sections).

2. The following steps are used for creating similar sets of data at each of the 2-D cross-sections:

- (a) From the data in step 1(c) above, select control

points that are of significance in defining the profile lines in all of the 2-D cross-sections. Tabulate the x-coordinates of these control points in increasing order. For reference purposes, this table is referred to as Table 100.

- (b) Use of the 'Interpolate' function expands the 2-D cross-sectional data of step 1(c) by linear interpolation for all of the control points listed in Table 100 for all of the profile lines and stores the data in separate tables; assigns Table numbers in increasing order starting with the user specified starting number and incrementing it by 1; assigns an identification number to each point; and positions the points in the 3-D model space. These tables contain the (x,z) coordinates of expanded 2-D cross-sectional data. A sample listing of the 'Interpolate' function and its dependency function 'zz' in *FISH* language is given in Figure 1. The starting table number used in the sample problem data file is 200.

3. The following steps are used for creating zones in the 3-D model space:

- (a) Tabulate the y-coordinates of the 2-D cross-sections in increasing y-direction. For reference purposes, this table is referred to as Table 101. The number of entries in Table 101 should equal the number of 2-D cross-sections marked in step 1(b).

- (b) Considering the spacing of x-coordinates of the control points in step 2(a), select the number of zones desired for each interval in the x-direction. Tabulate these values for all of the intervals in the increasing x-direction. For reference purposes, this table is referred to as Table 102. The number of entries in Table 102 should be one less than those in Table 100.

- (c) Considering the spacing between the 2-D cross-sections in the y-direction, select the number of zones desired for each interval in the y-direction. Tabulate these values for all of the intervals in the increasing y-direction. For reference purposes, this table is referred to as Table 103. The number of entries in Table 103 should be one less than the number of 2-D cross-sections.

- (d) Considering the spacing of the profile lines in the z-direction, select the number of zones desired for each material horizon in the z-direction. Tabulate these values for all of the intervals in the increasing z-direction. For reference purposes, this table is referred to as Table 104. The number of entries in Table 104 should be one less than the number of profile lines.

- (e) Use of the 'Fill_grid' function generates a brick mesh and assigns a group name to each 3-D volume zone. A sample listing of the 'Fill_grid' function in *FISH* language is given in Figure 2.

```

def zz
zz=table(t_n,xx)
end

def interpolate
loop j (js,je); profile line #s -
; js is for the bottom, je is for top
dt_n=dt_n_s+j; dt_n is destination table number
loop i (is,ie); is is the first interpolation #,
; ie is the last interpolation #
xx=xtable(100,i); x-coordinate of the
;interpolation point
command
set t_n=j
end_command
table(dt_n,xx)=zz
id_pt=id_pt+1
x_pt=xtable(dt_n,i)
y_pt=y_pt
z_pt=ytable(dt_n,i)
command
generate point id id_pt x_pt y_pt z_pt
end_command
endloop
endloop
end

```

Figure 1. Listing of the 'Interpolate' function and its dependency function 'zz' in *FISH* language.

```

def fill_grid
i_n=table_size(102)
j_n=table_size(103)
k_n=table_size(104)
loop jy (1,j_n)
ny=xtable(103,jy)
p0_d=(jy-1)*(i_n+1)*(k_n+1)
loop kz (1,k_n)
nz=xtable(104,kz)
if kz=1 then
material='shale'
endif
if kz=2 then
material='ns'; native_soil
endif
if kz=3 then
material='msw'; municipal_solid_waste
x_toe=xtable(105,jy)
endif
loop ix (1,i_n)
if kz=3 then
xx_toe=xtable(100,ix)
if xx_toe < x_toe then
material='mswt'
endif
endif
nx=xtable(102,ix)
p0_d=p0_d+1
p3_d=(p0_d+i_n+1)
p6_d=(p3_d+1)
p1_d=(p0_d+1)
p2_d=((i_n+1)*(k_n+1)+p0_d)
p5_d=(p2_d+(i_n+1))
p7_d=(p5_d+1)
p4_d=(p2_d+1)
command
generate zone brick size nx,ny,nz ratio 1,1,1 &
p0=point (p0_d) p3=point (p3_d) &
p6=point (p6_d) p1=point (p1_d) &
p2=point (p2_d) p5=point (p5_d) &
p7=point (p7_d) p4=point (p4_d) group material
end_command
if kz=3 then
material='msw'
endif
end_loop
p0_d=p0_d+1
end_loop
end_loop
end

```

Figure 2. Listing of 'FILL_GRID' function in *FISH* language.

5 COMMENTS

- (1) Use of a Brick mesh with an 8-point description is versatile and allows for creation of degenerated brick forms through the use of multiple points with different identification numbers occupying the same (x,y,z) coordinate location in the 3-D model space.
- (2) During the development of the grid, it is possible to assign group names to different segments of the model. This information can be useful in modifying the generated grid.
- (3) Expanding the (x,y,z) location data for all 2-D cross-sections to a common control number of locations via interpolations facilitates the programming of the automatic grid-generation procedure.
- (4) In engineering practice, it is generally desirable to analyze a few 2-D cross-sections at select locations prior to conducting a 3-D analysis. Because development of data for 2-D cross-sections is one of the steps for use of the proposed procedure, it is relatively easy to conduct a 2-D analysis using the 2-D cross-sectional data and the program *FLAC*.
- (5) The program instructions listed in Figures 1 and 2 can be modified to accommodate geometry and other problem details that are different or more complex than those encountered in the sample problem described in Section 6.

6 SAMPLE PROBLEM

The problem used to illustrate the proposed 3-D mesh generation procedure is the 1996 slide in a waste containment facility near Cincinnati, Ohio (Stark & Eid 1998, Eid et al. 2000). Figure 3 is an aerial view of the slide. Figure 4 is the plan view of the landfill and shows the location of the sixteen cross-sections used to construct a *FLAC3D* model of the site (the project data shown are in Imperial units). There are three material horizons bounded by four profile lines, and a liquid level present at this site. Figure 5 shows the 2-D cross-sectional views of the site at the 16-locations prior to failure (the available project data were converted to SI units and this conversion lead to numerical values with fractional parts). Figure 6 shows a partial listing of the data file for the sample problem with the following details:

Table 100 lists the x-coordinates of the 22 control points considered significant from the sixteen 2-D cross-sectional data.

Table 101 lists the y-coordinates of the sixteen 2-D cross-section locations.



Figure 3. Sample problem – Aerial view of Cincinnati landfill failure (from Eid et al. 2000). (Reproduced by permission of the publisher, ASCE).

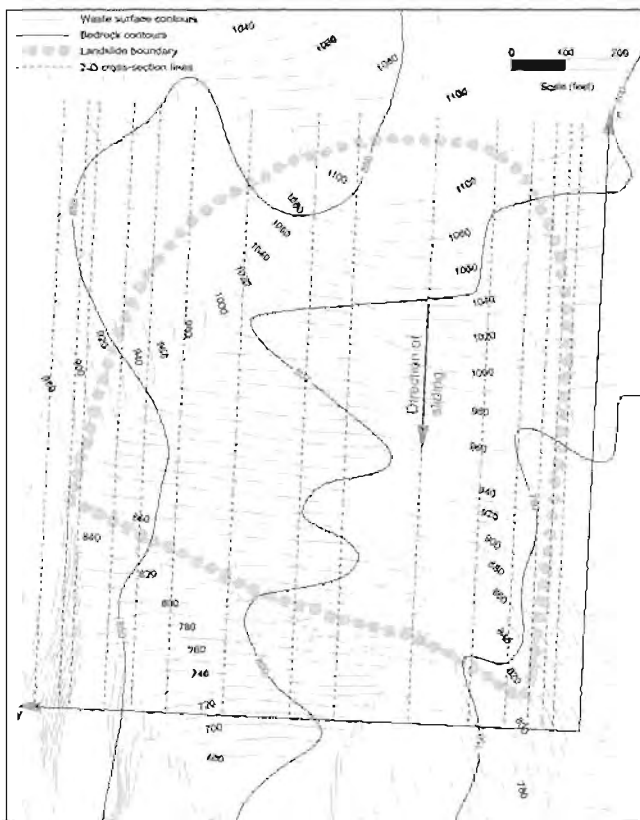


Figure 4. Plan view of the sample problem showing locations of selected 2-D sections.

Table 102 lists the number of zones desired in each of the 21 segments in the x-direction.

Table 103 lists the number of zones desired in each of the 15 segments in the y-direction.

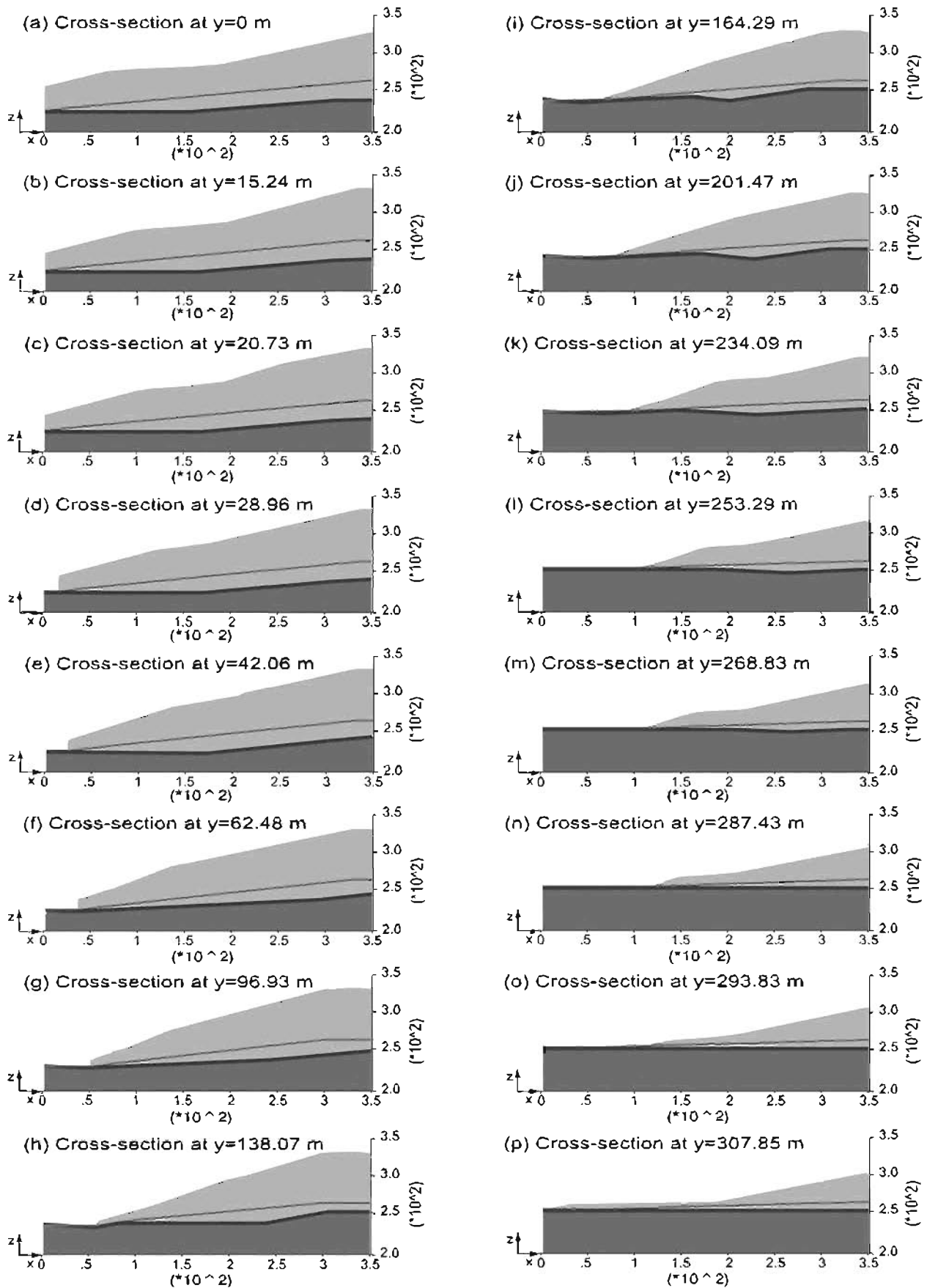
Table 104 lists the number of zones desired in each of the 3 material horizons at the site.

Table 105 lists the x-coordinates of the toe locations of the top profile line in the 2-D cross-sections in the increasing y-direction.

For each cross-section, x- and z-coordinates for data points defining the profile lines are recorded in individual tables numbered as Table 1 for profile line 1 data, Table 2 for profile line 2 data, Table 3 for profile line 3 data, and Table 4 for profile line 4 data in the data file shown in Figure 6. Profile lines are numbered from 1 to 4 in the increasing z-direction and each profile line uses a different number of data points to define the line. For cross-sections where the top profile line terminates in a vertical cut at the toe, the top profile line was extended to $x = 0$.

For each cross-section and for each of the four profile lines, the x-coordinate locations identified in Table 100 are used to create data by interpolation at each of the 22 control points. For the sample problem, this amounts to 88 pairs of (x,z) coordinates per cross-section, and the y-coordinate of the data points is read from Table 101. Thus, the x-, y-, and z-coordinates for all of the points defined and (or) interpolated are known. Each point is assigned a numeric identity number (id #) starting with one and incrementing by one. The data points are located in the 3-D model space using their id # and x-, y-, z-coordinates. This task is accomplished using the 'Interpolate' function and its listing in FISH language is given in Figure 1. At the end of this task, all of the defined and (or) interpolated points with an assigned id # have been located in the 3-D model space.

The connectivity of data points to define volume discretization is accomplished in the function named 'Fill_grid'. For each interval in the location of cross-sections in the y-direction (Table 103), and for each material horizon between the profile lines in the z-direction (Table 104), and for each interval in the x-direction (Table 102), the values of number of zones desired in the x, y, and z-direction and the id #s of points in the 3-D model space are used in the 'GENERATE zone brick p0, p1, ...p8' command of FLAC3D for a regular 8-noded brick mesh. The material between the profile lines is assigned a group name for ease of modifying the grid and for convenience in assigning material properties and/or addressing them for some other reason. This task is also accomplished in the function named 'Fill_grid'



Legend: Shale Natural soil Municipal solid waste Water table

Figure 5. 2-D cross-sectional views of the sample problem.

```

; Rumpke landfill site; Data are in metric units
set g=0,0,-9.81

; table 100 is for the x-coordinates of
; the desired 3-D grid
table 100 0,1 13.11,2 15.54,3 22.86,4 34.75,5
table 100 42.67,6 49.07,7 57.61,8 63.70,9
table 100 64.92,10 72.54,11 78.94,12 92.66,13
table 100 100.89,14 107.90,15 115.21,16
table 100 158.50,17 199.64,18 284.38,19
table 100 318.52,20 337.72,21 348.08,22

; table 101 is for y-coordinates of the
; 2-D cross-section locations
table 101 0,1 15.24,2 20.73,3 28.96,4 42.06,5
table 101 62.48,6 96.93,7 138.07,8 164.29,9
table 101 201.47,10 234.09,11 253.29,12
table 101 268.83,13 287.43,14 293.83,15
table 101 307.85,16

; table 102 is for the number of zones
; desired in the x-direction
table 102 2,1 1,2 1,3 2,4 1,5 1,6 1,7 1,8 1,9
table 102 1,10 1,11 2,12 1,13 1,14 1,15 5,16
table 102 5,17 10,18 4,19 2,20 2,21

; table 103 is for the number of zones
; desired in the y-direction
table 103 2,1 1,2 1,3 2,4 2,5 3,6 4,7 3,8 4,9
table 103 3,10 2,11 2,12 2,13 1,14 2,15

; table 104 is for the number of zones
; desired in the z-direction
table 104 5,1 3,2 10,3

; table 105 is for the x-coordinates of the
; receding toe
table 105 0,1 0,2 15.54,3 22.86,4 34.75,5
table 105 49.07,6 57.61,7 64.92,8 78.94,9
table 105 92.66,10 100.89,11 107.90,12
table 105 115.21,13 63.70,14 0,15

set is=1 ie=22
set js=1 je=4
set id_pt=0
set dt_n_s=200

; Station at y=0
set y_pt=0
table 1 -100,200 500,200
table 2 0,223.60 154.23,223.60 307.24,238.84
table 2 348.08,239.14
table 3 0,228.60 154.23,228.60 307.24,243.84
table 3 348.08,244.14
table 4 0,260.00 66.45,280.42 98.15,283.46
table 4 156.67,286.51 187.15,289.56
table 4 348.08,332.54
interpolate

; station at y=15.24 m
set y_pt=15.24
table 2 erase
table 3 erase
table 4 erase
set dt_n_s=dt_n
table 2 0,223.60 163.07,223.60 306.02,238.84
table 2 348.08,240.67
table 3 0,228.60 163.07,228.60 306.02,243.84
table 3 348.08,245.67
table 4 0,251.46 91.14,280.42 107.90,283.46
table 4 144.48,286.51 169.77,289.56
table 4 194.46,292.61 332.54,338.33
table 4 348.08,338.33
interpolate
.
.
.
; station at y=307.85 m
set y_pt=307.85
table 2 erase
table 3 erase
table 4 erase
set dt_n_s=dt_n
table 2 0,254.08 348.08,254.08
table 3 0,259.08 348.08,259.08

```

```

table 4 0,261.08 29.87,265.18 185.93,268.22
table 4 348.08,307.24
interpolate

fill_grid

delete range group mswt

; water surface
water den=1 table &
face 0,0,228.60 0,15.24,228.60 &
332.54,15.24,268.22 &
face 0,0,228.60 332.54,15.24,268.22 &
348.08,15.24,268.22 &
face 0,0,228.60 348.08,15.24,268.22 &
348.08,0,268.22 & ;interval # 1
face 0,15.24,228.60 0,20.73,228.60 &
340.77,20.73,268.22 &
face 0,15.24,228.60 340.77,20.73,268.22 &
348.08,20.73,268.22 &
face 0,15.24,228.60 348.08,20.73,268.22 &
332.54,15.24,268.22 &
face 332.54,15.24,268.22 348.08,20.73,268.22 &
348.08,15.24,268.22 &;interval # 2
.
.
.
face 0,293.83,259.08 0,307.85,259.08 &
63.70,307.85,259.08 &
face 0,293.83,259.08 63.70,307.85,259.08 &
348.08,307.85,268.22 &
face 0,293.83,259.08 348.08,307.85,268.22 &
63.70,293.83,259.08 &
face 63.70,293.83,259.08 348.08,307.85,268.22 &
348.08,293.83,268.22;interval # 15

save cin_3D_grid.sav

```

Figure 6. Partial listing of the data file for the sample problem for *FLAC3D*.

and its listing in *FISH* language is given in Figure 2. Table 105 data are used to assign a group name 'mswt' to the zones past the vertical cut which are later deleted using the **DELETE** command with the **range** defined by the **group** name 'mswt'. At the end of this task, a 3-D grid of specification exists in the region-of-interest. For the sample problem, the generated 3-D grid is shown in Figure 7. The representation of continuity of the vertical cut at the toe of the slope (as seen in 2-D cross-sections, Figure 5) in the 3-D model can be improved by increasing the number of 2-D cross-sections.

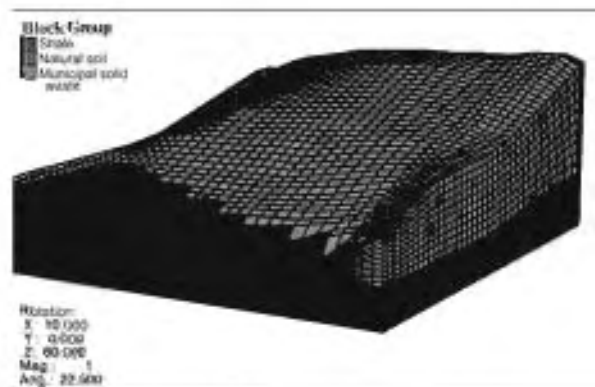
7 ADVANTAGES OF THE PROPOSED PROCEDURE

- (1) The proposed procedure for describing 3-D field conditions utilizes 2-D cross-sections which are essentially the same as commonly used by geologists and engineers to describe the field conditions. Linear variation in geometry, material horizons, and groundwater descriptions between known data points is generally accepted.
- (2) Changes in field data can be incorporated in the numerical model by updating the affected tables.

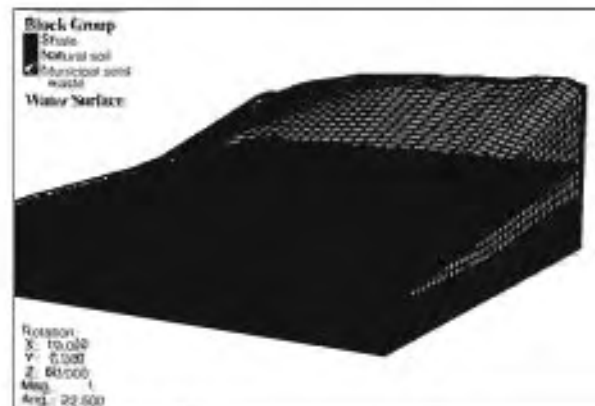
- (3) New cross-sections can be introduced or old cross-sections deleted and a new discretization of the continuum made quickly.
- (4) Describing the spatial location of data in a 3-D space followed by descriptions of their connectivity is a simple yet powerful way of constructing a 3-D numerical model for analysis purposes.
- (5) The proposed procedure produces regions with acceptable geometries, i.e., no conflicts in connectivity.
- (6) Changes in discretization due to changes in field data or due to numerical considerations can be included in the proposed procedure efficiently and a new discretization accomplished.
- (7) Number of discretized volume units in different parts of the numerical model is estimated at the start of the problem solving effort. If it becomes necessary to change or refine the discretization, very little effort is needed to change the tabular data and the procedure is then rerun to obtain an updated 3-D mesh.
- (8) A complete brick element is used to generate other degenerated volume element shapes.
- (9) Because the proposed procedure is based on simple and commonly used ideas, it should be adaptable when using computer programs or procedures other than *FLAC3D* to perform numerical analysis work. The program instructions can be rewritten in other programming languages.

8 SUMMARY

To facilitate 3-D analyses using *FLAC3D* or other software, an automated procedure is presented to create a 3-D mesh. The procedure utilizes commonly used techniques for drawing 2-D cross-sections and interpolation between 2-D cross-sections to portray spatial variations of geometry and distribution of materials in 3-D.



(a) without the water surface



(b) with the water surface

Figure 7. 3-D mesh for the sample problem.

9 REFERENCES

- Eid, H.T., Stark, T.D., Evans, W.D. & Sherry, P.E. 2000. Municipal solid waste slope failure. II Stability analyses. *Journal of Geotechnical and Geoenvironmental Engineering*, Vol. 126, No. 5, pp. 408-419.
- Stark, T.D. & Eid, H.T. 1998. Performance of three-dimensional slope stability methods in practice. *Journal of Geotechnical and Geoenvironmental Engineering*, Vol. 124, No. 11, pp. 1049-1060.

Appendix D

Part 6 Average Engineering Properties of Compacted Soils from the Western United States

This table is from reference [2]: *Design of Small Dams*, Bureau of Reclamation,
Denver, Colorado, pp. 96-97, 2004.

Table 5-1 Average engineering properties of compacted soils [2]

Unified classification	Soil type	Specific gravity		Compaction						Shear strength				Values listed	
		No. 4 minus	No. 4 plus	Laboratory			Index unit weight			Avg. placement		Effective stress			
				Maximum unit weight, lb/ft ³		Optimum moisture content, %	Max., lb/ft ³		Min., lb/ft ³	Unit weight, lb/ft ³	Moisture content, %		c' lb/in ²		φ' °
GW	Well-graded clean gravels, gravel-sand mixture	2.69	2.58	124.2		11.4	133.6		108.8	-	-		-	-	Average of all values
		0.02	0.08	3.2		1.2	10.4		10.2	-	-		-	-	Standard deviation
		2.65	2.39	119.1		9.9	113.0		88.5	-	-		-	-	Minimum value
		2.75	2.67	127.5		13.3	145.6		132.9	-	-		-	-	Maximum value
		16	9		5			16				0			Total number of tests
GP	Poorly graded clean gravels, gravel sand mixture	2.68	2.57	121.7		11.2	137.2		112.5	127.5	6.5		5.9	41.4	Average of all values
		0.03	0.07	5.9		2.2	6.3		8.3	7.2	1.2		-	2.5	Standard deviation
		2.61	2.42	104.9		9.1	118.3		85.9	117.4	5.3		5.9	38.0	Minimum value
		2.76	2.65	127.7		17.7	148.8		123.7	133.9	8.0		5.9	43.7	Maximum value
		35	12		15			34				3			Total number of tests
GM	Silty gravels, poorly graded gravel-sand-silt	2.73	2.43	113.3		15.8	132.0		108.0	125.9	10.3		13.4	34.0	Average of all values
		0.07	0.18	11.5		5.8	3.1		0.2	0.9	1.2		3.7	2.6	Standard deviation
		2.65	2.19	87.0		5.8	128.9		107.8	125.0	9.1		9.7	31.4	Minimum value
		2.92	2.92	133.0		29.5	135.1		108.1	126.9	11.5		17.0	36.5	Maximum value
		34	17		36			2				2			Total number of tests
GC	Clayey gravels, poorly graded gravel-sand-clay	2.73	2.57	116.6		13.9	-		-	111.1	15.9		10.2	27.5	Average of all values
		0.08	0.21	7.8		3.8	-		-	10.4	1.6		1.5	7.2	Standard deviation
		2.67	2.38	96.0		6.0	-		-	96.8	11.2		5.0	17.7	Minimum value
		3.11	2.94	129.0		23.6	-		-	120.9	22.2		16.0	35.0	Maximum value
		34	6		37			0				3			Total number of tests
SW	Well-graded clean sands, gravelly sands	2.67	2.57	126.1		9.1	125.0		99.5	-	-		-	-	Average of all values
		0.03	0.03	6.0		1.7	6.0		7.1	-	-		-	-	Standard deviation
		2.61	2.51	118.1		7.4	116.7		87.4	-	-		-	-	Minimum value
		2.72	2.59	135.0		11.2	137.8		109.8	-	-		-	-	Maximum value
		13	2		1			12				0			Total number of tests
SP	Poorly graded clean sands, sand-gravel mixture	2.65	2.62	115.6		10.8	115.1		93.4	103.4	5.4		5.5	37.4	Average of all values
		0.03	0.10	9.7		2.0	7.2		8.8	14.6	-		3.0	2.0	Standard deviation

Table 5-1 Average engineering properties of compacted soils [2]

Unified classification	Soil type	Specific gravity		Compaction						Shear strength				Values listed	
		No. 4 minus	No. 4 plus	Laboratory			Index unit weight			Avg. placement		Effective stress			
				Maximum unit weight, lb/ft ³		Optimum moisture content, %	Max., lb/ft ³		Min., lb/ft ³	Unit weight, lb/ft ³	Moisture content, %		c' lb/in ²		φ' °
		2.60	2.52	106.5		7.8	105.9		78.2	88.8	5.4		2.5	35.4	Minimum value
		2.77	2.75	134.8		13.4	137.3		122.4	118.1	5.4		8.4	39.4	Maximum value
		36	3		7			39				2			Total number of tests
SM	Silty sands, poorly graded sand-silt mixture	2.68	2.18	116.6		12.5	110.1		84.9	112.0	12.7		6.6	33.6	Average of all values
		0.06	0.11	8.9		3.4	8.7		7.9	11.1	5.4		5.6	5.7	Standard deviation
		2.51	2.24	92.9		6.8	88.5		61.6	91.1	1.6		0.2	23.3	Minimum value
		3.11	2.63	132.6		25.5	122.9		97.1	132.5	25.0		21.2	45.0	Maximum value
		149	9					21				17			Total number of tests
SC	Clayey sands, poorly graded sand-clay mixture	2.69	2.17	118.9		12.4	-		-	115.6	14.2		5.0	33.9	Average of all values
		0.04	0.18	5.9	23	2.3	-		-	14.1	5.7		2.5	2.9	Standard deviation
		2.56	2.17	104.3		6.7	-		-	91.1	7.5		0.7	28.4	Minimum value
		2.81	2.59	131.7		18.2	-		-	131.8	22.7		8.5	38.3	Maximum value
		88	4		73			0				10			Total number of tests
ML	Inorganic silts and clayed silts	2.69	-	103.3		19.7	-		-	98.9	22.1		3.6	34.0	Average of all values
		0.09	-	10.4		5.7	-		-	11.5	8.9		4.3	3.1	Standard deviation
		2.52	-	81.6			-		-	80.7	11.1		0.1	25.2	Minimum value
		3.10	-	126.0		34.6	-		-	119.3	40.3		11.9	37.7	Maximum value
		65	0		39			0				14			Total number of tests
CL	Inorganic clays of low to medium plasticity	2.71	2.59	109.3		16.7	-		-	106.5	17.7		10.3	25.1	Average of all values
		0.05	0.13	5.5		2.9	-		-	7.8	5.1		7.6	7.0	Standard deviation
		2.56	2.42	90.0		6.4	-		-	85.6	11.6		0.9	8.0	Minimum value
		2.87	2.75	121.4		29.2	-		-	118.7	35.0		23.8	33.8	Maximum value
		270	3					0				31			Total number of tests
MH	Inorganic clayey silts, elastic silts	2.79	-	85.1		33.6	-		-	-	-		-	-	Average of all values
		0.25	-	2.3	21	1.6	-		-	-	-		-	-	Standard deviation
		2.47	-	82.9		31.5	-		-	-	-		-	-	Minimum value
		3.50	-	89.0		35.5	-		-	-	-		-	-	Maximum value

Table 5-1 Average engineering properties of compacted soils [2]

Unified classification	Soil type	Specific gravity		Compaction						Shear strength				Values listed	
		No. 4 minus	No. 4 plus	Laboratory			Index unit weight			Avg. placement		Effective stress			
				Maximum unit weight, lb/ft ³		Optimum moisture content, %	Max., lb/ft ³		Min., lb/ft ³	Unit weight, lb/ft ³	Moisture content, %		c' lb/in ²		φ' °
		10	0		5			0				0			Total number of tests
CH	Inorganic clays of high plasticity	2.73	-	95.3		25.0	-		-	93.6	25.7		11.5	16.8	Average of all values
		0.06	-	6.6		5.4	-		-	8.1	5.7		7.4	7.2	Standard deviation
		2.51	-	82.3			-		-	79.3	17.9		1.5	4.0	Minimum value
		2.89	-	107.3		41.8	-		-	104.9	35.3		21.5	27.5	Maximum value
		74	0		36				0			12			Total number of tests

Appendix D

Part 7 Strength, Stress-Strain and Bulk Modulus Parameters for Finite Element Analyses of Stresses and Movements in Soil Masses, by J.M. Duncan, P. Byrne, K.S. Wong, and P. Mabry

This report was published as Report No. UCB/GT/80-01, University of California, Berkeley, California, 1980. Tables 5 and 6 of this report are reproduced herein with permission of the first author, Prof. J. M. Duncan, currently the Distinguished Professor Emeritus, 1600 Carlson Drive, Blacksburg, VA 24060.

Table 5. Stress-Strain and Strength Parameters for Soils Tested under Drained Conditions

Soil	Group	Soil Description	References	Grain Size (mm)			LL	PI	Compaction				Incl. Void Ratio	Relative Density	Degree of Saturation	Railing	Particle Shape	Stress Range (TSF)	Number of Tests	C (TSF)	Friction Angle	K	n	R _s	K _s	m	
				D ₆₀	D ₃₀	D ₁₀			Type	Max. Dry Unit Wt. (pcf)	Opt. w/c	Dry Unit Wt. (pcf)															w/c
GW	GW-1	Conglomerate Rockfill (Nezahu. Dam)	Marsal et al (38)	47.	7.5	0.9						118.9	0.380	70	**	Sub-angular	1.9-25.5	3	0.00	50 (10)	540	0.43	0.64	135	-0.34		
GW	GW-2	Granitic Gneiss Rockfill (Mica Dam)	Casagrande (10) / Marsal (38)	79.	24.	4.						123.7	0.320	95	**	Sub-angular	5.1-25.6	3	0.00	44 (8)	210	0.51	0.64	100	-0.34		
GW	GW-3	Quartzite Rockfill (Furnas Dam Shell)	Casagrande (10)	10.	-	-									**	Sub-rounded	4.1-36.9	4	0.00	49 (6)	560	0.48	0.65	330	-0.33		
GW	GW-4	Quartzite Rockfill (Furnas Dam Transit.)	Casagrande (10)	25.											**	Sub-rounded	4.1-36.9	4	0.00	53 (7)	950	0.52	0.59	470	-0.52		
GW	GW-5	Furnas Dam Transition	Casagrande (10)	10.											**	Sub-rounded	4.1-36.9	4	0.00	50 (7)	690	0.57	0.51	360	0.57		
GW	GW-6	Plinçandapan Gravel	Marsal et al (38)	21.	2.7	0.25						132.1	0.340	65	**	Sub-rounded	0.4-26.5	6	0.00	51 (9)	690	0.45	0.59	170	0.22		
GW	GW-7	Diorite Rockfill (El Infiernillo Dam)	Marsal et al (38)	93.	42.	17.						105.7	0.560	50	**	Angular	0.4-17.0	7	0.00	46 (9)	340	0.28	0.71	52	0.18		
GP	GP-2	Sandy Gravel (Mica Dam Shell)	Casagrande (10)	22.	1.2	0.23								50	**	Sub-angular	7.2-32.5	3	0.00	41 (3)	420	0.50	0.78	125	0.46		
GP	GP-3	Basalt Rockfill	Casagrande (10) / Marsal (38)	19.	3.6	1.						133.8	0.300	95	**	Angular	5.1-25.6	3	0.00	52 (10)	450	0.37	0.61	265	0.18		
GP	GP-6	Silty Sandy Gravel (Oroville Dam)	Hell & Gordon (25)	18.	4.8	0.4	21	3				148.0	0.210	100	**	Rounded	9.0-46.8	4	0.00	53 (8)	1300	0.40	0.72	900	0.22		
GP	GP-7	Amphibolite Gravel (Oroville Dam Shell)	Marachi (37)	13.2	4.6	0.36						152.0	0.200	100	**	Rounded	2.2-28.6	4	0.00	51 (6)	1780	0.39	0.67	1300	0.16		
GP	GP-11	Crushed Basaltic Rock (Round Butte Dam)	Shannon & Wilson (41)	15.	12.	6.						91.6	0.99.0	3.20	99	**	Angular	2.0-14.1	3	0.00	51 (14)	410	0.21	0.71	195	0.00	
GP	GP-13	Sandy Gravel (Rowallan Dam)	Boughton (5)	10.	3.	0.6						135.0	0.233	100	**	Rounded	1.8-10.8	4	0.00	58 (10)	2500	0.21	0.75	1400	0.00		
GC	GC-1	Clay Gravel (New Hogan Dam Core)	Bird (3)	12.	0.6	-	51	30				113.0	10.8	107.0	10.80	51	**		1.1- 4.3	3	0.28	19	99	0.70	0.86	45	0.00
SW	SW-1	Angiite Rockfill (Pyramid Dam Shell)	Marachi (37)	4.1	1.8	0.6						111.6	0.460	100	*	Angular	2.2-46.8	4	0.00	53 (9)	1600	0.08	0.72	600	0.00		
SW	SW-2	Crushed Olivine Basalt	Marachi (37)	4.1	1.8	0.6						125.4	0.430	100	*	Angular	2.2-46.8	4	0.00	55 (10)	1000	0.22	0.70	390	0.14		
SW	SW-3	Silty Sand, Some Gravel (Round Butte Dam)	Shannon & Wilson (41)	1.7	0.09	0.009	NP	NP	16,450	120.0	13.2	108.7	13.50		*	Sub-rounded	2.0-14.0	3	0.00	38 (3)	260	0.50	0.76	100	0.50		
SW	SW-5	Venato Sandstone (0.5 in max. size)	Becker, Chan & Seed (2)	0.17	0.07	0.025	NP	NP		118.3		117.5	0.470	93	*	Angular	2.2-28.6	4	0.00	43 (4)	330	0.46	0.51	110	0.46		
SP	SP-3	Glacial Outwash Sand	Hirschfeld & Poulos (26)	0.03	0.4	0.14						112.3	0.500	80	**	Sub-rounded	1.0-41.1	6	0.00	44 (4)	190	0.70	0.57	190	0.35		
SP	SP-4A	Sacramento River Sand	Lee (34)	0.22	0.17	0.15						89.5	0.870	38	*	Rounded	1.0-41.1	8	0.00	35 (2)	430	0.27	0.84	230	0.02		
SP	SP-4B	Sacramento River Sand	Lee (34)	0.22	0.17	0.15						94.0	0.780	60	*	Rounded	1.0-13.0	4	0.00	37 (2)	410	0.69	0.90	260	0.15		
SP	SP-4C	Sacramento River Sand	Lee (34)	0.22	0.17	0.15						97.8	0.710	78	*	Rounded	1.0-41.1	8	0.00	41 (5)	1100	0.36	0.85	900	0.00		
SP	SP-4D	Sacramento River Sand	Lee (34)	0.22	0.17	0.15						103.9	0.610	100	*	Rounded	3.0-41.1	6	0.00	45 (7)	1200	0.48	0.85	1500	0.00		
SP	SP-5A	Ham River Sand	Bishop (4)	0.25	0.17	0.15						0.820	Loose	**	Rounded	7.2-287.9	4	0.00	31 (2)	890	0.26	0.78	360	0.11			
SP	SP-5B	Ham River Sand	Bishop (4)	0.25	0.17	0.15						0.640	Dense	**	Rounded	7.2-71.3	3	0.00	47 (9)	1100	0.57	0.86	2250	0.00			
SP	SP-7A	Poorly Graded Sand (Port Allen Lock)	Sherman & Trahan (44)	0.2	0.17	0.12	NP	NP		100.0	13.0	95.5	0.730	49	**	Rounded	0.9- 3.9	3	0.00	39 (0)	410	0.65	0.84				
SP	SP-7B	Poorly Graded Sand (Port Allen Lock)	Sherman & Trahan (44)	0.2	0.17	0.12	NP	NP		100.0	13.0	100.0	0.650	73	**	Rounded	0.9- 3.9	3	0.00	40 (1)	400	0.48	0.77				
SP	SP-7C	Poorly Graded Sand (Port Allen Lock)	Sherman & Trahan (44)	0.2	0.17	0.12	NP	NP		100.0	13.0	105.1	0.570	98	**	Rounded	0.9- 3.9	3	0.00	44 (3)	750	0.77	0.83				
SP	SP-12	Coarse to Fine Sand (Round Butte Dam)	Shannon & Wilson (41)				NP	NP				74.8	1.220	70	**	Angular	2.0-14.0	3	0.00	39 (6)	280	0.37	0.71	95	0.21		
SP	SP-13	Pumicecus Sand (Round Butte Dam)	Shannon & Wilson (41)	0.85	0.41	0.24						87.4		84.2	18.00	77	*	Angular	2.0-14.1	3	0.00	48 (10)	340	0.45	0.70	230	0.06
SP	SP-14	Pumicecus Sand (Round Butte Dam)	Shannon & Wilson (41)	1.0	0.5	0.24						80.7		76.9	25.00	71	*	Angular	2.0-14.1	3	0.00	49 (12)	650	0.38	0.77	380	0.05
SP	SP-18A	Fine Silica Sand (Loose)	Duncan & Chang (22)	0.27	0.2	0.165							0.650	38	**	Rounded	1.0- 5.1	3	0.00	30 (0)	280	0.65	0.93	110	0.85		
SP	SP-18B	Fine Silica Sand (Dense)	Duncan & Chang (22)	0.27	0.2	0.165							0.540	100	**	Rounded	1.0- 5.1	3	0.00	37 (0)	1400	0.74	0.90	1080	0.15		
SP	SP-17A	Monterey No. 0 Sand (Cylind. specimen)	Lade (33)	0.43	0.37	0.29	NP	NP					0.780	27	**	Rounded	0.3- 1.2	3	0.00	35 (0)	920	0.79	0.96	485	0.32		
SP	SP-17B	Monterey No. 0 Sand (Cubical specimen)	Lade (33)	0.43	0.37	0.29	NP	NP					0.780	27	**	Rounded	0.3- 1.2	3	0.00	39 (0)	510	0.51	0.97	370	0.22		
SP	SP-17C	Monterey No. 0 Sand (Cylind. specimen)	Lade (33)	0.43	0.37	0.29	NP	NP					0.570	98	**	Rounded	0.3- 1.2	3	0.00	45 (3)	3200	0.78	0.92	1400	0.45		
SP	SP-17D	Monterey No. 0 Sand (Cubical specimen)	Lade (33)	0.43	0.37	0.29	NP	NP					0.570	98	**	Rounded	0.3- 1.2	3	0.00	47 (5)	1500	0.76	0.91	1100	0.52		
SP	SP-18	Basaltic Sand (Round Butte Dam)	Shannon & Wilson (42)	3.	9.	0.13						120.1	9.5	120.0	9.50	**	Angular	2.0-14.0	3	0.00	39 (13)	1600	0.08	0.63	750	0.80	
SM	SM-4	Silty Sand (Chalfield Dam)	COE, Omaha District (19)	0.62	0.16	0.026	20	0	Std. AASHTO	123.0	9.5	116.7	9.40		**	Sub-rounded	6.0-10.0	3	0.00	37 (0)	100	1.07	0.62				
SM	SM-5	Silty Gravelly Sand (Chalfield Dam)	COE, Omaha District (19)	1.15	0.28	0.05	NP	NP	Std. AASHTO	132.0	8.1	124.5	7.53		*	Sub-rounded	6.0-10.0	3	0.00	41 (0)	530	0.51	0.82	640	0.00		
SM	SM-6	Silty Sand w/Pebbles (Round Butte Dam)	Shannon & Wilson (41)	0.31	0.1	0.04	NP	NP	16,450	110.6	17.5	108.1	17.50		**	Angular	2.0-14.0	3	0.00	46 (8)	700	0.35	0.75				
SM	SM-9	Silty Sand w/Pumice (Round Butte Dam)	Shannon & Wilson (41)	0.15	0.054	0.013	NP	NP	16,450	91.7	19.5	88.4	19.00		**	Angular	2.0-13.7	3	0.00	43 (8)	670	0.25	0.72	500	0.00		
SM	SM-13	Silty Sand (Round Butte Dam)	Shannon & Wilson (43)	0.27	0.027	0.0022				105.6	16.4	104.5	15.00		*	Sub-angular	2.0-14.1	3	0.00	36 (5)	530	0.28	0.74	470	0.00		
SM	SM-16	Silty Sand & Gravel (Round Butte Dam)	Shannon & Wilson (42)	0.45	0.052	0.012				109.3	12.9	109.0	12.00		**	Sub-angular	2.0-14.0	3	0.00	36 (11)	800	0.20	0.67	600	0.00		
SM-SC	SM-SC-1A	Silty Clayey Sand (Mica Dam Core)	Casagrande (10) / Insley & Hillis (27)	0.34	0.03	0.002	21	4	Std. AASHTO	136.0	9.8	131.1	7.70		**		3.6-32.4	6	0.31	33	700	0.37	0.80	280	0.19		
SM-SC	SM-SC-1B	Silty Clayey Sand (Mica Dam Core)	Casagrande (10) / Insley & Hillis (27)	0.34	0.03	0.002	21	4	Std. AASHTO	136.0	9.8	134.0	9.70		**		3.6-18.0	4	0.85	34	425	0.58	0.70	205	0.44		
SM-SC	SM-SC-1C	Silty Clayey Sand (Mica Dam Core)	Casagrande (10) / Insley & Hillis (27)	0.34	0.03	0.0002	21	4	Std. AASHTO	136.0	9.8	128.2	11.90		**		3.6-32.4	6	0.40	34	160	0.81	0.63	65	0.81		
ML	ML-1	Cannonville Silt (Undisturbed)	Hirschfeld & Poulos (26)	0.033	0.018	0.005						108.0	0.570		*		1.5- 7.4	4	0.00	45 (6)	200	1.07	0.57	200	0.89		
ML	ML-4	Sandy Silty w/Pumice (Round Butte Dam)	Shannon & Wilson (41)	0.078	0.032	0.0064	NP	NP	16,450	97.0	19.0	92.8	17.70		*		2.0-13.9	2	0.00	42 (7)	500	0.45	0.82	400	0.00		
ML	ML-5	Sandy Silty w/Pumice (Round Butte Dam)	Shannon & Wilson (41)	0.1	0.025	0.0052	NP	NP	16,																		

Table 6. Stress-Strain and Strength Parameters for Soils Tested under Unconsolidated-Undrained Conditions

Soil	Group	Soil Description	References	Grain Size (mm)			LL	PI	Compaction				Degree of Saturation	Rating	Particle Shape	Stress Range (TSF)	Number of Tests	C (TSF)	Friction Angle	K	n	R _i	K _s	m	
				D ₆₀	D ₃₀	D ₁₀			Type	Max. Dry Unit Wt. (pcf)	Opt. w/c	Dry Unit Wt. (pcf)													w/c
GC	GC-2A	Sandy Gravel (Oroville Dam Core)	Dept. of Water Resources (21)	9.	0.12	0.005	30	16	Std. AASHO	138.6	8.1	139.0	8.1	*		3.6-10.9	2	1.50	24	540	0.51	0.84			
GC	GC-2B	Sandy Gravel (Oroville Dam Core)	Dept. of Water Resources (21)	9.	0.12	0.005	30	16	Std. AASHO	138.6	8.1	139.0	8.1	*		27.9-43.3	2	10.01	3	190	0.95	0.97			
SP	SP-8D	Poorly Graded Sand (Rodman Dam)	COE, Jacksonville District (16)	0.38	0.26	0.16	17	NP	Mod. AASHO	109.5	11.8	104.0	11.8	55	***	Sub-rounded	1.0-3.0	3	0.	37 (4)	590	1.10	0.89		
SP	SP-8E	Poorly Graded Sand (Rodman Dam)	COE, Jacksonville District (16)	0.38	0.26	0.16	17	NP	Mod. AASHO	109.5	11.8	98.6	11.8	47	*	Sub-rounded	1.0-3.0	2	0.	37 (8)	770	-0.14	0.87		
SP	SP-8F	Poorly Graded Sand (Rodman Dam)	COE, Jacksonville District (16)	0.38	0.26	0.16	17	NP	Mod. AASHO	109.5	11.8	110.0	11.2	61	**	Sub-rounded	1.0-3.0	3	0.	43 (9)	940	0.	0.82		
SP	SP-9D	Poorly Graded Silty Sand (Rodman Dam)	COE, Jacksonville District (16)	0.16	0.14	0.084	23	NP	Mod. AASHO	101.1	13.6	101.3	13.4	57	***	Sub-rounded	1.0-3.0	3	0.	44 (6)	420	0.67	0.76		
SP	SP-9E	Poorly Graded Silty Sand (Rodman Dam)	COE, Jacksonville District (16)	0.16	0.14	0.084	23	NP	Mod. AASHO	101.1	13.6	96.2	13.3	50	*	Sub-rounded	1.0-2.0	2	0.	44 (11)	850	0.79	0.92		
SP	SP-9F	Poorly Graded Silty Sand (Rodman Dam)	COE, Jacksonville District (16)	0.16	0.14	0.084	23	NP	Mod. AASHO	101.1	13.8	92.0	12.4	42	***	Sub-rounded	1.0-3.0	3	0.	40 (8)	470	0.51	0.86		
SM	SM-1	Gravelly Silty Sand (Ball Mountain Dam)	Linell & Shea (36)	0.80	0.074	0.05	NP	NP	Std. AASHO	122.9	10.0	124.0	9.4	71	**		1.1-4.3	3	0	42 (5)	430	0.38	0.57		
SM	SM-3A	Silty Sand (Somerville Dam)	COE, Fort Worth District (15)	0.108	0.095	0.004	NP	NP	Std. AASHO	109.1	13.4	109.3	13.4	70	**		0.5-6.0	4	0.	40 (2)	350	0.91	0.69		
SM	SM-3B	Silty Sand (Somerville Dam)	COE, Fort Worth District (15)	0.108	0.095	0.004	NP	NP	Std. AASHO	109.1	13.4	104.1	13.2	60	**		0.5-6.0	4	0.	40 (6)	420	0.84	0.75		
SM	SM-3C	Silty Sand (Somerville Dam)	COE, Fort Worth District (15)	0.108	0.055	0.004	NP	NP	Std. AASHO	109.1	13.4	103.6	16.7	75	**		0.5-6.0	4	0.	39 (4)	340	0.64	0.72		
SM-SC	SM-SC-2	Silty Clayey Sand (Hopkinson Dam)	Linell & Shea (36)	0.22	0.014	0.001	21	7	Std. AASHO	129.2	9.2	131.0	8.8	83	**		1.0-6.0	3	0.98	31	320	0.35	0.86		
SC	SC-2	Clayey Sand (Thomaston Dam)	Linell & Shea (36)	0.4	0.028	0.003	29	12	Std. AASHO	123.3	12.0	122.0	12.0	85	**		1.1-4.3	3	0.92	18	39	0.61	0.55		
SC	SC-3	Clayey Sand (New Don Pedro Dam Core)	Bechtel (1)	0.54	0.02	0.005	27	11	20,000	125.8	9.8	123.2	9.6	73	**		5.4-21.6	3	2.60	26	3900	-0.08	0.93	12000	-0.99
SC	SC-5	Clayey Gravelly Sand (Proctor Dam)	COE, Fort Worth District (15)	0.54	0.08	-	28	18	Std. AASHO	120.1	11.2	126.0	8.3	70	*		0.5-1.5	2	1.80	4	510	0.37	0.64	250	0.
SC	SC-6A	Clayey Sand (Chatfield Dam)	COE, Omaha District (19)	0.24	0.04	-	22	7	Std. AASHO	122.0	11.7	116.2	14.7	90	*		6.0-10.0	2	1.30	0	52	0.	0.76		
SC	SC-7B	Clayey Sand (Chatfield Dam)	COE, Omaha District (19)	0.11	0.01	-	32	18	Std. AASHO	115.0	15.0	110.0	17.0	88	*		6.0-10.0	2	1.10	0	250	0.	0.97		
ML	ML-2A	Sandy Silt (Chatfield Dam)	COE, Omaha District (19)	0.09	0.03	0.003	25	4	Std. AASHO	115.0	12.8	108.7	15.6	77	***		6.0-10.0	3	1.80	19	200	0.59	0.86		
ML	ML-2B	Sandy Silt (Chatfield Dam)	COE, Omaha District (19)	0.09	0.03	0.003	25	4	Std. AASHO	115.0	12.8	109.3	12.7	63	***		6.0-10.0	3	0.39	30	27	1.43	0.72		
ML	ML-3A	Sandy Silt (Birch Dam Shell)	COE, Tulsa District (20)	0.070	0.045	0.013	19	1	Std. AASHO	108.8	13.6	104.0	11.6	53	***		0.5-6.0	4	0.42	31	240	0.31	0.83		
ML	ML-3B	Sandy Silt (Birch Dam Shell)	COE, Tulsa District (20)	0.070	0.045	0.013	19	1	Std. AASHO	108.8	13.6	104.0	13.6	62	***		1.5-6.0	3	0.19	31	270	0.38	0.82		
ML	ML-3C	Sandy Silt (Birch Dam Shell)	COE, Tulsa District (20)	0.070	0.045	0.013	19	1	Std. AASHO	108.8	13.6	104.0	16.6	74	***		1.5-6.0	3	0.54	27	100	0.84	0.77		
CL	CL-1A	Silty Clay (Arkabulla Dam)	Casagrande et al (9)	0.023	0.01	-	40	20	Std. AASHO	110.0	18.0	108.7	16.7	81	***		1.0-12.3	4	0.53	29	260	0.60	0.87		
CL	CL-1B	Silty Clay (Arkabulla Dam)	Casagrande et al (9)	0.023	0.01	-	40	20	Std. AASHO	110.0	18.0	107.0	19.5	89	*		1.0-8.2	4	1.20	14	39	0.48	0.58		
CL	CL-2A	Lean Clay (Monroe Dam)	COE, Louisville District (18)	0.023	0.001	-	40	23	Std. AASHO	110.5	16.4	107.1	19.1	87	*		0.7-2.9	2	0.95	0	66	0.	0.75		
CL	CL-2B	Lean Clay (Monroe Dam)	COE, Louisville District (18)	0.023	0.001	-	40	23	Std. AASHO	110.5	16.4	104.0	21.2	89	**		0.7-2.9	3	0.42	0	10	0.03	0.52		
CL	CL-3	Lean Clay (Monroe Dam)	COE, Louisville District (18)	0.015	0.0044	-	44	22	Std. AASHO	106.8	18.0	102.0	21.7	92	*		0.7-2.9	2	1.00	0	36	0.	0.57		
CL	CL-5A	Pittsburg Silty Clay	Kulhawey, Duncan & Seed (32)	0.04	0.003	-	35	16	Mod. AASHO	118.9	13.5	105.4	11.5	52	**		1.0-3.0	2	0.92	31	650	-0.68	0.90	190	0.81
CL	CL-5B	Pittsburg Silty Clay	Kulhawey, Duncan & Seed (32)	0.04	0.003	-	35	16	Mod. AASHO	118.9	13.5	109.1	14.3	71	**		1.0-6.0	3	1.50	17	760	-0.14	0.93	240	-0.21
CL	CL-5C	Pittsburg Silty Clay	Kulhawey, Duncan & Seed (32)	0.04	0.003	-	35	16	Mod. AASHO	118.9	13.5	109.0	16.8	83	**		1.0-6.0	2	1.30	6	430	0.10	0.93	115	0.10
CL	CL-5E	Pittsburg Silty Clay	Kulhawey, Duncan & Seed (32)	0.04	0.003	-	35	16	Mod. AASHO	118.9	13.5	112.7	11.5	63	**		1.0-6.0	3	1.80	24	2400	-0.74	0.92	740	-0.96
CL	CL-5F	Pittsburg Silty Clay	Kulhawey, Duncan & Seed (32)	0.04	0.003	-	35	16	Mod. AASHO	118.9	13.5	114.7	14.5	84	**		1.0-3.0	2	1.90	13	2000	-0.30	0.87	460	-0.64
CL	CL-5H	Pittsburg Silty Clay	Kulhawey, Duncan & Seed (32)	0.04	0.003	-	35	16	Mod. AASHO	118.9	13.5	108.8	8.71	43	**		1.0-6.0	3	1.50	32	8900	-1.10	0.94	1900	-1.1
CL	CL-5I	Pittsburg Silty Clay	Kulhawey, Duncan & Seed (32)	0.04	0.003	-	35	16	Mod. AASHO	118.9	13.5	119.3	11.7	77	**		1.0-6.0	3	3.30	18	5000	-0.28	0.95	1400	-0.33
CL	CL-6A	Sandy Clay (Birch Dam Core)	COE, Tulsa District (20)	0.045	0.01	-	29	15	Std. AASHO	110.3	14.5	105.0	12.5	57	**		1.5-6.0	3	0.64	29	320	-0.21	0.80		
CL	CL-6B	Sandy Clay (Birch Dam Core)	COE, Tulsa District (20)	0.045	0.01	-	29	15	Std. AASHO	110.3	14.5	105.0	14.5	66	***		0.5-6.0	3	0.50	25	190	0.02	0.81		
CL	CL-7A	Sandy Clay (Somerville Core)	COE, Fort Worth District (15)	0.06	0.003	-	43	30	Std. AASHO	107.5	17.2	107.9	17.2	87	**		0.5-6.0	4	1.00	2	74	0.23	0.87		
CL	CL-7B	Sandy Clay (Somerville Core)	COE, Fort Worth District (15)	0.06	0.003	-	43	30	Std. AASHO	107.5	17.2	107.2	17.0	74	**		0.5-6.0	4	1.00	1	68	-0.05	0.84		
CL	CL-7C	Sandy Clay (Somerville Core)	COE, Fort Worth District (15)	0.06	0.003	-	43	30	Std. AASHO	107.5	17.2	102.6	20.0	88	**		0.5-6.0	4	0.45	1	27	0.18	0.85		
CL	CL-8B	Sandy Clay (Somerville Core)	COE, Fort Worth District (15)	0.085	0.0055	-	28	16	Std. AASHO	113.3	14.5	108.3	14.6	74	**		0.5-6.0	4	0.57	25	320	0.29	0.85		
CL	CL-9A	Sandy Clay (Somerville Core)	COE, Fort Worth District (15)	0.052	0.0085	-	49	32	Std. AASHO	95.7	23.3	96.5	23.2	89	**		0.5-6.0	3	1.50	4	200	0.29	0.89		
CL	CL-9B	Sandy Clay (Somerville Core)	COE, Fort Worth District (15)	0.052	0.0085	-	49	32	Std. AASHO	95.7	23.3	91.7	23.3	77	**		1.5-6.0	3	1.20	3	100	0.18	0.86		
CL	CL-9C	Sandy Clay (Somerville Core)	COE, Fort Worth District (15)	0.052	0.0085	-	49	32	Std. AASHO	95.7	23.3	90.8	26.7	87	**		0.5-6.0	3	0.64	1	53	0.14	0.90		
CL	CL-10A	Sandy Clay (Somerville Core)	COE, Fort Worth District (15)	0.085	0.004	-	29	16	Std. AASHO	110.7	15.0	111.8	15.1	86	**		0.5-6.0	4	0.84	22	160	0.34	0.78		
CL	CL-10B	Sandy Clay (Somerville Core)	COE, Fort Worth District (15)	0.085	0.004	-	29	16	Std. AASHO	110.7	15.0	106.5	15.0	74	***		0.5-6.0	4	0.55	22	290	0.27	0.91		
CL	CL-11A	Sandy Clay (Somerville Core)	COE, Fort Worth District (15)	0.06	0.002	-	25	12	Std. AASHO	107.5	16.8	100.3	13.5	58	**		0.5-6.0	4	0.78	28	680	-0.36	0.84		
CL	CL-11B	Sandy Clay (Somerville Core)	COE, Fort Worth District (15)	0.06	0.002	-	25	12	Std. AASHO	107.5	16.8	106.5	13.3	66	**		0.5-6.0	4	1.50	25	600	0.18	0.68		

Table 6. Stress-Strain and Strength Parameters for Soils Tested under Unconsolidated-Undrained Conditions (continued)

Soil	Group	Soil Description	References	Grain Size (mm)			LL	PI	Compaction				Degree of Saturation	Rating	Particle Shape	Stress Range (TSF)	Number of Tests	C (TSF)	Friction Angle	K	n	R _i	K _s	m
				D ₆₀	D ₃₀	D ₁₀			Type	Max. Dry Unit Wt. (pcf)	Opt. w/c	Dry Unit Wt. (pcf)												
CL	CL-11C	Sandy Clay (Somerville Dam)	COE, Fort Worth District (15)	0.06	0.002	-	25	12	Std. AASHO	107.5	168.8	102.6	19.3	87	*	0.5- 6.0	4	0.74	6	23	0.32	0.61		
CL	CL-11D	Sandy Clay (Somerville Dam)	COE, Fort Worth District (15)	0.06	0.002	-	25	12	Std. AASHO	107.5	168.8	106.7	16.7	85	*	0.5- 6.0	4	0.91	18	280	0.60	0.93		
CL	CL-11E	Sandy Clay (Somerville Dam)	COE, Fort Worth District (15)	0.06	0.002	-	25	12	Std. AASHO	107.5	16.8	101.5	16.3	72	*	0.5- 6.0	4	0.66	20	220	0.23	0.90		
CL	CL-12A	Sandy Clay (Somerville Dam)	COE, Fort Worth District (15)	0.065	0.0055	0.001	38	25	Std. AASHO	106.1	17.2	105.0	18.6	89	*	0.5- 6.0	4	1.30	8	140	0.20	0.84		
CL	CL-12C	Sandy Clay (Somerville Dam)	COE, Fort Worth District (15)	0.065	0.0055	0.001	38	25	Std. AASHO	106.1	17.2	101.9	17.1	75	**	0.5- 6.0	4	1.00	13	120	0.09	0.83		
CL	CL-12D	Sandy Clay (Somerville Dam)	COE, Fort Worth District (15)	0.065	0.0055	0.001	38	25	Std. AASHO	106.1	17.2	103.0	19.7	89	*	0.5- 6.0	4	0.80	2	47	0.33	0.82		
CL	CL-12E	Sandy Clay (Somerville Dam)	COE, Fort Worth District (15)	0.065	0.0055	0.001	38	25	Std. AASHO	106.1	17.2	106.5	13.9	70	**	0.5- 6.0	4	1.50	24	950	-0.15	0.90		
CL	CL-12F	Sandy Clay (Somerville Dam)	COE, Fort Worth District (15)	0.065	0.0055	0.001	38	25	Std. AASHO	106.1	17.2	108.3	16.9	89	*	0.5- 6.0	4	1.50	8	470	0.0	0.95		
CL	CL-13A	Sandy Clay (Somerville Dam)	COE, Fort Worth District (15)	0.046	0.0045	-	36	23	Std. AASHO	104.9	17.6	98.7	20.8	86	**	0.5- 6.0	4	0.67	4	75	0.44	0.88		
CL	CL-13B	Sandy Clay (Somerville Dam)	COE, Fort Worth District (15)	0.046	0.0045	-	36	23	Std. AASHO	104.9	17.6	104.9	14.8	72	*	0.5- 6.0	4	1.80	23	840	-0.19	0.84		
CL	CL-13C	Sandy Clay (Somerville Dam)	COE, Fort Worth District (15)	0.046	0.0045	-	36	23	Std. AASHO	104.9	17.6	101.2	17.4	76	*	0.5- 6.0	4	1.20	12	270	0.06	0.87		
CL	CL-13D	Sandy Clay (Somerville Dam)	COE, Fort Worth District (15)	0.046	0.0045	-	36	23	Std. AASHO	104.9	17.6	100.5	14.2	62	*	0.5- 6.0	4	1.40	29	1100	-0.36	0.83		
CL	CL-13E	Sandy Clay (Somerville Dam)	COE, Fort Worth District (15)	0.046	0.0045	-	36	23	Std. AASHO	104.9	17.6	104.4	17.5	84	*	0.5- 6.0	3	1.40	13	410	0.15	0.87		
CL	CL-14	Lean Clay (Clinton Dam)	COE, Kansas City District (17)	-	-	-	46	27	Std. AASHO	103.0	21.2	98.0	24.0	92	**	1.0- 5.0	3	0.77	2	57	0.43	0.86		
CL	CL-16C	Lean Clay (Clinton Dam)	COE, Kansas City District (17)	-	-	-	37	18	Std. AASHO	105.0	20.2	99.7	22.9	91	**	1.0- 3.0	2	0.97	1	110	0.43	0.90		
CL	CL-17A	Lean Clay (Clinton Dam)	COE, Kansas City District (17)	-	-	-	43	24	Std. AASHO	101.0	20.1	99.1	22.7	90	**	2.0- 6.0	3	1.10	2	100	0.27	0.89		
CL	CL-17B	Lean Clay (Clinton Dam)	COE, Kansas City District (17)	-	-	-	43	24	Std. AASHO	101.0	20.1	98.1	23.9	90	**	2.0- 6.0	3	0.99	1	160	0.54	0.97		
CL	CL-17C	Lean Clay (Clinton Dam)	COE, Kansas City District (17)	-	-	-	43	24	Std. AASHO	101.0	20.1	98.9	22.7	90	**	2.0- 6.0	3	1.10	3	130	0.46	0.91		
CL	CL-19A	Lean Clay (Clinton Dam)	COE, Kansas City District (17)	-	-	-	42	26	Std. AASHO	102.0	19.9	96.8	22.7	83	**	2.0- 6.0	3	0.78	2	53	0.41	0.85		
CL	CL-24A	Sandy Clay (Chatfield Dam)	COE, Omaha District (19)	0.016	-	-	43	24	Std. AASHO	104.0	19.3	97.6	23.4	90	*	6.0- 10.0	2	1.20	0	240	0.0	0.95		
CL	CL-25A	Sandy Clay (Chatfield Dam)	COE, Omaha District (19)	0.09	0.007	-	34	18	Std. AASHO	113.0	15.1	107.4	18.1	86	*	6.0- 10.0	2	0.95	0	160	0.0	0.93		
CL	CL-28	Sandy Clay (Proctor Dam)	COE, Fort Worth District (15)	0.033	0.002	-	31	20	Std. AASHO	115.0	14.6	114.8	12.2	72	**	1.5- 6.0	2	1.60	12	150	0.16	0.79		
CL	CL-29A	Silty Clay (Canyon Dam)	Casagrande & Hirschfeld (8)	0.037	0.008	-	34	19	Harvard	116.2	15.2	110.9	13.0	67	*	1.0- 14.3	5	2.00	20	440	0.17	0.85		
CL	CL-29B	Silty Clay (Canyon Dam)	Casagrande & Hirschfeld (8)	0.037	0.008	-	34	19	Harvard	116.2	15.2	115.8	13.1	77	*	1.0- 14.3	4	2.50	20	440	0.34	0.86		
CL	CL-30A	Silty Clay (Canyon Dam)	Casagrande & Hirschfeld (8)	0.037	0.008	-	34	19	Harvard	112.8	16.7	111.0	16.2	84	*	1.0- 6.3	4	1.00	16	110	0.94	0.91		
CL	CL-30B	Silty Clay (Canyon Dam)	Casagrande & Hirschfeld (8)	0.037	0.008	-	34	19	Harvard	112.8	16.7	112.2	16.6	88	*	1.0- 4.1	3	1.40	11	67	0.71	0.77		
CL	CL-30D	Silty Clay (Canyon Dam)	Casagrande & Hirschfeld (8)	0.037	0.008	-	34	19	Harvard	112.8	16.7	110.3	17.3	88	*	1.1- 4.1	3	1.00	9	37	0.37	0.65		
CL	CL-33B	Silty Clay (Canyon Dam)	Casagrande & Hirschfeld (7)	0.037	0.008	-	34	19	Harvard	108.8	18.0	106.3	16.2	75	**	4.1- 13.5	4	2.20	3	71	1.06	0.98		
CH	CH-1	Fat Clay (Clinton Dam)	COE, Kansas City District (17)	-	-	-	60	38	Std. AASHO	94.0	26.5	90.0	28.8	90	**	1.0- 3.0	2	0.61	4	92	0.21	0.89		
CH	CH-3A	Fat Clay (Monroe Dam)	COE, Louisville District (18)	0.0067	-	-	61	36	Std. AASHO	95.5	26.5	89.3	31.1	93	*	0.7- 2.9	2	0.37	0	21	0.0	0.65		
CH	CH-3B	Fat Clay (Monroe Dam)	COE, Louisville District (18)	0.0067	-	-	61	36	Std. AASHO	95.5	26.5	92.6	28.6	93	**	0.7- 2.9	3	0.51	1	67	0.02	0.79		
CH	CH-4	Fat Clay (Monroe Dam)	COE, Louisville District (18)	0.018	-	-	69	45	Std. AASHO	100.0	22.7	96.4	26.5	94	**	1.1- 2.9	2	0.63	1	65	0.14	0.77		
CH	CH-5A	Fat Clay (Chatfield Dam)	COE, Omaha District (19)	0.0095	-	-	54	36	Std. AASHO	95.0	24.4	90.3	27.4	84	*	6.0- 10.0	3	1.20	0	36	0.72	0.91		
CH	CH-5B	Fat Clay (Chatfield Dam)	COE, Omaha District (19)	0.0095	-	-	54	36	Std. AASHO	95.0	24.4	90.7	24.4	76	***	6.0- 10.0	3	1.50	2	52	0.66	0.89		